Mariam Kaynia

Analysis and Improvement of Wireless Ad Hoc Network Performance Through MAC and PHY Layer Design

Thesis for the degree of Philosophiae Doctor

Trondheim, November 2010

Norwegian University of Science and Technology
Faculty of Information Technology,
Mathematics and Electrical Engineering
Department of Electronics and Telecommunications

NTNU – Trondheim
Norwegian University of
Science and Technology

NTNU
Norwegian University of Science and Technology

Thesis for the degree of Philosophiae Doctor

Faculty of Information Technology, Mathematics and Electrical Engineering
Department of Electronics and Telecommunications

ISBN 978-82-471-2442-0 (printed ver.)
ISBN 978-82-471-2443-7 (electronic ver.)
ISSN 1503-8181

Doctoral theses at NTNU, 2010:227

Printed by NTNU-trykk

Abstract

In this dissertation, we investigate the performance of point-to-point wireless ad hoc networks. The performance evaluation is performed in terms of outage probability, which is defined as the probability of receiving messages correctly. This metric is stochastic, and closely related to the ubiquitous notions of throughput and transmission capacity. In order to make the analysis tractable, we establish a proper analytical framework, and make reasonable approximations in the derivations.

Approaching the design of ad hoc networks through the medium access control (MAC) layer, analytical expressions are obtained for the outage probability of a given mobile ad hoc network in an unbounded (infinite) region. We consider the following MAC protocols: slotted and unslotted ALOHA, carrier sensing multiple access (CSMA) with transmitter sensing, and CSMA with receiver sensing. Moreover, we investigate the impact of various ad hoc network characteristics on the outage probability. In particular, we add fading to the path loss channel model and measure the degradation it causes; we bound the network domain to investigate the edge effects; and we introduce fading within a bounded network. In each case, new outage probability expressions are derived.

Having established a fundamental understanding of the behavior of various flavors of mobile ad hoc networks, we propose MAC layer techniques to improve the performance. Three schemes are proposed: 1) optimization of the sensing threshold in CSMA, 2) addition of a feedback channel between each transmitter and its receiver for improving the decision making stage of CSMA, and 3) introduction of bandwidth partitioning. In each scenario, new outage probability expressions are derived both in non-fading and fading networks.

Finally, we step into the domain of multiple input multiple output (MIMO) communications, allowing for multiple antennas at transmitters and receivers. Within an ad hoc setting with no channel state information (CSI) at the transmitters, lower and upper bounds are derived on the outage probability and ergodic capacity. In the particular case of multiple

input single output (MISO) channels, different transmission schemes are proposed in order to achieve the best usage of transmit antennas. With the addition of CSI at the transmitters, we consider various interference management schemes, with focus on the high SNR regime. We propose a binary power control scheme that ensures an increase in the sum rate of the MIMO network with many users, and that operates in a distributed manner, regardless of the interference management algorithm applied.

Preface

This dissertation is submitted in partial fulfillment of the requirements for the degree of Philosophiae Doctor (PhD) at the Department of Electronics and Telecommunications, Norwegian University of Science and Technology (NTNU). The PhD study has been carried out in the period from August 2007 to August 2010.

The PhD requirement at NTNU comprises of research, half a year of full-time compulsory courses, and corresponding to one year of teaching duties. As part of the latter, I have taught in several undergraduate and graduate courses, and supervised graduate students on their Master thesis or term projects. Also, I have served as Treasurer in IEEE Norway, and as chair for the IEEE Norway Student Branch. Moreover, I have been the project leader for NTNU Alumni at the Department of Electronics and Telecommunications, and a PhD representative in the steering committee of the Faculty of Information Technology, Mathematics and Electrical Engineering at NTNU.

As a PhD student, I had the pleasure of having several visiting researcher appointments abroad. First, from January to July 2009, I was at Stanford University, as a member of the Wireless Systems Laboratory, headed by Prof. Andrea J. Goldsmith. Second, from September 2009 to February 2010, I was at EURECOM in Sophia-Antipolis, France, working in collaboration with Prof. David Gesbert. Moreover, I have had shorter visits to: University of Minnesota, Twin Cities, working with Prof. Nihar Jindal (who was also my Master's thesis advisor); University of Bologna in Italy, working with Prof. Roberto Verdone and his research group; and finally Politecnico di Torino in Italy, working with Post-Doctoral fellow, Dr. Giusi Alfano.

The work included in this thesis has been funded partly by the Research Council of Norway (NFR), and partly by the Department of Electronics and Telecommunications, NTNU. The teaching assistantship has been funded by the Department of Electronics and Telecommunications, NTNU. The stay at Stanford University and EURECOM were funded by NFR through

the VERDIKT Programme, while the shorter visiting scholar appointments have in part been funded by the COST 2100 Action and the Department of Electronics and Telecommunications.

Acknowledgements

There are a number of people I wish to thank for making my experience as a PhD student one of the most rewarding periods of my life. First off, I would like to thank my advisor at NTNU, Prof. Geir E. Øien, for his continuous support both on a technical and a personal level. His excellent supervising skills and commitment to his students have been not only of tremendous help in achieving my academic goals, but also extremely inspirational. The increasing trust and faith that Prof. Øien has shown me through my PhD studies, have allowed me to work independently and to develop myself as a self-driven researcher.

Through Prof. Øien's wide range of academic acquaintances, I was introduced to many distinguished researchers on an international basis. In particular, I would like to mention Prof. Andrea J. Goldsmith and Prof. David Gesbert, with whom I had the opportunity to work with for one year of my studies. I would hereby like to express my deep gratitude for their support and contributions. Their academic excellence and great social skills have been motivational for me. Also, I would like to thank Prof. Roberto Verdone, who has a remarkable ability to take initiatives and bring new ideas to the table. Working with him has been of great joy and our collaboration has been extremely efficient and fruitful. I am also grateful to Prof. Are Hjørungnes for his support during the writing stage of my thesis, and for providing me an office at UNIK University Graduate Center.

I am also deeply thankful to Prof. Nihar Jindal, who I was first introduced to as my Master's thesis advisor at the University of Minnesota. His remarkable knowledge of matters and ability to view problems from new and creative aspects is admirable and has been of immense contribution to my PhD work. Our continuing collaboration in the years after my Master's has been fruitful and personally rewarding.

I would also like to thank my other co-authors for great collaboration and insightful discussions that resulted in many solid results. Moreover, I am grateful to my colleagues at NTNU, Stanford, and EURECOM, whose friendship and support have been of the utmost importance, both on an academic and personal level. Without them, as well as my friends outside the university, my experience as a PhD student would not have been so

enjoyable and memorable.

At last, but not least, I would like to express my deep gratitude to my parents whose guidance and support through the years have been indispensable. Through them I was introduced to the academic life at an early age, and I developed a passion for education and research that has been the driving force in my life choices. I am indebted to them and so I dedicate this thesis to them.

Contents

Contents vii

List of Figures xi

Abbreviations xv

Nomenclature xix

1 Introduction 1
- 1.1 Background and Motivation . . . 2
  - 1.1.1 Medium Access Control (MAC) Protocols . . . 3
  - 1.1.2 Ad Hoc Network Characteristics . . . 6
  - 1.1.3 Performance Evaluation Metrics . . . 8
  - 1.1.4 Multiple Antenna Systems . . . 10
- 1.2 Overview of Contributions . . . 13
  - 1.2.1 Works Not Included in This Thesis . . . 14

2 Performance Analysis 19
- 2.1 System Model . . . 21
  - 2.1.1 Justification of Assumptions . . . 25
- 2.2 Method of Analysis . . . 26
- 2.3 Outage Probability of ALOHA . . . 28
  - 2.3.1 Slotted ALOHA . . . 28
  - 2.3.2 Unslotted ALOHA . . . 29
- 2.4 Outage Probability of CSMA . . . 30
  - 2.4.1 CSMA with Transmitter Sensing . . . 30
  - 2.4.2 CSMA with Receiver Sensing . . . 35
- 2.5 Proof of Theorems for CSMA . . . 37
  - 2.5.1 Proof of Theorem 2.3 . . . 37
  - 2.5.2 Proof of Theorem 2.4 . . . 40
- 2.6 Numerical Results . . . 42

2.7 Summary 47

3 Impact of Network Characteristics 49
3.1 Impact of Fading 49
3.1.1 System Model 50
3.1.2 The ALOHA Protocol 52
3.1.3 The CSMA Protocol 54
3.1.4 Numerical Results 58
3.2 Bounded Networks 62
3.2.1 System Model 62
3.2.2 The ALOHA Protocol 64
3.2.3 The CSMA Protocol 67
3.2.4 Numerical Results 71
3.3 Bounded Networks with Fading 74
3.3.1 System Model 74
3.3.2 The ALOHA Protocol 75
3.3.3 The CSMA Protocol 76
3.3.4 Numerical Results 79
3.4 Summary 83

4 Performance Improvement Through Advanced CSMA 85
4.1 Optimizing CSMA's Sensing Threshold 85
4.1.1 System Model 86
4.1.2 Performance in the Absence of Fading 87
4.1.3 Performance in the Presence of Fading 95
4.1.4 Numerical Results 99
4.2 CSMA With Joint Transmitter-Receiver Sensing 103
4.2.1 System Model 103
4.2.2 Performance in the Absence of Fading 104
4.2.3 Performance in the Presence of Fading 108
4.2.4 Optimizing the Sensing Thresholds 111
4.2.5 Numerical Results 117
4.3 Summary 123

5 Performance Improvement Through Bandwidth Partitioning 125
5.1 System Model 126
5.2 Performance in the Absence of Fading 128
5.2.1 The ALOHA Protocol 128
5.2.2 The CSMA Protocol With Random Selection of a Subband 130
5.2.3 The CSMA Protocol With Sensing Across Subbands 133

5.3 Performance in the Presence of Fading 134
5.3.1 The ALOHA Protocol 135
5.3.2 The CSMA Protocol 136
5.4 Numerical Results 139
5.5 Summary 145

6 Performance Improvement With MIMO Techniques 147
6.1 Usage of Antennas in Absence of CSI 148
6.1.1 System Model 150
6.1.2 MIMO Interference Channels 152
6.1.3 MISO Interference Channels 159
6.1.4 Optimal Use of Antennas in MISO Channels 164
6.2 Use of CSI to Improve System Performance 171
6.2.1 System Model 171
6.2.2 Interference Alignment and Feasibility 173
6.2.3 Binary Power Control to Ensure Feasibility 175
6.3 Summary 180

7 Conclusions and Future Work 181
7.1 Detailed Contributions of This Thesis 182
7.2 Subjects for Further Research 185

References 189

List of Figures

1.1 The 7-layer OSI model. 3
1.2 Setup to illustrate the hidden and exposed node problems of CSMA. 5
1.3 Illustration of SISO, SIMO, MISO, and MIMO channels. 11

2.1 Illustration of our ad hoc network and traffic model. 22
2.2 Guard zone of RX_0, denoted $B(\mathrm{RX}_0, s)$, with an interfering transmitter, TX_1. 27
2.3 Algorithm for numerically solving the various probabilities to find $P_{out}(\mathrm{CSMA}_{\mathrm{TX}})$. 32
2.4 Area of overlap between $B(\mathrm{RX}_0, s)$ and $B(\mathrm{TX}_0, s)$. 33
2.5 The setup used to analyze the outage probability of CSMA. . . 39
2.6 The setup used to analyze the outage probability of $\mathrm{CSMA}_{\mathrm{RX}}$. 41
2.7 The setup used in the derivation of P_{during} for $\mathrm{CSMA}_{\mathrm{RX}}$. 42
2.8 Outage probability of ALOHA along with the backoff probability of CSMA, as a function of λ for $(M, N) = (1, 0)$. 43
2.9 Outage probability of ALOHA and CSMA as a function of λ. . 44
2.10 Ratio of the outage probability of CSMA over that of unslotted ALOHA as a function of λ. 44
2.11 Average transmission delay as a function of the number of retransmissions, N for $\lambda = 0.05$, and in CSMA, $M = 3$. 45
2.12 Dependence of the outage probability on the transmitter-receiver distance R for $\lambda = 0.01$. 46
2.13 Dependence of the outage probability on the path loss exponent α for $\lambda = 0.05$ and $(M, N) = (2, 1)$. 47

3.1 Outage probability of ALOHA and CSMA as a function of the packet arrival density λ. 59
3.2 Outage probability ratio of CSMA over unslotted ALOHA as a function of λ for $(M, N) = (2, 1)$. 59

3.3 Outage probability with fading over outage probability without fading, as a function of λ. 60
3.4 Behavior of the outage probability in the presence of fading as a function of R, with $\lambda = 0.01$ and $(M, N) = (2, 1)$. 61
3.5 Partitioning of the finite area into 8 circular subregions. 64
3.6 Outage probability of ALOHA and CSMA in a bounded non-fading network with $L = 3.3$ m, as a function of λ. 71
3.7 Outage probability of ALOHA and CSMA in a bounded non-fading network, as a function of L. 72
3.8 Outage probability of ALOHA and CSMA in a bounded 3 m $\times$ 3 m network with fading as a function of λ. 79
3.9 Outage probability ratio of the unslotted protocols over that of slotted ALOHA as a function of λ for $(M, N) = (1, 0)$. 80
3.10 Outage probability of ALOHA and CSMA in a fading network as a function of L. 81
3.11 Outage probability of CSMA_{RX} for bounded and infinite networks, both in the absence and presence of fading, for $(M, N) = (2, 1)$. 81

4.1 Area of overlap between $B(\text{RX}_0, s)$ and $B(\text{TX}_0, s_b)$ for the derivation of the outage probability of CSMA. 88
4.2 Setup for derivation of $P_{rx|transmit}$ in CSMA_{RX}. 91
4.3 Setup to illustrate the rate of increase in P_b and decrease in P_{during} as s_b increases. 93
4.4 Outage probability in the absence of fading with $\lambda = 0.02$ and $\beta = 0$ dB, as a function of β_b/β 99
4.5 The outage probability in the presence of fading with $\lambda = 0.02$ and $\beta = 0$ dB. 100
4.6 Ratio of the outage probability of the unslotted protocols over that of slotted ALOHA in a non-fading network with $(M, N) = (1, 0)$, as a function of β_b/β. 101
4.7 Ratio of the outage probability of unslotted ALOHA and CSMA over that of slotted ALOHA as a function of $\beta_b = \beta$ for $\lambda = 0.2$ and $(M, N) = (1, 0)$. 102
4.8 Illustration of the sensing zones $B(\text{RX}_0, s_r)$ and $B(\text{TX}_0, s_t)$. . . 105
4.9 Derivative of the outage probability of $\text{CSMA}_{\text{TXRX}}$ for $\lambda = 0.01$, $\beta = 10$ dB, $M = 1$, and $N = 0$. 115
4.10 Derivative of the outage probability of $\text{CSMA}_{\text{TXRX}}$ in a fading network as a fucntion of β_t, for $\beta = 0$ dB. 117
4.11 Outage probability of $\text{CSMA}_{\text{TXRX}}$ in a non-fading network with $\beta_t = \beta_r = \beta = 0$ dB. 118

4.12 Outage probability of $\text{CSMA}_{\text{TXRX}}$ in a fading network with $\beta_t = \beta_r = \beta = 0$ dB. 119
4.13 Outage probability of $\text{CSMA}_{\text{TXRX}}$ as a function of the sensing thresholds, for a non-fading network with $\lambda = 0.01$, $\beta = 10$ dB and $(M, N) = (1, 0)$. 120
4.14 Outage probability of $\text{CSMA}_{\text{TXRX}}$ as a function of the sensing thresholds, for a fading network with $\lambda = 0.03$, $\beta = 0$ dB, and $(M, N) = (1, 0)$. 120
4.15 Outage probability of $\text{CSMA}_{\text{TXRX}}$ as a function of β_t and M, for a non-fading network with $\lambda = 0.1$, $\beta = \beta_r = 0$ dB, and $N = 0$. 121
4.16 Outage probability of $\text{CSMA}_{\text{TXRX}}$ as a function of the number of backoffs, M, for a non-fading network with $\lambda = 0.1$ and $N = 0$. 122
4.17 Outage probability of $\text{CSMA}_{\text{TXRX}}$ as a function of the number of retransmissions, N, for a non-fading network with $\lambda = 0.03$ and $M = 2$. 122

5.1 Outage probability of ALOHA and CSMA in a non-fading network with $\beta = 0$ dB and $K = 3$ subbands. 139
5.2 Outage probability of ALOHA and CSMA in a fading network with $\beta = 0$ dB, and $K = 3$ subbands. 140
5.3 Outage probability of ALOHA and CSMA in a non-fading network with $(M, N) = (2, 1)$, as a function of K. 141
5.4 Outage probability of ALOHA and CSMA in a fading network with $(M, N) = (2, 1)$, as a function of K. 142
5.5 Outage probability of CSMA with and without fading with sensing across all K subbands, for $\lambda = 0.01$ and $(M, N) = (2, 1)$. 143
5.6 Outage probability of ALOHA and CSMA with and without fading as a function of M, for $\lambda = 0.01$ and $(M, N) = (2, 1)$ . . 144

6.1 Illustration of a κ link MIMO network. 151
6.2 Illustration of a 2 link MIMO interference channel. 153
6.3 Ergodic link capacity, along with derived lower and upper bounds, of a 2 link MIMO channel, as a function of $\tau = N_t/N_r$ with $N_r = 8$. 157
6.4 Outage probability of a 2 link MIMO interference channel for $g_{12}/g = 0.5$ and $R_{req} = 3$, as a function of $\tau = N_t/N_r$. 158
6.5 Example of a star configuration where the distances between a given receiver and its interferers are equal. 160
6.6 Ergodic capacity of a $\kappa = 5$ link MISO interference channel as a function of N_t, both for different channel gain ratios. 163

6.7 Outage probability of a $\kappa = 5$ link MISO interference channel as a function of N_t, both for different channel gain ratios. 164
6.8 An example for the distribution of the capacity. 165
6.9 Derivative of the outage probability of a $\kappa = 2, 3, 4$ link MISO network to find ε_t. 166
6.10 Outage probability of a 2 link MISO interference channel as a function of N_t, both for $\varepsilon = \frac{\rho_I g_I}{\rho g}(2^{R_{req}} - 1) \leq 1$ and $\varepsilon > 1$. . . . 167
6.11 Outage probability of a 2 link MISO interference channel when $\varepsilon > 1$, with various techniques applied. 168
6.12 Outage probability of a $\kappa = 6$ link MISO interference channel with $g_I/g = 0.08$, where TDMA does not improve the performance. 170
6.13 Interference alignment of a 3 user interference channel [1]. . . 174
6.14 Simplified illustration of mapping the desired signal onto a subspace orthogonal to the interfering signal. 174
6.15 The sum rate of "maximizing SINR" interference alignment [2] of a network with 3, 4, 5, or 6 users, as a function of SNR. . . . 178
6.16 The sum rate of the "alternated minimization" interference alignment [3] of a network with 3, 4, 5, or 6 users, as a function of SNR. 178
6.17 The sum rate of the "sum rate optimization" interference alignment [4] of a network with 3, 4, 5, or 6 users, as a function of SNR. 179

Abbreviations

3G	3rd generation
3GPP	3rd generation partnership project
ACK	Acknowledge character
ARQ	Automatic repeat-request
ASE	Average spectral efficiency
AWGN	Additive white Gaussian noise
BER	Bit error rate
BPC	Binary power control
BS	Base station
BW	Bandwidth
cdf	Cumulative distribution function
CDMA	Code division multiple access
CSI	Channel state information
CSIR	CSI at the receiver
CSIT	CSI at the transmitter
CSMA	Carrier sensing multiple access
CSMA/CA	CSMA with collision avoidance
CSMA/CD	CSMA with collision detection
CTS	Clear to send
dB	Decibel

DS-CDMA	Direct sequence CDMA
FDMA	Frequency division multiple access
FH-CDMA	Frequence hopping CDMA
GPS	Global Positioning System
GSM	Global system for mobile communications
IC	Interference channel
IP	Internet protocol
iid	Independent and identically distributed
IEEE	Institute of Electrical and Electronics Engineers
LTE	Long term evolution
MAC	Medium access control
MANET	Mobile ad hoc netowrk
MMSE	Minimum mean square error
MIMO	Multiple input multiple output
MISO	Multiple input single output
NACK	Negative acknowledge character
OFDM	Orthogonal frequency division multiplexing
OFDMA	Orthogonal frequency division multiple access
OSI	Open system interconnect
pdf	Probability density function
QoS	Quality of service
PSK	Phase shift keying
RTS	Request to send
SIMO	Single input multiple output
SINR	Signal to interference plus noise ratio
SISO	Single input single output
SNR	Signal to noise ratio

TDMA	Time division multiple access
UMTS	Universal mobile telecommunications system
WiMAX	Worldwide interoperability for microwave access
w.l.o.g.	Without loss of generality

Nomenclature

α	Path loss exponent
β	Sensing threshold for determining correct reception of packets
β_b	Sensing threshold for backoff decision making of CSMA
β_r	Sensing threshold for the receiver in $\text{CSMA}_{\text{TXRX}}$
β_t	Sensing threshold for the transmitter in $\text{CSMA}_{\text{TXRX}}$
b	Average transmission rate per successful packet
$\mathbb{C}$	Set of complex numbers
$\mathbf{C}_i$	Covariance matrix of the received interference plus noise of user i
$\mathcal{C}_{erg}$	Ergodic channel capacity
$\mathcal{C}_i$	Instantaneous channel capacity of user i
$\mathcal{C}_\infty$	Deterministic channel capacity when the number of antennas goes to infinity
$\mathcal{C}_\Sigma^\kappa$	Sum capacity of a network with κ links
$\mathcal{D}$	2-D square network deployment region
$\Delta(M, N)$	Increase in the density of packet arrivals due to M backoffs and N retransmissions
ΔP_{out}	Change in outage probability
ϵ	Outage probability constraint imposed by application
ε	Constant determining the optimal number of antennas to apply in MISO channels

ε_t	Optimal value of ε used as threshold on the system parameters
ε_{tdma}	Auxiliary constant in deriving the outage probability of TDMA
η	Noise power
$\mathbb{E}_x$	Expected value with respect to random variable x
ϕ	Auxiliary variable for integration of angles
$F_X(x)$	Cumulative distribution function of random variable X
$f_X(x)$	Probability distribution function of random variable X
$\mathbf{G}_{ij}$	Channel gains from multi-antenna transmitter j to multi-antenna receiver i
g_{ij}	Variance of the elements of channel matrix $\mathbf{G}_{ij}$
γ	Angular integration limit for derivation of outage probability of CSMA
h_{ij}	Channel fading coefficient from transmitter j to receiver i
$\mathbf{H}_{ij}$	Channel gains from multi-antenna transmitter j to multi-antenna receiver i with unit variance
κ	Number of transmitter-receiver pairs in the network
K	Number of subbands the system bandwidth is divided into
λ	Spatial density of new packet arrivals [packets/m^2]
λ^s	Spatial density of transmitter nodes [nodes/m^2]
λ^t	Temporal density of packet arrivals at each transmitter node [packets/sec/node]
L	Length of the side of a square communication region
M	Number of backoffs per packet using CSMA
max	Maximum value
min	Minimum value
ν	Angular integration limit for derivation of outage probability of CSMA

N	Number of retransmissions per packet
N_r	Number of receive antennas at a multi-antenna receiver
N_t	Number of transmit antennas at a multi-antenna transmitter
P_{during}	Probability that error occurs in the middle of an active transmission
P_{out}	Outage probability
P_{rx}	Probability that a packet is in error at its receiver at the start of a retransmission
$P_{rx\|transmit}$	Probability that a packet is in error at the receiver at the start of its first transmission
$\Pr(a)$	Probability of event a
ρ	Constant transmit power
ρ_i	Transmit power of user i
$r_{1,i}, r_{i,2}$	Integration limits for radius r inside $\mathcal{D}$, given by a table
$\mathcal{R}$	Network deployment region
R	Distance between a transmitter and its own receiver
R_{req}	Required rate of transmission for correct packet reception
$R_{req,b}$	Required rate of transmission for backoff decision making of CSMA
RX_i	Receiver of packet i
$\mathcal{S}$	Network throughput
s	Radius of sensing zone for correct reception of packets
s_b	Radius of sensing zone for backoff decision making (either by receiver or transmitter)
s_r	Radius of sensing zone for backoff decision making of the receiver in $\mathrm{CSMA}_{\mathrm{TXRX}}$
s_t	Radius of sensing zone for backoff decision making of the transmitter in $\mathrm{CSMA}_{\mathrm{TXRX}}$
σ	Standard deviation of a random variable

SINR_i	SINR of node i
$\theta(r, x, y)$	Angular portion of a circle of radius r centered at (x, y) inside region $\mathcal{D}$
τ	Ratio of number of transmit antennas over receive antennas, N_t / N_r
T	Length of packets in time [sec]
TX_i	Transmitter of packet i
W	Total system bandwidth
$\mathcal{W}_0(x)$	Lambert function with parameter x
$\mathbf{x}^\dagger$	Conjugate transpose of vector $\mathbf{x}$
$\mathbf{x}_i$	Transmitted signal vector of multi-antenna transmitter i
x^{opt}	Optimal value of variable x
ζ	Mean value of a Rayleigh distributed random variable, $\frac{1}{\zeta} = \mathbb{E}[h_{ij}]$

Chapter 1

Introduction

Wireless communications is a well-established and expanding technology that has been embraced in most homes and work places, and is omnipresent in our everyday lives. High speed Internet connections allow for real-time interaction through video and audio on a global level. Wireless communication takes this one step further by moving the Internet out of the home and with you wherever you go. Being incorporated into communication devices such as cell phones, laptops, and Global Positioning Systems (GPS), wireless communications has become an indispensable part of life. That is, consumers desire seamless, high quality connectivity at all times and from virtually all locations. There has also been significant interest lately for all businesses to set up mobile computing workplaces for their employees and also mobile computing for other functions of the business from distributors, suppliers, and service providers. Wireless is being adopted for many new applications such as to connect computers, to allow remote monitoring and data acquisition, to enable control and security, and to provide a solution for environments where wires may not be the best implementation.

Due to such great interest and widespread adoption of wireless, the deployment and need for high quality wireless technologies is ever increasing. Despite the immense progress made in resolving constraints in rate and quality of wireless networks, much still remains to be done. Ultimately, there is a desire to replicate, and if possible, even surpass, the wired experience in a wireless fashion. With these visions in mind, the objective of this thesis is to establish a deeper understanding of network qualities and to improve the performance of wireless networks. The remainder of this chapter provides the motivation for our work and the necessary background material on the topics to be touched upon in the following chapters, as well as

outlining the specific contributions of this thesis.

1.1 Background and Motivation

Within the domain of wireless communications, *ad hoc networks* have received great interest due to their dynamic nature and their vast range of applications. A wireless ad hoc network consists of point-to-point[1] links distributed randomly in space, carrying out packet transmissions without a centralized control. These networks have the advantage of avoiding the cost, installation, and maintenance of network infrastructures, as well as having the ability to be rapidly formed from whatever nodes available. They can be deployed and reconfigured based on the requirements of the applications, while exhibiting great robustness, due to their distributed nature, node redundancy, and lack of single points of failure. Such networks, in particular mobile ad hoc networks (MANETs), can be observed in many of today's wireless applications, such as military battlefields, emergency operations, and environmental detection and surveillance.

Despite the great advantages brought about by ad hoc networks, their inherently flexible nature also brings about many design challenges. In particular, since the number and the positions of links in ad hoc networks are random and unknown, *interference* becomes one of the main issues to counteract in the design of such networks. Interference denotes the undesired received electromagnetic signals transmitted by devices in the vicinity of a receiver but intended for other receivers. If not managed properly, interference can be disruptive to the desired operation of the network. Such disruptions are readily exemplified by the poor performance of current Wi-Fi access points in dense housing complexes or convention centers. With the greater number of wireless enabled devices and sensors, the density of future networks will increase, and interference will become a fundamental hindrance to the operation of wireless networks, unless some measures are taken to counteract its negative effects.

Many techniques have been proposed to mitigate the destructive impact of interference, while efficiently allocating the scarce resources of the network [3; 5–9]. One popular way to approach such problems is through Medium Access Control (MAC) layer design. The quality-of-service (QoS) of networks is critically dependent on the MAC protocol used for communication between the nodes. The challenge of designing an ad hoc network

[1] With "point-to-point" we mean that each message is communicated between a single sender and a single destination, allowing for simultaneous communication between transmitter-receiver pairs.

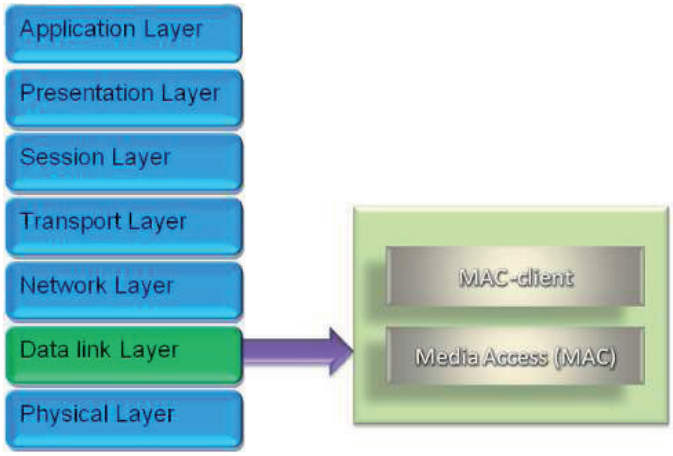

Figure 1.1: The 7-layer OSI model.

then becomes to decide which MAC protocol to apply in order to get the best performance, what evaluation metric and system parameters to apply and optimize, and how to employ external measures (such as bandwidth partitioning, interference cancellation, feedback channels, or multiple antennas) in order to improve the system performance. In the following, general descriptions and background information are provided on the specific domains that set the basis of this thesis.

1.1.1 Medium Access Control (MAC) Protocols

In most data applications, data packets are generated at random time instances and the system typically has more users than can be accommodated simultaneously. This is where *random access* strategies come into the picture, making sure that the channel and other resources in the network are shared in an efficient manner between the active users. Random access techniques are based on the premise of packetized data, and the resulting schemes are usually termed *packet radios*. Using a shared transmission medium in random access channels introduces many design challenges, which may be collectively addressed through the Data Layer of the 7-layered Open System Interface (OSI) model, as shown in Figure 1.1. By means of medium access control (MAC) techniques and MAC clients, algorithms can be performed locally at each node to obtain an efficient access to and a fair share of the communication resources, such as radio frequency, bandwidth, or time slots.

Random access techniques were pioneered by Norman Abrahamson with the *ALOHA* MAC protocol in 1970 [10]. In ALOHA, data is packetized at the transmitter, which initiates its packet transmissions whenever there is data to be sent. That is, packets are transmitted regardless of the channel conditions. In *unslotted ALOHA* (also termed pure ALOHA), transmissions are initiated immediately upon the packet formation. This property allows for partial overlap of packets, something that makes unslotted ALOHA an inefficient protocol. In order to improve the performance of unslotted ALOHA, a slotted version of it was introduced [10], in which time is divided into slots, and a packet transmission can only be initiated at the start of the next time slot after it has been formed. This significantly improves the performance of the network in terms of correct packet reception. However, slotted ALOHA requires a system with synchronization abilities, something that is costly, complex, and in some scenarios even impossible to achieve.

In order to improve the performance of ALOHA further, various modifications were introduced, including carrier sensing [5; 11; 12], collision avoidance [13; 14], and collision detection [5; 12]. These extensions are all under-categories of the *carrier sensing multiple access (CSMA)* protocol. In CSMA, which was proposed by Kleinrock and Tobagi in 1975 [5], the transmitters sense the channel around them and delay their packet transmissions if they sense the channel to be busy, i.e., if they expect their transmission not to be successful. The transmitter then waits a random time before a new channel sensing is performed. Such delay in the transmission is called *random backoff*. CSMA only works when each transmitter can sense the signal transmission of all other transmitters and when the propagation delay is small. These assumptions are reasonable in networks that are not too large, i.e. in LANs, MANs, and in cases where the transmission time of each packet is relatively small compared to the length of the packet.

There are a few problems inherent to the CSMA protocol, namely the *hidden* and *exposed terminal problems*. The hidden node problem occurs when the node making the backoff decision does not hear an ongoing transmission, while the exposed node problem denotes the occurrence of a backoff when that packet transmission would in fact not have caused error for other transmissions. To better understand these problems, consider Figure 1.2 where each node can only hear its neighboring nodes, as is represented by the lines connecting the terminals. In this setting, a packet transmission is considered unsuccessful if there are more than one packet at a receiving node, i.e., if there is a collision of signals. Now referring to the setup of Figure 1.2 for the hidden terminal problem, say both node 1 and 5 wish to send data to node 3. Since node 5 cannot sense node 1, and vice versa, both

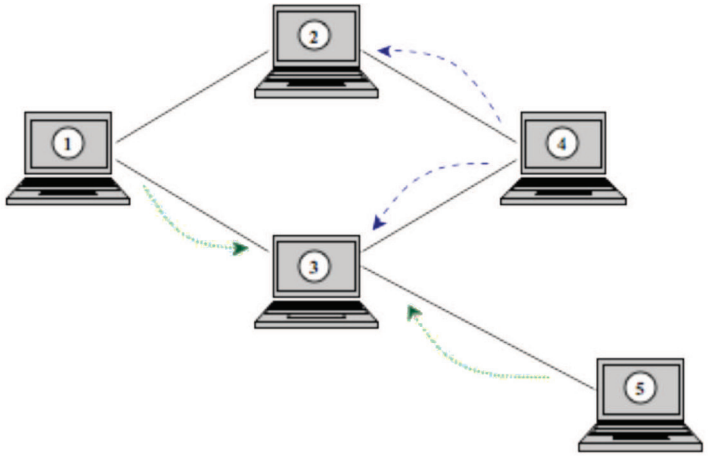

Figure 1.2: Setup to illustrate the hidden and exposed node problems of CSMA.

nodes will transmit their packets simultaneously, and node 3 will thus receive a collision of signals. For the exposed terminal problem, imagine that node 3 wishes to send a packet to node 5, at the same time as node 4 is sending a packet to node 2. When node 3 senses its channel, it detects node 4's transmission and assumes the channel is busy. Node 3 will hence back off, although no collisions would have occurred. Note that a "collision" in the context of point-to-point communication (as is the case in the work of this thesis) is characterized differently; it is defined as when the aggregation of interfering signal powers exceeds a predefined threshold.

The hidden and exposed terminal problems of CSMA result in inefficiencies in the channel utilization. Hence, to overcome the negative impact of these problems, several modifications to the CSMA protocol are proposed, most of which were introduced by Kleirock and Tobagi more than 30 years ago [5]. We provide a brief description of the main CSMA flavors.

- **Non-persistent, 1-persistent, and p-persistent CSMA**: In non-persistent CSMA, if the medium is idle, packet transmissions are initiated immediately. Otherwise, the transmitter waits a random amount of time before transmitting again. In 1-persistent CSMA, when the medium is busy, the transmitter continues to listen until the medium becomes idle, and then transmits immediately. This reduces the waste of idle time, but results in a collision if two nodes want to retransmit at the same time. In the p-persistent CSMA pro-

tocol, when the medium is idle, data is transmitted with probability p, and delayed with probability $(1 - p)$. If the medium is busy, the transmitter continues to listen until the medium becomes idle. The p-persistent CSMA thus balances between the trade-offs of the non-persistent and the 1-persistent CSMA. In short, the different degrees of persistence indicate how long a backoff should last before the packet is retransmitted.

- **CSMA with Collision Detection (CSMA/CD)**: In this version of CSMA, the channel is under frequent sensing during a packet transmission. If the channel becomes busy (meaning that the amount of interference detected surpasses a specified threshold) throughout a packet duration, the transmitter stops its packet transmission and waits a random backoff time before trying to retransmit its packet. This simple modification increases the probability of successfully delivering the packet to its receiver on retry.

- **CSMA with Collision Avoidance (CSMA/CA)**: In this version of CSMA, handshaking[2] is introduced. The handshaking comprises of a *request-to-send (RTS)* packet and a *clear-to-send (CTS)* packet prior to each transmission. The node that wishes to send a packet first sends an RTS packet. If the potential receiver perceives the channel to be idle, it will respond with a CTS signal, which authorizes the initiating node to transmit its data packet. All other nodes that overhear the RTS and CTS packets, will know which transmitter and receiver pair are communicating, and will thus refrain from sending information if their transmission is expected to collide with the ongoing transmission.

1.1.2 Ad Hoc Network Characteristics

Perhaps the main characteristic of ad hoc networks, in particular MANETs, is the fact that nodes can be efficiently repositioned and moved. Rapid deployment of wireless communications in areas with no infrastructure often implies that the users must explore and sense their surroundings, communicate based on the sensed conditions, and if necessary form teams that in turn coordinate among themselves to create a taskforce or a mission [15]. The choice of the *mobility* model, such as individual random mobility, group mobility, and motion along preplanned routes, has a major

[2]Handshaking refers to some kind of agreement between the transmitter and receiver in order to avoid collisions.

impact on the selection of a routing scheme and can thus strongly affect the network performance. E.g., assuming a highly individually mobile network, reduces the temporal and spatial correlations between transmission attempts, but also complicates the estimation of the channel conditions.

One of the main attributes of ad hoc networks is *scalability*. This is the ability of a network to maintain good performance under growing amounts of traffic, by using additional resources [16]. In applications where the ad hoc network can grow to several thousand nodes (such as sensor networks or emergency operations), it is useful to allow for scalability. For wireless "infrastructure" networks, scalability is handled by a hierarchical construction, where mobile IP or local handoff techniques may be used to overcome the problem of limited mobility. The main motivation behind the design for scalability is reduced cost and effort.

The distribution of interferers and the channel characteristics are also of great importance for the behavior of ad hoc networks. These factors impacts the interference power detected and thus the average network performance. In most wireless networks, there is the phenomenon of *fading*, which denotes rapid variations of received signal power due to constructive and destructive addition of the signal's multipath components. This is an additional factor to the distance-dependent path loss, and usually results in significant deviation from the expected value of interference obtained from a large-scale path loss model. The introduction of fading often results in degradation of the average performance of networks and complicates the estimation of the interference powers.

Furthermore, the topology of the communication domain plays a significant role on the system performance. This is due to the fact that the amount of interference is proportional to the number of users detected in the vicinity of a transmission, which is again dependent on the size and shape of the deployment region. That is, whether a network is bounded in size or grows indefinitely must be taken into account in the analysis. Although many networks are often modeled as infinite planes, we will show that *edge effects* in small bounded networks play a great role in the network performance.

Finally, we note that besides the network geometry, the traffic patterns and the path a packet takes from a sender to its receiver also affects the system performance. A common example of this is seen in single-hop communication versus multi-hop (or relay) networks. A multihop network is a network where the path from source to destination traverses several other nodes. Ad hoc networks often use multiple hops for obstacle negotiation, spectrum reuse, and energy conservation [6]. The communication between the two nodes in every hop uses the same concepts of single-hop wireless

signal transmissions, with a given routing protocol at the basis of the communication.

In this thesis (mainly in Chapter 3), we will touch upon most of the network characteristics mentioned above, and investigate their impact on the performance of wireless ad hoc networks.

1.1.3 Performance Evaluation Metrics

The performance of wireless networks can be evaluated based on various metrics, such as transmission capacity, ergodic capacity, outage probability, throughput, sum rate, and transmission delay. The metric selected reflects the Quality of Service (QoS) requirements and the application constraints of the network. In this thesis, our focus is on outage probability and ergodic capacity for our performance evaluation, but we will also touch upon the other metrics from time to time. Hence, we provide a brief overview of all the above-mentioned metrics.

Capacity denotes the amount of information traversing a network. This notion is not concerned with how many packets that are actually received correctly; it merely indicates the potential of the channel to transfer information. The relationship between the capacity of an additive white Gaussian noise (AWGN) channel and the stochastic SINR measure is given by the Shannon capacity formula [17]: $\mathcal{C} = W \log(1 + \mathrm{SINR})$, where W is the system bandwidth. In ergodic channels[3], there is the concept of *ergodic capacity*, which is defined as the average capacity of the network. The averaging is often performed over time, or equivalently, over many channel instances. That is,

$$\mathcal{C}_{erg} \;=\; W\, \mathbb{E}\big[\log(1+\mathrm{SINR})\big], \tag{1.1}$$

where $\mathbb{E}$ denotes the expectation operator, which is taken over the sources of randomness in the SINR expression. These could be fading coefficients or distance to interferers. In many applications, the overall performance of the network is more important than that of individual users. In this case, a common metric is *sum rate*, which is the sum of the capacity or ergodic capacity of all active users in the network. In some scenarios, it might be beneficial in terms of sum capacity to give some users the full channel access, while others have limited or no access. This metric is used specifically in Chapter 6.

[3] An ergodic channel denotes a channel where the time average is equal to the ensemble average.

Outage probability is a key concept in wireless communications. It is defined as the probability that a received signal, often given in terms of signal over interference plus noise ratio (SINR), falls below the predefined threshold required for a receiver to successfully decode its packet. An alternative way to define outage probability is to consider the rate of communications; if the required transmission rate is higher than the channel capacity, $\mathcal{C}$, data will be lost in the channel and packets will be received in outage. Mathematically, and in a simplified manner (i.e., assuming no specific protocol and allowing for no retransmissions), outage probability is defined as follows:

$$P_{out} \;=\; \Pr\left(\text{SINR} \leq \beta\right) \;=\; \Pr\left[\mathcal{C} \leq R_{req}\right], \tag{1.2}$$

where β is defined as the SINR threshold required for correct packet reception, and R_{req} is the requested rate of transmissions. In most applications, the QoS requirement is often specified as an outage probability constraint. This is the case for networks where the main concern is correct reception of packets. The outage probability in wireless ad hoc networks depends on various factors: the node distribution, the applied MAC scheme, the network topology, and the models used for the path loss attenuation and fading effects. These factors will be considered in the following chapters.

Throughput is defined as the amount of information that is actually delivered correctly to a destination. In the conventional sense, throughput of a randomized MAC in a Poisson distributed network is given as $\mathcal{S}_{Poisson} = Ge^{-\xi G}$ [10], where G denotes the intensity of attempted transmissions per time slot (this may be given as the density of transmissions times the rate or each transmission), and $e^{-\xi G}$ is the success probability. In a more general manner (i.e., for any distribution of nodes), throughput can be defined as

$$\mathcal{S} \;=\; \lambda \, \frac{R_{req}}{W} \left(1 - P_{out}\right), \tag{1.3}$$

where λ is the spatial density of packet arrivals, R_{req}/W [bits/s/Hz per packet] is the average rate that a successful packet achieves, normalized with respect to the bandwidth W, and P_{out} is the outage probability. Throughput has units [bits/s/Hz/m^2].

Transmission capacity is closely related to the notion of throughput. It was proposed in [18] due to the fact that the throughput metric often obscures the fact that high throughput is sometimes obtained at the expense of unacceptably high outages. As a simple example, consider the classic slotted ALOHA protocol with throughput of the form Ge^{-G}. This throughput is maximized for an attempt rate of $G = 1$, which corresponds to an

optimal throughput of $1/e \approx 0.32\%$, corresponding to an outage probability of $1 - 1/e \approx 0.68$. A 68% outage probability is unacceptable for many common network applications, such as streaming media. Such "wasting" of transmissions also indicates the existence of unnecessary interference for other nodes, as well as the waste of precious energy. Hence, transmission capacity considers the achievable rates from an outage perspective. It is given as

$$\mathcal{S}(\epsilon) \;=\; \lambda_\epsilon \, \frac{R_{req}}{W} \, (1 - \epsilon), \tag{1.4}$$

where λ_ϵ is the maximum spatial density of attempted transmissions with an outage probability constraint ϵ. Also note that transmission capacity is a modified version of the ubiquitous *transport capacity* metric, introduced by Gupta and Kumar in [19] and extended to random channels in [20]. The main distinction is that transmission capacity allows for a stochastic outage probability requirement.

Transmission delay is often a main concern in many networks, such as real-time voice and video communication systems. Often reducing delay results in an increase in the outage probability, and equivalently, a reduction in the throughput. Hence, the application that the ad hoc network is tailored for often specifies a delay constraint. As the main concern of this thesis is correct reception of packets, we will not impose such a constraint, but will evaluate the amount of delay our network design entails.

Note that many other metrics than the aforementioned ones can be applied for the performance evaluation of wireless networks. Some of these are power consumption, spectral efficiency, bandwidth usage, etc. The metrics discussed above are simply some of the most common measures used to evaluate the average performance of ad hoc networks, and are therefore also employed in this thesis.

1.1.4 Multiple Antenna Systems

All our discussions thus far have assumed single antenna systems, i.e., single input single output (SISO) channels. The application of multiple antennas have assumed great popularity because of their ability to reach remarkably higher transmission rates and better signal qualities compared to SISO systems [12; 1; 21]. Multiple antennas can be applied at both transmitters and receivers, or either of them, as shown in Figure 1.3. Multiple input multiple output (MIMO) denotes systems where multiple antennas are used at both the transmitter and receiver; single input multiple output (SIMO) refers to systems where only the receiver has multiple antennas;

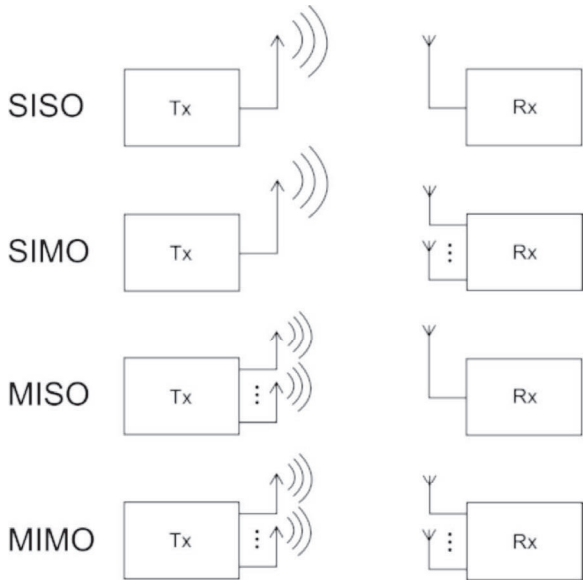

Figure 1.3: Illustration of SISO, SIMO, MISO, and MIMO channels.

and finally, in multiple input single output (MISO) channels, multiple antennas are applied at the transmitter only.

MIMO point-to-point *interference channels* have come in focus only in recent years, with prominent works such as [1; 3; 8; 22; 23]. An interference channel is a model for studying networks with two or more source-destination pairs and where the source signals interfere with each other at the receivers. One of the main qualities of an interference channel is the fact that a change in some system parameters not only affects the performance of the link under observation, but also the impact of this link on the rest of the network. This complicates the prediction of how nodes in an uncoordinated network will perform and thus the performance of a link. Understanding the behavior of MIMO interference channels is of great importance in today's communication networks, as there is an increasing demand for enabling simultaneous transmissions between independent multi-antenna transmitter-receiver pairs.

Many various MIMO techniques have been proposed to achieve an efficient use of the antennas. These can be sub-divided into three main categories [24], as listed below.

- **Precoding**: In general terms, precoding denotes all spatial processing that occurs at the transmitter. From an antenna design perspec-

tive, one common type of precoding is beamforming, which is the act of emitting the same or different signals from each of the transmit antennas with appropriate phase and gain weighting such that the signal power is maximized at the receiver side. The benefit of beamforming is the ability to increase the signal gain from constructive interference and to reduce the degradation from multipath fading effects and interfering signals. Precoding requires knowledge of the channel state information (CSI) at the transmitter. Precoding/beamforming techniques were first published by J. Winters and J. Salz at Bell Laboratories [25].

- **Spatial multiplexing**: In this technique, a high rate signal is split into multiple lower rate streams and each stream is transmitted from a different transmit antenna in the same frequency channel. If these signals arrive at the receiver antenna array with sufficiently different spatial signatures, the receiver can separate these streams, creating parallel channels. Spatial multiplexing is a powerful technique for increasing channel capacity at high signal-to-noise ratio (SNR) values. The maximum number of spatial streams is limited by the lesser of the number of antennas at the transmitter or receiver. This method can be used with or without transmit channel knowledge. It can also be combined with precoding when the channel is known at the transmitter. Spatial multiplexing was proposed and patented by A. Paulraj and T. Kailath in 1993 [7].

- **Diversity coding**: This technique is used, in particular, when there is no channel knowledge at the transmitter. In diversity methods, a single stream (unlike multiple streams in spatial multiplexing) is coded using techniques called *space-time coding* and emitted from each of the transmit antennas. Diversity coding exploits the independent fading in the multiple antenna links to enhance signal quality. Because there is no channel knowledge, there is no beamforming or array gain. Diversity coding can be combined with spatial multiplexing when decoding reliability is in trade-off, as was established by L. Zheng and D. Tse in 2003 [26].

The IEEE 802.16e standard [27] incorporates MIMO (in combination with orthogonal frequency division multiple access (OFDMA)). Furthermore, MIMO is planned to be used in mobile radio telephone standards such as the 3GPP (including the long term evolution (LTE) standard) and 3GPP2 standards [28].

Finally, we give a brief introduction to the newly proposed scheme of

interference alignment [1; 2; 8]. In this approach, interference coming from several nodes in the network is steered to superpose into a subspace of the received signal space at each receiver. The remaining dimensions are free from interference, thus providing notable improvement in the quality and sum rate of the network. This scheme will be discussed in more details in Chapter 6.

1.2 Overview of Contributions

Having established the motivation behind our work, along with the necessary background material, we now describe the specific contributions of this thesis. Specifically, we address the following questions:

- How do point-to-point ad hoc networks using various MAC protocols behave in terms of outage probability as a function of various network parameters?
- What network characteristics are essential for the behavior of MAC protocols, and how do these impact the outage performance of ad hoc networks?
- Can the performance of CSMA be improved by optimization of the sensing threshold, or by allowing for cooperation between transmitters and receivers?
- From a MAC layer perspective, can the outage probability of ad hoc networks be reduced by introducing bandwidth partitioning?
- With the introduction of cross-layer design, how does the application of multiple antennas in interference channels impact their performance, and in what way should the antennas be applied in order to improve the performance of ad hoc networks?

Answers to the above questions are given in the following chapters in the same order as listed above. In Chapter 2, we analyze the system performance of the ALOHA and CSMA MAC protocols as a function of the density of nodes, rate of packet arrivals, transmission power, communication range, required SINR threshold, and number of backoff and retransmission attempts. A precise analytical framework is established, where we assume an infinite network, with AWGN channels and only path-loss attenuation effects. Expressions for the outage probability of the ALOHA

and CSMA protocols (in their various incarnations) are derived, and their performances are compared.

In Chapter 3, we investigate different channel models, and derive new outage probability expressions for our MAC protocols. The various model characteristics investigated are: the addition of fading to the path loss model, bounding of the communication domain and considering the impact of edge effects, and allowing for fading in bounded networks. The obtained results are compared to those of Chapter 2, and the significance of correct modeling of the communication system is underlined.

Having analyzed the performance of the ALOHA and CSMA protocols within different network settings, we then take a step further in Chapters 4 and 5 to *improve* the outage probability performance of these protocols. MAC layer techniques such as threshold optimization, improved decision making abilities by means of feedback channels, and bandwidth partitioning are investigated. For all the proposed schemes, the outage probability is derived as a function of the additional parameters introduced by the various techniques, and optimization is performed.

Next, in Chapter 6, we attempt to improve the performance of ad hoc networks through multiple antenna design. This paves the way for cross-layer design between the PHY and MAC layers. We first establish an understanding for the behavior of MIMO and MISO interference channels in terms of outage probability and ergodic capacity, when no CSI is available at the transmitters. Moreover, we investigate the optimal number and usage of antennas. When CSI is available at the transmitters (CSIT), we briefly touch upon interference alignment techniques and propose a distributed power control algorithm that can improve the performance of interference alignment in certain operation regimes.

Finally, in Chapter 7, we finalize this thesis by summarizing the conclusions of our work, and we propose possible extensions to the various topics covered in this thesis. Note that the related work done within each of the above-mentioned topics will be discussed in their corresponding chapters.

1.2.1 Works Not Included in This Thesis

In addition to the publications that this thesis is based on, the author has participated in the writing of some other papers, as mentioned briefly in the following.

- P. H. J. Nardelli, M. Kaynia, P. Cardieri, and M. Latva-aho, "Optimal transmission capacity of ad hoc networks with packet retransmissions", to be submitted to *IEEE Trans. on Communications*, Sept.

2010.

In this paper, we address the optimal transmission capacity of wireless networks, where each packet is given an arbitrary number of transmissions. For this study, four different medium access protocols are considered, namely slotted and unslotted ALOHA, CSMA with transmitter sensing, and CSMA with receiver sensing. For each of these schemes, the number of allowed retransmissions that optimizes the transmission capacity is derived as a function of the transmission density and the outage constraint. Moreover, the behavior of the transmission capacity of the various protocols are compared and evaluated with respect to various system parameters.

- M. Kaynia, P. H. J. Nardelli, P. Cardieri, and M. Latva-aho, "On the optimal design of MAC protocols in multi-hop ad hoc networks", in *Proc. IEEE International Symposium of Modeling and Optimization in Mobile, Ad Hoc, and Wireless Networks (WiOpt)*, pp. 424-429, June 2010.

  We consider the performance of MAC protocols in multi-hop wireless ad hoc networks in terms of the newly proposed metric "aggregate multi-hop information efficiency". This metric captures the impact of the traffic conditions, the quality of service requirements for rate and correct packet reception, the number of hops and distance between a sender and its destination, and the outage probability for packet transmissions. Our network model resembles that of Chapter 2, with the difference that each packet traverses multiple hops to get to its destination. Approximate expressions are derived for the outage probability of the ALOHA and CSMA MAC protocols, and validated with Monte Carlo simulations. Moreover, an analytical procedure is presented to optimally design the communication so the multi-hop information efficiency performance of the network can be maximized.

- P. H. J. Nardelli, M. Kaynia, and M. Latva-aho, "Efficiency of the ALOHA protocol in multi-hop networks", in *Proc. IEEE International Workshop on Signal Processing Advances for Wireless Communications (SPAWC)*, Marrakech, Morocco, June 2010.

  This paper presents the evaluation of the "multi-hop aggregate information efficiency" of the slotted and unslotted ALOHA protocols.

Closed-form lower bounds are derived on the outage probability as a function of the required communication rate, the single-hop distance, the number of hops and the maximum number of retransmissions. Moreover, we show that it is possible to optimize the network efficiency by properly setting the required rate for a given packet density. It is also established that in some scenarios, the use of retransmissions and multiple hops degrades the performance of single-hop links without retransmissions.

- M. Kaynia, P. H. J. Nardelli, and M. Latva-aho, "Evaluating the information efficiency of multi-hop networks with carrier sensing capability", submitted to *IEEE International Conference on Communications (ICC)*, Kyoto, Japan, June 2011.

  We consider the performance of the CSMA MAC protocol in multi-hop ad hoc networks in terms of "aggregate multi-hop information efficiency". Approximate analytical expressions are derived for the outage probability of CSMA in its various incarnations, considering different values for the sensing threshold (related to the backoff decision) and the required communication threshold (which determines a correct packet reception). Our results indicate the existence of optimal operating points for the transmission density, the communication rate, the maximum number of permitted backoffs, and the number of hops in order to achieve maximum efficiency.

- J. E. Corneliussen, M. Kaynia, and G. E. Øien, "Optimal tradeoff between transmission rate and packet duration in wireless ad hoc networks", in *Proc. IEEE Wireless Communications and Networking Conference (WCNC)*, pp. 1-6, April 2010.

  This paper considers the tradeoff between bursty and continuous transmissions in wireless ad hoc networks. Packets belonging to specific transmitters arrive randomly in space and time according to a 3-D Poisson point process, and are then transmitted to their intended destinations using a fully-distributed MAC protocol (ALOHA or CSMA). The objective of this work is to maximize the probability of successful transmissions by optimizing the transmission rate and duration of packets. Based on derived outage probability expressions, the optimal spectral efficiency and packet duration of ALOHA is found analytically, and that of CSMA is obtained through simulations. CSMA is shown to yield the best performance both

in terms of the minimum achievable outage probability and the corresponding spectral efficiency.

- C.-S. Chen, M. Kaynia, G. E. Øien, and A. Gjendemsjø, "Cooperative multi-cell power control under imperfect channel knowledge: A comparative study", in *Proc. 2nd COST 2100 Workshop on MIMO and Cooperative Communications*, Trondheim, Norway, June 2008.

  Radio resource management is important in enhancing spectrum utilization efficiency in broadband wireless services. Multi-cell binary power control (BPC) in full-reuse networks is a promising candidate in system optimization for this purpose. While the BPC scheme is inherently simple, the sum rate maximization by cooperative BPC across cells/links is almost as good as the best achievable non-binary solution. For practical use, the issue of imperfect channel knowledge should also be considered for these schemes. In this paper, we conduct an investigation of the performance of BPC and compare it to the best known non-binary optimization, as well as to full-power transmission. Performance under two different link gain measurement error models is reported. When measurement errors occur, BPC achieves a better and more robust performance than an optimized non-binary power allocation. The simple full power scheme is seen to be severely suboptimal when perfect channel state knowledge or moderate channel state error levels are considered, but it can actually outperform BPC and also GP-based optimization in some scenarios with severely erroneous channel knowledge.

Chapter 2

Performance Analysis

In this chapter, we consider a mobile wireless ad hoc network model in which nodes are randomly distributed in space and packets arrive randomly in time, and we address the problem of interference through MAC layer design. The ALOHA and CSMA MAC protocols are employed for communication, and the outage probability of packet transmissions is investigated. In particular, we ask the following questions: (a) Given a fixed signal to interference plus noise ratio (SINR) threshold for each transmitter-receiver link in the network, what is the probability of successful transmission for ALOHA and CSMA, (b) how do the various MAC protocols behave with respect to the density of transmissions, transmitter-receiver distance, and other network parameters, and (c) what is the impact of multiple backoffs and retransmissions on the outage probability of the MAC protocols?

There has been a notable amount of research done on the performance of ALOHA in wireless ad hoc networks. A number of researchers have analyzed slotted ALOHA using a Poisson model for transmitter locations, considering transmission capacity and success probability of the network [35; 18; 36; 37]. Ferrari and Tonguz [38] have analyzed the transport capacity of slotted ALOHA and CSMA, showing that for low transmission densities, this capacity of slotted ALOHA is almost twice that of CSMA. However, for increasing densities, while the capacity of ALOHA drops to zero, the capacity of CSMA increases, making CSMA more beneficial at higher transmission densities. Other related works have evaluated the performance of ALOHA and CSMA in terms of throughput and bit error rate [19; 38; 39]. Some of these also assert CSMA's superiority over ALOHA, which is naturally followed by tradeoffs in other domains such as transmission rate and delay [5; 39]. Some recent works have also considered the

performance of ALOHA, showing that the scaling of transport capacity depends on the amount of attenuation in the channel [19]. It is shown that in the low-attenuation regime, the capacity of the network can be unbounded, while in the high-attenuation regime, the capacity is bounded by the total available power and thus scales as a function of the number of nodes in the network.

The seminal paper of Gupta and Kumar [19] considers an ad hoc network model that consists of Poisson distributed point-to-point transmissions. This model resembles a slotted version of our model. However, their analysis, as well as most of the other works done in this area, focuses on a deterministic SINR model, and employs a deterministic channel access scheme, thereby precluding the occurrence of outages. Weber et al. [18] revise this model by considering a stochastic SINR-based model, within which they find tight lower and upper bounds to the outage probability of slotted ALOHA as a function of the node density. We consider the model used in [18], and extend it to also cover unslotted systems. Other spatial models considered for analyzing the performance of MAC protocols can be found in [40–42]. In [40], the outage probability of the ALOHA protocol with arbitrary number of retransmissions is derived. However, the model used in this paper does not appear to be straight-forward to extend to cover CSMA-like protocols. In [41], the throughput and fairness of CSMA/CA is evaluated based on a Markovian analysis. In [42], an analytical framework is introduced to evaluate the per-flow throughput of CSMA in a multi-hop environment. However, in the two latter works, a single communication link is considered; thus, the complexity of link performances and decisions being dependent on each other, as is the case in *interference channels*, is ignored. In contrast, this is considered in our model.

Despite all the research done on MAC protocols thus far, only a limited number of works have considered a model that is both stochastic, continuous in time, and allows for simultaneous communication between nodes [18; 35; 36; 38]. Perhaps the closest work is that of Hasan and Andrews [36], where the success probability of slotted ALOHA is analyzed within such a stochastic ad hoc wireless network model. *Success probability* is defined as the probability that a transmission is received successfully at the receiver, i.e., that the measured SINR is above a certain threshold, β, for the duration of the packet. This is equal to $1 - P_{out}$, where P_{out} denotes the outage probability. In their work, Hasan and Andrews assume the use of a scheduling mechanism that creates an interferer-free *guard zone*, which is in effect a theoretical circle around the receiver, within which no interfering transmitters are allowed. By means of geometrical analysis, an optimal guard zone radius is derived that maximizes the density of successful transmissions in

slotted ALOHA under a specified outage constraint. In the same manner as in [18] (which considers slotted ALOHA only), we adopt the concept of guard zones in our analysis, with the difference that instead of incorporating into the protocol a guard zone within which no transmitter are *permitted*, we consider actual MAC protocols that employ virtual guard zones in order to make the backoff decision and evaluate the outage probability.

The work of this chapter is published in [43; 44], and a revision of [45] is submitted for possible publication in IEEE Trans. on Wireless Communications.

2.1 System Model

As a starting point, consider a mobile wireless network in which transmitters are randomly placed on an infinite 2-D plane according to a homogeneous Poisson point process (PPP) with spatial density λ^s [nodes/m^2] and moving independently of each other. At each transmitter, a series of packets, each with a fixed duration T, arrives according to an independent homogeneous 1-D PPP in time with intensity λ^t [packets/sec/node]. These packets are then sent with a constant power ρ to their intended receiver, which is assumed to lie a fixed distance R away. The assumptions made on the system parameters will be justified in Subsection 2.1.1. In this network model, the spatial PPP is first fixed and each transmitter generates its own traffic of packets. This means that at each time instant, the average number of nodes per unit area that have formed a new packet during the last T seconds is: $\lambda = \lambda^s \lambda^t T$ [packets/m^2]. Futhermore, each packet is given M backoffs and N retransmission attempts. Hence, due to the ability to backoff from transmissions (in CSMA) and retransmit in the case of erroneous packet reception, we have an increase of $\lambda\Delta(M,N)$ to the spatial density of packets, when the network is in a steady state. That is, the density of packets attempting to access the channel at each time instant is $\lambda(1+\Delta(M,N))$, where $\Delta(M,N)$ is a function of the number of backoffs and retransmissions, depending on the applied protocol. If no backoffs or retransmissions are allowed, i.e., $(M,N)=(1,0)$, we have that $\Delta(M,N)=0$ for all the protocols. Note that the number of backoffs M is always strictly greater than 0 for CSMA. Finally, the number of packets attempting to access the channel over the area A is: $\lambda^s\lambda^t A\ T(1+\Delta(M,N))$ [packets].

Since this network model entails two independent Poisson distributions, in order to derive the outage probability, we would have to average over both the spatial and temporal statistics. Because of the involved expressions and the complicated analysis this would entail, instead we con-

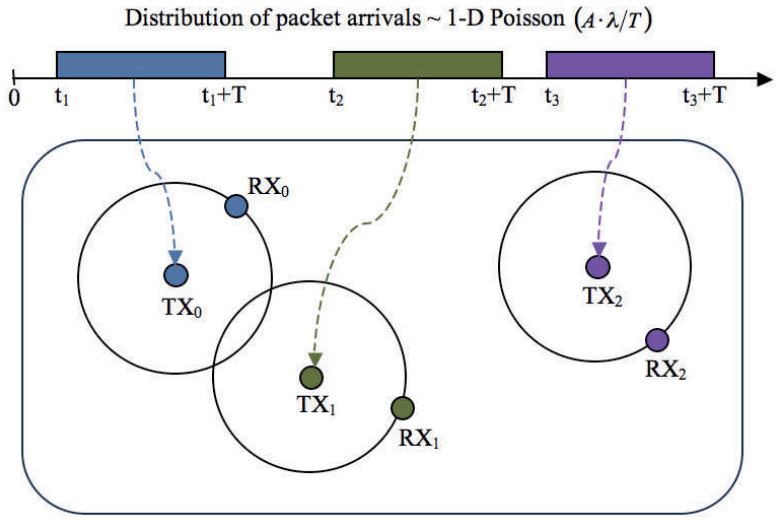

Figure 2.1: Illustration of our ad hoc network and traffic model.

sider our wireless network from an alternative point of view. Instead of fixing the user locations first and then generating traffic for each user, we rather consider the packet arrivals to be the only random process and incorporate the spatial PPP into the temporal PPP. This is done as follows: Consider a single queue of packet arrivals with density $\lambda^s \lambda^t A$. Upon the arrival of each packet, it is assigned to a transmitter node, which is then randomly placed on a 2-D plane (uniformly distributed in area A), as illustrated in Figure 2.1. The intended receiver of this packet is located, with random orientation, a fixed distance R away. The transmission is then initiated according to the specified MAC protocol. When the packet has been served (successfully or not), the corresponding transmitter-receiver pair disappears from the plane. When the maximum number of backoffs and retransmissions is not reached, the packet is placed back in the packet arrival queue, with a new transmission time. The retransmitted packet will be located in a new position, which is most reasonable in networks with high mobility. The density of packets attempting to access the channel, including those due to backoffs and retransmissions, is $\lambda(1 + \Delta(M, N))$.

Note that the temporal PPP of packet arrivals at each node is independent of the PPP of transmitter locations in space. Due to the high mobilility presumed in our network, different sets of packets are active between times t_0 and $t_0 + T$. In a network domain of 35 m $\times$ 35 m, with a packet time of

100 sec, high mobility would indicate a speed of about 0.17 m/sec. This is in accordance with proposed sensor network designs, such as [46], where a node mobility of 0.15 m/sec is assumed. Since the waiting time from one transmission attempt to the next is set to be greater than T, and because of the high mobility assumption, there are no spatial and temporal correlations between retransmission attempts of a packet. This conclusion agrees with the results of [47], where it is concluded that in a standard path loss model, the spatio-temporal correlation coefficient (defined as the ratio of the interference covariance over the interference variance) is indeed 0. The reason for this result is that the nearest interferer is the main contributor to the interference, and having independence between the location of interferers at time t_0 and those at time $t_0 + T$ makes the correlation coefficient go to 0. As a result of this independence, and the basic properties of PPPs, the number of nodes in any random selection of an area at any random point in time still follows a PPP [48; 49]. Hence, our space-time model entails a 3-D PPP with density $\lambda^s\lambda^t(1 + \Delta(M, N))$ [packets/m^2/sec]. Considering the entire plane at a fixed point in time, we observe the behaviour of the space-time model's spatial 2-D PPP with density $\lambda = \lambda^s\lambda^t T(1 + \Delta(M, N))$. Equivalently, the total expected number of packets in area A during a time interval T is $\lambda^s\lambda^t A\ T(1 + \Delta(M, N))$. Thus, we see that our alternative 3-D *space-time model* is a good representation of the ad hoc network initially described, as it entails a Poisson distribution of nodes in space and of packet arrivals in time, with the same density of packets accessing the channel as the initial model. Hence, we adopt this model for our analysis, as it allows us to only consider a single random process describing both the temporal and spatial variations of the system. Such unification of the sources of randomness simplifies the analysis, as well as making many complex derivations (e.g., for the outage probability of CSMA) tractable.

Finally, we also investigate what happens when the network area tends to infinity. Consider our 3-D PPP with spatial density λ. Let A_k be the area of a circle of radius k in this space. By the Borel-Cantelli lemma [48], we have that for dimensions ≥ 2, the number of points inside A_k as $k \to \infty$ is equal to λA, where $A = \lim_{k\to\infty} A_k$. The bearing of this lemma is that, although the number of nodes goes to infinity, the density remains a finite value of λ when the area increases to infinity.

We emphasize the following attributes of our traffic model that are of significance for the derivations:

- Our network is highly mobile, meaning that different and independent sets of nodes are observed on the plane from one slot (of length T) to the next.

- Upon retransmission of a packet, it is treated as a new packet arrival and placed in a new location (justified by the preceding assumption), resulting in no spatial correlation between transmission attempts.
- The waiting time between retransmission attempts is set to be $t_{wait} > T$, which because of the high mobility assumption, results in no temporal correlation between retransmission attempts.

For the channel model, we consider only path loss attenuation effects (with path loss exponent $\alpha > 2$[1]), ignoring both short term and long term fading. The channel is assumed to be constant for the duration of a transmission. Each receiver sees interference from all active transmitters on the plane, and these interference powers are added to the channel noise, η, to result in a certain SINR at each receiver. If this received SINR falls below a required SINR threshold, β, at any time during the packet transmission, the packet is received *erroneously*, with probability

$$P_{error} = \Pr\left(\min_{0 \le t < T} \frac{\rho R^{-\alpha}}{\eta + \sum_{i(t)} \rho r_i^{-\alpha}} \le \beta \right), \tag{2.1}$$

where r_i is the distance between the node under observation and the i-th interfering transmitter, and the summation is over all active interferers on the plane at time t.

The MAC protocols ALOHA and CSMA are applied for the communication between nodes. In the case of unslotted ALOHA, each transmission starts as soon as the packet arrives, regardless of the channel condition. Slotted ALOHA improves the performance by removing partial outages, but this requires synchronization. If the packet is received erroneously, it is retransmitted. Each packet has a maximum of N retransmission attempts in order to be received correctly. In the CSMA protocol, the channel is sensed at the beginning of each packet (i.e., the radio measures the energy received on its available radio channel). If the measured SINR is above β_b,[2] the packet transmission is initiated; otherwise, it is backed off. Each packet is given a maximum of M backoffs, before it is dropped. Since evaluating the backoff scheme is outside the scope of this thesis[3], we simply assume that

[1] $\alpha = 2$ is for propagation in free space.

[2] The subscript b is used, because the backoff decision is made based on this sensing threshold. Equivalently, the backoff probability is denoted P_b.

[3] Various backoff schemes are evaluated in [50]. Although the Fibonacci increment backoff is shown to yield the best performance in terms of throughput and delay, the difference between the various schemes is very small.

the backoff times are random, uncorrelated, and exponentially distributed (this also maintains the Poisson distribution of packets). Once the transmission is initiated, but the packet is received erroneously, i.e., its SINR $< \beta$, it is retransmitted. If still received in error after N retransmissions, the packet is counted to be in *outage*. Finally, all communication between the transmitter and its receiver is assumed to occur over an orthogonal control channel, and the delay introduced by the feedback is assumed to be insignificant compared to the packet length.

The outage probability of ALOHA and CSMA is defined mathematically as

$$\begin{aligned} P_{out}(\text{ALOHA}) &= \Pr\big[\text{SINR} < \beta \text{ at some } [0,T) \;\; N+1 \text{ times}\big] \\ P_{out}(\text{CSMA}) &= \Pr\big[\text{SINR} < \beta_b \;\; M \text{ times} \;\; \cup \;\; \text{SINR}_t < \beta \;\; N+1 \text{ times}\big], \end{aligned} \tag{2.2}$$

where SINR_0 is defined as the SINR at time $t = 0$, i.e., at the start of the packet, and SINR_t denotes the SINR at some $t \in (0, T)$. As the goal of this chapter is to establish an understanding on the outage probability of various MAC protocols, with focus on the analysis technique, in the following we assume that $\beta_b = \beta$.

The throughput $\mathcal{S}$ of this network is given as

$$\mathcal{S} = \lambda \left(1 + \Delta(M, N)\right) \frac{R_{req}}{W} \left(1 - P_{out}\right) \tag{2.3}$$

where R_{req}/W [bits/s/Hz per packet] is the average rate that a successful packet achieves, normalized with respect to the system bandwidth, W. The unit of $\mathcal{S}$ is [bits/s/Hz/m^2]. Since the outage probability is the only unknown term in the throughput expression, we will solely focus on this metric in the analytical derivations of this chapter.

2.1.1 Justification of Assumptions

For ad hoc networks with single-hop communication links and substantial mobility or indiscriminate node placement, such as a dense sensor network, an assumption of Poisson distributed nodes in space is reasonable and commonly used [35; 36; 51; 52]. However, in many networks, such as *clustered* or *multi-hop* networks, this assumption might not be valid anymore, as transmissions are often correlated with each other in both time and space. Assuming no fading is not always reasonable. This assumption is made in this chapter because we wish to find the outage probability of MAC protocols under optimal conditions, as in [18; 36]. In Chapter 3, we add fading to our model, and rederive the outage probability of the various

protocols. Independent fading is there shown to deteriorate the average performance of single-antenna networks.

The assumption of fixed packet length T is reasonable, because in most applications, data is packetized before transmission, and each packet is then of the same constant length. The fixed distance, R, between all transmitter-receiver pairs (which is also assumed in [18; 19; 51]) is often not a natural assumption. However, note that the whole network with a fixed R could be viewed as a snapshot of a multi-hop wireless network, where R is the bounded *average* inter-relay distance resulting from the specific routing protocol used. Furthermore, for low densities and zero ambient noise, the outage probability is a convex function of R, making our outage probability analysis yield a lower bound to the case when R is variable. As a simple proof of this fact, consider the outage probability of slotted ALOHA with no retransmissions (as we will derive in Subsection 2.3): $P_{out} = 1 - e^{-\lambda\pi\beta^{2/\alpha}R^2}$. Setting $k = \pi\lambda\beta^{2/\alpha}$, we have that

$$\frac{d^2P_{out}}{dR^2} \;=\; 2\,k\,e^{-kR^2}(1-2\,k\,R^2). \tag{2.4}$$

For $2\,k\,R^2 \leq 1$, we have that $\frac{d^2P_{out}}{dR^2} \geq 0$, indicating convexity. Hence, we may conclude that for low enough values of $k = \pi\,\lambda\,\beta^{2/\alpha}$ (which is the case when the density is low), P_{out} is a convex function of R.

2.2 Method of Analysis

The evaluation of outage probability consists of solving Eq. (2.2). However, the consideration of all interfering contributions in the denominator of Eq. (2.2) turns out to be impractical for the analytical derivations. For this reason, we focus on the probability of having a single *closest* interferer, whose received interference power alone is strong enough to result in outage for the packet of interest. Denote a randomly selected active receiver on the plane as RX_0. In order to consider the closest interferer as the determinant for outage probability, we first establish the notion of *guard zones* [36]. The guard zone of RX_0 is a circle $B(\mathrm{RX}_0, s)$ centered on RX_0 with radius s, defined such that if a single interferer, TX_1, is located at a distance less than s away from RX_0, the packet of RX_0 will be received in error. The radius s is derived to be

$$s \;=\; \left(\frac{R^{-\alpha}}{\beta} - \frac{\eta}{\rho}\right)^{-1/\alpha}. \tag{2.5}$$

Through Eq. (2.5), β_b corresponds to s_b, β_r to s_r, etc. This convention will be used in the following chapters.

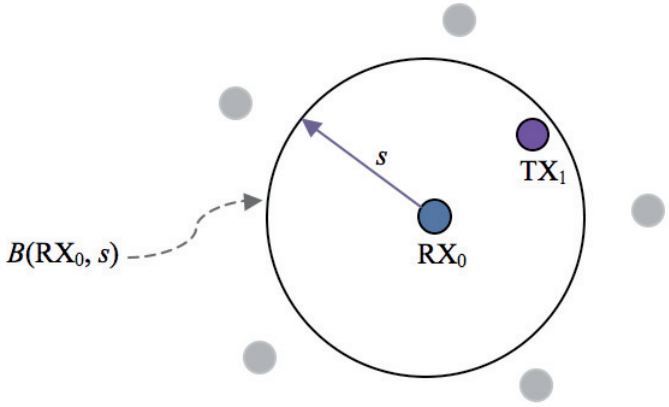

Figure 2.2: Guard zone of RX_0, denoted $B(\mathrm{RX}_0, s)$, with an interfering transmitter, TX_1.

The guard zone $B(\mathrm{RX}_0, s)$ is a circle of radius s around RX_0, as illustrated in Figure 2.2. One situation that would cause RX_0 to go into outage is if the accumulation of powers from all the interfering nodes *outside* $B(\mathrm{RX}_0, s)$ results in the SINR at RX_0 to fall below the threshold β. Another situation that will lead to erroneous reception of a packet is if at least one active transmitter, other than RX_0's own transmitter, TX_0, falls inside $B(\mathrm{RX}_0, s)$ at some $t \in [0, T)$. Considering only the latter event yields a *lower bound* to the outage probability. It has previously been shown that this lower bound is in fact fairly tight around the actual outage probability [18], and hence, we only focus on this bound in our analysis.

Due to the Poisson distribution of packets over space and time, with density λ, the probability of having at least one interferer within a given area A and during a given time interval Δt is given by

$$P_{A\Delta t} = 1 - e^{-\mathbb{E}[\#\text{ of interferers in } A \text{ during } \Delta t]} = 1 - e^{-\lambda A \Delta t}. \tag{2.6}$$

This expression is valid because of a property of the PPP, namely that removing one point from the process does not change the distribution, which means that the *interferers* of the node under observation also follow a homogeneous PPP with the same intensity. The derivation of the outage probability of ALOHA and CSMA in non-fading networks is based on the techniques described above.

2.3 Outage Probability of ALOHA

In this section, we derive the outage probability of the ALOHA protocol, following the analysis technique described in Section 2.2. Both the slotted and unslotted ALOHA protocols are considered.

2.3.1 Slotted ALOHA

Due to the slotting of time in slotted ALOHA, there is no problem of partial overlap of packets, something that is intuitively expected to decrease the outage probability compared to unslotted algorithms. This performance improvement comes, however, at the expense of a need for synchronization. Using the concept of guard zones, a lower bound to the outage probability of slotted ALOHA is given by the following theorem.

Theorem 2.1
The outage probability of slotted ALOHA may be lower bounded by $P_{out}^{lb}(\textit{Slotted ALOHA}) = P_{rt,s}^{N+1}$, *where* $P_{rt,s}$ *is the solution to*[4]

$$P_{rt,s} \;=\; 1 - \exp\left\{-\lambda\,\frac{1-P_{rt,s}^{N+1}}{1-P_{rt,s}}\,\pi\,s^2\right\}. \tag{2.7}$$

Proof: Consider the communication link of TX_0-RX_0. Due to the slotting of time, only packets arriving during the last T seconds start simultaneously with the one generated by TX_0, and have thus the potential to result in an erroneous packet reception at RX_0. Based on the concept of guard zones, we have that

$$\mathbb{E}\big[\#\text{ of interferers inside } B(\mathrm{RX}_0, s) \text{ at some } t \in [-T, 0)\big] \;\approx\; \lambda_{slotted}\,\pi\,s^2, \tag{2.8}$$

where $\lambda_{slotted}$ is the density of packets accessing the channel. Allowing for retransmissions is equivalent to increasing the number of packets that attempt to access the channel. Since the waiting times are random and uncorrelated (by assuming $t_{wait} > T$), there is no correlation between the amount of interference detected in each retransmission attempt. Given the probability of a packet being retransmitted is $P_{rt,s}$, the density of packets in the channel at each time instant is

$$\lambda_{slotted} \;=\; \lambda(1 + P_{rt,s} + P_{rt,s}^2 + ... + P_{rt,s}^N) \;=\; \lambda\,\frac{1-P_{rt,s}^{N+1}}{1-P_{rt,s}}. \tag{2.9}$$

[4]The subscript "rt,s" denotes ReTransmission for Slotted ALOHA.

The probability of having an erroneous packet transmission in a Poisson distributed network is $P_{rt,s} = 1 - e^{-\mathbb{E}[\#\text{ of interferers}]}$. Furthermore, a packet is retransmitted the k-th time if it is erroneously received all $k-1$ previous attempts. Hence, a packet is counted to be in outage if it is received erroneously on the N-th retransmission attempt, resulting in $P_{out}^{lb}(\text{Slotted ALOHA}) = P_{rt,s}^{N+1}$. □

In [53], the *exact* outage probability of slotted ALOHA for $\alpha = 4$ and $(M, N) = (1, 0)$ was derived to be

$$P_{out}^{exact}(\text{Slotted ALOHA}) = 1 - \text{erfc}(\sqrt{\pi\,\beta}\,\lambda\,\pi\,R^2/2). \tag{2.10}$$

We will consider this expression for the sake of comparison with our lower bound in Section 2.6.

2.3.2 Unslotted ALOHA

Unslotted protocols are particularly of interest in systems that have no synchronization abilities. Intuitively, we expect the outage probability of unslotted ALOHA to exceed that of the slotted case, due to the partial overlap of transmissions. With the same reasoning as for slotted ALOHA, we obtain the following theorem.

Theorem 2.2
The outage probability of unslotted ALOHA may be lower bounded by $P_{out}^{lb}(\textit{Unslotted ALOHA}) = P_{rt,u}^{N+1}$, *where* $P_{rt,u}$ *is the solution to*

$$P_{rt,u} = 1 - \exp\left\{-2\,\lambda\,\frac{1 - P_{rt,u}^{N+1}}{1 - P_{rt,u}}\pi\,s^2\right\}. \tag{2.11}$$

Proof: Due to the unslottedness of the system, any transmission that started less than time T before the start of TX_0's transmission and up to time T later, will be interfering with the packet of RX_0 and thus contribute to its outage probability. Since the number of packet arrivals at times t_0 and $t_0 + T$ are independent, we have that

$$\begin{aligned} P_{rt,u} &= 1 - \Pr\left(\text{No interferers inside } B(\text{RX}_0, s) \text{ during } [-T, T)\right) \\ &= 1 - \Pr\left(\text{No interf. during } [-T, 0)\right) \cdot \Pr\left(\text{No interf. during } [-0, T)\right) \\ &= 1 - e^{-2\,\lambda_{unslotted}\,\pi\,s^2}, \end{aligned}$$

where $\lambda_{unslotted} = \lambda\frac{1-P_{rt,u}^{N+1}}{1-P_{rt,u}}$ as explained in the proof of Theorem 2.1. Given N retransmissions for each packet, the outage probability becomes $P_{rt,u}^{N+1}$. □

Extending the result of [53] for the outage probability of slotted ALOHA for $\alpha = 4$ and $(M, N) = (1, 0)$ to the unslotted case, we obtain

$$P_{out}^{exact}(\text{Unslotted ALOHA}) \;=\; 1 - \text{erfc}(\sqrt{\pi\,\beta}\,\lambda\,\pi\,R^2/2)^2. \qquad (2.12)$$

This is also evaluated with simulations in Section 2.6.

For lower densities and when $\frac{1-P_{rt,s}^{N+1}}{1-P_{rt,s}} \;\approx\; \frac{1-P_{rt,u}^{N+1}}{1-P_{rt,u}} \;\approx\; 1$ (where equality signs may be used when $N = 0$), we may apply the Taylor expansion on Eqs. (2.7) and (2.11), obtaining

$$P_{out}(\text{Slotted ALOHA}) \;\approx\; \left(\lambda\,\pi\,s^2\right)^{N+1}$$
$$P_{out}(\text{Unslotted ALOHA}) \;\approx\; \left(2\,\lambda\,\pi\,s^2\right)^{N+1}$$

This shows that for lower densities, slotted ALOHA outperforms its unslotted version by a factor of 2^{N+1}. When no retransmissions are allowed, $P_{out}(\text{Unslotted ALOHA}) \;\approx\; 2\,P_{out}(\text{Slotted ALOHA})$, which is consistent with the results obtained in the conventional model [10].

2.4 Outage Probability of CSMA

In this section, we derive the outage probability of the CSMA protocol. We consider two basic forms of the protocol; CSMA_{TX} where the transmitter makes the backoff decision, and CSMA_{RX} where the receiver is the decision maker. Moreover, we assume that the sensing threshold, β_b, based on which the backoff decision is made, is constant and equal to the required SINR for correct reception of packets, β. The assumption on $\beta_b = \beta$ is made because the aim of this section is primarily to establish an understanding for the behavior of the CSMA protocol and our analysis technique.

2.4.1 CSMA with Transmitter Sensing

This protocol, denoted by CSMA_{TX}, is the conventional CSMA protocol which is employed in many of today's network standards, such as IEEE 802.11 and 802.16. In CSMA_{TX}, the *transmitter* is the backoff decision maker. That is, when a new packet arrives, the transmitter immediately measures the aggregate interference power. If this is greater than $\left(\frac{\rho\,R^{-\alpha}}{\beta} - \eta\right)$, it backs off; otherwise, it starts transmitting immediately. The outage probability of this protocol is established by the following theorem.

Theorem 2.3
The outage probability of $CSMA_{TX}$ is given by[5]

$$P_{out}(CSMA_{TX}) \;=\; P_b^M + \left(1 - P_b^M\right)\, P_{rt1}\, P_{rt}^N, \tag{2.13}$$

where:

- *P_b is the backoff probability, approximated by the solution to*

$$\tilde{P}_b = 1 - e^{-\pi\, s^2 \lambda \left(1 - \tilde{P}_b^M + \left(1 - \tilde{P}_b^M\right) \tilde{P}_{rt1}\, \frac{1 - \tilde{P}_{rt}^N}{1 - \tilde{P}_{rt}}\right)}. \tag{2.14}$$

- *$P_{rt} = P_b + (1 - P_b)\; P_{during}$ is the probability that a packet is received in error during a retransmission attempt and must thus be retransmitted again. P_{during} is the probability that the error has occurred at some $t \in (0, T)$, approximated by*

$$\tilde{P}_{during} \;=\; 1 - e^{-\int_{\lceil s-R \rceil^+}^{s} \lambda_{csma}^{TX} \left[2\pi - 2\cos^{-1}\left(\frac{r^2 + R^2 - s^2}{2Rr}\right)\right] r\, dr}. \tag{2.15}$$

- *$P_{rt1} \;=\; P_{rx|transmit} + \left(1 - P_{rx|transmit}\right)\, P_{during}$ is the probability that the packet is received in error at its first transmission attempt. $P_{rx|transmit}$ is the probability that the received packet is in outage upon arrival, approximated by*

$$\tilde{P}_{rx|transmit} = \tilde{P}_b \left[1 - \frac{1}{\pi s^2}\left(2s^2 \cos^{-1}\left(\frac{R}{2s}\right) - Rs\sqrt{1 - \frac{R^2}{4s^2}}\right)\right]. \tag{2.16}$$

- *The density of packets attempting to access the channel is given by*

$$\lambda_{csma}^{TX} \;\approx\; \lambda \left[\frac{1 - \tilde{P}_b^M}{1 - \tilde{P}_b} + (1 - \tilde{P}_b^M)\, \tilde{P}_{rt1}\, \frac{1 - \tilde{P}_{rt}^N}{1 - \tilde{P}_{rt}}\right]. \tag{2.17}$$

Proof: The proof of Theorem 2.3 is given in the Subsection 2.5.1. □

The reason why Eqs. (2.14)-(2.17) are approximations is that the concept of guard zones is used to derive a lower bound, while the assumption that all new interferers ignore each other and make their backoff decision based on TX_0 only, gives a higher outage probability than the lower bound.

[5]Note that in the following, we omit the superscript TX or RX for the various probability expressions, in order to avoid confusion with the exponents. That is, we refer to the backoff probability of both $CSMA_{TX}$ and $CSMA_{RX}$ by P_b, but the values of these are different.

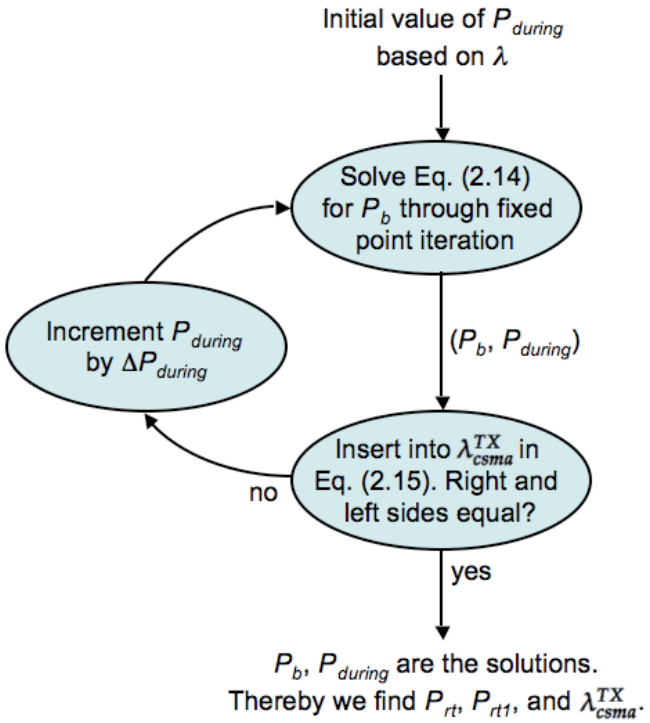

Figure 2.3: Algorithm for numerically solving the various probabilities to find $P_{out}(\text{CSMA}_{\text{TX}})$.

Due to the interdependence between the various probabilities in Theorem 2.3, their values must be solved numerically. Here we give an explanation to how this may be done. Insert the equations for P_{rt}, P_{rt1}, and λ_{csma}^{TX} into the expressions for P_b and P_{during}, and observe that these two latter probabilities are the only ones dependent on each other when $N > 0$. The procedure for finding these probabilities is illustrated in Figure 2.3. First, find an initial value for P_{during} by replacing λ_{csma}^{TX} with λ in Eq. (2.15). Insert this value for P_{during} into Eq. (2.14), and find the corresponding P_b through fixed point iteration. Then insert the values for P_b and P_{during} into λ_{csma}^{TX} in Eq. (2.15), and check whether the left and right sides of the expression are equal. If not, increment P_{during} by a small step[6], insert it into Eq. (2.14), and repeat the procedure just described until both sides of Eq. (2.15) become equal. The values for P_b and P_{during} are then the correct solutions, based on

[6]The reason we can *increase* P_{during} is that when $N > 0$, $\lambda_{csma}^{TX} > \lambda$, meaning that P_{during} cannot fall below its corresponding value with λ.

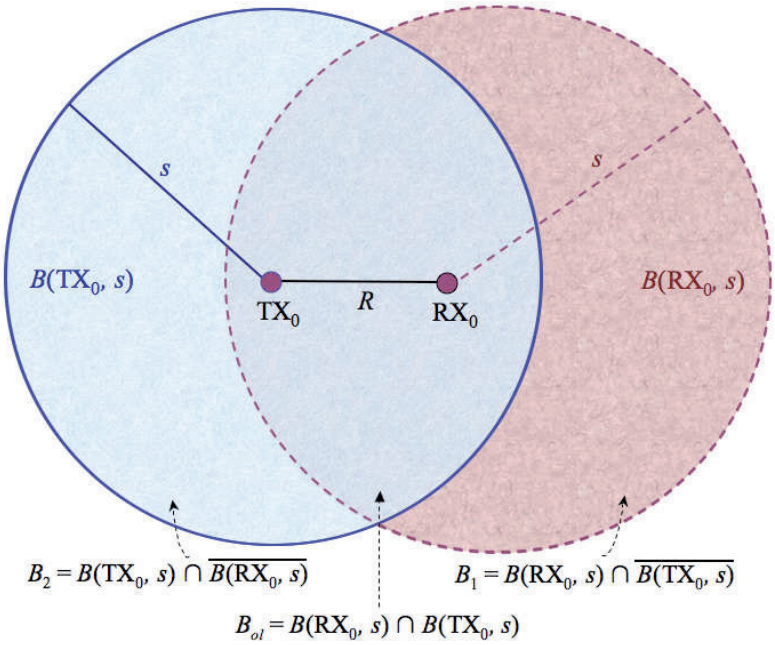

Figure 2.4: Area of overlap between $B(\mathrm{RX}_0, s)$ and $B(\mathrm{TX}_0, s)$.

which we can find P_{rt}, P_{rt1}, and thereby $P_{out}(\mathrm{CSMA_{TX}})$. If $N = 0$, P_{during} is dependent on P_b, but not vice versa, meaning that the solution will be reached after only one iteration.

Note that the outage probability of $\mathrm{CSMA_{TX}}$ is due to the hidden and exposed node problems. The hidden node problem occurs when a new interferer TX_i is located inside $B_1 = B(\mathrm{RX}_0, s) \cap \overline{B(\mathrm{TX}_0, s)}$, where TX_0 is *hidden* to TX_i, in each of the N retransmission attempts of the packet of TX_0-RX_0. The exposed node problem occurs when TX_i backs off in cases when its transmission would not have contributed to any outage, i.e., when TX_i is located inside $B_2 = B(\mathrm{TX}_0, s) \cap \overline{B(\mathrm{RX}_0, s)}$ during all the M backoffs. The regions B_1 and B_2 are shown in Figure 2.4.

Compared to unslotted ALOHA, the impact of the carrier sensing in $\mathrm{CSMA_{TX}}$ is two-fold;

a) The benefit that CSMA provides over unslotted ALOHA is to prevent interferers from being placed inside $B_{ol} = B(\mathrm{RX}_0, s) \cap B(\mathrm{TX}_0, s)$ during the transmission of TX_0-RX_0 (because in this region, the interferer would back off). The area of this region is denoted $A_{ol}(s)$, and

is given as

$$A_{ol}(s) \;=\; 2s^2 \cos^{-1}\left(\frac{R}{2s}\right) - Rs\sqrt{1-\left(\frac{R}{2s}\right)^2}. \tag{2.18}$$

Hence, the outage probability of unslotted ALOHA is reduced by the probability that interferers are located in area $A_{ol}(s)$ during all N retransmission attempts, namely $\left(1-e^{-\lambda_{csma}^{TX} A_{ol}(s)}\right)^N$.

b) There is also a probability that a packet is dropped without making any transmission attempts (i.e., it is backed off M times), while it could in fact have been received without errors at its receiver, if it had been transmitted. This is the exposed node problem, and is a result of the transmitter being the decision maker. The probability of this is determined by active interferers on the plane being located in the vicinity of the transmission of TX_0 but out of the hearing range of RX_0, i.e., inside $B_2 = B(\mathrm{TX}_0, s) \cap \overline{B(\mathrm{RX}_0, s)}$. The area of this region is $\pi s^2 - A_{ol}(s)$, and the increase in the probability is $(1-e^{-\lambda_{active}(\pi s^2 - A_{ol}(s))})$.

Considering the outage probability decrease caused by factor a) and the outage probability increase of factor b) yields

$$\begin{aligned} P_{out}(\mathrm{CSMA_{TX}}) \;\approx\; & P_{out}(\text{Unslotted ALOHA}) - \left(1-e^{-\lambda_{csma}^{TX} A_{ol}(s)}\right)^N \\ & + \left(1-e^{-\lambda_{active}\left(\pi s^2 - A_{ol}(s)\right)}\right)^M, \end{aligned} \tag{2.19}$$

where λ_{active} is the density of active transmissions, given by

$$\lambda_{active} \;=\; \lambda\left(1 - P_b^M + (1-P_b^M)\, P_{rt1}\, \frac{1-{P_{rt}}^N}{1-P_{rt}}\right). \tag{2.20}$$

The approximation of Eq. (2.19) works best for low transmission densities, i.e., when $\lambda_{csma}^{TX} \approx \lambda_{active} \approx \lambda_{unslotted}$.

Note that only the first term of Eq. (2.17) is multiplied by $(1-P_b)$, because once a transmitter-receiver pair has decided to transmit, it will not perform new sensing and make a new decision at every retransmission attempt. If the channel was sensed at the start of each retransmission also, the density of active transmissions would have been $\lambda_{csma}^{TX}(1-P_b)$. This yields a lower density of interferers compared to λ_{active}, something that would

improve the performance of CSMA, at the expense of higher complexity of the hardware. In this thesis, we follow the same scheme as CSMA/CA in the IEEE 802.11 and 802.16 standards, i.e., we assume that once a packet has been activated, but must be retransmitted, it does *not* perform new sensing for each retransmission. Hence, the density of active transmissions is given by λ_{active} in Eq. (2.20).

To better understand the behavior of the backoff probability, consider the particular case of $(M, N) = (1, 0)$, i.e., we do not allow for any retransmissions and when a packet backs off it is essentially dropped. In this case, P_b can be expressed in terms of the Lambert function, $\mathcal{W}_0(\cdot)$ [54]

$$P_b \;=\; 1 - \frac{1}{\lambda\,\pi\,s^2}\,\mathcal{W}_0\left(\lambda\pi s^2\right) \;=\; 1 - \frac{1}{\lambda\,\pi\,s^2}\sum_{n=1}^{\infty}\frac{(-n)^{n-1}}{n!}\left(\lambda\pi s^2\right)^n. \quad (2.21)$$

Let $x = \lambda\pi s^2$ in Eq. (2.14). Dividing the backoff probability by the outage probability of slotted ALOHA, letting the density go to 0, and applying l'Hopital's rule multiple times, yields

$$\begin{aligned}
&\lim_{x\to 0}\frac{P_b}{P_{out}(\text{Slotted ALOHA})} \;=\; \lim_{x\to 0}\frac{1-\frac{1}{x}\mathcal{W}_0(x)}{1-e^{-x}} \;=\; \lim_{x\to 0}\frac{x-\mathcal{W}_0(x)}{x(1-e^{-x})}\\
&=\; \lim_{x\to 0}\frac{1-\frac{d\mathcal{W}_0(x)}{dx}}{1-e^{-x}+xe^{-x}} \;\overset{(3)}{=}\; \lim_{x\to 0}\frac{e^{\mathcal{W}_0(x)}+x-1}{\left(e^{\mathcal{W}_0(x)}+x\right)\left[e^{-x}(x-1)+1\right]}\\
&=\; \lim_{x\to 0}\frac{e^{\mathcal{W}_0(x)}\frac{d\mathcal{W}_0(x)}{dx}+1}{\left(e^{\mathcal{W}_0(x)}\frac{d\mathcal{W}_0(x)}{dx}+1\right)\left[e^{-x}(x-1)+1\right]+\left(e^{\mathcal{W}_0(x)}+x\right)\left[-e^{-x}(x-1)+e^{-x}\right]}\\
&\overset{(5)}{=}\; 1.
\end{aligned}$$

This proves that as $\lambda \to 0$, $P_b \to P_{out}(\text{Slotted ALOHA})$. In step 3 of the above derivation, we apply the result $\frac{d\mathcal{W}_0(x)}{dx} = \frac{1}{(1+\mathcal{W}_0(x))e^{\mathcal{W}_0(x)}} = \frac{1}{e^{\mathcal{W}_0(x)}+x}$, and in step 5, we use that $\lim_{x\to 0}\mathcal{W}_0(x) = 0$ and $\lim_{x\to 0}\frac{d\mathcal{W}_0(x)}{dx} = 1$.

Moreover, for low values of P_b, we have that $\lambda_{active} \approx \lambda_{slotted}$, while as P_b increases, the density of *active* transmissions in CSMA may no longer be approximated by that in slotted ALOHA. Due to the reduced number of interferers, P_b is less than the case when *all* prior arrivals are activated. Hence, while Eq. (2.14) is an approximate measure of P_b, Eq. (2.7) operates as an upper bound.

2.4.2 CSMA with Receiver Sensing

In this subsection, we consider a variation of the CSMA protocol, termed CSMA_{RX}. In this protocol, the *receiver* senses the channel and subsequently

determines whether or not the packet transmission should be initiated. Since the information determining a backoff is binary ("transmit" or "don't transmit"), the communication between the receiver and its transmitter is assumed to occur over a 1 bit control channel (per packet), which is orthogonal to the control channel. This means that there are no interference issues between the control signals and the data packets. Moreover, the delay introduced by the feedback is assumed to be small and insignificant compared to the packet length.

Note that the main difference between the proposed CSMA_{RX} protocol and the popular CSMA/CA protocol used in the IEEE 802.11 and 802.16 standards family is that in the latter, *all* nodes in the channel hear the request-to-send (RTS) and clear-to-send (CTS) signals, whereas in CSMA_{RX}, we assume that the communication of control signals is between a receiver and its own transmitter only. Assuming that this control channel is much smaller than the system bandwidth, we do not consider in our analysis the "stealing" of resources that it entails. The outage probability of CSMA_{RX} is given by the following theorem.

Theorem 2.4

The outage probability of $CSMA_{RX}$ is given by

$$P_{out}(CSMA_{RX}) \;=\; P_b^M + \left(1 - P_b^M\right)\, P_{during}\, P_{rt}^N, \tag{2.22}$$

where:

- *P_b is the backoff probability, approximated by the solution to*

$$\tilde{P}_b \;=\; 1 - e^{-\pi s^2 \lambda \left(1 - \tilde{P}_b^M + \left(1 - \tilde{P}_b^M\right)\, \tilde{P}_{during}\, \frac{1 - \tilde{P}_{rt}^N}{1 - \tilde{P}_{rt}}\right)}. \tag{2.23}$$

- *$P_{rt} = P_b + (1 - P_b)\, P_{during}$ is the probability that a packet is received in error during a retransmission attempt. P_{during} is the probability that the error has occurred at some $t \in (0, T)$, approximated by*

$$\tilde{P}_{during} \;=\; 1 - e^{-\int_{s-R}^{s} \int_{\nu(r)}^{2\pi - \nu(r)} \lambda_{csma}^{RX}\, P(active \mid r, \phi)\, r\, d\phi\, dr}, \tag{2.24}$$

with $P(active|r, \phi)$ and $\nu(r)$ given by:

$$P(active|r, \phi) \;=\; 1 - \frac{1}{\pi} \cos^{-1}\left(\frac{r^2 + 2R^2 - s^2 - 2Rr\cos\phi}{2R\sqrt{r^2 + R^2 - 2Rr\cos\phi}}\right) \tag{2.25}$$

$$\nu(r) \;=\; \cos^{-1}\left(\frac{r^2 + 2Rs - s^2}{2Rr}\right). \tag{2.26}$$

- *The density of packets attempting to access the channel is given by*

$$\lambda_{csma}^{RX} \approx \lambda \left[\frac{1-\tilde{P}_b^M}{1-\tilde{P}_b} + (1-\tilde{P}_b^M)\,\tilde{P}_{during}\,\frac{1-\tilde{P}_{rt}^N}{1-\tilde{P}_{rt}} \right]. \tag{2.27}$$

Proof: The proof of Theorem 2.4 is given in the Subsection 2.5.2. □

The outage probability of CSMA_{RX} is due to the hidden node problem, which occurs when an interferer, TX_i, is located too close to RX_0, while its receiver is located too far away from TX_0 to detect its transmission. That is, TX_i is located inside $B_1 = B(\text{RX}_0, s) \cap \overline{B(\text{TX}_0, s)}$, as shown in Figure 2.4.

Compared to unslotted ALOHA, the impact of the carrier sensing in CSMA_{RX} is only positive; it prevents interferers from being placed inside $B(\text{RX}_0, s) \cap B(\text{TX}_0, s-R)$ during the transmission of TX_0-RX_0. Here we presume that $s \geq R$, which is a reasonable assumption, as the sensing range of the receiver should at least cover the distance to its own transmitter. The area of this region is $A_{ol}(s) = \pi\,(s-R)^2$. Moreover, the receiver of the interfering node must be outside of $B(\text{TX}_0, s)$ to be activated. The probability of this is

$$P_{activation} = 1 - \frac{1}{\pi}\cos^{-1}\left(\frac{2R^2-s^2}{2R^2}\right). \tag{2.28}$$

Hence, the outage probability of unslotted ALOHA is reduced by the probability of the activation of interferers inside $A_{ol}(s)$ during all N retransmission attempts, resulting in

$$\begin{aligned} P_{out}(\text{CSMA}_{\text{RX}}) \approx\ & P_{out}(\text{Unslotted ALOHA}) \\ & - \left[1 - e^{-\lambda_{csma}^{RX}\left[1-\frac{1}{\pi}\cos^{-1}\left(\frac{2R^2-s^2}{2R^2}\right)\right]\pi\,(s-R)^2}\right]^N, \end{aligned} \tag{2.29}$$

where λ_{csma}^{RX} is given by Eq. (2.27).

2.5 Proof of Theorems for CSMA

In this section, we provide proof for the theorems on the outage probability of CSMA, as given in Section 2.4.

2.5.1 Proof of Theorem 2.3

Denote the received SINR of the receiver under observation, RX_0, by SINR_0. The packet transmission of TX_0-RX_0 is counted to be in outage if one or both of the following events occur:

a) The packet is backed off (i.e., $\text{SINR}_0 < \beta$ upon packet arrival) M times and thus dropped.

b) Once the packet transmission is initiated, one or both of the following subevents occur $N+1$ times:

b_1) $\text{SINR}_0 < \beta$ at the start of the packet, i.e., at $t = 0$.

b_2) $\text{SINR}_0 < \beta$ at some $t \in (0, T)$.

where events (*a*) and (*b*) are independent except at the first transmission attempt. This yields

$$\begin{aligned} P_{out}(\text{CSMA}) &= \Pr(a) + (1 - \Pr(a)) \Pr(b_1 \cup b_2 | \overline{a})^{N+1} \\ &= \Pr(a) + (1 - \Pr(a)) \Pr(b_1 \cup b_2 | \overline{a}) \Pr(b_1 \cup b_2)^N \end{aligned} \quad (2.30)$$

Based on Eq. (2.30), the probability that event (*a*) occurs in CSMA_{TX} is $\Pr(a) = P_b^M$, where P_b can be lower bounded by considering packet arrivals inside $B(\text{TX}_0, s)$ during $[-T, 0)$. The density of packets attempting to access the channel is

$$\lambda_{csma}^{TX} = \begin{cases} \lambda \sum_{m=0}^{M-1} P_b^m & ;\text{for } N = 0 \\ \lambda \left[\sum_{m=0}^{M-1} P_b^m + (1 - P_b^M) P_{rt1} \sum_{n=0}^{N-1} P_{rt}^n \right] & ;\text{for } N \geq 1 \end{cases}$$

which yields Eq. (2.17). We assume that the number of *active* interferers on the plane follows a PPP (which will be proven by the simulation results to be reasonable) with density λ_{active}. This density is derived by multiplying the first term of Eq. (2.17) by $(1 - P_b)$, since only *new* packet arrivals perform channel sensing. This yields

$$\lambda_{active} = \lambda \left(\frac{1 - P_b^M}{\cancel{1 - P_b}} \cancel{(1 - P_b)} + (1 - P_b^M) \, P_{rt1} \, \frac{1 - P_{rt}^N}{1 - P_{rt}} \right). \quad (2.31)$$

Applying the error proability expression for PPPs, $1 - e^{-\mathbb{E}[\#\text{ of interferers}]}$ with density λ_{active}, we obtain $Pr(a)$, as given in Eq. (2.14).

Event b_1 is concerned with packet arrivals during $[-T, 0)$. When $\beta_b = \beta$, we have that $\Pr(b_1) = P_b$. For the first transmission attempt, $\Pr(b_1|a)$ is found geometrically as the ratio of the area of $B_1 = B(\text{RX}_0, s) \cap \overline{B(\text{TX}_0, s)}$ over the area of $B(\text{RX}_0, s)$, as given by Eq. (2.16).

$\Pr(b_2)$ is lower bounded by the probability that one or more interfering transmitters are located and activated inside $B(\text{RX}_0, s)$ at some $t \in (0, T)$. To derive this probability, consider the homogeneous PPP of packet arrivals with density λ_{csma}^{TX}. Once a packet has been activated, outage occurs if the SINR at RX_0, SINR_0, falls below β at some $t \in (0, T)$. This happens if there

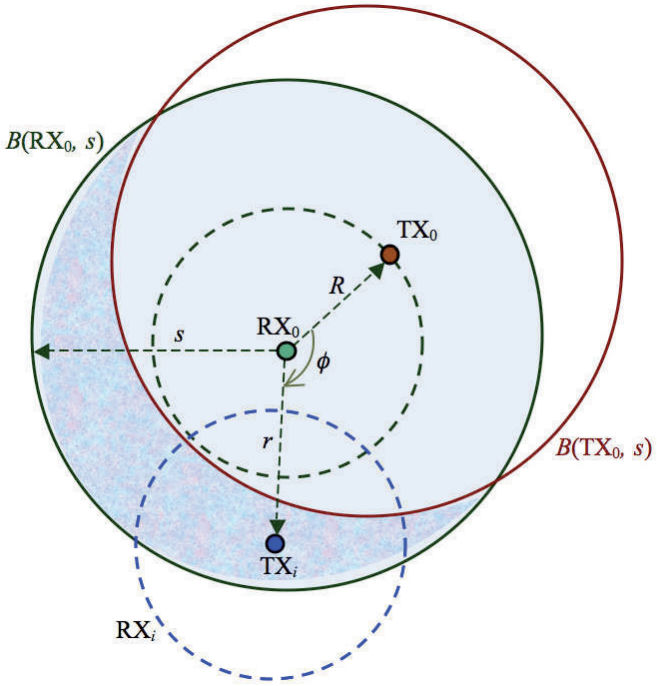

Figure 2.5: The setup used to analyze the outage probability of CSMA.

are one or more packets activated inside $B(\mathrm{RX}_0, s)$ at some $t \in (0, T)$. We have that:

$$\Pr\left[\mathrm{SINR}_0 < \beta \text{ at some } t \in (0,T) \middle| \text{ active}\right] \geq \Pr\left[\geq 1 \text{ interferer in } B(\mathrm{RX}_0, s) \text{ at some } t \in (0,T) \middle| \text{ active}\right].$$

Next, we assume that all interferers (following a PPP with density λ_{csma}^{TX}) base their backoff decision on the interference they see only from TX_0. Since $\frac{\rho R^{-\alpha}}{\eta + \text{interf. from TX}_0} \geq \frac{\rho R^{-\alpha}}{\eta + \text{interf. from TX}_0 \text{ and all other interferers}}$:

$$\Pr\left[\geq 1 \text{ interferer in } B(\mathrm{RX}_0, s) \text{ at some } t \in (0,T) \middle| \text{ active}\right] \leq \Pr\left[\geq 1 \text{ interferer in } B(\mathrm{RX}_0, s) \text{ at some } t \in (0,T) \text{ based only on } \mathrm{TX}_0 \middle| \text{ active}\right].$$

This means that we no longer have a lower bound, but rather an *approximate* measure to $\Pr(b_2)$. For the interferer of RX_0 to be activated, it must be placed at least a distance s away from TX_0. Hence, $\Pr(b_2) = P_{during}$ is derived by considering the area $B_1 = B(\mathrm{RX}_0, s) \cap \overline{B(\mathrm{TX}_0, s)}$ (the darkly

shaded region in Figure 2.5):

$$\mathbb{E}[\#\text{ of interferers in } B_1] \;=\; \int_{\lceil s-R\rceil^+}^{s} \int_{\gamma(r)}^{2\pi-\gamma(r)} \lambda_{csma}^{TX}\, r\, d\phi\, dr, \tag{2.32}$$

where $\gamma(r)$ in the integration limit found by using the cosine-rule:

$$s^2 = r^2 + R^2 - 2Rr\cos(\gamma) \quad \Rightarrow \quad \gamma(r) = \cos^{-1}\left(\frac{r^2+R^2-s^2}{2Rr}\right). \tag{2.33}$$

Solving the integral of Eq. (2.32) with respect to ϕ, and inserting it into $1 - e^{-\mathbb{E}[\#\text{ of interferers in } B_1]}$, yields Eq. (2.15). Note that for high densities and for large values of N, P_{during} loses its accuracy, partly due to the fact that the portion of λ_{csma}^{TX} that is due to retransmissions, does not perform any channel sensing, meaning that this portion can be placed anywhere inside $B(\mathrm{RX}_0, s)$ (and not only inside B_1 as we assume here). However, at high densities, the outage probability is will be too high to be applied in practical scenarios.

Inserting these expressions back into Eq. (2.30) yields Theorem 2.3.

2.5.2 Proof of Theorem 2.4

As for $\mathrm{CSMA_{TX}}$, $\Pr(a) \approx P_b^M$ in $\mathrm{CSMA_{RX}}$. Moreover, $P(b_1|a) = 0$, because once the receiver decides that its packet transmission is activated, it is sure to not have any interferers inside $B(\mathrm{RX}_0, s)$ at the start of its first transmission.

In order to derive $\Pr(b_2) = P_{during}$, we apply the fact that the process of packets starting in $B(\mathrm{RX}_0, s)$ at some $t \in (0, T)$ is a inhomogeneous PPP with intensity $\mu(x, y)$.

$$\begin{aligned}
\mu(x,y) &= \Pr[\text{ packet starts at location (x,y)}] \\
&= \Pr[\text{ packet arrives at } (x,y) \cap \text{ packet is activated}] \\
&= \Pr[\text{ packet arrives at } (x,y)] \cdot \Pr[\text{ packet activated } |(x,y)] \\
&= \lambda_{csma}^{RX} \cdot \Pr(\text{ active } |x,y).
\end{aligned}$$

As in Subsection 2.5.1, we use the approximation that all interferers, TX_i, base their backoff decision only on the interference from TX_0. Hence, in order for TX_i to be activated, its receiver, RX_i, must be placed a distance s away from TX_0. Hence, outage occurs if TX_i falls inside $B_3 = B(\mathrm{RX}_0, s) \cap \overline{B(\mathrm{TX}_0, s-R)}$, as shown in Figure 2.6. Integrating $\mu(x, y)$ over B_2 with polar

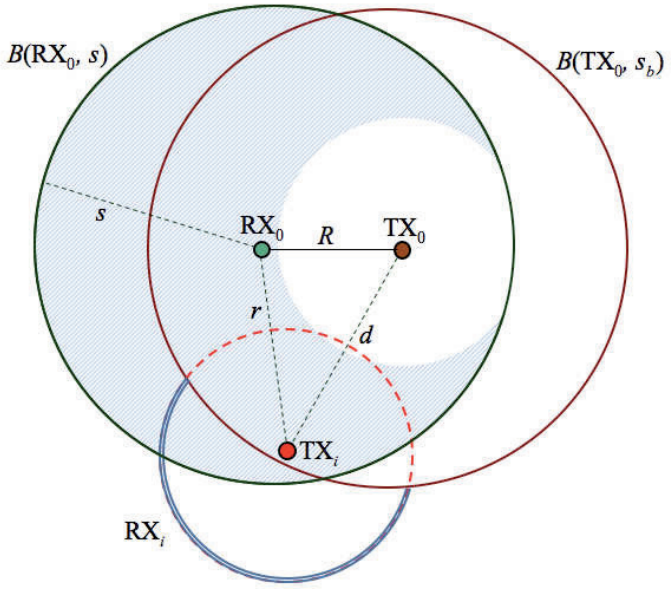

Figure 2.6: The setup used to analyze the outage probability of CSMA_{RX}.

coordinates, yields:

$$\begin{aligned}\mathbb{E}\left[\#\text{ of interferers in } B_3 \text{ during } (0,T)\right] &= \iint_{B_2} \mu(x,y)\,dx\,dy \qquad (2.34)\\ &= \int_{s-R}^{s}\int_{\nu(r)}^{2\pi-\nu(r)} \lambda_{csma}^{RX}\, P(\text{active}|r,\phi)\, r\,dr\,d\phi.\end{aligned}$$

$\nu(r)$ is found by using the cosine rule as described in Subsection 2.5.1. $P(\text{active}|r,\phi)$ is the probability that TX_i initiates its transmission, and is in effect a thinning process of the rate of packet arrivals. Consider Figure 2.7, and the triangle TX_1-RX_0-TX_0. Using the cosine rule, we have: $d = \sqrt{r^2+R^2-2Rr\cos\phi}$. Next, consider the triangle P-TX_1-TX_0. Again by applying the cosine rule, we derive θ to be: $\theta = \cos^{-1}\left(\frac{d^2+R^2-s^2}{2Rd}\right)$. Furthermore, RX_i must be placed outside of $B(\text{TX}_0, s)$. Thus, the probability that an interfering packet is activated is $P(\text{active}|r,\phi) = \frac{2\pi-2\theta}{2\pi}$, as given in Eq. (2.25).

Inserting these expressions back into Eq. (2.34), and using the probability expression $P_{during} = 1 - e^{-\mathbb{E}[\#\text{ of interferers in } B_3]}$, we arrive at Theorem 2.4.

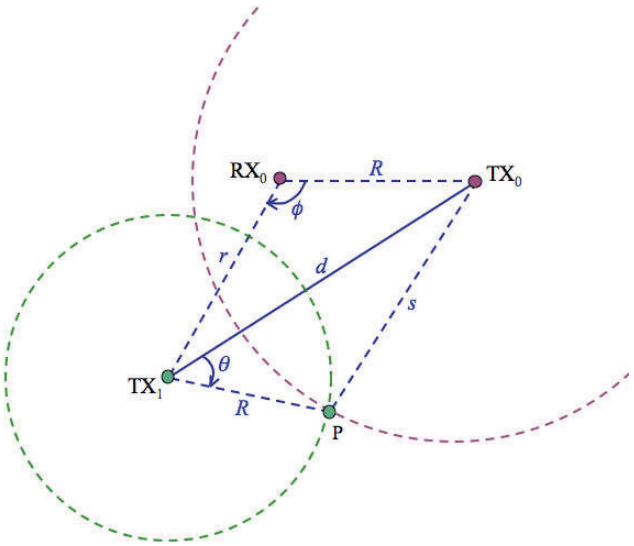

Figure 2.7: The setup used in the derivation of P_{during} for CSMA_{RX}.

2.6 Numerical Results

For the simulations, we employ MATLAB to generate a total of 10000 packets, each of which are located at a random (x, y)-coordinate on 35 m $\times$ 35 m communication domain (which is, compared to the transmission range, a good representation of an infinite network). Transmissions are initiated according to the applied MAC protocol, and depending on other simultaneous transmissions and interferer locations. The outage probability is calculated by dividing the number of packets that are received erroneously after M backoffs and N retransmissions by the total number of transmitted packets. Unless stated otherwise, we set the transmitter-receiver distance $R = 1$ m, the transmission power $\rho = 1$ mW, the path loss exponent $\alpha = 4$, and the SINR threshold $\beta_b = \beta = 0$ dB (which corresponds to $s_b = s \approx R$). The value 0 dB is chosen in order for the analytical outage probability to have little dependence on the path loss exponent α.

The derived formulas for slotted and unslotted ALOHA are plotted in Figure 2.8 for $(M, N) = (1, 0)$. The curves confirm Theorems 2.1 and 2.2, as the analytical results follow the simulations tightly. Moreover, we observe that the slotted system outperforms the unslotted one by approximately a factor of 2. This is consistent with the result obtained in Subsection 2.3.2, as well as from the conventional ALOHA model [10]. The exact outage

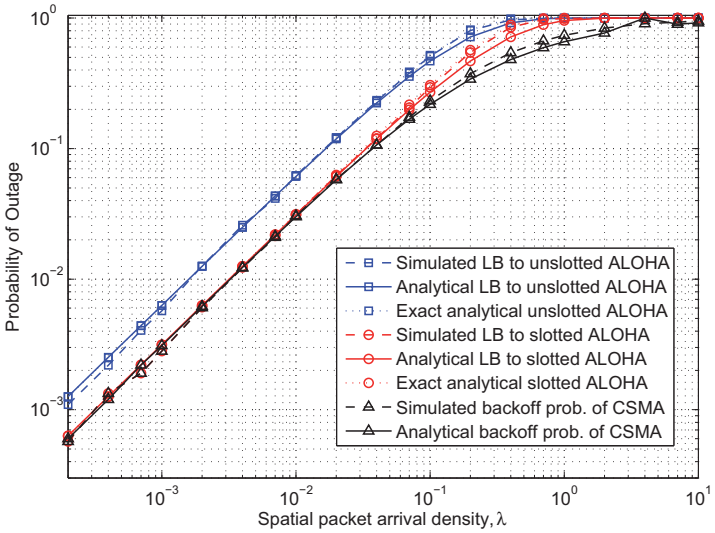

Figure 2.8: Outage probability of ALOHA along with the backoff probability of CSMA, as a function of λ for $(M, N) = (1, 0)$.

probability expressions as given in Eqs. (2.10) and (2.12) are also plotted in Figure 2.8.

Moreover, we observe that the outage probability of ALOHA increases linearly with the number of interferers on the plane (which is equal to the number of packet arrivals), until it reaches a saturation point where $P_{out} \approx 1$. For the sake of the discussions in Section 2.4.1, the backoff probability of CSMA, P_b, is also plotted in Figure 2.8. For low densities, P_b is approximately equal to the outage probability of slotted ALOHA. For higher densities, due to fewer active interferers in CSMA, $P_b < P_{out}(\text{Slotted ALOHA})$.

Figure 2.9 shows the outage probability performance of CSMA_{TX} and CSMA_{RX} for $(M, N) = (1, 0)$ and $(M, N) = (2, 1)$. While the analytical expressions are seen to follow the simulations tightly for $(M, N) = (1, 0)$, some discrepancies are observed for $(M, N) = (2, 1)$. This is due to the fact that the guard zone approximation is used multiple times when $M > 1$ and $N > 0$. For $(M, N) = (1, 0)$, approximately 60% of the outage probability is due to backoffs and 40% is due to errors occurring during an active transmission. Clearly, the addition of several backoffs and retransmissions improves the outage probability performance of CSMA considerably, and this difference increases for lower densities.

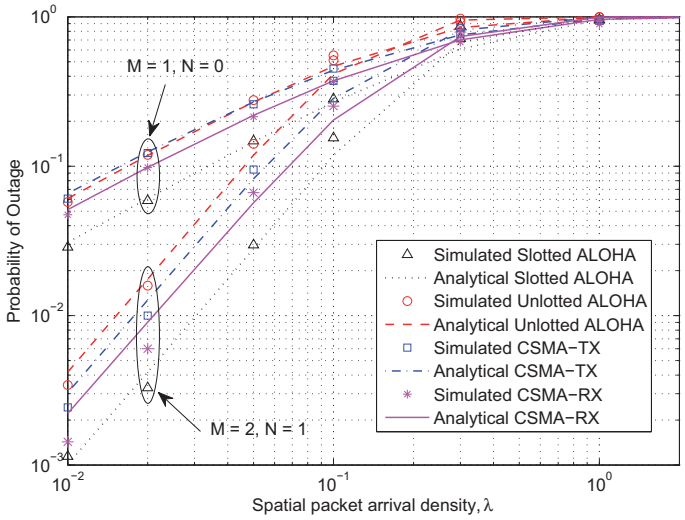

Figure 2.9: Outage probability of ALOHA and CSMA as a function of λ.

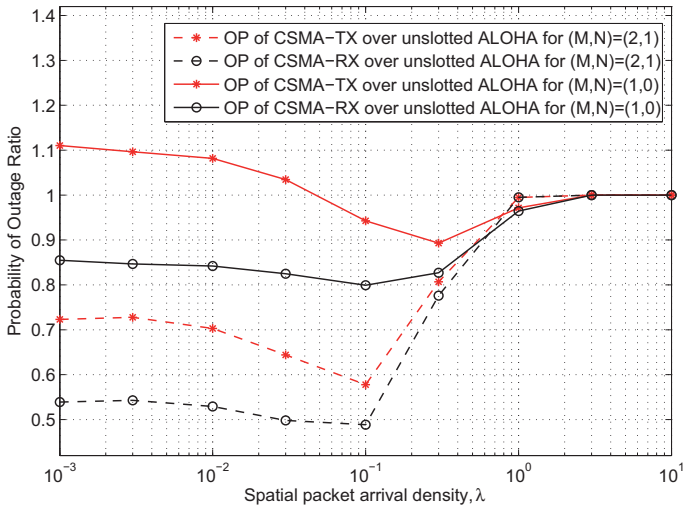

Figure 2.10: Ratio of the outage probability of CSMA over that of unslotted ALOHA as a function of λ.

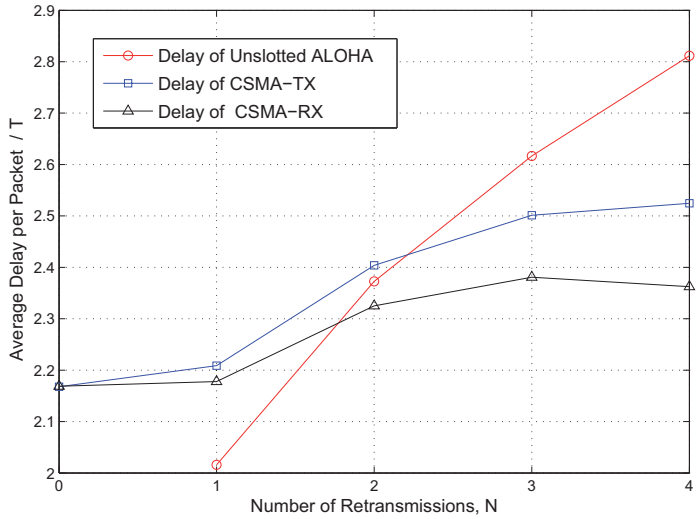

Figure 2.11: Average transmission delay as a function of the number of retransmissions, N for $\lambda = 0.05$, and in CSMA, $M = 3$.

In order to compare the different protocols, in Figure 2.10, the ratio of the outage probability of CSMA_{TX} and CSMA_{RX} over that of slotted ALOHA is plotted for both $(M, N) = (1, 0)$ and $(M, N) = (2, 1)$. Interestingly, we see that for lower densities and $(M, N) = (1, 0)$, CSMA_{TX} actually performs worse than unslotted ALOHA, having about 10% more outage probability. This is due to the exposed node problem, as discussed in Section 2.4.1. The outage probability of slotted ALOHA is almost two orders of magnitude lower than that of CSMA_{TX}, as was also concluded in [38]. However, for higher values of M and N, CSMA_{TX} becomes more efficient than unslotted ALOHA, outperforming it by approximately 25% in terms of outage probability. As the density increases, so does P_b, thus decreasing the level of interference in the channel and making CSMA more advantageous. The introduction of the simple feedback channel in CSMA_{RX} emphasizes the advantage of the backoff property, providing a performance gain of up to 25% compared to CSMA_{TX} when $(M, N) = (1, 0)$ and 20% when $(M, N) = (2, 1)$.

Figure 2.11 shows the performance of the MAC protocols in terms of the average transmission delay per transmitted packet as a function of N, for a fixed density of $\lambda = 0.05$ and $M = 3$. This delay is the average time from

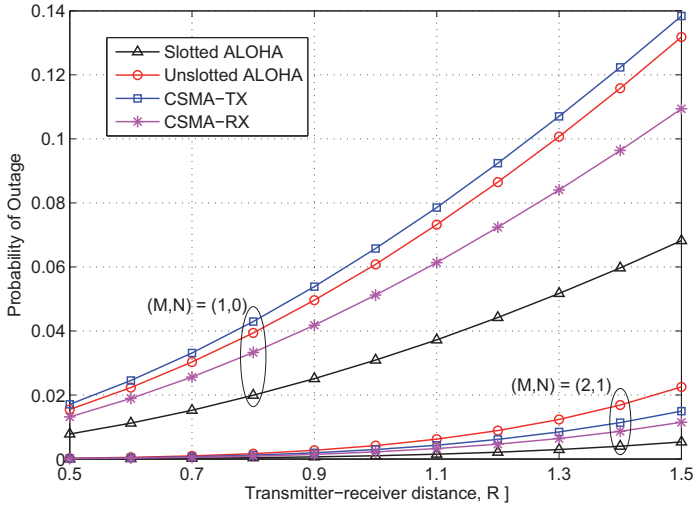

Figure 2.12: Dependence of the outage probability on the transmitter-receiver distance R for $\lambda = 0.01$.

the instant of the packet arrival at the transmitter till the entire packet is received correctly at the receiver, and is solely based on simulations. As seen from the figure, the average delay increases with N, and this rate of increase is highest for ALOHA. E.g., for $N = 1$, the average delay of CSMA_{RX} is approximately 16% *more* than that of unslotted ALOHA, whereas for $N = 4$, CSMA_{RX} yields 32% *lower* delay than ALOHA. This result emphasizes the benefit of using CSMA (in particular CSMA_{RX}) over unslotted ALOHA.

In Figure 2.12, we investigate the behavior of the outage probability as the transmitter-receiver distance, R, varies. For higher values of R, the outage probability increases approximately linearly. Moreover, we note that a change in R has a greater impact on the outage probablity for lower values of M and N. For $(M, N) = (1, 0)$, the rate of increase is approximately 50%, while for $(M, N) = (2, 1)$, it is 22%.

Finally, we evaluate the dependence of the outage probability on the path loss exponent α, as shown in Figure 2.13 for a moderate packet density of $\lambda = 0.05$. When α is very low, the interfering signals are not affected too much from the path loss, and thus, the aggregation of the interference powers becomes too destructive, resulting in a high outage probability. As α increases, the destruction from the aggregate interference powers reduces, and the interference detected becomes closer to that of only one closest in-

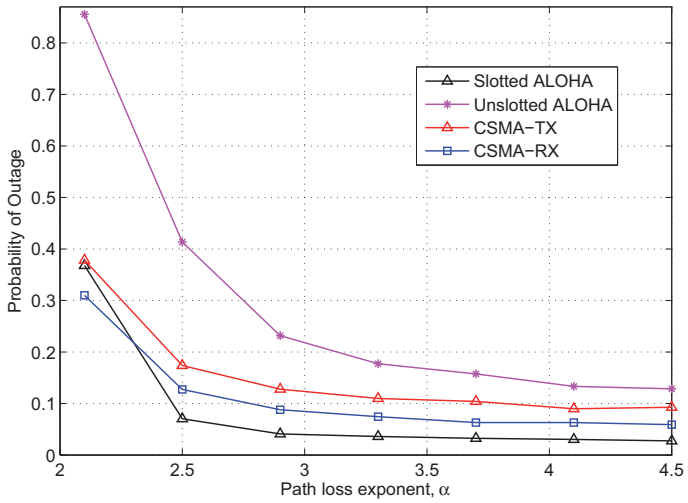

Figure 2.13: Dependence of the outage probability on the path loss exponent α for $\lambda = 0.05$ and $(M, N) = (2, 1)$.

terferer. Consequently, the outage probability converges towards a constant value. Note that this effect is only observed in the simulation, because the analytical results do not consider the aggregate interference.

2.7 Summary

In this chapter, we have considered the performance of the ALOHA and CSMA MAC protocols in terms of outage probability. The ad hoc network model applied for this work represents a communication system in which transmitter-receiver pairs are randomly placed on a 2-D plane, and packets arrive continuously in time based on a 1-D PPP. Having established a new analytical framework for analyzing this network, we derive expressions for the outage probability of slotted and unslotted ALOHA, CSMA with transmitter sensing (CSMA_{TX}) and CSMA with receiver sensing (CSMA_{RX}). Our derived analytical expressions are consistent with the simulations, and an intuitive understanding is established on the benefits that CSMA provides over ALOHA. It is confirmed that CSMA is more effective than ALOHA for higher densities, as there is a greater probability of backoff, and thus less interference in the network.

An interesting result is that when no backoffs or retransmissions are allowed, $CSMA_{TX}$ actually performs worse than unslotted ALOHA for low densities due to the exposed node problem, i.e., transmitters back off in situations where their transmissions would not have caused outage for other packets. By allowing the *receiver* to sense the channel in $CSMA_{RX}$ and inform its transmitter over a control channel whether or not to initiate its transmission, the performance of the conventional CSMA protocol is significantly improved. However, note that this improvement is achieved at the expense of additional feedback (1 bit per packet). Some challenges related to this, which are not considered in our analysis, are collisions between control signals and the usage of extra bandwidth (although this additional bandwidth is significantly small compared to the system bandwidth).

Chapter 3

Impact of Network Characteristics

In this chapter, we evaluate the impact of various channel characteristics on the outage probability performance of the ALOHA and CSMA MAC protocols. In particular, we consider the addition of fading attenuation in infinite ad hoc networks, edge effects in bounded networks (without fading), and finally the influence of fading in bounded networks. Each of these network characteristics has devoted to it a separate section, in the same order as listed above.

The work of this chapter is partly published in [55–57], and partly submitted to IEEE Trans. on Vehicular Communications [58].

3.1 Impact of Fading

The issue of interference is more involved than simply estimating the location of interferers. In most networks, there is also the phenomenon of *fading*, which denotes rapid variations of received signal power due to constructive and destructive addition of the signal's multipath components. This is an additional factor to the path loss, and usually results in significant instantaneous deviation from the expected value of interference obtained from a large-scale path loss model. The introduction of fading often results in degradation of the network performance, and complicates the estimation of the interference powers.

Much work has been done on fading and its effects in communication networks. In [59], Baccelli *et. al.* evaluate the outage capacity of ALOHA

in a Rayleigh-fading environment. The aggregate co-channel interference is characterized under distance attenuation with random fading as a stable random process. The focus of their work is on optimizing the transmit power and the access probability (which is the product of the number of simultaneously successful transmissions per unit space by the average range of each transmission). In [35], the success probability ($P_s = 1 - P_{out}$) of slotted ALOHA is derived in various fading scenarios, obtaining similar results as the formulas we apply in our analysis of unslotted protocols. The work of [35] is extended in [60] to evaluate the transmission capacity and outage probability of a stationary and isotropic Poisson cluster process in the presence of Rayleigh fading. The system evaluates the spread-spectrum systems DS-CDMA and FH-CDMA, and complicated formulas are derived for the performance of clustered networks.

In [61], a new fading model is proposed that combines uncertainties in the transmission distance with small-scale fading. In this model, where transmitters are Poisson distributed and fading is assumed to be Rayleigh, it is established that the effect of fading is a *thinning* in the geographical domain in the same manner as path loss effects. The role of fading on networks with regular topologies and deterministic node placements are considered in [62], specifically for square, triangular, and hexagon networks. Ilow and Hatzinakos [63] consider the impact of random channel effects on the aggregate co-channel interference in an ad hoc network where nodes are distributed according to a PPP. Whereas their focus is on identifying the impact of fading on the parameters of the characteristic function of the interference, we concentrate on the MAC layer design and evaluate the outage probability of various MAC protocols in the presence of fading.

In the same manner as in [18], Weber *et. al.* evaluate in [64] the transmission capacity of slotted ALOHA in a fading ad hoc network with Poisson distributed node locations. It is shown that in the absence of CSI, fading can significantly reduce the transmission capacity. Rather than setting a constraint on the outage probability, as is done in the transmission capacity metric, we evaluate the performance of our ad hoc network in terms of outage probability for given transmission densities. Furthermore, our work extends the results of [35] and [64] to consider the unslotted ALOHA and CSMA protocols.

3.1.1 System Model

The traffic model of this section is similar to the one explained in Section 2.1. That is, packets are generated according a 3-D PPP with a density of *new* packet arrivals of $\lambda = \lambda^s \lambda^t T$ [packets/m^2], where λ^s [nodes/m^2] is the

density of nodes on the 2-D plane, λ^t [packets/sec/node] is the density of packet arrivals in time, and T [sec] is the fixed packet length. Each packet is transmitted with a constant power ρ to its destination, which is located a fixed distance R away[1]. The ALOHA and CSMA protocols are applied in a distributed manner to grant channel access to the packets. Each packet is given M backoffs and N retransmissions before it is dropped and counted to be in outage. Following the same setup as in Chapter 2, we set the sensing threshold of CSMA, β_b, equal to the communication threshold, β, which is specified by the QoS requirement, i.e., $\beta_b = \beta$.

The only difference between the model of this section and the one used in Chapter 2 is the channel model, where we now add fading effects to the path loss attenuation. Although our derivations apply to potentially any fading distribution, we will assume the particular case of Rayleigh fading, as this is the only distribution that yields a closed form expression for the error probability [65] (page 160). Each node i potentially sees interference from all transmitters on the plane, and these independent interference powers are added to the channel noise power, η, resulting in a signal to interference plus noise ratio of

$$\text{SINR}_i^f \;=\; \frac{\rho\, h_{00}\, R^{-\alpha}}{\eta + \sum_i \rho\, h_{0i}\, r_i^{-\alpha}}, \tag{3.1}$$

where r_i and h_{0i} are, respectively, the distance and the fading coefficient between the node under observation (this could be either the transmitter or receiver of the packet we are considering) and the i-th interfering transmitter. h_{00} represents the fading effects between the receiver under observation and its designated transmitter. The summation is over all active interfering transmissions at a particular snapshot in time.

If the received SINR falls below the required SINR threshold β during the packet transmission, the packet is received in *error*. This happens with probability P_{error}^f, given as

$$P_{error}^f \;=\; \Pr\left(\frac{\rho R^{-\alpha} h_{00}}{\eta + \sum_i \rho\, r_i^{-\alpha} h_{0i}} < \beta\right). \tag{3.2}$$

In the following subsections, we derive the outage probability of ALOHA and CSMA based on Eq. (3.2).

[1]For justification of the use of a fixed R, please refer to Subsection 2.1.1. Moreover, it has been rigorously shown in [6] that variable transmit distances in the presence of fading do not result in fundamentally different performances.

3.1.2 The ALOHA Protocol

When introducing fading, we can no longer use the concept of guard zones and distance to evaluate the outage probability. Instead, we consider the probability of having a *dominant* interferer, i.e., one whose received interference power is strong enough to alone cause outage for the receiver under observation, RX_0. Considering a PPP of dominant interferers, and allowing each packet to retransmit up to a maximum of N times, yields the following theorem for slotted ALOHA.

Theorem 3.1

The outage probability of slotted ALOHA in the presence of Rayleigh fading may be approximated by $\tilde{P}_{out}(\textit{Slotted ALOHA}) = \overline{P}_{rt,s}^{N+1}$, *where* $\overline{P}_{rt,s}$ *is the solution to*

$$\overline{P}_{rt,s} \;=\; 1 - \exp\left\{ -\lambda \frac{1-\overline{P}_{rt,s}^{N+1}}{1-\overline{P}_{rt,s}}\, \pi\, R^2\, \beta^{2/\alpha} \frac{2\pi/\alpha}{\sin(2\pi/\alpha)} \right\}. \tag{3.3}$$

Proof: To derive the error probability in Eq. (3.3), define $s^f(h_{00}, h_{0i})$ to be the distance to the *dominant* interferer on the plane, given as

$$s^f(h_{00}, h_{0i}) \;=\; h_{0i}^{1/\alpha} \left(\frac{h_{00} R^{-\alpha}}{\beta} - \frac{\eta}{\rho} \right)^{-1/\alpha}. \tag{3.4}$$

Due to the presence of fading, this distance is clearly a function of the fading coefficients h_{00} and h_{0i}. Since interferers are distributed uniformly in space according to a PPP, we apply the error-probability expression

$$P_{rt,s}(h_{00}, h_{0i}) \;=\; 1 - e^{-\mathbb{E}\left[\#\text{ of interferers within a distance } s^f(h_{00},h_{0i}) \text{ away }\right]}. \tag{3.5}$$

Now, following the same reasoning as for non-fading networks in Section 2.3, we replace s by $s^f(h_{00}, h_{0i})$ in Eq. (2.7).

Taking the expectation with respect to h_{00} and h_{0i}, yields [9]

$$\begin{aligned} \overline{P}_{rt,s} &= 1 - \mathbb{E}\Big[\exp\left\{ -\lambda_{slotted}\, \pi\, h_{0i}^{\frac{2}{\alpha}} \left(\frac{h_{00} R^{-\alpha}}{\beta} - \frac{\eta}{\rho} \right)^{-\frac{2}{\alpha}} \right\} \Big] \\ &\approx 1 - \exp\left\{ -\lambda_{slotted}\, \pi\, \mathbb{E}\left[h_{0i}^{\frac{2}{\alpha}} \right] \mathbb{E}\left[\left(\frac{h_{00} R^{-\alpha}}{\beta} - \frac{\eta}{\rho} \right)^{-\frac{2}{\alpha}} \right] \right\}. \end{aligned} \tag{3.6}$$

where $\lambda_{slotted} = \lambda \frac{1-\overline{P}_{rt,s}^{N+1}}{1-\overline{P}_{rt,s}}$. As path loss and fading are assumed to be the main sources of signal degradation, for the sake of simplifying the analysis,

we set the noise power η to 0. This results in

$$\overline{P}_{rt,s} \approx 1 - e^{-\lambda \frac{1-\overline{P}_{rt,u}^{N+1}}{1-\overline{P}_{rt,u}} \pi R^2 \beta^{2/\alpha} \mathbb{E}\left[h_{0i}^{2/\alpha}\right] \mathbb{E}\left[h_{00}^{-2/\alpha}\right]}. \tag{3.7}$$

For Rayleigh fading channels, $\mathbb{E}\left[h_{00}^{-2/\alpha}\right]$ and $\mathbb{E}\left[h_{0i}^{2/\alpha}\right]$ are Gamma functions [64], and thus we have that

$$\mathbb{E}\left[h_{00}^{-2/\alpha}\right] \mathbb{E}\left[h_{0i}^{2/\alpha}\right] = \frac{2\pi/\alpha}{\sin(2\pi/\alpha)}. \tag{3.8}$$

Note that other fading distributions may be assumed, such as Rician or Nakagami-m. However, if the received signal strength from the desired transmitter is not Rayleigh fading, there are no known closed-form expressions for the outage [65]. Log-normal shadowing was considered in [64], and an integral form expression was derived for the outage probability of slotted ALOHA.

Inserting Eq. (3.8) back into Eq. (3.7), we arrive at Eq. (3.3). With a maximum of N retransmissions for each packet, the outage probability is equal to $\overline{P}_{rt,s}^{N+1}$. □

In the same manner as in Subsection 2.3.2, we also evaluate the performance of unslotted ALOHA. Accounting for the partial overlap of a packet with its dominant interfering packets, we obtain the following theorem.

Theorem 3.2

The outage probability of unslotted ALOHA in the presence of Rayleigh fading may be approximated by $\tilde{P}_{out}(\textit{Unslotted ALOHA}) = \overline{P}_{rt,u}^{N+1}$, *where* $\overline{P}_{rt,u}$ *is the solution to*

$$\overline{P}_{rt,u} = 1 - \exp\left\{-2\lambda \frac{1-\overline{P}_{rt,u}^{N+1}}{1-\overline{P}_{rt,u}} \pi R^2 \beta^{2/\alpha} \frac{2\pi/\alpha}{\sin(2\pi/\alpha)}\right\}. \tag{3.9}$$

Proof: In the same manner as in the case of non-fading, as explained in the proof of Theorem 2.2, in unslotted ALOHA, outage occurs if the received SINR falls below β either at the start of the packet or at any time during its transmission. This means that rather than considering packet arrivals only in $[-T, 0)$ (as is the case for slotted ALOHA, given in Theorem 3.1), we now consider the period $[-T, T)$. Due to independence between packet arrivals in each slot (of length T), we arrive at $\overline{P}_{rt,u}$ in Eq. (3.9). Given N retransmissions for each packet, the outage probability becomes $\overline{P}_{rt,u}^{N+1}$. □

For lower densities and when $\frac{1-\overline{P}_{rt,s}^{N+1}}{1-\overline{P}_{rt,s}} \approx \frac{1-\overline{P}_{rt,u}^{N+1}}{1-\overline{P}_{rt,u}} \approx 1$, we may apply the Taylor expansion formula on Eqs. (3.3) and (3.9), obtaining

$$\overline{P}_{rt,s} \approx \lambda\, \pi\, R^2 \beta^{2/\alpha}\, \frac{2\pi/\alpha}{\sin(2\pi/\alpha)} \quad \wedge \quad \overline{P}_{rt,u} \approx 2\,\lambda\, \pi\, R^2 \beta^{2/\alpha}\, \frac{2\pi/\alpha}{\sin(2\pi/\alpha)}$$

This shows that for lower densities, unslotted ALOHA is outperformed in terms of outage probability by its slotted version, by a factor of 2^{N+1}.

3.1.3 The CSMA Protocol

In this subsection, we derive the outage probability in the presence of fading for both versions of the CSMA protocol discussed in Chapter 2, namely CSMA_{TX}, where the transmitter performs the channel sensing and makes the backoff decision, and CSMA_{RX}, where the receiver is the decision-maker.

3.1.3.1 Outage Probability of CSMA_{TX}

With M backoffs and N retransmission attempts per packet, the outage probability of CSMA_{TX} is given by the following theorem.

Theorem 3.3
The outage probability of $CSMA_{TX}$ in the presence of Rayleigh fading is given by

$$P_{out}(CSMA_{TX}) \;=\; \overline{P}_b^{\,M} + \left(1 - \overline{P}_b^{\,M}\right) \overline{P}_{rt1}\, \overline{P}_{rt}^{\,N}, \tag{3.10}$$

where:

- $\overline{P}_b$ *is the average backoff probability, approximated by the solution to*

$$\overline{P}_b \;=\; 1 - e^{-\lambda\left(1-\overline{P}_b^{\,M}+\left(1-\overline{P}_b^{\,M}\right)\overline{P}_{rt1}\,\frac{1-\overline{P}_{rt}^{\,N}}{1-\overline{P}_{rt}}\right)\pi R^2\beta^{2/\alpha}\frac{2\pi/\alpha}{\sin(2\pi/\alpha)}}. \tag{3.11}$$

- $\overline{P}_{rt} \;=\; \mathbb{E}_{h_{00}}\left[\overline{P}_b + \left(1-\overline{P}_b\right) P_{during}(h_{00})\right]$ *is the average probability that a packet is received in error during a retransmission attempt. $P_{during}(h_{00})$ is the probability that the error has occurred at some $t \in (0, T)$, approximated by*

$$\tilde{P}_{during}(h_{00}) = 1 - e^{-\int_0^\infty 2\pi\lambda_{csma}^{TX}\left(1-\exp\left\{-\frac{\mathbb{E}[h_{ii}]R^{-\alpha}r^{\alpha}}{\beta}\right\}\right)\exp\left\{-\frac{h_{00}R^{-\alpha}r^{\alpha}}{\beta}\right\}rdr} \tag{3.12}$$

- $\overline{P}_{rt1} = \mathbb{E}_{h_{00}}\left[P_{rx|transmit}(h_{00}) + \left(1 - P_{rx|transmit}(h_{00})\right) P_{during}(h_{00})\right]$ *is the probability that the packet is received in error at its first transmission attempt.* $P_{rx|transmit}(h_{00})$ *is the probability that the received packet is in outage upon arrival, approximated by*

$$\tilde{P}_{rx|transmit}(h_{00}) = \overline{P}_b \left[1 - \frac{1}{\pi s^{f2}} \left(2s^{f2}\cos^{-1}\left(\frac{R}{2s^f}\right) - Rs^f\sqrt{1 - \frac{R^2}{4s^{f2}}}\right)\right]. \tag{3.13}$$

  where $s^f = s^f(h_{00}, \mathbb{E}[h_{0i}])$ *is given by Eq.* (3.4).
- *The density of packets attempting to access the channel is given by*

$$\lambda_{csma}^{TX} \approx \lambda \left[\frac{1 - \overline{P}_b^M}{1 - \overline{P}_b} + (1 - \overline{P}_b^M)\,\overline{P}_{rt1}\,\frac{1 - \overline{P}_{rt}^N}{1 - \overline{P}_{rt}}\right]. \tag{3.14}$$

Proof: The expression for the total outage probability of CSMA_{TX} is as explained in Subsection 2.5.1, with P_b, P_{rt1}, and P_{rt} being replaced by their average values with respect to h_{00} and h_{0i}, denoted by $\overline{P}_b$, $\overline{P}_{rt1}$, and $\overline{P}_{rt}$, respectively. To derive the average backoff probability of CSMA_{TX}, $\overline{P}_b$, we note that the sensing at the start of the packet is dependent on the number of packet arrivals during the last T seconds. Thus, we apply Eq. (3.3), with the density of *active* transmissions as derived in Eq. (2.20). Assuming that the active interferers are still Poisson distributed (an approximation that is proven to be reasonable by our Monte Carlo simulations), we have that

$$\overline{P}_b^f = 1 - \exp\left\{-\lambda_{active}\,\pi\,R^2\,\beta^{2/\alpha}\frac{2\pi/\alpha}{\sin(2\pi/\alpha)}\right\}, \tag{3.15}$$

where we have applied the result $\mathbb{E}\left[h_{00}^{-2/\alpha}\right]\mathbb{E}\left[h_{0i}^{2/\alpha}\right] = \frac{2\pi/\alpha}{\sin(2\pi/\alpha)}$, as explained in the proof of Theorem 3.1.

Next, we derive an expression for the probability that a packet goes into outage at some time during its transmission, denoted by $P_{during}(h_{00})$. This is found by considering all the active dominant interferers, TX_i, on the plane (i.e., all transmitters that started their transmissions during the last T seconds, and that each can alone cause outage for the ongoing packet transmission of TX_0-RX_0):

$$\begin{aligned}\mu^f &= \text{Intensity of active dominant interferers for } \text{RX}_0 \qquad (3.16)\\ &= \Pr\left(\text{TX}_i \text{ placed at } (x,y) \text{ during } (0,T]\right)\Pr\left(\text{TX}_i \text{ activated} \mid (x,y)\right)\\ &\quad \times \Pr\left(\text{TX}_i \text{ causes outage for } \text{RX}_0 \mid \text{TX}_i \text{ active at } (x,y)\right).\end{aligned}$$

The first term in (3.16) is equal to λ_{csma}^{TX}. To derive the second term, we assume that the interferer TX_i makes its backoff decision based on the interference from TX_0 only. This approximation is reasonable, because once TX_i is a dominant interferer for RX_0, it is likely that TX_0 is a dominant interferer for RX_i (due to the distance-dependence of the outage probability). Moreover, we assume that the distance TX_i-RX_0 is approximately equal to the distance TX_0-RX_i, denoted by r. This yields:

$$\begin{aligned}\Pr(\text{TX}_i \text{ activated} \mid (x,y), h_{ii}) &= \Pr(\text{SINR}_i \geq \beta \mid (x,y), h_{ii}) \\ &\geq \Pr(\text{SINR}_i \geq \beta \text{ based on TX}_0 \text{ only} \mid (x,y), h_{ii}) \\ &= \Pr(h_{i0} \leq \frac{h_{ii} R^{-\alpha} r^{\alpha}}{\beta} \mid (r,\phi), h_{ii}) \\ &= F_{H_i}\left(\frac{h_{ii} R^{-\alpha} r^{\alpha}}{\beta}\right), \end{aligned} \tag{3.17}$$

where $F_{H_i}(h_{i0})$ is the cdf of h_{i0}. Finally, we derive an expression for the last term of Eq. (3.16):

$$\begin{aligned}&\Pr\left(\text{TX}_i \text{ causes outage for RX}_0 \mid \text{TX}_i \text{ active at } (x,y), h_{00}\right) \\ &\qquad = \Pr\left(\text{SINR}_0 < \beta \mid \text{TX}_i \text{ active at } (x,y)\right) \\ &\qquad = \Pr\left(h_{0i} > \frac{h_{00} R^{-\alpha} r^{\alpha}}{\beta} \mid \text{TX}_i \text{ active at } (r,\phi), h_{00}\right) \\ &\qquad = 1 - F_{H_i}\left(\frac{h_{00} R^{-\alpha} r^{\alpha}}{\beta}\right). \end{aligned} \tag{3.18}$$

Inserting Eqs. (3.17) and (3.18) back into Eq. (3.16) yields:

$$\begin{aligned}\mu^f &\approx \int_0^{\infty}\int_0^{2\pi} \lambda_{csma}^{TX} F_{H_i}\left(\frac{h_{ii} R^{-\alpha} r^{\alpha}}{\beta}\right)\left[1 - F_{H_i}\left(\frac{h_{00} R^{-\alpha} r^{\alpha}}{\beta}\right)\right] r\, d\phi\, dr \\ &= \int_0^{\frac{h_{ii} R^{-\alpha} r^{\alpha}}{\beta}} f_{H_i}(h_{0i})\, dh_{0i} \int_{\frac{h_{00} R^{-\alpha} r^{\alpha}}{\beta}}^{\infty} f_{H_i}(h_{i0})\, dH_i. \end{aligned} \tag{3.19}$$

Assuming we have a Rayleigh fading channel, h_{i0} and h_{0i} are exponentially distributed, with pdf: $f_{H_i}(h) = \zeta e^{-\zeta h}$, where $\frac{1}{\zeta}$ is the mean value of H_i. The expected total number of interferers that can alone cause outage for the packet of RX_0 is then

$$\begin{aligned}\mathbb{E}\left[\,\#\text{ dominant interferers for RX}_0 \mid h_{00}, h_{ii}\right] &= \iint_A \mu^f\, r\, dr\, d\phi \\ &= \int_0^{\infty}\int_0^{2\pi} \lambda_{csma}^{TX}\left(1 - e^{-\frac{\mathbb{E}[h_{ii}] R^{-\alpha} r^{\alpha}}{\beta}}\right) e^{-\frac{h_{00} R^{-\alpha} r^{\alpha}}{\beta}}\, r\, d\phi\, dr. \end{aligned}$$

Based on the Poisson distribution of packets, we derive the probability that a packet is received in error at some time during its transmission to be

$$\overline{P}_{during} \;=\; 1 - \mathbb{E}_{h_{00},h_{ii}}\left[e^{-\iint_A \mu^f \; r \; dr \; d\phi}\right]. \tag{3.20}$$

This is given by Eq. (3.12).

To find $P_{rx|transmit}(h_{00})$, we approximate this by considering a portion of the probability that the packet is in error at the start of its transmission, $\overline{P}_b$. To derive this portion, we treat the area within which there is a probability of having a dominant interferer at the start of the packet, given h_{00} and h_{0i}, as a circle with radius $s^f = s^f(h_{00}, [h_{0i}])$. This probability is then equal to $\frac{\text{area of } B(\text{RX}_0, s^f) \cap \overline{B(\text{TX}_0, s^f)}}{\pi {s^f}^2}$, which yields Eq. (3.13). □

Due to the interdependence of the different probability expressions in Theorem 3.3, their values are found through numerical iterations, in the same manner as was described in Chapter 2. This procedure was illustrated in Figure 2.3.

3.1.3.2 Outage Probability of CSMA$_{\text{RX}}$

Allowing the receiver to sense the channel and make the backoff decision, as in CSMA$_{\text{RX}}$, improves the performance over that of CSMA$_{\text{TX}}$, as it ensures that the packet is not in error at the start of its first transmission attempt. In the same manner as for CSMA$_{\text{TX}}$, we derive the outage probability of CSMA$_{\text{RX}}$ as expressed by the following theorem.

Theorem 3.4

The outage probability of CSMA$_{RX}$ in the presence of Rayleigh fading is given by

$$P_{out}(CSMA_{RX}) \;=\; \overline{P}_b^M + \left(1 - \overline{P}_b^M\right) \overline{P}_{during}\, \overline{P}_{rt}^N, \tag{3.21}$$

where:

- $\overline{P}_b$ *is the average backoff probability, approximated by*

$$\overline{P}_b \;=\; 1 - e^{-\lambda\left(1-\overline{P}_b^M + \left(1-\overline{P}_b^M\right)\overline{P}_{during}\frac{1-\overline{P}_{rt}^N}{1-\overline{P}_{rt}}\right)\pi R^2 \beta^{2/\alpha}\frac{2\pi/\alpha}{\sin(2\pi/\alpha)}}. \tag{3.22}$$

- $\overline{P}_{rt} \;=\; \mathbb{E}_{h_{00}}\left[\overline{P}_b + \left(1-\overline{P}_b\right) P_{during}(h_{00})\right]$ *is the average probability that a packet is received in error after a retransmission attempt.* $\overline{P}_{during} =$

$\mathbb{E}_{h_{00}}\left[P_{during}(h_{00})\right]$ *is the average probability that the error has occurred at some* $t \in (0,T)$*, where* $P_{during}(h_{00})$ *is approximated by*

$$\tilde{P}_{during}(h_{00}) = 1 - e^{-\int_0^\infty 2\pi\lambda_{csma}^{RX}\left(1-\exp\left\{-\frac{\mathbb{E}[h_{ii}]R^{-\alpha}r^{\alpha}}{\beta}\right\}\right)\exp\left\{-\frac{h_{00}R^{-\alpha}r^{\alpha}}{\beta}\right\}rdr} \quad (3.23)$$

- *The density of packets attempting to access the channel is given by*

$$\lambda_{csma}^{RX} \approx \lambda\left[\frac{1-\overline{P}_b^M}{1-\overline{P}_b} + (1-\overline{P}_b^M)\,\overline{P}_{during}\,\frac{1-\overline{P}_{rt}^N}{1-\overline{P}_{rt}}\right]. \quad (3.24)$$

Proof: The proof of Theorem 3.4 is similar to that of Theorem 3.3. The only difference is that $\overline{P}_{rx|transmit}(h_{00}) = 0$, resulting in $\overline{P}_{rt1} = \overline{P}_{during}$. This is because once the receiver decides to transmit, it is sure to not to be in outage at the start of its first transmission attempt. □

3.1.4 Numerical Results

Monte Carlo simulations are generated using MATLAB, to confirm the derived expressions of this section. The averaging is performed over 4000 channel instances[2]. Unless stated otherwise, we use the following parameter values: fixed transmitter-receiver distance $R = 1$ m, transmission power $\rho = 1$ mW, path-loss exponent $\alpha = 4$, SINR threshold $\beta_b = \beta = 0$ dB, fading with parameter $\zeta = 1$, number of backoffs $M = 2$, and number of retransmissions $N = 1$.

Figure 3.1 shows the outage probability of all the MAC protocols in the presence of fading. As expected, CSMA_{RX} yields the lowest outage probability of all the continuous-time protocols. For $(M,N) = (1,0)$ and low transmission densities (i.e., when $\lambda \ll 1$), approximately 60% of the total outage probability of CSMA_{RX} is due to backoff, and 40% is due to outage occurring during transmission. The effect of fading on the backoff probability can be observed by the effect that fading has on ALOHA for low densities. Fading also has an impact on the hidden and exposed node problems, which are intensified by the fact that new packet arrivals base their decisions on their own channel conditions, and are not concerned with the destruction they cause for other active packet transmissions on the plane.

As was also the case in non-fading networks, when $(M,N) = (1,0)$, the outage probability of CSMA_{TX} is 10% higher than that of unslotted

[2]This number is lower than for non-fading networks due to memory limitations of MATLAB.

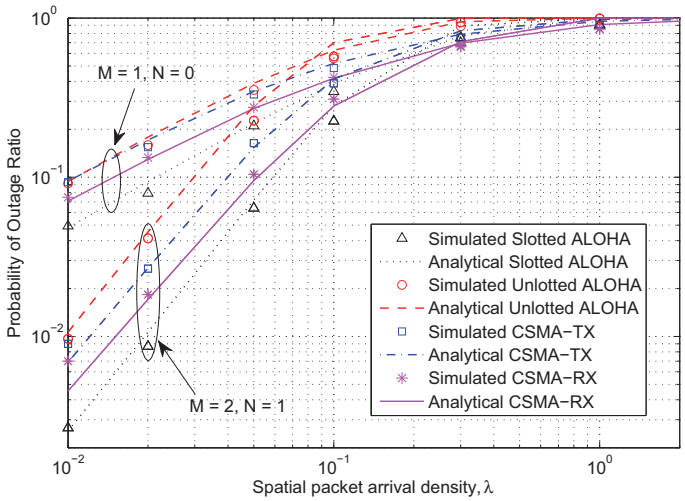

Figure 3.1: Outage probability of ALOHA and CSMA as a function of the packet arrival density λ.

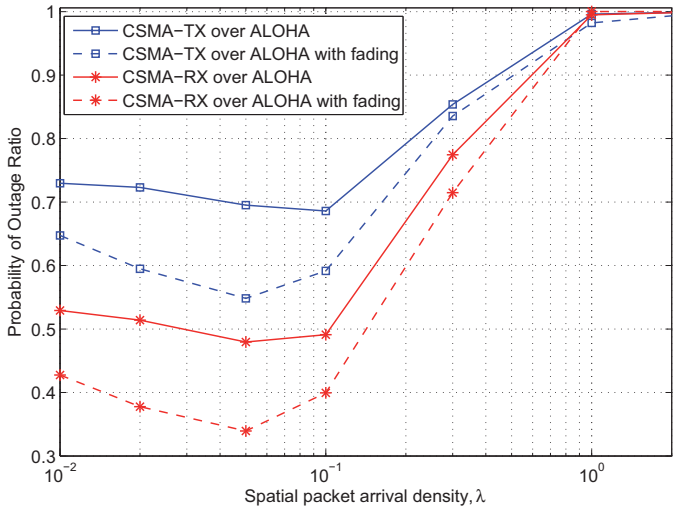

Figure 3.2: Outage probability ratio of CSMA over unslotted ALOHA as a function of λ for $(M, N) = (2, 1)$.

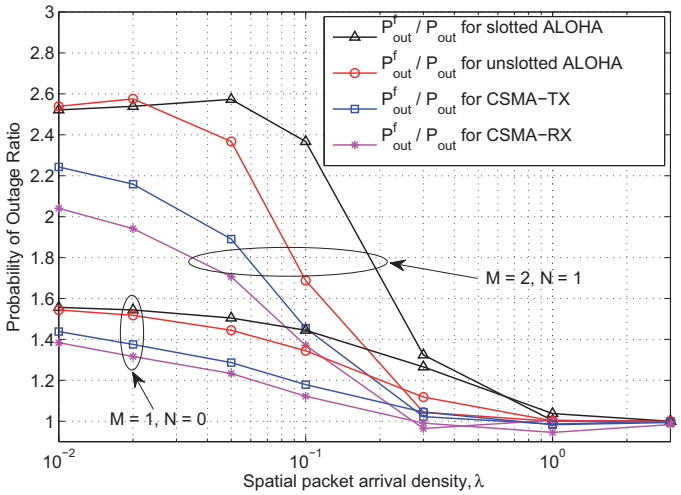

Figure 3.3: Outage probability with fading over outage probability without fading, as a function of λ.

ALOHA. This is due to the exposed node problem. As the density of nodes increases, however, the benefit of channel sensing becomes more evident, and CSMA_{TX} can then provide up to 18% less outage probability. The simple feedback channel introduced in CSMA_{RX} results in significant improvement in the performance of CSMA_{TX}, by approximately 30% for low densities. Note that the outage probability of CSMA_{RX} is primarily due to the hidden node problem, while the outage probability of CSMA_{TX} is due to both the hidden and exposed node problems. As λ increases, the exposed node problem of CSMA_{TX} is reduced, while the hidden node problem increases. Similarly, for higher values of M and N, the hidden and exposed node problems become less destructive.

As M and N increase, so does the difference between the various protocols. This difference is emphasized in Figure 3.2 for $(M, N) = (2, 1)$. Compared to unslotted ALOHA, CSMA_{TX} provides up to 35% lower outage probability as opposed to 28% in non-fading networks. CSMA_{RX} performs even better, providing up to 65% improvement (compared to 50% in the absence of fading).

Figure 3.3 illustrates the impact of fading on the outage probability of ALOHA and CSMA. Compared to a non-faded network, the average outage probability in the presence of fading increases by up to 58% for ALOHA

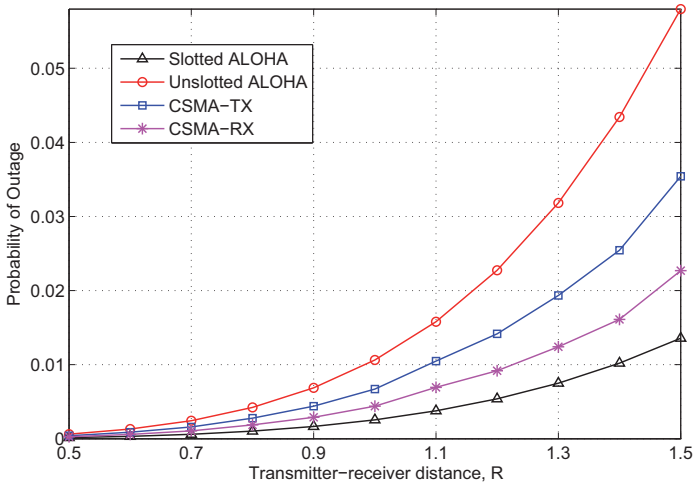

Figure 3.4: Behavior of the outage probability in the presence of fading as a function of R, with $\lambda = 0.01$ and $(M, N) = (2, 1)$.

and up to 47% for CSMA. When $(M, N) = (2, 1)$, the impact of fading increases, yielding up to 160% higher outage probability for ALOHA and approximately 120% for CSMA. This is to be expected, as independent channel fading is known to degrade communication links, at least as long as we cannot apply techniques such as opportunistic scheduling. As the transmission density increases, the difference between the outage probability of a fading network and a non-fading network decreases. This is because for higher densities, the outage probability approaches 1 in both cases, meaning that both networks have saturated.

Finally, in Figure 3.4, we investigate the dependence of a fading network on the transmitter-receiver distance. Although at a higher outage probability, the rate of increase with R is approximately the same as that in non-fading networks, observed in Section 2.6. On a logarithmic scale, this increase is linear.

3.2 Bounded Networks

Assuming an *infinite* network, as has been done thus far in this thesis, is not always an appropriate model. In many ad hoc networks, such as military battlefields or sensor networks, the communication domain is bounded. Interference, being one of the most challenging issues in the design of ad hoc networks, is closely related to the network topology, such as the physical size and shape of the communication domain. These factors, as well as the location of the node of interest, play a great role in the amount of interference that this node detects.

Only a few works have evaluated the significance of the boundedness of regions and the impact of the node position. In [66], distance distributions of uniformly and Gaussian distributed nodes in a rectangular area are considered. Other network types and shapes, such as Manhattan networks, hypercubes, and shufflenets are investigated in [67]. In [68], the capacity of networks with a regular structure, using slotted ALOHA, is evaluated. For linear networks, it is shown that the capacity is almost constant with respect to the network size. In two-dimensional networks, on the other hand, the capacity grows in proportion to the square root of the area of the deployment region. Moreover, the mean transmission distance between two randomly selected points in a square Manhattan network of unit size is determined to be 2/3.

The edge effects due to the finiteness of deployment region have been initially considered in [69]. Extensions of this work can be seen in [70], where the specific case of a square domain is analyzed in detail. With geometrical considerations, the probability that a randomly chosen node is not isolated, is derived. However, the two latter works only focus on connectivity, while no indication is given about its implications on the performance at MAC layer. The MAC layer perspective is added in [56], where we evaluate the impact of edge effects in a bounded square network. The MAC protocols considered in [56] are simplified in that no backoffs or retransmissions are allowed. This restriction is removed in this section.

3.2.1 System Model

Our model resembles that of Chapter 2, with the difference of having a bounded region. Consider a finite 2-D region $\mathcal{R}$, where transmitter nodes are deployed according to a homogeneous PPP with spatial node density λ^s [nodes/m^2]. At each transmitter, data packets of a fixed duration T arrive in time according to an independent 1-D PPP with temporal density λ^t [packets/sec/node]. As before, the spatial density of *new* packets ar-

rivals at each time instant is $\lambda = \lambda^s \lambda^t T$ [packets/m^2]. Upon the formation of each packet, it is transmitted with constant power ρ to its intended receiver, which is located a fixed distance R away. The packet transmissions are initiated according to either the ALOHA or CSMA MAC protocol. The SINR threshold determining an erroneous packet reception is β, and the threshold based on which the backoff decision in CSMA is made is $\beta_b = \beta$. Each packet is given N retransmissions, and in the case of CSMA M backoffs, before it is dropped and counted to be in outage.

For the channel model, we again consider only deterministic path loss attenuation effects (with exponent $\alpha > 2$). That is, additional fading and shadowing effects are ignored. Each receiver potentially sees interference from all transmitters, and these independent interference powers are added to the channel noise η, resulting in

$$\text{SINR}_i = \frac{\rho R^{-\alpha}}{\eta + \sum_i \rho\, r_i^{-\alpha}}, \tag{3.25}$$

where r_i is the distance between the node under observation and the i-th interfering transmitter, and the sum is over all active interferers on the bounded plane, $\mathcal{R}$. If the received SINR falls below β at any time during a packet transmission, that transmission is said to be received *erroneously* with probability P_{error};

$$P_{error} = \Pr\left(\frac{\rho\, R^{-\alpha}}{\eta + \sum_i \rho\, r_i^{-\alpha}} < \beta\right). \tag{3.26}$$

The outage probability of the various MAC protocols is derived as different combinations of error events.

In order to address the problem of edge effects in space, we devote our attention to a square domain of size $L \times L$, denoted as $\mathcal{D}$, and we only consider those nodes that fall inside this region. The origin of our coordinates system is placed in the center of the square. For the sake of the analysis carried out in the following subsections, we consider the tessellation proposed in [70], i.e., we divide our network domain into eight circular subregions, as shown in Figure 3.5. The advantage of this tessellation is that we can switch to polar coordinates very easily, owing to the decomposition of the surface into sectors of annuli. Specifically, given whatever node position (x, y) inside the square, we may obtain the number of interferers inside a circle of radius r centered at (x, y), by considering the area of overlap between this circle and the domain $\mathcal{D}$. Denoting the fraction of the circle overlapping $\mathcal{D}$ by $\Delta\mathcal{D}$, we have that

$$\Delta\mathcal{D} = \frac{\theta_i(r, x, y)}{\pi}, \tag{3.27}$$

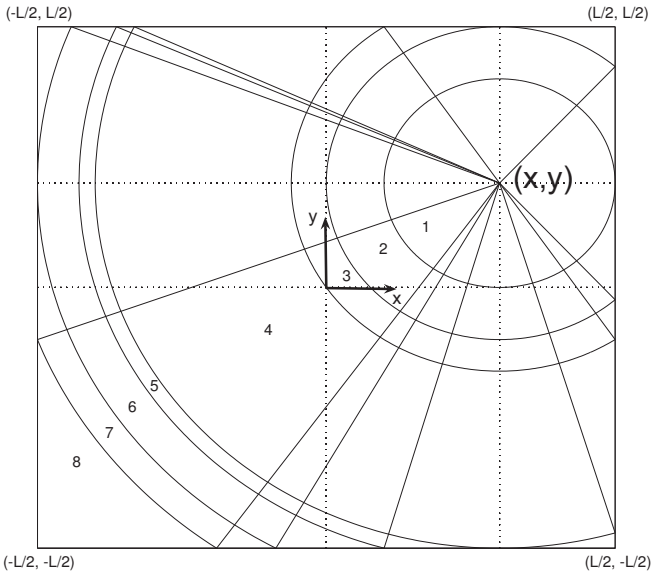

Figure 3.5: Partitioning of the finite area into 8 circular subregions.

where $\theta_i(r, x, y)$ is given in Table 3.2. $\theta_i(r, x, y)$ is dependent on the size of r, which ranges from $r_{1,i}(x, y)$ to $r_{2,i}(x, y)$ for each subregion i of the 8 sectors of $\mathcal{D}$. These are defined in Table 3.1. The entries of these tables were derived in [70].

3.2.2 The ALOHA Protocol

The evaluation of outage probability consists of solving Eq. (3.26) in the specific case of the square domain $\mathcal{D}$. However, the consideration of all interfering contributions in the denominator of Eq. (3.26) turns out to be unpractical. For this reason we focus on the probability of having a single *closest* interferer, whose received interference power alone is strong enough to result in outage for the packet of RX_0. This technique was described in details in Chapter 2. Hence, our problem is now reduced to finding the areas of intersection between the circles $B(\mathrm{RX}_0, s)$, $B(\mathrm{TX}_0, s)$, and the square domain $\mathcal{D}$ for every (x, y)-coordinate of the network.

Following the concept of guard zones, as was explained in Section 2.2, we incorporate the boundedness of the network into the geometrical anal-

Table 3.1: Boundary values for r in the eight regions.

Region	Range: $r_{1,i}(x,y) \leq r \leq r_{2,i}(x,y)$
1	$0 \leq r \leq \frac{L}{2} - x$
2	$\frac{L}{2} - x \leq r \leq \frac{L}{2} - y$
3	$\frac{L}{2} - y \leq r \leq \sqrt{\left(\frac{L}{2}-x\right)^2 + \left(\frac{L}{2}-y\right)^2}$
4	$\sqrt{\left(\frac{L}{2}-x\right)^2 + \left(\frac{L}{2}-y\right)^2} \leq r \leq \frac{L}{2} + y$
5	$\frac{L}{2} + y \leq r \leq \sqrt{\left(\frac{L}{2}-x\right)^2 + \left(\frac{L}{2}+y\right)^2}$
6	$\sqrt{\left(\frac{L}{2}-x\right)^2 + \left(\frac{L}{2}+y\right)^2} \leq r \leq \frac{L}{2} + x$
7	$\frac{L}{2} + x \leq r \leq \sqrt{\left(\frac{L}{2}+x\right)^2 + \left(\frac{L}{2}-y\right)^2}$
8	$\sqrt{\left(\frac{L}{2}+x\right)^2 + \left(\frac{L}{2}-y\right)^2} \leq r \leq \sqrt{\left(\frac{L}{2}+x\right)^2 + \left(\frac{L}{2}+y\right)^2}$

Table 3.2: Boundary values for the angle θ in the eight subregions.

Region	$\theta_i(r,x,y)$
1	π
2	$\frac{\pi}{2} + \arcsin \frac{\frac{L}{2}-x}{r}$
3	$\frac{\pi}{2} + \arcsin \frac{\frac{L}{2}-x}{r} - \arccos \frac{\frac{L}{2}-y}{r}$
4	$\frac{\pi}{2} + \frac{1}{2}\left(\arcsin \frac{\frac{L}{2}-x}{r} - \arccos \frac{\frac{L}{2}-y}{r}\right)$
5	$\frac{\pi}{2} - \arccos \frac{\frac{L}{2}+y}{r} + \frac{1}{2}\left(\arcsin \frac{\frac{L}{2}-x}{r} - \arccos \frac{\frac{L}{2}-y}{r}\right)$
6	$\frac{\pi}{2} - \frac{1}{2}\left(\arccos \frac{\frac{L}{2}+y}{r} + \arccos \frac{\frac{L}{2}-y}{r}\right)$
7	$\frac{1}{2}\left(\arcsin \frac{\frac{L}{2}-y}{r} + \arcsin \frac{\frac{L}{2}+y}{r}\right) - \arccos \frac{\frac{L}{2}+x}{r}$
8	$\frac{1}{2}\left(\arcsin \frac{\frac{L}{2}+y}{r} - \arccos \frac{\frac{L}{2}+x}{r}\right)$

ysis by considering the area of the intersection between $\mathcal{D}$ and $B(\mathrm{RX}_0, s)$. This yields the following theorem for slotted ALOHA.

Theorem 3.5 (Slotted ALOHA)
The outage probability of slotted ALOHA in a bounded region (without fading) can

be lower bounded by $P_{out}^{lb}(\textit{Slotted ALOHA}) = \overline{P}_{rt,s}^{N+1}$, *where* $\overline{P}_{rt,s}$ *is the solution to*

$$\overline{P}_{rt,s} \;=\; \mathbb{E}_{x,y}\left[1 - e^{-\lambda \frac{1-\overline{P}_{rt,s}^{N+1}}{1-\overline{P}_{rt,s}} \sum_{i=1}^{8} \int_{r_{1,i}(x,y)}^{r_{2,i}(x,y)} 2\,\theta_i(r,x,y)\, r\, u(s-r)\, dr}\right], \quad (3.28)$$

where $u(\cdot)$ *is the step function, and* $r_{1,i}(x,y)$, $r_{2,i}(x,y)$, *and* $\theta_i(r,x,y)$ *are given in Tables 3.1 and 3.2, respectively.*

Proof: Observing the packet transmission of a randomly chosen transmitter-receiver pair TX_0-RX_0, starting at time 0, we know that with slotted ALOHA, all packet arrivals during the time period $[-T, 0)$ are potential interferers for RX_0. Moreover, with the concept of guard zones to derive a lower bound to the outage probability, all packet arrivals during $[-T, 0)$ inside RX_0's guard zone $B(\text{RX}_0, s)$, can cause outage for the packet reception at RX_0. Hence, we evaluate the number of packet arrivals inside $\mathcal{D} \cap B(\text{RX}_0, s)$, which is the intersection between a circle of radius s around the receiver under observation, RX_0, and the square domain $\mathcal{D}$ where the nodes are deployed. We denote the area of this region by $A_{\mathcal{D}}$, and derive it by integrating $\theta_i(r,x,y)$ with respect to r, and using Table 3.1 for the integration limits.

The interferers of RX_0 (located at (x,y)) are Poisson distributed with density $\lambda_{slotted}$. This density is given by Eq. (2.9), where $P_{rt,s}$ is replaced by $\overline{P}_{rt,s} = \mathbb{E}[P_{rt,s}(x,y)]$. Based on this, we have that the lower bound to the probability of erroneous packet reception is:

$$\Pr\left(\geq 1 \text{ transmitter inside } \mathcal{D} \cap B(\text{RX}_0, s) \text{ during } [0,T)\right) = 1 - e^{-\lambda_{slotted} A_{\mathcal{D}}(x,y)},$$

A packet is then in outage if it is received erroneously during all its $N+1$ transmission attempts, resulting in Theorem 2.1.

Note that since nodes are uniformly distributed in space, and because of symmetry, the average of Eq. (2.7) with respect to x and y may be obtained by only considering the lower half of the first quadrant of Figure 3.5 and then multiplying the result by 8. □

For unslotted ALOHA, we must consider two time slots, as this protocol allows for partial overlap of packets. Compared to slotted ALOHA, the unslotted nature of the system increases the outage probability, which is given by the following theorem.

Theorem 3.6 (Unslotted ALOHA)
The average outage probability of unslotted ALOHA in a bounded region (without fading) can be lower bounded by $P_{out}^{lb}(\textit{Unslotted ALOHA}) = \overline{P}_{rt,u}^{N+1}$, *where* $\overline{P}_{rt,u}$ *is the solution to*

$$\overline{P}_{rt,u} = \mathbb{E}_{x,y}\left[1 - e^{-2\lambda \frac{1-\overline{P}_{rt,u}^{N+1}}{1-\overline{P}_{rt,u}} \sum_{i=1}^{8} \int_{r_{1,i}(x,y)}^{r_{2,i}(x,y)} 2\,\theta_i(r,x,y)\, r\, u(s-r)\, dr}\right], \quad (3.29)$$

where $u(\cdot)$ *is the step function, and* $r_{1,i}(x,y)$, $r_{2,i}(x,y)$, *and* $\theta_i(r,x,y)$ *are given in Tables 3.1 and 3.2, respectively.*

Proof: This proof for unslotted ALOHA is similar to that for slotted ALOHA, with the only difference that in the unslotted case, we have to consider all packet arrivals during $[-T, T)$. Note that the number of packet arrivals (and hence, the amount of interference) in $[-T, 0)$ is independent from that in $[0, T)$. Thus, the only difference between Eqs. (2.7) and (2.11) is the factor 2 in the exponent of the $\exp(\cdot)$-expression. □

3.2.3 The CSMA Protocol

The derivation of the outage probability of CSMA in a bounded region follows the same concept as for ALOHA, with the difference that if a packet is expected to be received in error at the start of its transmission, it is backed off and the transmission is reattempted after a random waiting time. Hence, at every given (x, y)-point, we evaluate the existence of interferers in the vicinity of this point, accounting for the edge effects by using Table 3.1 for the integration limits of the interferer distance r.

In CSMA_{TX}, it is the transmitter that makes the backoff decision. With M backoffs and N retransmissions, we arrive at the following theorem.

Theorem 3.7 (CSMA_{TX})
The outage probability of $CSMA_{TX}$ *in a bounded region (without fading) is given by*

$$P_{out}(CSMA_{TX}) \;=\; \overline{P}_b^M + (1 - \overline{P}_b^M)\, \overline{P}_{rt1}\, \overline{P}_{rt}^N, \quad (3.30)$$

where:

- $\overline{P}_b = \mathbb{E}_{x,y}\left[P_b(x,y)\right]$ *is the average backoff probability for a transmitter* TX_0 *with its receiver* RX_0 *being located in* (x,y)*. This probability is approximated by the solution to*

$$\overline{P}_b = \mathbb{E}_{x,y}\left[1 - e^{-\lambda\left(1-\overline{P}_b^M+(1-\overline{P}_b^M)\overline{P}_{rt1}\frac{1-\overline{P}_{rt}^N}{1-\overline{P}_{rt}}\right)\sum_{i=1}^{8}\int_{r_{1,i}(x,y)}^{r_{2,i}(x,y)} 2\theta_i(r,x,y)\, r\, u(s-r)\, dr}\right], \tag{3.31}$$

with $r_{1,i}(x,y)$*,* $r_{2,i}(x,y)$*, and* $\theta_i(r,x,y)$ *as given in Tables 3.1 and 3.2, respectively.*

- $\overline{P}_{rt} = \mathbb{E}_{x,y}\left[P_b(x,y) + (1-P_b(x,y))\, P_{during}(x,y)\right]$ *is the approximate average probability that a packet located at* (x,y) *is received in error during a retransmission attempt.* $P_{during}(x,y)$ *is approximated by*

$$\begin{aligned}\tilde{P}_{during}(x,y) \;=\; & \sum_{i=1}^{8}\int_{r_{1,i}(x,y)^2}^{r_{2,i}(x,y)^2} \lambda_{csma}^{TX}\,\theta_i(r,x,y)\, e^{-\lambda_{csma}^{TX}\theta_i(r,x,y)\, r^2} \\ & \times \left[1-\tfrac{1}{\pi}\cos^{-1}\left(\tfrac{r^2+R^2-s^2}{2Rr}\right)\right]\,\text{rect}\left(\tfrac{r-s+R/2}{R}\right)\, d(r^2),\end{aligned} \tag{3.32}$$

where $\text{rect}\left(\dfrac{t-a}{b}\right) = u\left(t-a+\tfrac{b}{2}\right) - u\left(t-a-\tfrac{b}{2}\right)$.

- $\overline{P}_{rt1} = \mathbb{E}_{x,y}\left[P_{rx|transmit}(x,y) + \left(1-P_{rx|transmit}(x,y)\right)\, P_{during}(x,y)\right]$ *is the average probability that the packet is received in outage at its first transmission attempt, with*

$$P_{rx|transmit}(x,y) \approx P_b(x,y)\left[1-\frac{1}{\pi s^2}\left(2s^2\cos^{-1}\left(\frac{R}{2s}\right) - Rs\sqrt{1-\frac{R^2}{4s^2}}\right)\right].$$

- *The density of packets attempting to access the channel is given by*

$$\lambda_{csma}^{TX} = \lambda\left[\frac{1-\overline{P}_b^M}{1-\overline{P}_b} + (1-\overline{P}_b^M)\,\overline{P}_{rt1}\,\frac{1-\overline{P}_{rt}^N}{1-\overline{P}_{rt}}\right], \tag{3.33}$$

Proof: The proof of the expressions in this theorem is similar to the proof of Theorem 2.3, given in Subsection 2.5.1. The difference is that the expressions derived above are for a given (x,y)-coordinate. The area of overlap considered for the derivation of $\overline{P}_b$ is $\mathcal{D}\cap B(\text{TX}_0, s)$. This is considered in the exponent of the $\exp(\cdot)$-expressions in Eq. (3.31), where the limits of r are taken from $r_{1,i}(x,y)$ to $r_{2,i}(x,y)$, which are given in Table 3.1.

In order to derive P_{during}, we apply a slightly different approach than in Chapter 2. Due to the boundedness of the network, we need to account for

both the angles specifying the region $B(\mathrm{RX}_0, s) \cap \overline{B(\mathrm{TX}_0, s)}$, at the same time as accounting for the angle of the region $\mathcal{D} \cap B(\mathrm{RX}_0, s)$. The most straightforward way to do this, is to consider the pdf of having an interferer a distance r away within an angle of $\theta_i(r, x, y)$. This is then integrated over the area of $B(\mathrm{RX}_0, s) \cap \overline{B(\mathrm{TX}_0, s)}$, as is done as follows.

Consider the pdf, $f_r(r; \psi)$, of the distance r to the nearest neighbor within the angle ψ. Assuming a PPP of interferers on an infinite plane, this is given as [70]

$$f_r(r; \psi) = \lambda_{csma}^{TX} \, r \, \psi \, e^{-\frac{\lambda_{csma}^{TX}}{2} \psi \, r^2}. \tag{3.34}$$

In a bounded square region, considering $\psi = 2\,\theta_i(r, x, y)$ (owing to the definition of $\theta_i(r, x, y)$ as a semi-angle defining the i-th subregion of the square domain), the same distribution becomes

$$f_r(r; x, y) = \begin{cases} 2\,\lambda_{csma}^{TX} \, r \, \theta_i(r) \, e^{-\lambda_{csma}^{TX} \theta_i(r,x,y) \, r^2} & ; r_{1,i}(x, y) \leq r \leq r_{2,i}(x, y) \\ 0 & ; \text{otherwise} \end{cases} \tag{3.35}$$

with $i = 1, \ldots, 8$. Furthermore, the distribution of r^2 may be easily obtained as $f_{r^2}^{(i)}(r^2; x, y) = \lambda_{csma}^{TX} \, \theta_i(r^2, x, y) \, e^{-\lambda_{csma}^{TX} \theta_i(r^2,x,y) \, r^2}$ for $r_{1,i}(x, y) \leq r \leq r_{2,i}(x, y)$. Using that the distribution of ϕ is $f_\phi(\phi) = \frac{1}{2\pi}$, we derive P_{during} to be

$$P_{during}(x, y) \;\approx\; \sum_{i=1}^{8} \int_{r_{1,i}(x,y)^2}^{r_{2,i}(x,y)^2} \int_{\gamma(r)}^{2\pi - \gamma(r)} \frac{\lambda_{csma}^{TX}}{2\pi} \, f_{r^2}^{(i)}(r^2; x, y) \, \mathrm{rect}\left(\tfrac{r - s + R/2}{R}\right) \, d\phi \, d(r^2).$$

Solving the first integral yields Eq. (3.32).

The probability expressions at a given (x, y)-coordinate must then be averaged over the entire domain $\mathcal{D}$. Due to symmetry, we may divide $\mathcal{D}$ into 8 triangles, average the outage probability expressions with respect to x and y within each of these triangles, and then multiply the result by 8. Inserting the derived expressions back into Eq. (3.30) yields the outage probability of $\mathrm{CSMA}_{\mathrm{TX}}$. □

With the addition of a simple 1-bit feedback channel between each receiver and its transmitter in $\mathrm{CSMA}_{\mathrm{RX}}$, as introduced in Section 2.4, the performance of the $\mathrm{CSMA}_{\mathrm{TX}}$ protocol is improved significantly. Within a bounded network, the outage probability of $\mathrm{CSMA}_{\mathrm{RX}}$ is given by the following theorem.

Theorem 3.8 ($\mathbf{CSMA_{RX}}$)
The outage probability of $CSMA_{RX}$ in a bounded region (without fading) may be approximated by

$$P_{out}(CSMA_{RX}) \;=\; \overline{P}_b^M + (1-\overline{P}_b^M)\,\overline{P}_{during}\,\overline{P}_{rt}^N, \tag{3.36}$$

where

- $\overline{P}_b = \mathbb{E}_{x,y}\left[P_b(x,y)\right]$ *is the average backoff probability, approximated by the solution to*

$$\overline{P}_b \;=\; \mathbb{E}_{x,y}\left[1 - e^{-\lambda\left(1-\overline{P}_b^M+(1-\overline{P}_b^M)\,\overline{P}_{rt1}\frac{1-\overline{P}_{rt}^N}{1-\overline{P}_{rt}}\right)\sum_{i=1}^{8}\int_{r_{1,i}(x,y)}^{r_{2,i}(x,y)} 2\,\theta_i(r,x,y)\,r\,u(s-r)dr}\right], \tag{3.37}$$

  with $r_{1,i}(x,y)$, $r_{2,i}(x,y)$, and $\theta_i(r,x,y)$ given in Tables 3.1 and 3.2, respectively.
- $\overline{P}_{rt} \;=\; \mathbb{E}_{x,y}\left[P_b(x,y) + (1-P_b(x,y))\,P_{during}(x,y)\right]$ *is the average probability that a packet is received in error after a retransmission attempt. $P_{during}(x,y)$ is approximated by*

$$\begin{aligned}\tilde{P}_{during}(x,y) \;=\; &\sum_{i=1}^{8}\int_{r_{1,i}(x,y)^2}^{r_{2,i}(x,y)^2}\int_{\nu(r)}^{2\pi-\nu(r)} \frac{\lambda_{csma}^{RX}}{2\pi}P(active|r,\phi)\theta_i(r,x,y)\\ &\times e^{-\lambda_{csma}^{RX}\theta_i(r,x,y)\,r^2}\,u(s-d)\,d\phi\,d(r^2),\end{aligned} \tag{3.38}$$

  where $P(active \mid r,\phi)$ and $\nu(r)$ given by

$$P(active|r,\phi) \;=\; 1 - \frac{1}{\pi}\cos^{-1}\left(\frac{r^2+2R^2-s^2-2Rr\cos\phi}{2R\sqrt{r^2+R^2-2Rr\cos\phi}}\right), \tag{3.39}$$

$$\nu(r) \;=\; \cos^{-1}\left(\frac{r^2+2Rs-s^2}{2Rr}\right). \tag{3.40}$$

- *The density of packets attempting to access the channel is given by*

$$\lambda_{csma}^{RX} \;=\; \lambda\left[\frac{1-\overline{P}_b^M}{1-\overline{P}_b} + (1-\overline{P}_b^M)\,\overline{P}_{during}\,\frac{1-\overline{P}_{rt}^N}{1-\overline{P}_{rt}}\right], \tag{3.41}$$

Proof: The derivation of Eqs. (3.37)-(3.40) is similar to that explained in Subsection 2.5.2, for a given (x,y)-coordinate. The limits introduced by the sides of $\mathcal{D}$ are incorporated into the expressions in the same manner as explained in the proof of Theorem 3.7. □

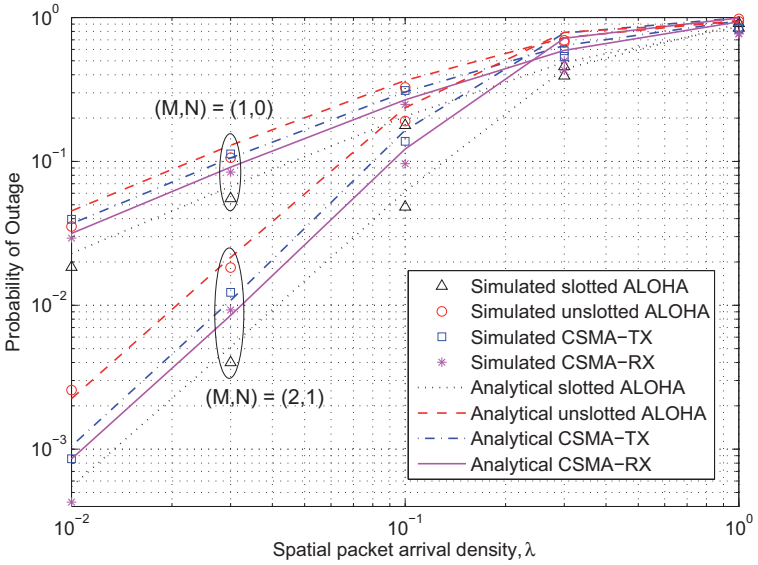

Figure 3.6: Outage probability of ALOHA and CSMA in a bounded non-fading network with $L = 3.3$ m, as a function of λ.

3.2.4 Numerical Results

The simulation model is as described in Subsection 3.2.1, and unless stated otherwise, we apply the following parameter values: a fixed transmitter-receiver distance $R = 1$ m, transmission power $\rho = 1$ mW, path-loss exponent $\alpha = 4$, and SINR threshold $\beta = 0$ dB. The analytical expressions are solved through numerical iterations, in the same manner as was described in Chapter 2, and illustrated in Figure 2.3.

Figure 3.6 shows the outage probability of the various MAC protocols as a function of the density for a 3.3×3.3 m^2 network. In both cases, the simulations are seen to follow the analytical results tightly, thus validating our derivations. As the density increases, so does the outage probability, until it reaches a saturation density above which the outage probability is approximately 1. Slotted ALOHA is seen to yield the lowest outage probability, due to the avoidance of partial overlap of packets. Among the unslotted protocols, CSMA$_{\text{RX}}$ performs the best, because by allowing the receiver to make the backoff decision, the exposed node problem is omitted. In the same manner as in infinite networks, for $(M, N) = (1, 0)$ and low densities, CSMA$_{\text{TX}}$ yields up to 10% higher outage probability than unslotted

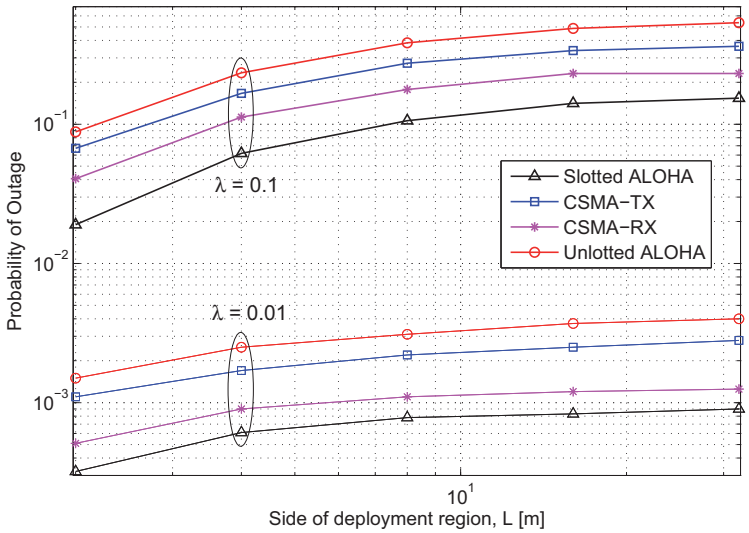

Figure 3.7: Outage probability of ALOHA and CSMA in a bounded non-fading network, as a function of L.

ALOHA. However, the outage probability of CSMA_{TX} is significantly reduced by allowing for more backoff attempts. When $(M, N) = (2, 1)$, the difference between the protocols increases, and CSMA_{TX} outperforms unslotted ALOHA by 30%, while it is outperformed by CSMA_{RX} with 50%. As the density increases, so does the backoff probability, and the amount of interference in the channel is thus less in the case of CSMA than ALOHA. Hence, for higher densities, the benefit of the carrier sensing capability in CSMA becomes more evident.

Having validated our model, we now evaluate the system performance as the size of the deployment region is changed. In Figure 3.7, the outage probability is plotted as a function of the length of the side of our square region, L, for fixed densities of $\lambda = 0.01$ and 0.1 [packets/m^2]. We observe that up to 85% of the outage probability is reduced due to edge effects when the side of the deployment region, L, is reduced to be of the same order as the radius of the guard zone, s. Our simulations show that the the outage probability of a node located in the corner is about 50% less than one located at the center of the communication region. As L increases, the outage probability converges towards that obtained in infinite networks. $L \approx 30 \times s$ is a good approximation for an infinite network.

Practical implications of these results include the possibility of deploying a greater density of nodes in indoor networks than predicted by previous models, due to the presence of walls and obstacles.

3.3 Bounded Networks with Fading

Having considered the impact of fading on infinite ad hoc networks and the edge effect in bounded non-fading networks, a natural question then becomes: How does a bounded network behave in the presence of fading? And moreover, knowing from Section 3.2 that interference is a greater problem in infinite networks than in bounded ones, we ask whether fading is more destructive in either network? These questions are addressed in this section.

The effect of fading on infinite wireless networks has been under extensive investigation, as described in Section 3.1, while only a few results exist in the literature on the the impact of fading in *bounded* networks. Related works on edge effects are discussed in Section 3.2. In [57], the outage probability performance of a bounded network with fading was investigated under simplified protocol assumptions (no backoffs and retransmissions were allowed). Removing these restrictions, we evaluate in the following the performance of MAC protocols in bounded fading ad hoc networks.

3.3.1 System Model

We employ the same traffic and network model as described in Section 3.2, but with the addition of fading, as explained in Subsection 3.1.1. In summary, the model used in this section is as follows. Consider a bounded network of size $L \times L$, with packets distributed in space and time according to a PPP with density $\lambda = \lambda^s \lambda^t T(1 + \Delta(M, N))$, where λ^s [nodes/m^2] is the density of nodes on the 2-D plane, λ^t [packets/sec/node] is the density of packet arrivals in time, T [sec] is the fixed packet length, and $\Delta(M, N)$ is the amount of increase in the number of packets that attempt to access the channel due to M backoffs and N retransmissions.

For the channel model, we consider fading effects in addition to the deterministic path loss attenuation effects explained in Subsection 3.2.1. The SINR of a received packet in the presence of fading is given by Eq. (3.1), and the probability that this SINR falls below the required SINR threshold β is given by the error probability in Eq. (3.2). As in the previous sections, we assume that $\beta_b = \beta$ in CSMA.

The evaluation of the outage probability consists of solving Eq. (3.2) over the square domain $\mathcal{D}$. In order to make the analysis tractable, we follow the same concept of lower bounding the outage probability as in the absence of fading. This is done by considering all *dominant* interferers, as explained in Section 3.1. Hence, to find the probability of outage, we derive the probability of having dominant interferers over the entire network

domain, $\mathcal{D}$. This yields

$$P^f_{error}(x,y) \;\geq\; \Pr\left(\frac{\rho\, h_{00}\, R^{-\alpha}}{\eta + \rho\, h_{0i}\, r^{-\alpha}} < \beta\right) \tag{3.42}$$

The outage probability is obtained as different combinations of error events.

3.3.2 The ALOHA Protocol

Combining the techniques of Sections 3.1 and 3.2, we can analytically evaluate the existence of dominant interferers in the square domain, $\mathcal{D}$, during the time period $[-T, 0)$. The outage probability is thus given by the following theorem.

Theorem 3.9 (Slotted ALOHA)
The average outage probability of slotted ALOHA in a bounded network with Rayleigh fading can be approximated by $\tilde{P}_{out}(\textit{Slotted ALOHA}) = \overline{P}^{N+1}_{rt,s}$, *where* $\overline{P}_{rt,s}$ *is the solution to*

$$\overline{P}_{rt,s} \;=\; \mathbb{E}_{x,y}\left[1 - e^{-\lambda \frac{1-\overline{P}^{N+1}_{rt,s}}{1-\overline{P}_{rt,s}} \sum_{i=1}^{8} \int_{r_{1,i}(x,y)}^{r_{2,i}(x,y)} 2\,\theta_i(r,x,y) \frac{\zeta\beta}{\zeta\beta + R^{-\alpha} r^{\alpha}}\, r\, dr}\right], \tag{3.43}$$

with $r_{1,i}(x,y)$, $r_{2,i}(x,y)$, *and* $\theta_i(r,x,y)$ *as given in Tables 3.1 and 3.2, respectively.*

Proof: Since interferers are Poisson distributed in $\mathcal{D}$, we may apply the expression $P_{rt,s}(x,y) = 1 - e^{-\mathbb{E}[\#\text{ of interferers}]}$. To find this, we first derive the expected number of dominant interferers when RX_0 is in (x,y) to be

$$\begin{aligned}
\mu^f(x,y) &= \iint_{\mathcal{D}} \lambda_{slotted} \Pr(\text{TX}_i \text{ causes outage for } \text{RX}_0 | (r,\theta))\, r\, dr\, d\theta \\
&\geq \iint_{\mathcal{D}} \lambda_{slotted} \Pr\left(\frac{\rho R^{-\alpha} h_{00}}{\eta + \rho r^{-\alpha} h_{0i}} < \beta \mid r\right) r\, dr\, d\theta
\end{aligned} \tag{3.44}$$

where $\lambda_{slotted}$ is given by Eq. (2.9).

Assuming Rayleigh fading, we have that the channel coefficients are exponentially distributed, i.e., $f_{H_i}(h_{0i}) = \zeta e^{-\zeta h_{0i}}$, where $\frac{1}{\zeta} = \mathbb{E}[h_{0i}]$. Therefore, taking the expectation of Eq. (3.42) yields

$$\begin{aligned}
P^f_{error}(x,y) &= 1 - \frac{\zeta R^{-\alpha} \exp(-\beta\eta / R^{-\alpha}\beta)}{\zeta R^{-\alpha} + \beta r^{-\alpha}} \\
&\approx \frac{\zeta\beta}{\zeta\beta + (r/R)^{\alpha}},
\end{aligned} \tag{3.45}$$

where we have assumed in the last step that the path loss and fading effects are the main sources of signal degradation, thus setting $\eta = 0$.

Inserting these formulas back into the expression for $P_{rt,s}$ and splitting the integral over the domain $\mathcal{D}$ into the 8 subregions listed in Table 3.1, yields Eq. (3.43). □

The extension of the results of Theorem 3.9 to unslotted ALOHA is straight forward, as two time slots must now be considered, as opposed to one in slotted ALOHA. This yields the following theorem.

Theorem 3.10 (Unslotted ALOHA)
The average outage probability of unslotted ALOHA in a bounded network with fading can be approximated by $\tilde{P}_{out}(\text{Unslotted ALOHA}) = \overline{P}_{rt,u}^{N+1}$, *where* $\overline{P}_{rt,u}$ *is the solution to*

$$\overline{P}_{rt,u} \;=\; \mathbb{E}_{x,y}\left[1 - e^{-2\lambda \frac{1-\overline{P}_{rt,u}^{N+1}}{1-\overline{P}_{rt,u}} \sum_{i=1}^{8} \int_{r_{1,i}(x,y)}^{r_{2,i}(x,y)} 2\,\theta_i(r,x,y)\, \frac{\zeta\beta}{\zeta\beta + R^{-\alpha} r^{\alpha}}\, r\, dr}\right], \quad (3.46)$$

with $r_{1,i}(x,y)$, $r_{2,i}(x,y)$, *and* $\theta_i(r,x,y)$ *as given in Tables 3.1 and 3.2, respectively.*

Proof: The outage probability of unslotted ALOHA is derived in the same manner as slotted ALOHA, with the difference that the period $[-T, 0)$ is now also considered in addition to $[0, T)$. Due to the assumption on high mobility and fixed packet length, the arrivals of interferers during $[-T, 0)$ and $[0, T)$ are independent, which results in a factor 2 in the exponent of the $\exp(\cdot)$-expression. □

3.3.3 The CSMA Protocol

The outage probability of CSMA is derived as a combination of the dropping of a packet due to M backoffs and, in the case of activation, because of erroneous packet reception after N retransmissions. For CSMA_{TX}, this probability is given by the following theorem.

Theorem 3.11 (CSMA_{TX})
The average outage probability of $CSMA_{TX}$ *in a bounded network with Rayleigh fading is given by*

$$P_{out}(CSMA_{TX}) \;=\; \overline{P}_b^{M} + (1 - \overline{P}_b^{M})\, \overline{P}_{rt1}\, \overline{P}_{rt}^{N}, \quad (3.47)$$

where

- $\overline{P}_b = \mathbb{E}_{x,y}\left[P_b(x,y)\right]$ *is the average backoff probability, approximated by the solution to*

$$\overline{P}_b \;=\; \mathbb{E}_{x,y}\left[1 - e^{-\lambda\left(1-\overline{P}_b^M+(1-\overline{P}_b^M)\overline{P}_{rt1}\frac{1-\overline{P}_{rt}^N}{1-\overline{P}_{rt}}\right)\sum_{i=1}^{8}\int_{r_{1,i}(x,y)}^{r_{2,i}(x,y)} 2\theta_i(r,x,y)\frac{\zeta\beta}{\zeta\beta+R^{-\alpha}r^{\alpha}}\,r\,dr}\right]. \tag{3.48}$$

- $\overline{P}_{rt} \;=\; \mathbb{E}_{x,y}\left[P_b(x,y) + (1-P_b(x,y))\,P_{during}(x,y)\right]$ *is the average probability that a packet is received in error after a retransmission attempt.* $P_{during}(x,y)$ *is the probability that a receiver at* (x,y) *receives its packet in error at some* $t \in (0,T)$*, approximated by*

$$\tilde{P}_{during}(x,y) \;=\; 1 - e^{-\lambda_{csma}^{TX}\sum_{i=1}^{8}\int_{r_{1,i}(x,y)^2}^{r_{2,i}(x,y)^2} 2\theta_i(r,x,y)\frac{\zeta\beta}{\zeta\beta+R^{-\alpha}r^{\alpha}}\left(1-\frac{\zeta\beta}{\zeta\beta+R^{-\alpha}r^{\alpha}}\right)r\,dr} \tag{3.49}$$

  with λ_{csma}^{TX} *as given by Eq.* (3.14)*.*

- $\overline{P}_{rt1} = \mathbb{E}_{x,y}\left[P_{rx|transmit}(x,y) + (1-P_{rx|transmit}(x,y))\,P_{during}(x,y)\right]$ *is the average probability that the packet is received in outage at its first transmission attempt.* $P_{rx|transmit}(x,y)$ *is the probability that the receiver located at* (x,y) *is in outage at the start of the transmission;*

$$\overline{P}_{rx|transmit} \;\approx\; \overline{P}_b\,\mathbb{E}_{h_{00}}\left[1-\frac{1}{\pi s^{f^2}}\left(2s^{f^2}\cos^{-1}\left(\frac{R}{2s^f}\right) - Rs^f\sqrt{1-\frac{R^2}{4s^{f^2}}}\right)\right], \tag{3.50}$$

where $s^f = s^f(h_{00}, \mathbb{E}[h_{0i}])$ *is given by Eq.* (3.4)*.*

Proof: The expression for the outage probability is derived as in the case of non-fading in Section 3.2. Also the backoff probability is derived as described in the proof of Theorem 3.3. In the same manner as for infinite fading networks in Section 3.1, we derive the density of dominant interferers to be

$$\mu^f(x,y) \;=\; \iint_{\mathcal{D}} \lambda_{csma}^{TX}\cdot P_{error}^f(x,y)\cdot \Pr(\text{TX}_i \text{ activated}|(r,\theta))\;r\,dr\,d\theta. \tag{3.51}$$

$P_{error}^f(x,y)$ is given in Eq. (3.45). When $\beta_b = \beta$, the probability that TX_i is activated is derived to be $1 - P_{error}^f(x,y)$.

Finally, the probability that a packet is in outage at the receiver at the start of its first transmission attempt, once its transmitter has decided to

transmit, is

$$P_{rx|transmit}(h_{00}, h_{0i}) \approx \overline{P}_b \left(\frac{\text{Area of } B(\text{RX}_0, s^f) \cap \overline{B(\text{TX}_0, s^f)}}{\text{Area of } B(\text{RX}_0, s^f)} \right), \quad (3.52)$$

which is given by Eq. (3.50). Inserting these derived expressions back into Eq. (3.10), yields the outage probability of CSMA_{TX}. □

By allowing the receiver to perform the channel sensing and make the backoff decision, significant performance gain may be obtained. In the same manner as in for CSMA_{TX}, we obtain the outage probability of CSMA_{RX}, as given by the following theorem.

Theorem 3.12 (CSMA_{RX})
The average outage probability of $CSMA_{RX}$ in a bounded network with Rayleigh fading is approximated by

$$P_{out}(CSMA_{RX}) = \overline{P}_b^M + (1 - \overline{P}_b^M)\, \overline{P}_{during}\, \overline{P}_{rt}^N, \quad (3.53)$$

where

- $\overline{P}_b = \mathbb{E}_{x,y}\left[P_b(x,y)\right]$ *is the average backoff probability, approximated by*

$$P_b(x,y) = 1 - e^{-\lambda \left(1-\overline{P}_b^M + (1-\overline{P}_b^M)\overline{P}_{during} \frac{1-\overline{P}_{rt}^N}{1-\overline{P}_{rt}}\right) \sum_{i=1}^{8} \int_{r_{1,i}(x,y)}^{r_{2,i}(x,y)} 2\theta_i(r,x,y) \frac{\zeta\beta}{\zeta\beta + R^{-\alpha} r^{\alpha}} r\, dr}. \quad (3.54)$$

- $\overline{P}_{during} = \mathbb{E}_{x,y}\left[P_{during}(x,y)\right]$ *is the average probability that the error occurs at some $t \in (0,T)$. $P_{during}(x,y)$ is the probability that a receiver located at (x,y) goes into outage at some $t \in (0,T)$, approximated by*

$$\tilde{P}_{during}(x,y) = 1 - e^{-\lambda_{csma}^{RX} \sum_{i=1}^{8} \int_{r_{1,i}(x,y)}^{r_{2,i}(x,y)} 2\theta_i(r,x,y) \frac{\zeta\beta}{\zeta\beta + R^{-\alpha} r^{\alpha}} \left(1 - \frac{\zeta\beta}{\zeta\beta + R^{-\alpha} r^{\alpha}}\right) r\, dr}, \quad (3.55)$$

  with λ_{csma}^{RX} as given by Eq. (3.24).
- $\overline{P}_{rt} = \mathbb{E}_{x,y}\Big[P_b(x,y) + (1 - P_b(x,y))\; P_{during}(x,y)\Big]$ *is the average probability that a packet is received in error after a retransmission attempt.*

Proof: The outage probability of CSMA_{RX} is obtained in the same manner as explained in the proof of Theorem 3.11. The main difference is that $\overline{P}_{rt1} = \overline{P}_{during}$, due to the fact that once the receiver dictates its transmitter to initiate the packet transmission, the packet is ensured to not be in outage at the start of its first transmission attempt. Hence, $P_{rx|transmit}(h_{00}, h_{0i}) = 0$. □

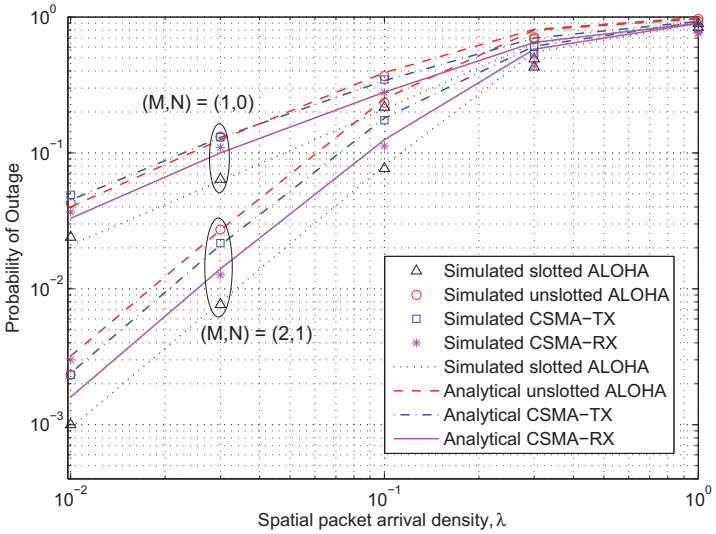

Figure 3.8: Outage probability of ALOHA and CSMA in a bounded 3 m $\times$ 3 m network with fading as a function of λ.

3.3.4 Numerical Results

Monte Carlo simulations are conducted in order to confirm the derived results of this section. As before, the simulation tool MATLAB is used, and the simulations are carried out as described in Section 2.6. The network model is as described in Subsection 3.3.1. Unless stated otherwise, we set the transmitter-receiver distance $R = 1$ m, transmission power $\rho = 1$ mW, path-loss exponent $\alpha = 4$, SINR threshold $\beta = 1$, number of backoffs $M = 2$, and number of retransmissions $N = 1$.

Figure 3.8 shows the outage probability of the various MAC protocols in a bounded fading network with $L = 3.3$ m, as a function of the packet arrival density λ. The simulations follow the analytical results tightly, thus validating our expressions. As in the case of non-fading networks, slotted ALOHA is seen to yield the lowest outage probability, outperforming its unslotted version by a factor of 2 when $N = 0$, and approximately by a factor of $2^{N+1} = 4$ for $N = 1$. However, this protocol requires perfect synchronization between nodes, something that is difficult to maintain. CSMA_{RX} yields approximately 30% lower outage probability than CSMA_{TX}, when $(M, N) = (1, 0)$, and 53% lower when $(M, N) = (2, 1)$. As the density increases, so does the backoff probability, and the benefit of the carrier sens-

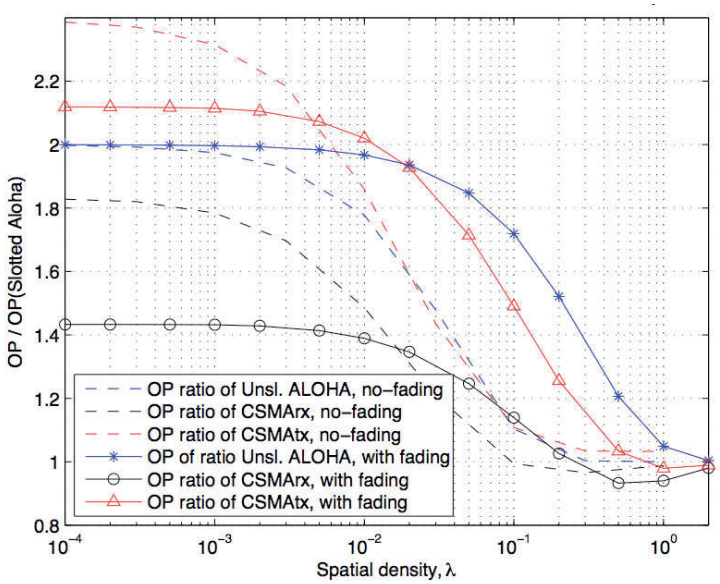

Figure 3.9: Outage probability ratio of the unslotted protocols over that of slotted ALOHA as a function of λ for $(M, N) = (1, 0)$.

ing capability in CSMA becomes more evident.

Compared to non-fading networks, the presence of fading results in approximately 35% higher outage probability for all the MAC protocols. Figure 3.9 emphasizes the difference between the various MAC protocols in the absence and presence of fading. In this figure, the ratio of the outage probability of all the unslotted protocols over that of slotted ALOHA is plotted for $(M, N) = (1, 0)$. We note that while the outage probability ratio of unslotted ALOHA over slotted ALOHA remains approximately the same (about 2 for low densities) in non-fading and fading networks, that of the CSMA protocols over slotted ALOHA changes considerably. That is, the degradation due to fading has a larger impact on CSMA than on ALOHA. E.g., in a non-fading network, CSMA_{RX} yields about 40% more outage probability than slotted ALOHA, while in a fading network, this difference is about 80%.

Having validated our model and analytical results, we now evaluate the system performance as the size of the deployment region is changed. In Figure 3.10, the outage probability is plotted as a function of the length of the side of our square domain, L, for fixed densities of $\lambda = 0.01$ and 0.1 [packets/m^2]. At the high density, up to 85% of the outage probability

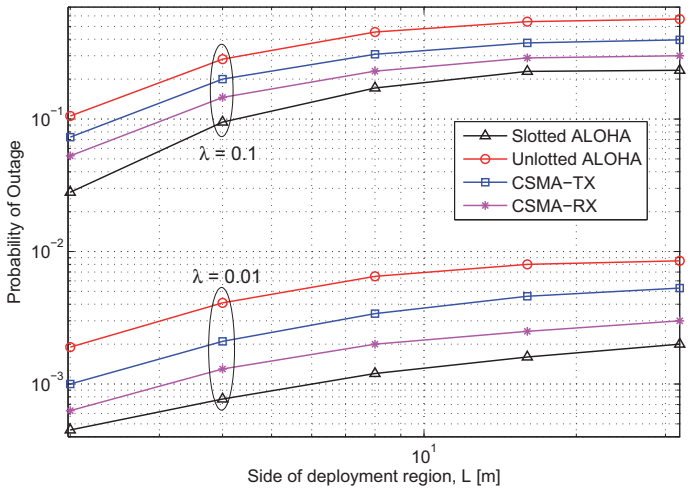

Figure 3.10: Outage probability of ALOHA and CSMA in a fading network as a function of L.

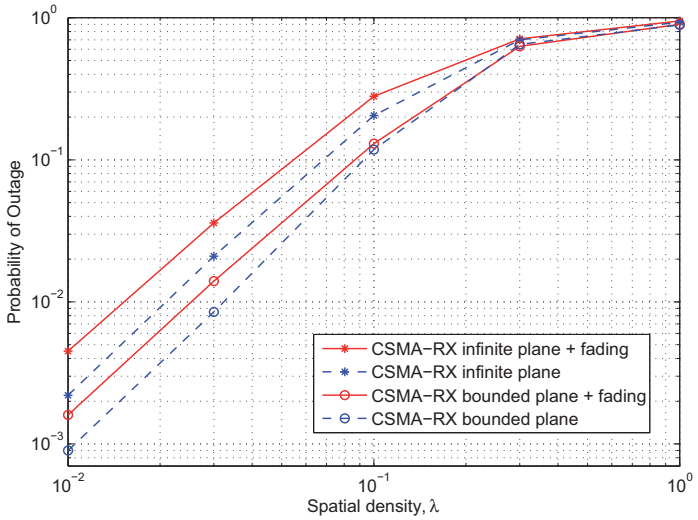

Figure 3.11: Outage probability of CSMA_{RX} for bounded and infinite networks, both in the absence and presence of fading, for $(M, N) = (2, 1)$.

is reduced due to edge effects when the side of the deployment region is reduced to be of the same order as the radius of the guard zone, s. Our simulations show that the outage probability of a node located in the corner is about 50% lower than one located in the center of the communication domain.

Finally, we compare the outage probability of a bounded region to that of an infinite network, as shown in Figure 3.11. We only consider CSMA_{RX}, as the other protocols behave in the same manner. In the absence of fading, the bounded network with side length $L = 3.3$ m yields up to 60% lower outage probability than the infinite network. The degradation due to fading is about 47% in infinite networks and about 38% in bounded networks. The reason for this difference is that there is a greater number of interferers in an infinite network. Consequently, when each interferer causes a greater destruction due to fading, the aggregate destruction becomes more significant as the number of interferers increases. Hence, the impact of fading is more severe in infinite networks compared to bounded ones.

3.4 Summary

In this chapter, we have evaluated the impact of various channel characteristics on the performance of ad hoc networks. In particular, we investigate the effects of fading, boundedness of the network domain, and a combination of these. In all the aforementioned network models, we derive approximate expressions for the outage probability of the ALOHA and CSMA MAC protocols. With Monte Carlo simulations our analytical expressions were validated in all scenarios, and our approximations are proven to be reasonable.

Moreover, the outage performance of the various protocols are compared. Without allowing for many backoffs relative to retransmissions, slotted ALOHA is shown to yield the best performance in all the network models considered, i.e., infinite fading networks, bounded non-fading networks, and bounded fading networks. However, if the network has no synchronization capabilities, then the most reliable protocol to use is CSMA with receiver sensing, CSMA_{RX}. This protocol is modified from the conventional CSMA protocol by introducing a simple feedback channel and allowing the receiver to sense its channel and make the backoff decision. This minor modification yields up to 30% improvement in the outage probability of CSMA both in the presence of fading in an infinite network and when the network region is bounded.

It is also observed that both in the absence and presence of fading, the outage probability is much lower in bounded networks compared to infinite ones. This is because the number of interferers is lower in bounded networks (i.e., the edges of the communication region behave as shields against potential interferers outside the region). Specifically, edge effects reduce the outage probability by up to 85% in both cases. Furthermore, fading is seen to degrade the system performance considerably, with up to 2.5 times higher outage probability (when $(M, N) = (2, 1)$). The degradation due to fading is about 20% higher in infinite networks than in bounded ones. This is again due to the fact that the number of interferers is higher in infinite networks, and so when the destruction from interfering signals increases, fading has a greater impact in infinite networks.

Finally, note that our findings on boundedness of networks also applies to other shapes of the communication domain. Clearly, the expressions and the values for outage probability will change, but the main conclusions remain intact. The fewer edges the domain has, the greater is the impact of edge effects, as the number of interferers decreases. This results in a greater difference between infinite networks and bounded ones. Practical implications of our results include the possibility of deploying a greater

density of nodes in indoor networks than predicted by infinite network models, due to the presence of walls and obstacles.

Chapter 4

Performance Improvement Through Advanced CSMA

In this chapter, we focus on the CSMA protocol, and we propose some MAC layer techniques to improve its performance. In particular, we first optimize the sensing threshold of CSMA_{TX} and CSMA_{RX}, in both non-fading and fading networks. Next, we propose a joint transmitter-receiver sensing and decision-making scheme in order to reduce the outage probability further. Each of these techniques is devoted a separate section.

Since the analysis techniques and the derivations were discussed in great detail in the proofs of the various theorems in Chapter 2 for non-fading networks, and in Section 3.1 for fading networks, in this chapter (and the next), we will be referring to these proofs and explain the changes made in this section in order to arrive at the new outage probability expressions. For the sake of fluency in the reading, this will be done in the body of the text (rather than in separate proofs, as was done in the preceding chapters).

The work of this chapter is partly published in [71], in revision for possible publication in IEEE Trans. on Wireless Communications [45], and submitted to IEEE Trans. on Communications [72].

4.1 Optimizing CSMA's Sensing Threshold

A good choice of the sensing threshold of CSMA, β_b, is of great importance for achieving an optimal performance. Hence, numerous works have been performed to determine the optimum value of this threshold. In [11],

the throughput of the CSMA protocol is evaluated in a multi-hop ad hoc network. It is shown that the optimal algorithm is to decrease the sensing range as long as the network remains sufficiently connected. In [73], it is claimed that in order to maximize the spatial reuse of the network, one must set $\beta_b \approx \rho \left(1 + \beta^{1/\alpha}\right)^{\alpha}$, where ρ represents the transmitted signal strength, α is the path loss exponent, and β is the minimum required SINR threshold for correct packet reception. The authors subsequently propose a distributed scheme in which the nodes would exchange their SINR measurements in order to adjust their sensing thresholds toward a common value.

In [74], an algorithm with joint adaptation of sensing threshold and transmit power is proposed. It is shown that the optimum sensing threshold of CSMA depends on the system design parameters, such as the distance between a transmitter and its receiver. The authors conclude that in order to minimize the outage probability, senders must keep the product of their transmit power and carrier sensing threshold equal to a fixed constant. However, this algorithm is not distributed, and is dependent on estimation of signal powers. Loosening these limitations, a new sensing threshold adaptation algorithm is proposed in [75], where each node chooses the β_b that maximizes the number of successful transmissions in its neighborhood. The drawback of this scheme is that it relies on the collection of information from the environment over a period of time, which entails high complexity and is not able to handle fast variations of the channel or the interference.

Our objective in this section is to optimize the sensing threshold, β_b, of CSMA in its various incarnations, in order to minimize the outage probability. In the analysis thus far, we have used a constant sensing threshold, namely $\beta_b = \beta = 0$ dB. This simplified the analysis, as we did not need to consider different ranges of β_b in the derivation of the formulas. In this section, we take into account variations in β_b (translating to s_b through Eq. (2.5)). We consider both CSMA_{TX} and CSMA_{RX}, and derive their outage probabilities in the following.

4.1.1 System Model

For the system model, we refer to the initial network model described in Chapter 2. The traffic generated follows a 3-D PPP with density $\lambda = \lambda^s \lambda^t T$, where λ^s [nodes/m^2] is the density of nodes on the 2-D plane, λ^t [packets/sec/node] is the density of packet arrivals in time, and T [sec] is the fixed packet length. Upon a packet arrival, it is transmitted to its destination located a fixed distance R away. Transmissions occur according to the

ALOHA and CSMA protocols in a fully-distributed manner. In ALOHA, a packet transmission is initiated upon its arrival, regardless of the channel conditions. In CSMA, a packet backs off a random time if the measured or estimated SINR at the start of the packet falls below the sensing threshold, β_b. Once a transmission is initiated, but the SINR falls below the threshold β at some time throughout its duration, the packet is received in error and must be retransmitted. If the packet is not received correctly after M backoffs and N retransmissions, it is dropped and counted to be in outage.

As before, we assume high mobility of nodes, meaning that a backed off or retransmitted packet is located in a new position on the plane. The waiting time between the transmission attempts, t_{wait}, is by design ensured to be more than T, meaning that new channel instances are observed for each transmission attempt. As a consequence, there are no spatial or temporal correlations between packet transmissions. For more details on the traffic and network model, we refer the reader to Section 2.1.

For the channel model, we first consider only deterministic path loss attenuation effects (with exponent $\alpha > 2$). This yields

$$\text{SINR}_i \;=\; \frac{\rho\, R^{-\alpha}}{\eta + \sum_i \rho\, r_i^{-\alpha}}, \tag{4.1}$$

where r_i is the distance between the node under observation and the i-th interfering transmitter, and the summation is over all active interferers on the plane at each time instant.

In Subsection 4.1.3, we will add fading effects to the deterministic path loss attenuation, in the same manner as was done in Subsection 3.1.1. This results in

$$\text{SINR}_i^f \;=\; \frac{\rho\, h_{00}\, R^{-\alpha}}{\eta + \sum_i \rho\, h_{0i}\, r_i^{-\alpha}}, \tag{4.2}$$

where r_i and h_{0i} are, respectively, the distance and fading coefficient between the node under observation and the i-th interfering transmitter. h_{00} represents the fading effects between the receiver under observation, RX_0, and its own transmitter, TX_0.

Initially, we assume that β stays constant (we set $\beta = 0$ dB, as in Chapter 2, which corresponds to $s \approx R$), while β_b varies. We will also investigate what happens when $\beta_b = \beta$ and both the thresholds vary simultaneously.

4.1.2 Performance in the Absence of Fading

In this subsection, we assume only distance-dependent attenuation in the signal transmissions. This allows us to translate the outage probability for-

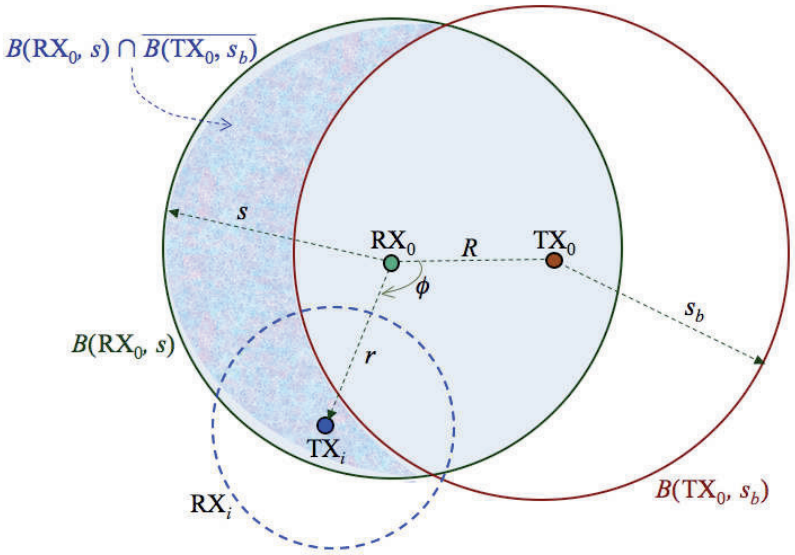

Figure 4.1: Area of overlap between $B(\mathrm{RX}_0, s)$ and $B(\mathrm{TX}_0, s_b)$ for the derivation of the outage probability of CSMA.

mulation, as stated in Eq. (2.2), into a distance problem. The analysis technique used is similar to the one explained in Section 2.2, but because of the variations in β_b, new expressions must be derived for the outage probability of CSMA. Hence, we apply similar geometrical considerations as before, with the difference that we also account for when s_b is different from s.

The outage probability of CSMA is given as

$$\begin{aligned} P_{out}(\mathrm{CSMA}) &= \Pr\left[\mathrm{SINR} < \beta_b \text{ at } t = 0\right]^M + \Big(1 - \Pr\left[\mathrm{SINR} < \beta_b \text{ at } t = 0\right]^M\Big) \\ &\quad \times \Pr\left[\mathrm{SINR} < \beta \text{ during } 1^{\mathrm{st}} \text{ transmission} | \text{active}\right] \\ &\quad \times \Pr\left[\mathrm{SINR} < \beta \text{ at some } t \in [0, T)\,\right]^N \\ &= P_b^M + (1 - P_b^M)\, P_{rt1}\, P_{rt}^N. \end{aligned} \tag{4.3}$$

As s_b changes, so does the area of $B(\mathrm{TX}_0, s_b)$, as shown in Figure 4.1. This impacts P_b, P_{rt1}, and P_{rt}.

We start with $\mathrm{CSMA}_{\mathrm{TX}}$, where the transmitter senses the channel state and makes the backoff decision. The backoff probability, P_b, is derived in same manner as described in Section 2.5. Once a packet transmission has

been activated, we have that:

$$P_{during} \approx \Pr\left[\geq 1 \text{ interferer inside } B(\mathrm{RX}_0, s) \cap \overline{B(\mathrm{TX}_0, s_b)} \text{ at some } t \in (0, T)\right].$$

For $s_b < R + s$, the derivation is as explained in Subsection 2.5.1. For $s_b > R + s$, $B(\mathrm{TX}_0, s_b)$ covers $B(\mathrm{RX}_0, s)$ completely, meaning that it is impossible for an interferer to fall inside $B(\mathrm{RX}_0, s)$ and at the same time be outside of $B(\mathrm{TX}_0, s)$.

Once a packet has been activated, there is still a chance that an error occurs at the start of its transmission. This is denoted $P_{rx|transmit}$ and is determined by the probability that at least one interferer is placed inside $B_1 = B(\mathrm{RX}_0, s) \cap \overline{B(\mathrm{TX}_0, s_b)}$ during $[-T, 0)$. This is approximated by the probability that the receiver is in outage at the start of the packet, P_{rx}, multiplied by the ratio $\frac{\text{Area of } B(\mathrm{RX}_0,s) \cap \overline{B(\mathrm{TX}_0,s_b)}}{\text{Area of } B(\mathrm{RX}_0,s)}$. Based on these considerations, in addition to the derivations carried out in Chapter 2, we arrive at the following theorem.

Theorem 4.1 ($\mathrm{CSMA_{TX}}$)
The outage probability of $CSMA_{TX}$ for variable sensing threshold is given by

$$P_{out}(CSMA_{TX}) = P_b^M + (1 - P_b^M)\, P_{rt1}\, P_{rt}^N, \tag{4.4}$$

where

- *P_b is the backoff probability, approximated by the solution to*

$$\tilde{P}_b = 1 - \exp\left\{-\pi\, s_b^2\, \lambda \left(1 - \tilde{P}_b^M + \left(1 - \tilde{P}_b^M\right) \tilde{P}_{rt1}\, \frac{1 - \tilde{P}_{rt}^N}{1 - \tilde{P}_{rt}}\right)\right\}. \tag{4.5}$$

- *$P_{rt} = P_{rx} + (1 - P_{rx})\, P_{during}$ is the probability that an activated packet is received erroneously in a retransmission attempt. P_{rx} is the probability that the receiver is in outage upon arrival in each retransmission attempt (since no backoff decision is made for each transmission), and is approximated by Eq. (4.5), with s_b replaced by s.*
- *P_{during} is the probability that the error occurs at some $t \in (0, T)$, approximated by*

$$\tilde{P}_{during} = \tag{4.6}$$
$$\begin{cases} 1 - e^{-\lambda_{csma}^{TX}\left[\int_0^{R-s_b} 2\pi\, r\, dr + \int_{R-s_b}^{s} 2\pi - 2\cos^{-1}\left(\frac{r^2+R^2-s_b^2}{2Rr}\right) rdr\right]} & ; s_b < R \\ 1 - e^{-\lambda_{csma}^{TX}\int_{s_b-R}^{s} 2\pi - 2\cos^{-1}\left(\frac{r^2+R^2-s_b^2}{2Rr}\right) rdr} & ; R \leq s_b < R+s \\ 0 & ; \textit{otherwise} \end{cases}$$

- $P_{rt1} = P_{rx|transmit} + (1 - P_{rx|transmit})\, P_{during}$ *is the probability that the first transmission is received erroneously.* $P_{rx|transmit}$ *is the probability that the receiver is in outage at the start of the packet, approximated by*

$$\tilde{P}_{rx|transmit} = \tag{4.7}$$
$$\begin{cases} \tilde{P}_{rx} - \tilde{P}_{rx}\frac{s_b^2}{\pi s^2}\cos^{-1}\left(\frac{R^2+s_b^2-s^2}{2Rs_b}\right) - \tilde{P}_{rx}\frac{1}{\pi}\cos^{-1}\left(\frac{R^2+s^2-s_b^2}{2Rs}\right) \\ \quad + \frac{\tilde{P}_{rx}}{2\pi s^2}\sqrt{(s_b+s-R)(s_b-s+R)(-s_b+s+R)(s_b+s+R)} & ; s_b < R+s \\ 0 & ; otherwise \end{cases}$$

Optimizing the sensing threshold in CSMA_{TX} yields an optimal tradeoff between the hidden and exposed node problems. As noted in Chapter 2, the *hidden node problem* occurs during an active packet transmission, when a newly arriving interferer, TX_i, is located less than a distance s away from RX_0, and simultaneously more than a distance s_b away from TX_0 (in order to be activated). That is, TX_i is activated because TX_0 is *hidden* to it. The *exposed node problem* occurs when a packet transmission is backed off even though its transmission would not have contributed to the outage probability. This is the case when TX_i is located within a distance s_b of TX_0, but more than a distance s away from RX_0. Clearly, an increase in one problem (due to changes in s_b) results in a decrease in the other, and vice versa.

Due to the complexity of our outage probability expressions, we are not able to analytically perform the optimization of the sensing threshold. Hence, this is done through simulations in Subsection 4.1.4. For the particular case of CSMA_{RX} with $(M, N) = (1, 0)$, we can apply approximate measures to find the sensing threshold analytically, as is done at the end of this subsection. As an approximation, the reasoning and final results obtained for CSMA_{RX} also apply to CSMA_{TX}. This is because P_b and P_{during} are approximately the same in these two versions of CSMA, leaving the main source of difference in the probability that an error occurs at the *start of the first* transmission attempt.

To derive the outage probability of CSMA_{RX}, we start with the same total outage probability expression as Eq. (4.4). Also the backoff probability expression is unchanged, because whether the transmitter or the receiver make the backoff decision, the same distribution and density of interferers are observed. To derive the probability that an activated transmission is received in error *during* its transmission, we consider the occurrence of an interferer, TX_i, inside $B(\text{RX}_0, s)$ at some $t \in (0, T)$, while its receiver, RX_i, is placed outside of $B(\text{TX}_0, s_b)$. As seen from Figure 4.1, when $s_b > 2R + s$,

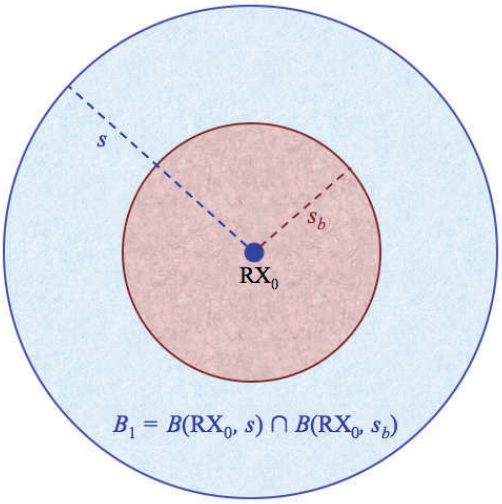

Figure 4.2: Setup for derivation of $P_{rx|transmit}$ in CSMA_{RX}.

$B(\text{TX}_0, s_b)$ covers $B(\text{RX}_0, s)$ completely with a margin R. This means that if TX_i falls anywhere inside $B(\text{RX}_0, s)$, RX_i will be inside $B(\text{TX}_0, s_b)$, and TX_i-RX_i would thus back off. For the other ranges of s_b, the integration limits are adjusted as to cover the area $B_1 = B(\text{RX}_0, s) \cap \overline{B(\text{TX}_0, s_b - R)}$, in the same manner as described in Subsection 2.5.2.

Furthermore, an error occurs at the start of the first transmission attempt, if at least one interferer is placed inside $B_1 = B(\text{RX}_0, s) \cap \overline{B(\text{RX}_0, s_b)}$, as shown in Figure 4.2. When $s < s_b$, the area of B_1 is 0, and so is $P_{rx|transmit}$. When $s \geq s_b$, this probability is equal to the probability that outage occurs at the start of the packet, P_{rx}, multiplied by the probability that the interferer is *not* inside $B(\text{RX}_0, s_b)$. These derivations, in addition to the ones in Chapter 2, lead to the following theorem.

Theorem 4.2 (CSMA_{RX})
The outage probability of $CSMA_{RX}$ for variable sensing threshold is given by Eq. (4.4)*, where:*

- $P_b \approx \tilde{P}_b$ *is given by the solution to Eq.* (4.5)*;* P_{rx} *is approximated by Eq.* (4.5)*, with* s_b *replaced by* s*.*
- $P_{rt} = P_{rx} + (1 - P_{rx})\, P_{during}$ *is the probability that an activated packet is received erroneously after a retransmission attempt.* P_{during} *is the probabil-*

ity that the error occurs at some $t \in (0, T)$, and is approximated by

$$\tilde{P}_{during} = \tag{4.8}$$
$$\begin{cases} 1-e^{-\lambda_{csma}^{RX}\left[\int_0^{s_b}\int_0^{2\pi} P(active|r,\phi)r\,d\phi dr + 2\int_{s_b}^{s}\int_{\nu(r)}^{\zeta(r)} P(active|r,\phi)r\,d\phi dr + \int_{s_b}^{s}[2\pi-2(\zeta(r)-\nu(r))]\,rdr\right]} & ;0<s_b<R \\ 1-e^{-\lambda_{csma}^{RX}\left[\int_0^{2R-s_b}\int_0^{2\pi} P(active|r,\phi)r\,d\phi dr + \int_{2R-s_b}^{s}\int_{\nu(r)}^{2\pi-\nu(r)} P(active|r,\phi)r\,d\phi dr\right]} & ;R\le s_b<2R \\ 1-e^{-\lambda_{csma}^{RX}\int_{s_b-2R}^{s}\int_{\nu(r)}^{2\pi-\nu(r)} P(active|r,\phi)r\,d\phi\,dr} & ;2R\le s_b<2R+s \\ 0 & ;otherwise \end{cases}$$

with $P(active|r,\phi)$ and $\nu(r)$ given in Eq. (2.25)*, with s replaced by s_b. Moreover, $\zeta(r) = \cos^{-1}\left(\frac{r^2-2Rs_b-s_b^2}{2Rr}\right)$.*

- *$P_{rt1} = P_{rx|transmit} + (1 - P_{rx|transmit})\,P_{during}$ is the probability that the first transmission attempt is erroneous, with $P_{rx|transmit}$ approximated by*

$$\tilde{P}_{rx|transmit} = \begin{cases} P_{rx}\left[1-\frac{s_b^2}{s^2}\right] & ;s_b<s \\ 0 & ;otherwise \end{cases} \tag{4.9}$$

Our simulation results indicate that the optimal sensing threshold in CSMA_{RX} is $\beta_b = \beta$ (equivalent to $s_b = s$). To confirm this analytically, we start by considering the case of $(M, N) = (1, 0)$, simplifying Eq. (4.4) to

$$\tilde{P}_{total} = \tilde{P}_{out}(\text{CSMA}_{\text{RX}}) = \begin{cases} \tilde{P}_{rx} + (1-\tilde{P}_{rx})\,\tilde{P}_{during} & ;s_b<s \\ \tilde{P}_b + (1-\tilde{P}_b)\,\tilde{P}_{during} & ;\text{otherwise} \end{cases} \tag{4.10}$$

Based on this, we now evaluate the rate of change of the different sources of outage, namely $\tilde{P}_b$ and $\tilde{P}_{during}$.

- When $s_b < s$:

$$\frac{d\tilde{P}_{total}}{ds_b} = [1-\tilde{P}_{rx}]\frac{d\tilde{P}_{during}}{ds_b}. \tag{4.11}$$

Since $\tilde{P}_{rx}$ is only a function of s, its derivative with respect to s_b is 0. $\tilde{P}_{during}$, on the other hand, is a monotonically decreasing function of s_b, which can be observed by considering Figure 4.3. As s_b increases with ds, the areas A and C shrink. As the decrease in these areas has

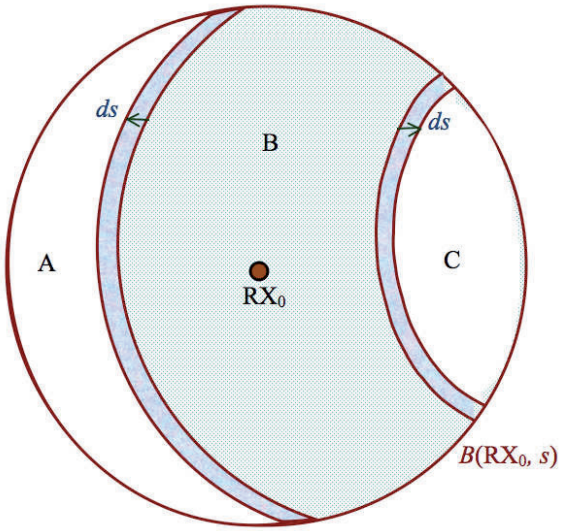

Figure 4.3: Setup to illustrate the rate of increase in P_b and decrease in P_{during} as s_b increases.

a greater impact on $\tilde{P}_{during}$ than the increase in area B (because in A and C, $P(\text{active}|r,\phi) = 1$), we get a decrease in $\tilde{P}_{during}$. Intuitively, this means that an increase in s_b results in more protection for an arriving TX-RX pair, resulting in a higher rate of backoff. Consequently, due to the reduced number of interferers, there is a smaller probability that a packet transmission is received in error once it has been activated. Hence, $\frac{d\tilde{P}_{total}}{ds_b} < 0$ for $s_b < s$.

- When $s_b \geq s$:

$$\frac{d\tilde{P}_{total}}{ds_b} = \left[1 - \tilde{P}_{during}\right] \frac{d\tilde{P}_b}{ds_b} + \left[1 - \tilde{P}_b\right] \frac{d\tilde{P}_{during}}{ds_b}. \tag{4.12}$$

When s_b increases by ds, $B(\text{RX}_0, s_b)$ grows and so does $\tilde{P}_b$. The rate of this increase is:

$$\frac{d\tilde{P}_b}{ds_b} \approx \frac{\pi(s_b + ds)^2 - \pi s_b^2}{\pi s_b^2} \frac{1}{ds} = \frac{ds^2 + 2\,s_b\,ds}{s_b^2} \frac{1}{ds}. \tag{4.13}$$

$\tilde{P}_{during}$, on the other hand, decreases with s_b. This change may be approximated by the decrease in the area around RX_0 within which

the occurrence of an interferer would cause outage, given by:

$$\frac{d\tilde{P}_{during}}{ds_b} \approx \frac{\left(\pi s^2 - \frac{\pi(s_b+ds-R)^2}{3}\right) - \left(\pi s^2 - \frac{\pi(s_b-R)^2}{3}\right)}{\pi s^2} \frac{1}{ds} = -\frac{2(s_b-R)ds + ds^2}{3\,s^2}\frac{1}{ds}. \quad (4.14)$$

To obtain the sign of $\frac{d\tilde{P}_{total}}{ds_b}$, we make some approximations. Since $ds \ll 1$, we set $(ds)^2 \approx 0$. Also, since $\beta = 1$, and the noise is small, we have $s \approx R$. The largest rate of decrease of Eq. (4.14) is when $s_b = s + R$. This yields $|\frac{d\tilde{P}_{during}}{ds_b}| \approx \frac{1}{3sds} < \frac{1}{2sds} \approx |\frac{d\tilde{P}_b}{ds_b}|$. Hence, since for all $s_b \geq s$, $|\frac{d\tilde{P}_{during}}{ds_b}| < |\frac{d\tilde{P}_b}{ds_b}|$ and $(1-\tilde{P}_b) \leq (1-\tilde{P}_{during})$, we have that the first term in Eq. (4.12) has a greater impact, resulting in $\frac{d\tilde{P}_{total}}{ds_b} > 0$ for $s_b \geq s$.

Thus, we conclude that the outage probability of CSMA_{RX} is minimized for $\beta_b^{opt} = \beta$ (i.e., $s_b^{opt} = s$). Similar behavior is observed for CSMA_{TX}. Note that the reduction in the outage probability by using β_b^{opt} is more evident for higher values of λ, as we will observe and discuss further in Subsection 4.1.4.

Extending the above optimization result to $M > 1$ and $N > 0$, results in solving the following equation

$$\frac{dP_{out}(\text{CSMA}_{\text{RX}})}{ds_b} = M\,P_b^{M-1}\left(1 - P_{rt}^{N+1}\right)\frac{dP_b}{ds_b} + (N+1)\,P_{rt}^{N}\,(1-P_b)(1-P_{rx})\,\frac{dP_{during}}{ds_b} = 0 \quad (4.15)$$

where $P_{rt} = P_{rx} + (1-P_{rx})\,P_{during}$, while $\frac{dP_b}{ds_b}$ and $\frac{dP_{during}}{ds_b}$ may be approximated by Eqs. (4.13) and (4.14), respectively. The evaluation of this expression depends on the values of M and N, and because of the complexity of the expressions, must be solved numerically. This is done by finding, for each value of s_t with ds increments, the values of P_b and P_{during} through numerical iterations, as described in Chapter 2, and illustrated in Figure 2.3. Inserting these values, along with the approximate values of $\frac{dP_b}{ds_b}$ and $\frac{dP_{during}}{ds_b}$ into Eq. (4.15), yields $\frac{dP_{out}(\text{CSMA}_{\text{RX}})}{ds_b}$. This can then be plotted as a function of s_b. The point where this curve crosses the 0-line yields s_b^{opt}.

Finally, we assume that both the sensing threshold and the required SINR threshold are varying, at the same time as remaining equal, i.e., $\beta_b = \beta$ (equivalently $s_b = s$).

Theorem 4.3 (CSMA with varying $s_b = s$)
The outage probability of CSMA$_{TX}$ when s_b is equal to s, is found by replacing s_b by s in Theorem 4.1, with the following differences:

- *The probability that the receiver is in outage at the start of its first transmission attempt is approximated by*

$$\tilde{P}_{rx|transmit} = \begin{cases} P_{rx} & ;s \leq \frac{R}{2} \\ P_{rx}\left[1 - \frac{2}{\pi}\cos^{-1}\left(\frac{R}{2s}\right) + \frac{R}{\pi s}\sqrt{1-\left(\frac{R}{2s}\right)^2}\right] & ;otherwise \end{cases} \tag{4.16}$$

- *The probability that a packet goes into outage at some $t \in (0, T)$ is approximated by*

$$\tilde{P}_{during} = \begin{cases} 1 - e^{-\lambda_{csma}^{TX}\pi s^2} & ;s < \frac{R}{2} \\ 1 - e^{-\lambda_{csma}^{TX}\left[\int_0^{R-s} 2\pi r dr + \int_{R-s}^{s} 2\pi - 2\cos^{-1}\left(\frac{r^2+R^2-s^2}{2Rr}\right) r dr\right]} & ;\frac{R}{2} < s < R \\ 1 - e^{-\lambda_{csma}^{TX}\int_{s-R}^{s}\left[2\pi - 2\cos^{-1}\left(\frac{r^2+R^2-s^2}{2Rr}\right)\right] r dr} & ;otherwise \end{cases} \tag{4.17}$$

The outage probability of CSMA$_{RX}$ is found by setting $s_b = s$ in Theorem 4.2, with the difference that the third line in Eq. (4.8) *is now valid for all $s \geq 2R$.*

4.1.3 Performance in the Presence of Fading

In this section, we add fading to the channel model, as described in Subsection 4.1.1. In the same manner as described in Subsection 3.1.3, the total outage probability of CSMA is given by

$$P_{out}(\text{CSMA}) \;=\; \overline{P}_b^M + \left(1 - \overline{P}_b^M\right)\, \overline{P}_{rt1}\, \overline{P}_{rt}^N, \tag{4.18}$$

where $\overline{P}_b$, $\overline{P}_{rt1}$, and $\overline{P}_{rt}$ are respectively the backoff probability, the probability that the packet is received in error at its first transmission attempt, and the probability of erroneous packet reception in a retransmission attempt, *averaged* with respect to the fading coefficients.

The density of packets that attempt to access the channel when the network is in a steady state, is (for both CSMA_{TX} and CSMA_{RX})

$$\lambda_{csma} \;=\; \lambda \left[\frac{1-\overline{P}_b^M}{1-\overline{P}_b} + (1-\overline{P}_b^M)\,\overline{P}_{rt1}\,\frac{1-\overline{P}_{rt}^N}{1-\overline{P}_{rt}} \right], \tag{4.19}$$

The backoff probability is derived using a modified version of the guard zone concept as discussed in Section 3.1. Once a transmission has been initiated, there is still a probability $\overline{P}_{rx|transmit}$ in CSMA_{TX} that the packet is in outage at the start of its first transmission attempt. To derive this probability, we refer to Eq. (3.4) for a strictly interference-limited channel, i.e.,

$$s^f(h_{00},h_{0i}) = h_{0i}^{1/\alpha}\left(\frac{h_{00}R^{-\alpha}}{\beta}\right)^{-1/\alpha} \;\wedge\; s_b^f(h_{00},h_{0i}) = h_{0i}^{1/\alpha}\left(\frac{h_{00}R^{-\alpha}}{\beta_b}\right)^{-1/\alpha} \tag{4.20}$$

These are the distances to the dominant interferers of RX_0 or TX_0 that cause the SINR to fall below β or β_b, respectively. For the sake of readability of the expressions, we use the simplified notation s_b^f for $s_b^f(h_{00},h_{i0})$ and s^f for $s^f(h_{00},h_{i0})$. Now consider the region of overlap $B_{ol} = B(\text{RX}_0,s^f)\cap B(\text{TX}_0,s_b^f)$. The area of this region is derived to be

$$A_{ol}(s^f,s_b^f) = \tag{4.21}$$
$$\begin{cases} 0 & ;\, s^f + s_b^f < R \\ \pi s_b^{f^2} & ;\, s^f > R + s_b^f \\ s^{f^2}\cos^{-1}\left(\frac{R^2+s^{f^2}-s_b^{f^2}}{2Rs^f}\right) + s_b^{f^2}\cos^{-1}\left(\frac{R^2+s_b^{f^2}-s^{f^2}}{2Rs_b^f}\right) & \\ \quad -\frac{1}{2}\sqrt{(s_b^f+s^f-R)(s_b^f-s^f+R)(-s_b^f+s^f+R)(s_b^f+s^f+R)} & ;\,\text{otherwise} \end{cases}$$

Given the probability that the packet is in error at the start of a transmission, $\overline{P}_{rx}$ (which is derived by using Eq. (3.11)), we have for CSMA_{TX} that

$$P_{rx|transmit}(h_{00},h_{0i}) \;\approx\; \overline{P}_{rx}\,\frac{\text{Area of } B(\text{RX}_0,s^f)\cup\overline{B(\text{TX}_0,s_b^f)}}{\text{Area of } B(\text{RX}_0,s^f)}. \tag{4.22}$$

To derive the probability that a packet goes into outage at some time during its transmission, $\overline{P}_{during}$, we use the Poissonianity of interferers and apply the following expression:

$$P_{during} \;=\; 1-\mathbb{E}_{h_{00},h_{ii}}\left[\exp\left\{-\iint_A \mu^f\, r\, dr\, d\phi\right\}\right], \tag{4.23}$$

where μ^f is the density of dominant interferers, TX_i, for the packet at RX_0, given as

$$\begin{aligned}\mu^f &= \mathbb{E}\left[\text{density of active dominant interferers for } RX_0\right] \qquad (4.24)\\ &= \Pr\left(TX_i \text{ placed at } (x,y)\right)\cdot \Pr(TX_i \text{ activated } |(x,y))\\ &\quad \times \Pr(TX_i \text{ causes error at } RX_0 \mid TX_i \text{ active at } (x,y)).\end{aligned}$$

The first term in Eq. (4.24) is equal to λ_{csma}^{TX} in $CSMA_{TX}$ and λ_{csma}^{RX} in $CSMA_{RX}$. As derived in Section 3.1, the second and third terms are, respectively, $\Pr(TX_i \text{ activated } |(x,y), h_{ii}) = 1 - \exp\left\{-\frac{h_{ii}R^{-\alpha}r^{\alpha}}{\beta_b}\right\}$ and $\Pr(TX_i \text{ causes error at } RX_0 | \ TX_i \text{ active at } (x,y), h_{00}) = \exp\left\{-\frac{h_{00}R^{-\alpha}r^{\alpha}}{\beta}\right\}$.

Taking the expectation with respect to h_{00} and h_{0i} of the above expressions, we arrive at the following theorem.

Theorem 4.4 ($CSMA_{TX}$)
The outage probability of $CSMA_{TX}$ in the presence of Rayleigh fading for variable sensing thresholds is given by Eq. (4.18)*, where:*

- $\overline{P}_b$ *is the average backoff probability, approximated by the solution to*

$$\overline{P}_b = 1 - e^{-\lambda\left(1-\overline{P}_b^M+\left(1-\overline{P}_b^M\right)\overline{P}_{rt1}\frac{1-\overline{P}_{rt}^N}{1-\overline{P}_{rt}}\right)\pi R^2 \beta_b^{2/\alpha}\frac{2\pi/\alpha}{\sin(2\pi/\alpha)}}. \qquad (4.25)$$

  $\overline{P}_{rx}$ *is the average probability that a packet is in error at the start of each of its retransmission attempts. This is given by Eq.* (4.25)*, with β_b replaced by β.*
- $\overline{P}_{rt} = \mathbb{E}_{h_{00}}\left[\overline{P}_{rx} + \left(1-\overline{P}_{rx}\right) P_{during}(h_{00})\right]$ *is the average probability that a packet is received in error during a retransmission attempt, with $P_{during}(h_{00})$ approximated by*

$$\tilde{P}_{during}(h_{00}) = 1 - e^{-\int_0^\infty 2\pi\lambda_{csma}^{TX}\left(1-e^{-\mathbb{E}[h_{ii}]R^{-\alpha}r^{\alpha}/\beta_b}\right)e^{-h_{00}R^{-\alpha}r^{\alpha}/\beta} r\,dr}, \qquad (4.26)$$

  where λ_{csma}^{TX} is the density of packets attempting to access the channel, as given by (4.19)*.*
- $\overline{P}_{rt1} = \mathbb{E}_{h_{00}}\left[P_{rx|transmit}(h_{00}) + \left(1 - P_{rx|transmit}(h_{00})\right) P_{during}(h_{00})\right]$ *is the average probability that the packet is received in error at its first transmission attempt. $P_{rx|transmit}(h_{00})$ is the probability that the received packet is*

in error upon its arrival, approximated by

$$\tilde{P}_{rx|transmit}(h_{00}) \approx \overline{P}_{rx}\, \mathbb{E}_{h_{0i}}\left[1 - \frac{A_{ol}\left(s^f(h_{00},h_{0i}), s_b^f(h_{00},h_{0i})\right)}{\pi\, s^f(h_{00},h_{0i})^2}\right], \tag{4.27}$$

where $A_{ol}\left(s^f(h_{00},h_{0i}), s_b^f(h_{00},h_{0i})\right)$ *is given by Eq.* (4.21).

The outage probability of CSMA_{RX} is derived in the same manner as for CSMA_{TX} with some minor differences. The main difference is the expression for $P_{rx|transmit}(h_{00})$, which is now dependent on the value of β_b with respect to β. When $\beta_b \geq \beta$, we have that $P_{rx|transmit}(h_{00}) = 0$, because once a packet using CSMA_{RX} has decided to transmit, its packet will surely not be received in error at the start of its first transmission attempt. When $\beta_b < \beta$, we have that $P_{rx|transmit}(h_{00},h_{0i}) \approx \overline{P}_{rx}\, \frac{\text{Area of } B(\text{RX}_0,s^f) \cap \overline{B(\text{RX}_0,s_b^f)}}{\text{Area of } B(\text{RX}_0,s^f)}$. Applying these changes to Theorem 4.4, we arrive at the following theorem for CSMA_{RX}.

Theorem 4.5 (CSMA_{RX})
The outage probability of $CSMA_{RX}$ *in the presence of Rayleigh fading for variable sensing threshold is given by Eq.* (4.18)*, where:*

- $\overline{P}_b$ *is the average backoff probability, approximated by the solution to Eq.* (4.25). $\overline{P}_{rx}$ *is given by Eq.* (4.25) *with* β_b *replaced by* β.
- $\overline{P}_{rt} = \mathbb{E}_{h_{00}}\left[\overline{P}_{rx} + \left(1-\overline{P}_{rx}\right) P_{during}(h_{00})\right]$ *is the average probability that a packet is received in error during a retransmission attempt, with* $P_{during}(h_{00})$ *approximated by Eq.* (4.26).
- $\overline{P}_{rt1} = \mathbb{E}_{h_{00}}\left[\overline{P}_{rx|transmit} + \left(1-\overline{P}_{rx|transmit}\right) P_{during}(h_{00})\right]$ *is the average probability that the packet is received in error at its first transmission attempt.* $P_{rx|transmit}$ *is the probability that the received packet is in outage upon arrival, approximated by*

$$\overline{P}_{rx|transmit} = \begin{cases} 0 & ;\ \textit{for } \beta_b \geq \beta \\ \overline{P}_{rx}\, \dfrac{\beta^{2/\alpha} - \beta_b^{2/\alpha}}{\beta^{2/\alpha}} & ;\ \textit{otherwise} \end{cases} \tag{4.28}$$

Optimization of the derived outage probability expressions as a function of the sensing threshold β_b is performed through simulations in the following subsection.

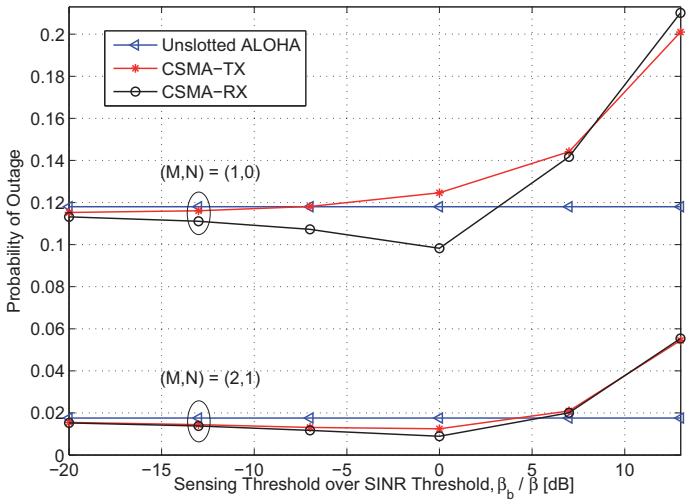

Figure 4.4: Outage probability in the absence of fading with $\lambda = 0.02$ and $\beta = 0$ dB, as a function of β_b/β

4.1.4 Numerical Results

For the Monte Carlo simulations, we apply the following values (unless stated otherwise): transmitter-receiver distance $R = 1$ m, transmission power $\rho = 1$ mW, path-loss exponent $\alpha = 4$, SINR threshold $\beta = 0$ dB, and fading parameter $\zeta = 1$. The averaging is performed over 10000 instances in the case of non-fading, and 4000 for fading networks.

In Figure 4.4, the outage probability of unslotted ALOHA and CSMA in a non-fading network is plotted as a function of the normalized sensing threshold β_b, for $\beta = 0$ dB and a low density of $\lambda = 0.02$. For $(M, N) = (1, 0)$, we observe that the outage probability of CSMA_{TX} increases monotonically with β_b, meaning that the outage probability is in fact minimized when no sensing is applied at all. This is due to the fact that for low values of β_b, $B(\text{TX}_0, s_b)$ is too small, and consequently transmitter-sensing provides minimal protection for its receiver, resulting in an approximately constant outage probability for all $\beta_b \leq \beta$. For higher values of β_b, P_b becomes the dominant source of outage, and with a higher rate of increase than the decrease in P_{during}, the total outage probability *increases* monotonically. For CSMA_{RX}, however, a slight improvement in the outage probability is observed when $\beta_b^{opt} = \beta$. For $(M, N) = (2, 1)$, on the other

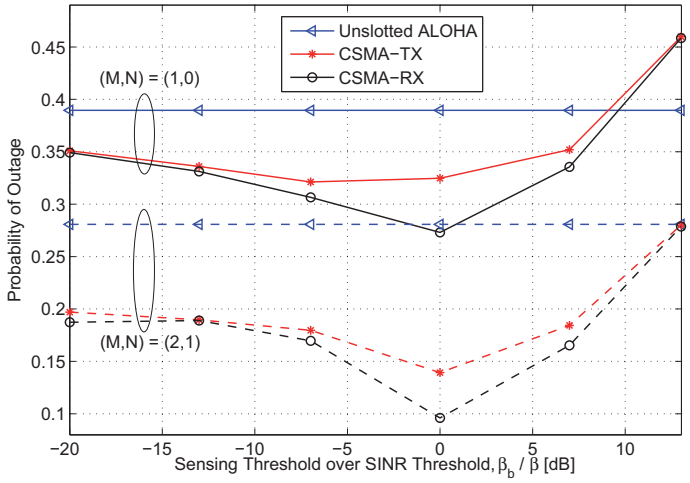

Figure 4.5: The outage probability in the presence of fading with $\lambda = 0.02$ and $\beta = 0$ dB.

hand, the benefit of optimizing the sensing threshold becomes more significant for both protocols. The outage probability is minimized for $\beta_b \approx \beta$ (as was also derived in Subsection 4.1.2), providing up to 50% improvement for CSMA_{RX} and 40% for CSMA_{TX}, compared to having no sensing (i.e., when $\beta_b = 0$).

Similarly, Figure 4.5 shows the outage performance of a fading network as a function of β_b/β for a fixed density of $\lambda = 0.02$. The outage probability of both CSMA protocols is minimized for $\beta_b = \beta = 0$ dB. When $(M, N) = (1, 0)$, the use of the optimal sensing threshold reduces the outage probability of CSMA_{RX} by up to 22% and that of CSMA_{TX} by 8%. For higher values of M and N, this improvement is increased; the outage probability of CSMA_{RX} can then be reduced by up to 50%.

To compare the various protocols, Figure 4.6 shows the the ratio of the outage probability of the unslotted protocols over that of slotted ALOHA for a non-fading network with $(M, N) = (1, 0)$ as a function of β_b/β. The advantage of the sensing threshold optimization is more apparent for higher densities. By using β_b^{opt} when $\lambda = 0.2$, the outage probability of CSMA_{TX} and CSMA_{RX} can be reduced by up to 40% and 42%, respectively. Note that the minimum outage probability occurs at a slightly higher sensing threshold than β. This is because the probability that outage occurs due

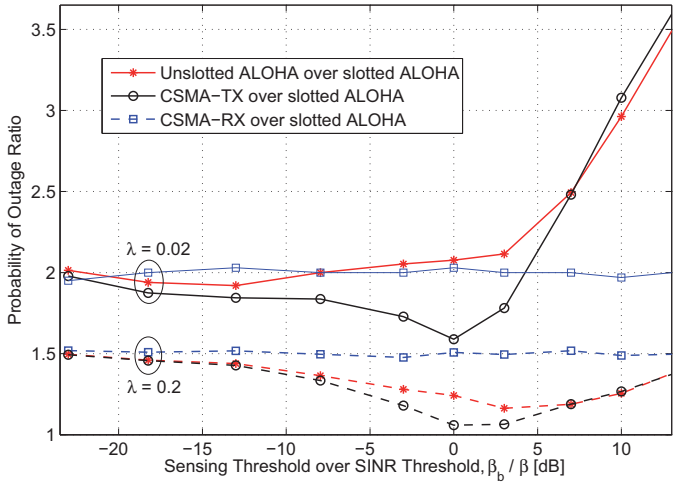

Figure 4.6: Ratio of the outage probability of the unslotted protocols over that of slotted ALOHA in a non-fading network with $(M, N) = (1, 0)$, as a function of β_b/β.

to the aggregate interference power from transmitters outside $B(\mathrm{RX}_0, s)$ increases with λ, and having a higher β_b provides greater protection against this event.

Figure 4.7 shows the ratio of the outage probability of unslotted ALOHA and CSMA over that of slotted ALOHA in a non-fading network, when $\beta_b = \beta$ and both varying, for $(M, N) = (2, 1)$ and a fixed high density of $\lambda = 0.2$. For low values of β, $\mathrm{CSMA}_{\mathrm{RX}}$ yields up to 10% lower outage probability compared to unslotted ALOHA, while $\mathrm{CSMA}_{\mathrm{TX}}$ yields 45% higher outage probability. However, as $\beta_b = \beta$ increases (i.e., for $\beta > -6$ dB), making both the sensing zone and the communication guard zone grow, the outage probability of $\mathrm{CSMA}_{\mathrm{TX}}$ decreases below that of unslotted ALOHA. This is because once a packet has been activated, the ratio of the area within which the arrival of an interferer causes outage in $\mathrm{CSMA}_{\mathrm{TX}}$ (i.e., $B(\mathrm{RX}_0, s) \cap \overline{B(\mathrm{TX}_0, s)}$) over that in ALOHA (i.e., $B(\mathrm{RX}_0, s)$) decreases with β.

More interestingly, for even higher values of β (i.e., for $\beta > 8$ dB), both CSMA protocols actually perform better than *slotted* ALOHA. This is because for large s, $B(\mathrm{TX}_0, s)$ and $B(\mathrm{RX}_0, s)$ overlap almost completely, such that the only source of outage in CSMA is if an interferer is placed inside

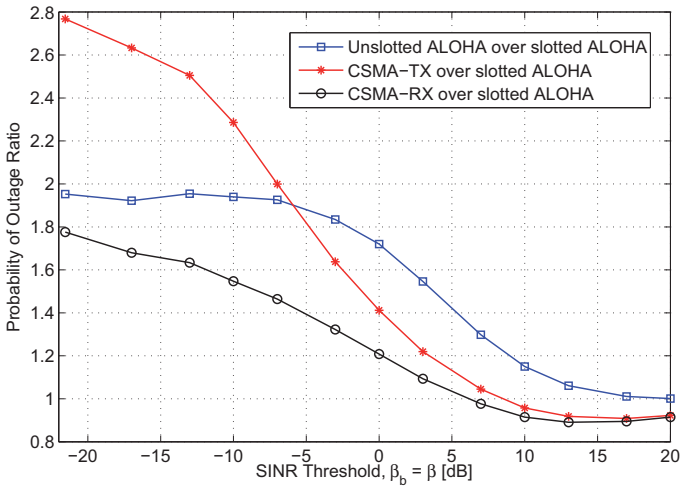

Figure 4.7: Ratio of the outage probability of unslotted ALOHA and CSMA over that of slotted ALOHA as a function of $\beta_b = \beta$ for $\lambda = 0.2$ and $(M, N) = (1, 0)$.

$B(\mathrm{RX}_0, s)$ during $[0, T)$, as is the case in slotted ALOHA. Moreover, due to the backoff property of CSMA, the density of interferers is lower than that of slotted ALOHA, making CSMA yield a lower outage probability. Similar behavior is observed for lower densities and other (M, N)-values.

4.2 CSMA With Joint Transmitter-Receiver Sensing

Having considered the performance of CSMA_{TX} and CSMA_{RX}, a potentially interesting follow-up question is: Can we improve the performance of CSMA further if we allow *both* the transmitter and its receiver to sense the channel, and subsequently let them *collectively* decide whether or not to initiate transmission of each packet? And moreover, what are the optimal sensing thresholds that minimize the outage probability of this new flavor of CSMA, both in the absence and presence of fading?

Hence, in the following, we will analyze the impact of such a joint back-off decision-making on the performance of the CSMA protocol. Following the same style of notation as in the preceding chapters, we refer to this flavor of CSMA as $\text{CSMA}_{\text{TXRX}}$. Not only is this analysis useful for future improvements made to CSMA, it also provides us with an understanding of the *hidden* and *exposed node problems*, which are the main sources of imperfection of this protocol. The hidden node problem occurs whenever a new node is unable to detect an ongoing transmission, so that it initiates its transmission and thereby causes outage for an already active packet. The exposed node problem is characterized by transmissions being prevented even though they could have taken place without harm to other ongoing transmissions. An increase in one of these problems, results in a decrease in the other, and vice versa. Choosing optimal values for the sensing thresholds β_t and β_r, will provide a balance between the hidden and exposed node problems, thus improving the system performance.

4.2.1 System Model

The ad hoc network model in this section resembles again that of Chapter 2. That is, we consider a single random process describing both the temporal and spatial variations of the system, by assuming a 3-D PPP of packet arrivals in time and space. The spatial density of new packet arrivals is as before $\lambda = \lambda^s \lambda^t T$, where λ^s [nodes/m^2] is the density of nodes on the 2-D plane, λ^t [packets/sec/node] is the density of packet arrivals in time at each node, and T [sec] is the fixed packet length.

The channel access is driven by the $\text{CSMA}_{\text{TXRX}}$ protocol. This protocol operates as follows: Whenever a packet is ready for transmission, its corresponding transmitter and receiver both perform physical carrier sensing (i.e., the radio measures the energy received on its available radio channel), calculate their SINRs individually, and compare them against their required sensing thresholds, β_t and β_r, respectively. If the SINR at the

transmitter is greater than β_t *and*[1] the SINR at the receiver is greater that β_r, the transmission is initiated. Otherwise, the channel is considered busy, and the packet is backed off. Once a transmission is initiated, there is a probability that it is received in error at its receiver, i.e., the received SINR is below β at some $t \in [0, T)$. In this case, the packet is retransmitted. Each packet is given M backoffs and N retransmissions before it is dropped and counted to be in outage.

For the channel model, we consider both non-fading and fading channels. In the former, only path loss attenuation effects are considered, with path loss exponent $\alpha > 2$. Each receiver potentially sees interference from all transmitters, and these independent interference powers are added to the channel noise η to cause signal degradation. The introduction of fading adds another source of randomness to the model, namely the channel coefficients h_{ij}. The SINR of a non-fading network and SINR^f of a fading network (for link i) are given as

$$\text{SINR}_i = \frac{\rho\, R^{-\alpha}}{\eta + \sum_i \rho\, r_i^{-\alpha}} \quad \wedge \quad \text{SINR}_i^f = \frac{\rho\, R^{-\alpha}\, h_{00}}{\eta + \sum_i \rho\, r_i^{-\alpha} h_{0i}}, \tag{4.29}$$

where r_i is the distance between the node under observation and the i-th interfering transmitter; h_{00} represents the fading effects between the receiver under observation, RX_0, and its designated transmitter, and h_{0i} is the fading coefficient between RX_0 and the i-th interfering transmitter. The summation is over all active interferers on the plane at each time instant.

Our performance metric is, as before, outage probability, which is defined as the probability that a packet is received erroneously at its receiver after M backoffs and N retransmission. In the following, we derive the outage probability of $\text{CSMA}_{\text{TXRX}}$ both in the absence and in the presence of fading. Moreover, the sensing thresholds of both the transmitter and the receiver are optimized.

4.2.2 Performance in the Absence of Fading

In this section, we assume no fading effects in the channel, i.e., the signal degradation is due to path loss only, as described in Subsection 4.2.1. Denoting the SINR based on the transmitter's sensing as SINR_t, and that based on the receiver's sensing as SINR_r, the outage probability of

[1] Using "or" here would mean that each node pair backs off less often than both CSMA_{TX} and CSMA_{RX}, and thus the outage probability of CSMA would increase and approach that of unslotted ALOHA.

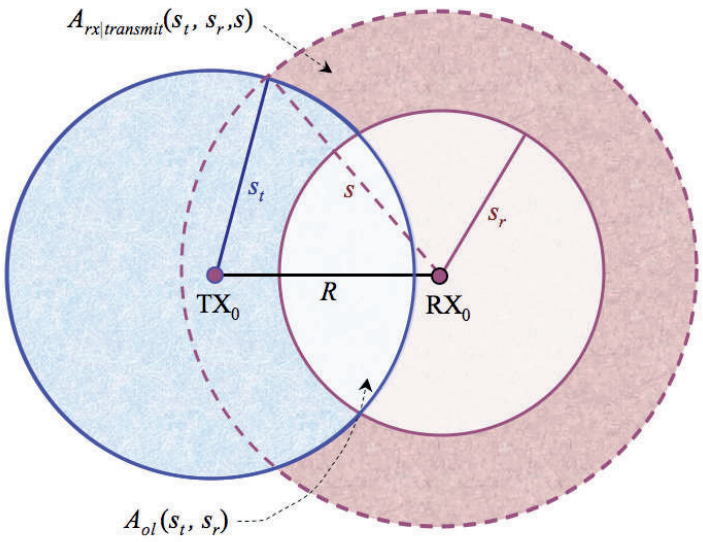

Figure 4.8: Illustration of the sensing zones $B(\mathrm{RX}_0, s_r)$ and $B(\mathrm{TX}_0, s_t)$.

$\mathrm{CSMA}_{\mathrm{TXRX}}$ is given by

$$\begin{aligned} P_{out}(\mathrm{CSMA}_{\mathrm{TXRX}}) &= \Pr\left[\mathrm{SINR}_t < \beta_t \cup \mathrm{SINR}_r < \beta_r \text{ at } t = 0\right]^M \\ &\quad - \left(1 - \Pr\left[\mathrm{SINR}_t < \beta_t \cup \mathrm{SINR}_r < \beta_r \text{ at } t = 0\right]^M\right) \\ &\qquad \times \Pr\left[\mathrm{SINR}_r < \beta \text{ at some } t \in [0, T)\right]^{N+1}. \end{aligned} \tag{4.30}$$

To derive the backoff probability, P_b, in the same manner as in the previous sections, we use the distance dependence of the interference and apply the concept of guard zones [36]. Defining s_t to be the distance between the transmitter under observation, TX_0, and its closest interferer, TX_i, and s_r as the distance between RX_0 and TX_i, yields

$$s_t = \left(\frac{R^{-\alpha}}{\beta_t} - \frac{\eta}{\rho}\right)^{-\frac{1}{\alpha}} \quad \wedge \quad s_r = \left(\frac{R^{-\alpha}}{\beta_r} - \frac{\eta}{\rho}\right)^{-\frac{1}{\alpha}}. \tag{4.31}$$

The sensing zone of RX_0 is then $B(\mathrm{RX}_0, s_r)$ and that of the transmitter is $B(\mathrm{TX}_0, s_t)$. This means that if there exists, upon the arrival of TX_0-RX_0, at least one transmission inside $B_1 = B(\mathrm{TX}_0, s_t) \cup B(\mathrm{RX}_0, s_r)$, this transmitter-receiver pair would back off from transmission. The area of B_1 is shown as the lightly shaded area (of the two smaller circles) in Figure 4.8, and given

as $\pi s_t^2 + \pi s_r^2 - A_{ol}(s_t, s_r)$, where $A_{ol}(s_t, s_r)$ is the area of overlap $B(\text{TX}_0, s_t) \cap B(\text{RX}_0, s_r)$, as given by Eq. (4.21).

Once TX_0-RX_0 decides to transmit, there is still a probability that their packet is in error at the start of its first transmission due to ongoing transmissions inside $B(\text{RX}_0, s)$ that were not detected in the backoff decision-making stage. That is, the packet must be retransmitted if an interfering transmission is detected inside $B(\text{RX}_0, s) \cap \overline{B(\text{TX}_0, s_t) \cup B(\text{RX}_0, s_r)}$. This area is the darkly shaded area shown in Figure 4.8, and is given by

$$A_{rx|transmit}(s_t, s_r, s) = \begin{cases} 0 & ; s_r \geq s \\ \pi s^2 - \pi s_r^2 - A_{ol}(s_t, s) & ; s_r < s \text{ and } s_t < R - s_r \\ \pi s^2 - \pi s_r^2 - A_{ol}(s_t, s) + A_{ol}(s_t, s_r) & ; s_r < s \text{ and } s_t < R + s_r \\ \pi s^2 - A_{ol}(s_t, s) & ; \text{otherwise} \end{cases} \tag{4.32}$$

Finally, given the packet transmission of TX_0-RX_0 is initiated, and it is not in error at the start of its transmission, then there is a probability that a new interferer, TX_i, enters the plane at some $t \in (0, T)$ and is located inside $B(\text{RX}_0, s)$, causing error for the packet of RX_0. Since, TX_i would back off if it detects the transmission of TX_0, this means that TX_i must be placed inside $B_2 = B(\text{RX}_0, s) \cap \overline{B(\text{TX}_0, s_t)}$, while its receiver RX_i is located outside of $B(\text{TX}_0, s_r)$, in order for it to cause outage for RX_0. The area of B_2, including the probability of activation on RX_i is given as

$$G_{active} = \tag{4.33}$$
$$\begin{cases} 0 & ; s_t \geq R + s \\ \int_{s_t - R}^{s} \int_{\gamma(r)}^{2\pi - \gamma(r)} P(\text{active}|r, \phi)\, r\, d\phi\, dr & ; R \leq s_t < R + s \\ \int_{0}^{R - s_t} \int_{0}^{2\pi} P(\text{active}|r, \phi) r\, d\phi\, dr + \int_{R - s_t}^{\min(s_r, s)} \int_{\gamma(r)}^{2\pi - \gamma(r)} P(\text{active}|r, \phi) r\, d\phi\, dr & \\ \quad + 2 \int_{s_r}^{\min(s_r, s)} \int_{\gamma(r)}^{\zeta(r)} P(\text{active}|r, \phi)\, r\, d\phi\, dr + \int_{\min(s_r, s)}^{s} (2\pi - 2\zeta(r))\, r\, dr & ; \text{otherwise} \end{cases}$$

where $P(\text{active}|r, \phi)$ is the probability that the receiver of the interferer, RX_i, is located out of the range of TX_0, i.e., outside $B(\text{TX}_0, s_r)$. It is derived in the same manner as explained in Subsection 2.5.2 The integration limits of the angle are derived with the cosine rule based on the points of intersection between $B(\text{TX}_0, s_t)$ and circles around RX_0 with various radi.

Due to the Poisson distribution of interferers, we apply the expression $P_{error} = 1 - \exp\left\{-\lambda_{csma}^{TXRX} A\right\}$, where A is the detection area, depending

on the particular error probability to be calculated. Moreover, the density λ_{csma}^{TXRX} is given as

$$\begin{aligned}\lambda_{csma}^{TXRX} &= \begin{cases}\lambda \sum_{m=0}^{M-1} P_b^m & ;\text{for } N=0\\ \lambda\left[\sum_{m=0}^{M-1} P_b^m + (1-P_b^M)\, P_{rt1} \sum_{n=0}^{N-1} P_{rt}^n\right] & ;\text{for } N \geq 1\end{cases}\\ &= \lambda\left[\frac{1-P_b^M}{1-P_b} + (1-P_b^M)\, P_{rt1}\, \frac{1-P_{rt}^N}{1-P_{rt}}\right], \end{aligned} \tag{4.34}$$

where P_b is the backoff probability, P_{rt1} is the probability that the packet is received in error at its first transmission attempt, and P_{rt} is the probability that the packet is received erroneously in a retransmission attempt. Based on the above derivations, we are now able to mathematically express the outage probability of $\text{CSMA}_{\text{TXRX}}$ in the following theorem.

Theorem 4.6

The outage probability of $CSMA_{TXRX}$ (in the absence of fading) with variable sensing thresholds is given by

$$P_{out}(CSMA_{TXRX}) \;=\; P_b^M + \left(1-P_b^M\right)\, P_{rt1}\, P_{rt}^N, \tag{4.35}$$

where:

- *P_b is the backoff probability, approximated by the solution to*

$$\tilde{P}_b \;=\; 1 - e^{-\lambda\left(1-\tilde{P}_b^M+\left(1-\tilde{P}_b^M\right)\tilde{P}_{rt1}\frac{1-\tilde{P}_{rt}^N}{1-\tilde{P}_{rt}}\right)\left(\pi s_t^2+\pi s_r^2-A_{ol}(s_t,s_r)\right)}, \tag{4.36}$$

  where $A_{ol}(s_t, s_r)$ is given by Eq. (4.21).

- *$P_{rt} = P_{rx} + (1-P_{rx})\; P_{during}$ is the probability that a packet is received in error in a retransmission attempt. P_{rx} is the probability that the packet is in error at the start of each of its retransmissions, approximated by*

$$\tilde{P}_{rx} \;=\; 1 - e^{-\lambda\left(1-\tilde{P}_b^M+\left(1-\tilde{P}_b^M\right)\tilde{P}_{rt1}\frac{1-\tilde{P}_{rt}^N}{1-\tilde{P}_{rt}}\right)\pi s^2}, \tag{4.37}$$

- *P_{during} is the probability that an error occurs at some $t \in (0, T)$, approximated by*

$$\tilde{P}_{during} \;=\; 1 - e^{-\lambda\left(\frac{1-\tilde{P}_b^M}{1-\tilde{P}_b}+\left(1-\tilde{P}_b^M\right)\tilde{P}_{rt1}\frac{1-\tilde{P}_{rt}^N}{1-\tilde{P}_{rt}}\right)G_{active}(s_t,s_r)}, \tag{4.38}$$

where $G_{active}(s_t, s_r)$ *is given by Eq.* (4.33)*, with* $P(active|r,\phi)$ *and the angles* $\nu(r)$*,* $\zeta(r)$*, and* $\gamma(r)$ *given by*

$$P(active|r,\phi) \;=\; 1 - \frac{1}{\pi}\cos^{-1}\left(\frac{r^2+2R^2-s_r^2-2Rr\cos\phi}{2R\sqrt{r^2+R^2-2Rr\cos\phi}}\right) \tag{4.39}$$

$$\nu(r) = \cos^{-1}\left(\frac{r^2+2Rs_t-s_t^2}{2Rr}\right) \quad \wedge \quad \zeta(r) = \cos^{-1}\left(\frac{r^2-2Rs_t-s_t^2}{2Rr}\right)$$

$$\gamma(r) = \cos^{-1}\left(\frac{r^2+R^2-s_t^2}{2Rr}\right).$$

- $P_{rt1} \;=\; P_{rx|transmit} + (1 - P_{rx|transmit})\, P_{during}$ *is the probability that the packet is received in error at its first transmission attempt.* $P_{rx|transmit}$ *is the probability that the receiver is in outage at the start of the packet, although it decides to initiate its transmission, approximated by*

$$\tilde{P}_{rx|transmit} \;=\; P_{rx}\,\frac{A_{rx|transmit}(s_t, s_r, s)}{\pi\, s^2}, \tag{4.40}$$

with $A_{rx|transmit}(s_t, s_r, s)$ *given by Eq.* (4.32)*.*

Optimization of the sensing thresholds is carried out in Subsection 4.2.4, and comparison between the outage probability of $\text{CSMA}_{\text{TXRX}}$ with the other versions of CSMA is performed through simulations in Subsection 4.2.5.

4.2.3 Performance in the Presence of Fading

In this section, we again add fading effects to the path loss attenuation, as described in Subsection 4.2.1. Due to the independence of the channel fading coefficients on distance, we now consider all the *dominant* interferers, which are transmitters whose interference power can alone result in outage for the packet under observation.

The outage probability expression in the case of fading is the same as Eq. (4.35), with the difference that P_b, P_{rt1}, and P_{rt} are replaced by their average values with respect to the fading coefficients: $\overline{P}_b$, $\overline{P}_{rt1}$, and $\overline{P}_{rt}$. Moreover, based on the same reasoning as in the case of non-fading networks, the density of packets attempting to access the channel is

$$\lambda_{csma}^{TXRX} = \lambda\left[\frac{1-\overline{P}_b^M}{1-\overline{P}_b} + (1-\overline{P}_b^M)\,\overline{P}_{rt1}\,\frac{1-\overline{P}_{rt}^N}{1-\overline{P}_{rt}}\right]. \tag{4.41}$$

The probability that a transmitter-receiver pair, TX_0-RX_0, backs off is given by the probability that the SINR at the start of the packet is below β_t at the transmitter, or below β_r at the receiver, or both. Hence, we have

$$\overline{P}_b \;=\; \overline{P}_{b1}(\beta_t) + \overline{P}_{b1}(\beta_r) - \Pr(\text{TX}_0 \text{ beg.} \;\cap\; \text{RX}_0 \text{ beg.}) \tag{4.42}$$

$\overline{P}_{b1}(\beta_t)$ (and similarly $\overline{P}_{b1}(\beta_r)$) is derived by using a modified version of the guard zone concept, as described in Section 3.1. That is, with an SINR constraint of β, the distance to the dominant interferer (given h_{00} and h_{0i}) is given in Eq. (3.4). Consequently, we have that the expected number of dominant interferers within a distance $s^f(h_{00}, h_{0i})$ away and with arrival time during $[-T, 0)$, is approximately: $\pi\,\lambda_{csma}^{TXRX}\, s^f(h_{00}, h_{0i})^2$. Assuming a strictly interference-limited network (i.e., $\eta \approx 0$) with Poisson distributed packets, we have

$$\overline{P}_{b1}(\beta_t) \;\approx\; 1 - \exp\left\{ -\pi\,\lambda_{active}\, \mathbb{E}\left[h_{0i}^{\frac{2}{\alpha}} \right] \mathbb{E}\left[\left(\frac{h_{00} R^{-\alpha}}{\beta_t} \right)^{-\frac{2}{\alpha}} \right] \right\}, \tag{4.43}$$

where $\lambda_{active} = \lambda \left[1 - \overline{P}_b^M + (1 - \overline{P}_b^M)\, \overline{P}_{rt1}\, \frac{1-\overline{P}_{rt}^N}{1-\overline{P}_{rt}} \right]$. The expectations in Eq. (4.43) can be simplified by using the result given in Eq. (3.8).

To derive $\Pr(\text{TX}_0 \text{ beg.} \cap \text{RX}_0 \text{ beg.})$, we refer to our geometrical analysis again. Assuming that $B(\text{TX}_0, s_t^f)$ and $B(\text{RX}_0, s_r^f)$ are approximately circular regions, as shown in Figure 4.8, we have after some manipulations

$$\begin{aligned} &\Pr(\text{RX}_0 \text{ beg.} \;\cap\; \text{TX}_0 \text{ beg.}) \qquad (4.44)\\ &\quad= \quad \Pr(\text{RX}_0 \text{ beg.}) - \Pr(\overline{\text{TX}_0 \text{ beg.}}) \cdot \Pr(\text{RX}_0 \text{ beg.} \mid \overline{\text{TX}_0 \text{ beg.}})\\ &\quad= \quad \overline{P}_{b1}(\beta_r) - \left(1 - \overline{P}_{b1}(\beta_t)\right)\, \overline{P}_{b1}(\beta_r)\, \frac{\pi s_r^{f^2} - A_{ol}(s_t^f, s_r^f)}{\pi s_r^{f^2}}. \end{aligned}$$

Inserting this expression back into Eq. (4.42), yields the backoff probability of $\text{CSMA}_{\text{TXRX}}$.

Once a transmission has been initiated, there is a probability $\overline{P}_{rx|transmit}$ that the packet is in error at the start of its first transmission attempt. Using geometric arguments again, this probability is given as the probability that an active interferer already exist on the plane inside $B(\text{RX}_0, s^f)$, that was not detected during the backoff decision-making stage. That is, the interferer TX_i must have been located inside $A_{rx|transmit}(s_t^f, s_r^f, s^f)$, as shown by the dark-shaded area in Figure 4.8.

To derive the probability that a packet goes into outage at some time during its transmission, denoted by $\overline{P}_{during}$, we use the Poissonianity of

interferers and apply the following expression:

$$\overline{P}_{during} \;=\; \mathbb{E}_{h_{00},h_{ii}}\left[1-\exp\left\{-\iint_A \mu^f\, r\, dr\, d\phi\right\}\right]. \tag{4.45}$$

where μ^f is the density of dominant interferers, TX_i, for the packet at RX_0, and is derived as

$$\begin{aligned}\mu^f &= \mathbb{E}\left[\text{density of active dominant interferers for } \mathrm{RX}_0\right]\\ &= \Pr\left(\mathrm{TX}_i \text{ placed at } (x,y)\right) \times \Pr(\mathrm{TX}_i\text{—}\mathrm{RX}_i \text{ activated } |(x,y))\\ &\qquad \times \Pr(\mathrm{TX}_i \text{ causes error at } \mathrm{RX}_0 | \mathrm{TX}_i \text{ active at } (x,y))\\ &= \lambda_{csma}^{TXRX}\left(1-e^{-\frac{h_{ii}R^{-\alpha}r^{\alpha}}{\beta_t}}\right)\left(1-e^{-\frac{h_{ii}R^{-\alpha}r^{\alpha}}{\beta_r}}\right)e^{-\frac{h_{00}R^{-\alpha}r^{\alpha}}{\beta}}.\end{aligned} \tag{4.46}$$

Based on the derivations given above, we arrive at the following theorem.

Theorem 4.7

The outage probability of $CSMA_{TXRX}$ in the presence of Rayleigh fading with variable sensing thresholds is given by

$$P_{out}(CSMA_{TXRX}) \;=\; \overline{P}_b^M + \left(1-\overline{P}_b^M\right)\overline{P}_{rt1}\,\overline{P}_{rt}^N, \tag{4.47}$$

where:

- $\overline{P}_b \approx \overline{P}_{b1}(\beta_t) + \left(1-\overline{P}_{b1}(\beta_t)\right)\overline{P}_{b1}(\beta_r)\frac{\pi {s_r^f}^2 - A_{ol}(s_t^f, s_r^f)}{\pi {s_r^f}^2}$ *is the average backoff probability, where $\overline{P}_{b1}(\beta_t)$ is the solution to*

$$\overline{P}_{b1}(\beta_t) \;=\; 1-e^{-\lambda\left(1-\overline{P}_b^M+\left(1-\overline{P}_b^M\right)\overline{P}_{rt1}\frac{1-\overline{P}_{rt}^N}{1-\overline{P}_{rt}}\right)\pi R^2 \beta_t^{2/\alpha}\frac{2\pi/\alpha}{\sin(2\pi/\alpha)}}, \tag{4.48}$$

  Similarly, $\overline{P}_{b1}(\beta_r)$ is given by replacing β_t by β_r in Eq. (4.48).

- $\overline{P}_{rt} = \mathbb{E}_{h_{00}}\left[\overline{P}_{rx} + \left(1-\overline{P}_{rx}\right)\,P_{during}(h_{00})\right]$ *is the probability that a packet is received in error in a retransmission attempt. $\overline{P}_{rx}$ is the average probability that the packet is in error at the start of each packet, approximated by*

$$\overline{P}_{rx} \;=\; 1-e^{-\lambda\left(1-\overline{P}_b^M+\left(1-\overline{P}_b^M\right)\overline{P}_{rt1}\frac{1-\overline{P}_{rt}^N}{1-\overline{P}_{rt}}\right)\pi R^2 \beta^{2/\alpha}\frac{2\pi/\alpha}{\sin(2\pi/\alpha)}}, \tag{4.49}$$

- $P_{during}(h_{00})$ *is the probability that an error occurs at some $t \in (0,T)$, approximated by*

$$\tilde{P}_{during}(h_{00}) = 1-e^{-\lambda_{csma}^{TXRX}\int_0^{\infty} 2\pi\left(1-e^{-\frac{\mathbb{E}[h_{ii}]R^{-\alpha}r^{\alpha}}{\beta_t}}\right)\left(1-e^{-\frac{\mathbb{E}[h_{ii}]R^{-\alpha}r^{\alpha}}{\beta_r}}\right)e^{-\frac{h_{00}R^{-\alpha}r^{\alpha}}{\beta}} r\, d}. \tag{4.50}$$

- $\overline{P}_{rt1} = \mathbb{E}_{h_{00}}\left[P_{rx|transmit}(h_{00}) + \left(1 - P_{rx|transmit}(h_{00})\right)\ P_{during}(h_{00})\right]$ *is the probability that the packet is received in error at its first transmission attempt.* $P_{rx|transmit}(h_{00})$ *is the probability that the packet is received in error at the start of its first transmission, approximated by*

$$\tilde{P}_{rx|transmit}(h_{00}) \ = \ \overline{P}_{rx}\ \mathbb{E}_{h_{0i}}\left[\frac{A_{rx|transmit}\left(s_t^f(h_{00},h_{0i}), s_r^f(h_{00},h_{0i})\right)}{\pi\, s^f(h_{00},h_{0i})^2}\right], \quad (4.51)$$

where $s^f(h_{00}, h_{0i})$ *is given by Eq.* (3.4).

4.2.4 Optimizing the Sensing Thresholds

In order to find the optimal sensing thresholds of $\text{CSMA}_{\text{TXRX}}$, β_t^{opt} and β_r^{opt}, such that the outage probability is minimized, we must in principle differentiate the outage probability expressions derived above with respect to β_t and β_r, and set the derivatives equal to 0. However, because of the complexity of our equations, this turns out to be a nontrivial task. Hence, we attack our optimization problem from another angle: Using the performance of CSMA_{RX}[2] as a reference point, we evaluate the outage probability of $\text{CSMA}_{\text{TXRX}}$ based on the change in the exposed and hidden node problems. For this, we first develop an understanding of the impact of transmitter and receiver sensing on the hidden and exposed node problems.

4.2.4.1 Understanding the Hidden and Exposed Node Problems

In order to establish a fundamental understanding of the inherent hidden and exposed node problems of CSMA, we solely focus on a non-fading network. The *hidden node problem* of CSMA occurs during an active packet transmission, when a newly arriving transmitter, TX_i, is located too close to the receiver under observation, RX_0, while TX_i and RX_i are simultaneously too far away from TX_0 to detect its transmission. That is, TX_i initiates its transmission and causes error for the packet reception of RX_0 because TX_0 is *hidden* to it and its receiver. The probability of such an event ocurring is:

$$\Pr(\text{hidden node}) \ \approx \ \Pr(\text{RX}_0 \text{ mid.} \mid \overline{\text{TX}_i \text{ beg.} \cap \ \text{RX}_i \text{ beg.}}).$$

Now, the probability that TX_0 is hidden to both TX_i and RX_i is less than the probability that it is hidden only to RX_i, which is the case in CSMA_{RX}.

[2] This protocol was evaluated in Section 4.1 for a variable sensing threshold. We assume low density of transmissions, where the outage probability expressions are reasonable approximations.

Hence, the transmitter sensing of $\text{CSMA}_{\text{TXRX}}$ reduces the hidden node problem, as the area around RX_0 within which an interferer may be activated and cause outage, is reduced. For a non-fading network, this yields the following approximation:

$$\tilde{P}_{during} \approx \tilde{P}^{RX}_{during} - \left(1 - e^{-\lambda^{TXRX}_{csma} A_{ol}(s_t, s_r)}\right), \tag{4.52}$$

where $A_{ol}(s_t, s_r)$ is the overlapping area of $B(\text{TX}_0, s_t)$ and $B(\text{RX}_0, s_r)$, as illustrated in Figure 4.8 and given by Eq. (4.21).

The *exposed node problem* occurs when a packet transmission is backed off even though its transmission would not have contributed to any outages. This is the case when TX_i or RX_i are located too close to the active transmission of TX_0, but far enough from RX_0 to not cause outage. That is:

$$\Pr(\text{exposed node}) \approx \Pr(\text{TX}_i \text{ beg.} \cup \text{RX}_i \text{ beg.} \mid \overline{\text{RX}_0 \text{ mid.}}).$$

The exposed node problem is a direct consequence of the transmitter making the backoff decision, because if the receiver detects TX_0's transmission, its decision to back off is legitimate. Hence, the exposed node problem occurs when TX_i is located inside $B(\text{TX}_0, s_t)$, and simultaneously outside of $B(\text{RX}_0, s)$. Since it is TX_i that is causing the outage, we consider *its* (and not RX_0's) position. Compared to CSMA_{RX}, we have:

$$\tilde{P}_b \approx \tilde{P}^{RX}_b + \left(1 - e^{-\lambda^{TXRX}_{csma}\left(\pi s_t^2 - A_{ol}(s_t, s_r)\right)}\right), \tag{4.53}$$

where $\tilde{P}^{RX}_b$ is the backoff probability of CSMA_{RX} as derived in Section 4.1, and $A_{ol}(s_t, s_r)$ is given by Eq. (4.21).

In summary, the joint transmitter-receiver sensing of $\text{CSMA}_{\text{TXRX}}$ results in a decrease in the hidden node problem compared to CSMA_{RX}, while it has the potential to increase the exposed node problem. The trade-off between these two problems allows us to derive the optimal sensing thresholds of $\text{CSMA}_{\text{TXRX}}$.

4.2.4.2 Optimization in the Absence of Fading for $M = 1$ and $N = 0$

In a non-fading network, we note that $P_{out}(\text{CSMA}_{\text{TXRX}})$ is a convex function of s_t and s_r for low densities. As a simplified proof for this claim (which was also proven for slotted ALOHA in Subsection 2.1.1), we note that the total outage probability of $\text{CSMA}_{\text{TXRX}}$ consists of the summation of error probability expressions, which are of the form $P_{error} = 1 - e^{-\lambda^{TXRX}_{csma} \pi s^2}$. Since the

sum of convex functions is also convex, we concentrate on P_{error}. Differentiating this expression twice with respect to $s = \{s_t, s_r\}$ yields

$$\frac{d^2 P_{error}}{ds^2} \;=\; 2\pi\,\lambda_{csma}^{TXRX}\, e^{-\pi\,\lambda_{csma}^{TXRX}\, s^2}\,(1 - 2\,\pi\,\lambda_{csma}^{TXRX}). \tag{4.54}$$

For $2\pi\lambda_{csma}^{TXRX} < 1$, we have that $\frac{d^2 P_{out}}{ds^2} > 0$, indicating convexity. Hence, we may conclude that for low enough values of the density (where our approximate expressions are reasonable), P_{out} is a convex function of s.

This means that in order to obtain β_t^{opt} and β_r^{opt} (equivalently s_t^{opt} and s_r^{opt}), we may minimize the outage probability with respect to each variable separately. Starting from Eq. (4.35), we have that the derivative of the outage probability for arbitrary values of M and N with respect to the sensing zone s_t (or equivalently s_r) is

$$\begin{aligned}\frac{dP_{out}(\text{CSMA}_{\text{TXRX}})}{ds_t} \;=\;& M\,P_b^{M-1}\left(1 - P_{rt}^{N+1}\right)\frac{dP_b}{ds_t} \\ &+(N+1)\,P_{rt}^{N}\,(1 - P_b^{M})(1 - P_{rx})\frac{dP_{during}}{ds_t},\end{aligned} \tag{4.55}$$

where $P_{rt} = P_{rx} + (1 - P_{rx})\,P_{during}$. The probabilities P_b and P_{during} are the only ones dependent on s_t, and may be approximated by Eqs. (4.52) and (4.53). The optimal value for s_t is then the solution to $\frac{dP_{out}(\text{CSMA}_{\text{TXRX}})}{ds_t} = 0$ (with P_b^{RX} and P_{during}^{RX} as given in Theorem 4.2), which must be solved numerically.

In order to find simpler expressions for the optimal values of s_t and s_r, we consider the particular case of $M = 1$ and $N = 0$. This yields

$$P_{out}(\text{CSMA}_{\text{TXRX}}) \;=\; \begin{cases} P_{rx} + (1 - P_{rx})\,P_{during} & ; s_r < s \\ P_b + (1 - P_b)\,P_{during} & ; \text{otherwise} \end{cases} \tag{4.56}$$

Firstly, we recall from Section 4.1 that the optimum s_r that minimizes the outage probability of CSMA_{RX} (which Eqs. (4.52) and (4.53) are based on) is $s_r^{opt} = s$, which corresponds to $\beta_r^{opt} = \beta$. The intuition behind this is as follows:

- For $s_r < s \Rightarrow B(\text{RX}_0, s_r) < B(\text{RX}_0, s) \Rightarrow$ lower probability of backoff $\Rightarrow$ higher probability that outage occurs during an active transmission. In addition, the reduction in the backoff probability does in fact not result in a reduction in the total outage probability, because even though $B(\text{RX}_0, s_r) < B(\text{RX}_0, s)$, any active transmissions inside

$B(\text{RX}_0, s)$ upon the arrival of TX_0-RX_0 will contribute to the outage. Hence, if $s_r < s$, the total outage probability will be higher than its minimum value.

- For $s_r > s \Rightarrow B(\text{RX}_0, s_r) > B(\text{RX}_0, s) \Rightarrow$ higher probability of backoff $\Rightarrow$ lower probability that outage occurs during an active transmission. However, this decrease is less than the increase in the backoff probability, because the change in the area of $B(\text{RX}_0, s_r)$ is larger than the decrease in the circumference of the circle around TX_i where RX_i can be located. Hence, the total outage probability increases as s_r increases beyond s.

Now, assuming that $s_r^{opt} = s$, we have that $P_{out}(\text{CSMA}_{\text{TXRX}})$ is a function of s_t only. In order to derive the optimal sensing radius of the transmitter, s_t^{opt}, we use Eqs. (4.52) and (4.53). Moreover, we note that $\tilde{P}_b^{RX}$ and $\tilde{P}_{during}^{RX}$ are functions of s and s_r only (and not of s_t), which yields:

$$\begin{aligned}\frac{P_{out}(\text{CSMA}_{\text{TXRX}})}{ds_t} &= (1-P_{during})\frac{dP_b}{ds_t} + (1-P_b)\frac{dP_{during}}{ds_t} \\ &= -(1-P_b)\,\lambda\, e^{-\lambda A_{ol}(s_t, s_r^{opt})}\frac{dA_{ol}(s_t, s_r^{opt})}{ds_t} \\ &\quad +(1-P_{during})\lambda e^{-\lambda\left(\pi s_t^2 - A_{ol}(s_t, s_r^{opt})\right)}\frac{d}{ds_t}(\pi s_t^2 - A_{ol}(s_t, s_r^{opt})).\end{aligned} \tag{4.57}$$

Setting this derivative equal to 0, we obtain:

$$\begin{aligned}&(1-P_b)e^{-\lambda A_{ol}(s_t, s_r^{opt})}\frac{dA_{ol}(s_t, s_r^{opt})}{ds_t} \\ &\quad -(1-P_{during})e^{-\lambda\left(\pi s_t^2 - A_{ol}(s_t, s_r^{opt})\right)}\left(2\pi s_t - \frac{dA_{ol}(s_t, s_r^{opt})}{ds_t}\right) = 0\end{aligned} \tag{4.58}$$

Note that for $s_r = s \approx R$, we have: $\frac{dA_{ol}(s_t, s_r)}{ds_t} = 2s_t \cos^{-1}\left(\frac{s_t}{2R}\right)$. For $s \leq R$, we have that $s_t^{opt} = 0$, i.e., it is beneficial to have no transmitter sensing at all, as is the case in CSMA_{RX}. For $s > R$, s_t^{opt} is found numerically as the nonzero solution to Eq. (4.58), which is plotted in Figure 4.9 for $\beta = 10$ dB. The reason we apply a high value for β (compared to the value of 0 dB that has been applied before), is to emphasize the benefit of the transmitter sensing. If β is small, such that $s \leq R$, then we have that $\beta_t^{opt} = 0$, and $\text{CSMA}_{\text{TXRX}}$ will not provide any benefit over CSMA_{RX}.

The point where the outage probability is decreasing at its highest rate, i.e., the minimum point of $\frac{dP_{out}(\text{CSMA}_{\text{TXRX}})}{ds_t}$, occurs for $s_t = s - R$. This corre-

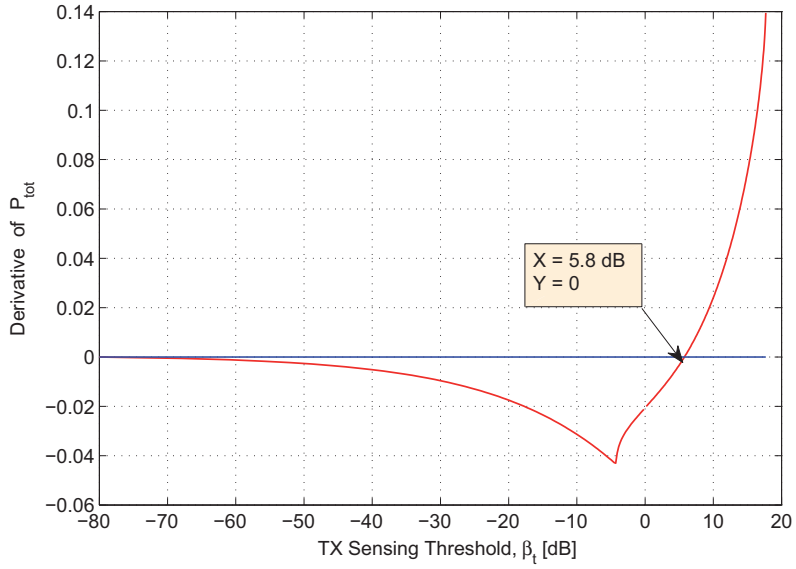

Figure 4.9: Derivative of the outage probability of $\text{CSMA}_{\text{TXRX}}$ for $\lambda = 0.01$, $\beta = 10$ dB, $M = 1$, and $N = 0$.

sponds to $\beta_t = \left(\beta^{1/\alpha} - 1\right)^{\alpha}$, which is in fact the optimal sensing threshold for CSMA_{TX}, and is in accordance with the result obtained in [73]. For this value of β_t, $B(\text{RX}_0, s)$ covers $B(\text{TX}_0, s_t)$ completely, meaning that the transmitter sensing of $\text{CSMA}_{\text{TXRX}}$ introduces no additional exposed node problem, while it at the same time provides some protection for its receiver, thus reducing the hidden node problem. For $s \geq R$, s_t can be increased up to $(s - R)$ without introducing any exposed node problems, meaning that in $\text{CSMA}_{\text{TXRX}}$ we always have that $\beta_t^{opt} \geq \left(\beta^{1/\alpha} - 1\right)^{\alpha}$.

4.2.4.3 Optimization in the Presence of Fading for $M = 1$ and $N = 0$

In the case of fading, the optimization problem becomes more complicated, as we can no longer translate it to a distance problem. Intuitively, we would expect $\text{CSMA}_{\text{TXRX}}$ to yield an optimal performance when $\beta_r = \beta$ and $\beta_t = 0$. The reason for this is as follows:

- If $\beta_r > \beta$, the exposed node problem is increased, while the hidden node problem is not reduced (because we do not consider the

aggregate interference power in our derivations). On the other hand, if $\beta_r < \beta$, there is no exposed node problem, but the hidden node problem is higher than when $\beta_r = \beta$. Hence, $\beta_r^{opt} = \beta$.

- Next, we evaluate the benefit that the transmitter sensing of $\text{CSMA}_{\text{TXRX}}$ provides. Since we have that the channel coefficient from TX_0 to an interfering transmitter TX_i is independent from the channel coefficient from TX_0 to RX_i, it means that the decision-making of the TX_i based on its own channel does not provide much benefit for the packet reception at its receiver in terms of the hidden node problem. In fact, the transmitter's decision to back off from transmission, when its receiver wishes to activate it, is only adding to the exposed node problem. Hence, $\beta_t^{opt} = 0$.

In order to validate the reasoning given above, we evaluate the derivative of the outage probability in the presence of fading for $M = 1$ and $N = 0$;

$$\frac{dP_{out}(\text{CSMA}_{\text{TXRX}})}{d\beta_t} \approx \left(1 - \overline{P}_{during}\right) \frac{d\overline{P}_b}{d\beta_t} + \left(1 - \overline{P}_b\right) \frac{d\overline{P}_{during}}{d\beta_t} = 0. \quad (4.59)$$

Firstly, we find the derivative of $\overline{P}_{during}$;

$$\frac{d\overline{P}_{during}}{d\beta_t} = 2\pi\lambda\, \mathbb{E}_{h_{00}}\Bigg[e^{-\lambda \int_0^\infty 2\pi \left(1-e^{-\frac{\mathbb{E}[h_{ii}]R^{-\alpha} r^\alpha}{\beta_t}}\right)\left(1-e^{-\frac{\mathbb{E}[h_{ii}]R^{-\alpha} r^\alpha}{\beta_r}}\right) e^{-\frac{h_{00}R^{-\alpha} r^\alpha}{\beta}} r\, dr} \quad (4.60)$$
$$\times \int_0^\infty \left(1 - e^{-\frac{\mathbb{E}[h_{ii}]R^{-\alpha} r^\alpha}{\beta_t}}\right) e^{-\frac{\mathbb{E}[h_{ii}]R^{-\alpha} r^\alpha}{\beta_r}} e^{-\frac{h_{00}R^{-\alpha} r^\alpha}{\beta}} \left(-\frac{\mathbb{E}[h_{ii}]R^{-\alpha} r^\alpha}{\beta_t^2}\right) r\, dr \Bigg].$$

For the backoff probability, $\overline{P}_b$, as given by Theorem 4.7, we obtain

$$\frac{d\overline{P}_b}{d\beta_t} = \frac{d\overline{P}_{b1}(\beta_t)}{d\beta_t} + \left(1 - \overline{P}_{b1}(\beta_t)\right) \overline{P}_{b1}(\beta_r)\, \mathbb{E}_{h_{00},h_{0i}} \left[\frac{1}{\pi s_r^{f^2}} \frac{dA_{ol}(s_t^f, s_r^f)}{d\beta_t} \right]$$
$$- \frac{d\overline{P}_{b1}(\beta_t)}{d\beta_t} \overline{P}_{b1}(\beta_r)\, \mathbb{E}_{h_{00},h_{0i}} \left[1 - \frac{A_{ol}(s_t^f, s_r^f)}{\pi s_r^{f^2}} \right], \quad (4.61)$$

where $A_{ol}(s_t^f, s_r^f)$ is given by Eq. (4.21). Now note that when $(M, N) = (1, 0)$, $\overline{P}_{b1}(\beta_t)$ may be expressed by the Lambert function $\mathcal{W}_0(\cdot)$, as given below:

$$\overline{P}_{b1}(\beta_t) = 1 - \frac{1}{\pi\lambda R^2 \beta_t^{2/\alpha} \frac{2\pi/\alpha}{\sin(2\pi/\alpha)}} \mathcal{W}_0\left(\pi\lambda R^2 \beta_t^{2/\alpha} \frac{2\pi/\alpha}{\sin(2\pi/\alpha)}\right). \quad (4.62)$$

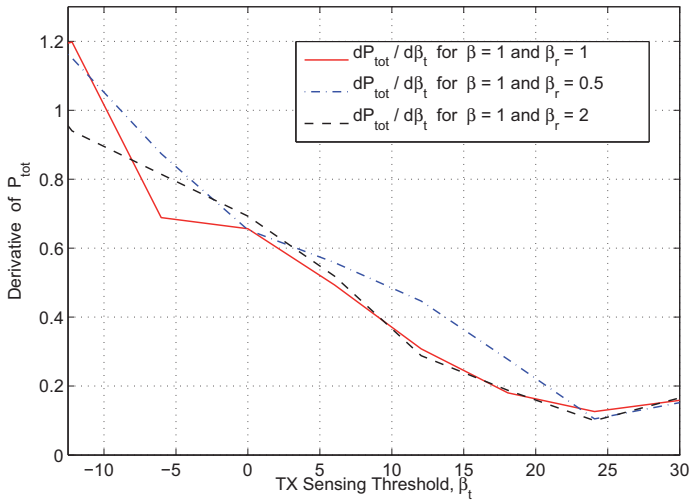

Figure 4.10: Derivative of the outage probability of $\text{CSMA}_{\text{TXRX}}$ in a fading network as a fucntion of β_t, for $\beta = 0$ dB.

Setting $x = \pi\lambda R^2 \beta_t^{2/\alpha} \frac{2\pi/\alpha}{\sin(2\pi/\alpha)}$, we have that

$$\frac{d\overline{P}_{b1}(\beta_t)}{d\beta_t} = \frac{\mathcal{W}_0(x)}{x^2} - \frac{1}{x} \cdot \frac{\mathcal{W}_0(x)}{x[1+\mathcal{W}_0(x)]} = \frac{\mathcal{W}_0(x)^2}{x^2\,[1+\mathcal{W}_0(x)]}. \tag{4.63}$$

Inserting these expressions back into Eq. (4.59), we can find the optimal value of β_t numerically. This is shown in Figure 4.10, where $\frac{dP_{out}(\text{CSMA}_{\text{TXRX}})}{d\beta_t}$ is plotted as a function of β_t for various values of β_r. β_t^{opt} is potentially the point where the derivative of $P_{out}(\text{CSMA}_{\text{TXRX}})$ becomes 0. As expected, we see that $\frac{dP_{out}(\text{CSMA}_{\text{TXRX}})}{d\beta_t}$ is positive for all β_t, meaning that it is always an increasing function of β_t. In other words, the outage probability of $\text{CSMA}_{\text{TXRX}}$ in the presence of fading is minimized for $\beta_r^{opt} = \beta$ and $\beta_t^{opt} = 0$.

4.2.5 Numerical Results

The derived results of Subsections 4.2.2 and 4.2.3 are validated through Monte Carlo simulations. We set the transmitter-receiver distance $R = 1$ m, path loss exponent $\alpha = 4$, and fading parameter $\zeta = 1$. In the case of non-fading, the averaging is performed over 10000 packets, while in the

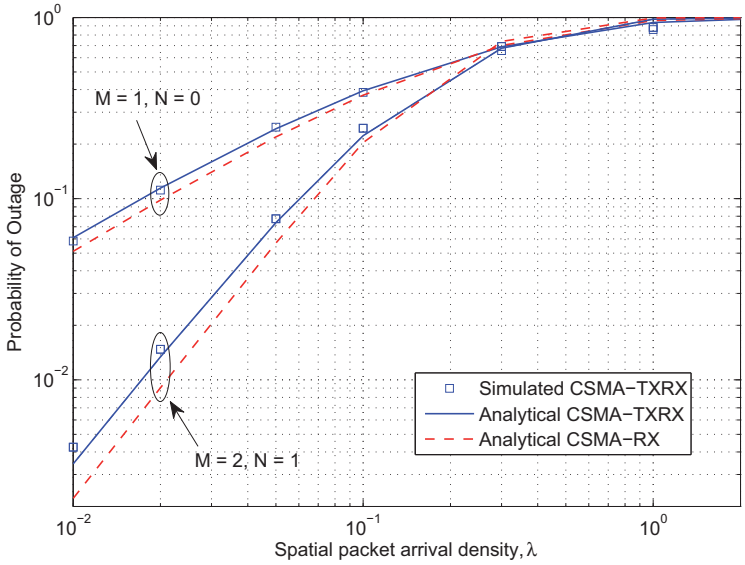

Figure 4.11: Outage probability of $\text{CSMA}_{\text{TXRX}}$ in a non-fading network with $\beta_t = \beta_r = \beta = 0$ dB.

fading network, 4000 packets are considered (due to memory constraints in MATLAB).

In Figures 4.11 and 4.12, the outage probability of $\text{CSMA}_{\text{TXRX}}$ and CSMA_{RX} (for the sake of comparison) is plotted as a function of the packet arrival density λ, for non-fading and fading networks, respectively. Firstly, our analytical expressions are validated as they follow the simulation results tightly. Secondly, we observe that as the density increases, so does the outage probability, until the network reaches a point of saturation, where $P_{out} \approx 1$. By increasing the number of backoffs and retransmissions, significant performance gain can be obtained. For low densities with $(M, N) = (2, 1)$, the outage probability is up to 10 times less than when $(M, N) = (1, 0)$. Thirdly, the addition of transmitter sensing in $\text{CSMA}_{\text{TXRX}}$ does not appear to provide any improvement compared to CSMA_{RX}. In fact, CSMA_{RX} outperforms $\text{CSMA}_{\text{TXRX}}$ by up to 20% in non-fading networks and up to 50% when fading is present. This is due to the exposed node problem caused by the transmitter sensing. That is, when M is small, the protection that the transmitter sensing provides does not counterbalance the backoff probability increase it generates.

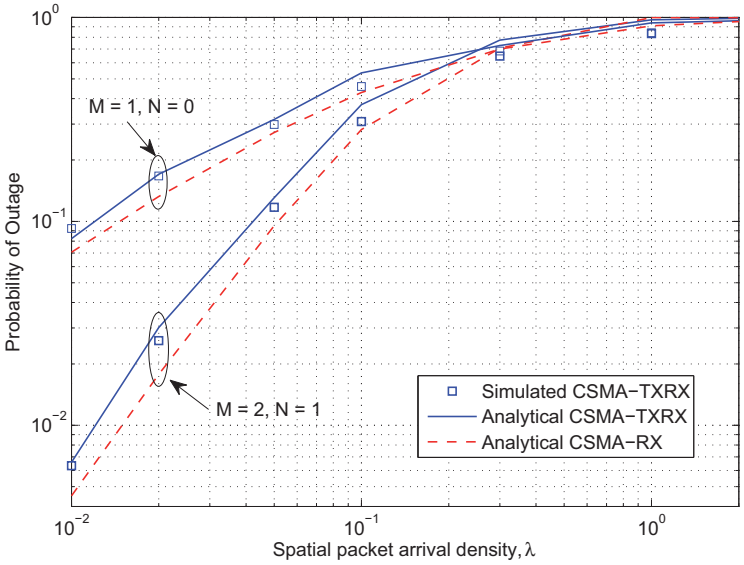

Figure 4.12: Outage probability of $\text{CSMA}_{\text{TXRX}}$ in a fading network with $\beta_t = \beta_r = \beta = 0$ dB.

In Figure 4.13, the outage probability of $\text{CSMA}_{\text{TXRX}}$ is plotted as a function of the sensing thresholds, β_t and β_r, for a fixed low density of $\lambda = 0.01$, $\beta = 10$ dB, and $(M, N) = (1, 0)$. The plot shows that $\beta_r^{opt} = \beta$ and $\beta_t^{opt} = 5.8$ dB, which is also obtained by numerically solving Eq. (4.58), thus confirming our conclusions from Subsection 4.2.4.2. Similarly, in Figure 4.14, the outage probability of $\text{CSMA}_{\text{TXRX}}$ is considered in a fading network with $\lambda = 0.03$, $\beta = 0$ dB, and $(M, N) = (1, 0)$. Again, our derivations from Subsection 4.2.4.3 are confirmed, i.e., $\beta_r^{opt} = \beta = 0$ dB and $\beta_t^{opt} = 0$.

The impact of the number of backoffs, M, is illustrated in Figure 4.15, where the receiver sensing threshold is assumed to be constant, $\beta_r = 0$ dB, while the transmitter sensing threshold and M are optimized jointly. As expected, the outage probability decreases monotonically with M. For each M, there is a different value for β_t^{opt}, although the range of this is very small. Hence, we conclude that the result of Eq. (4.58) to find s_t^{opt} analytically for $M = 1$, can be applied as an approximation for other values of M as well.

Figure 4.16 emphasizes the effect of M on the outage probability of $\text{CSMA}_{\text{TXRX}}$, as compared to CSMA_{TX} and CSMA_{RX}. In this plot, we set $N = 0$ and a high density of $\lambda = 0.1$ is chosen. When only $M = 1$ channel

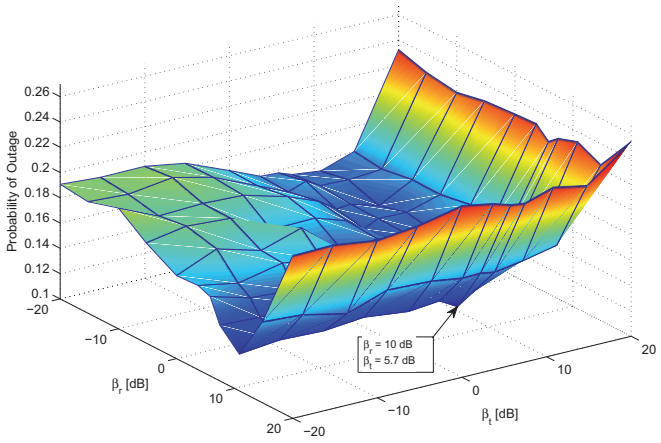

Figure 4.13: Outage probability of $\text{CSMA}_{\text{TXRX}}$ as a function of the sensing thresholds, for a non-fading network with $\lambda = 0.01$, $\beta = 10$ dB and $(M, N) = (1, 0)$.

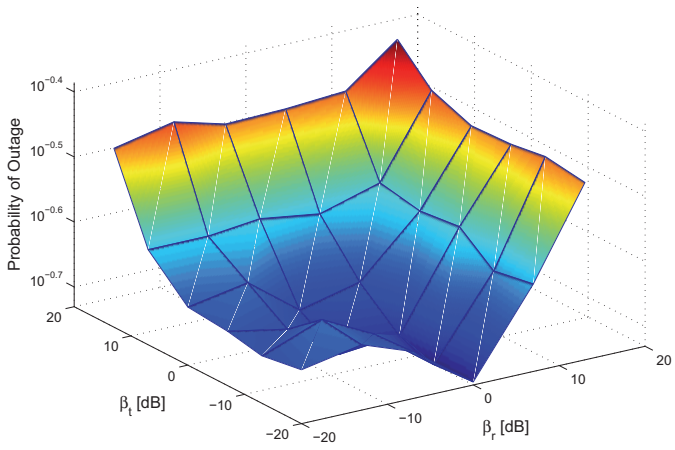

Figure 4.14: Outage probability of $\text{CSMA}_{\text{TXRX}}$ as a function of the sensing thresholds, for a fading network with $\lambda = 0.03$, $\beta = 0$ dB, and $(M, N) = (1, 0)$.

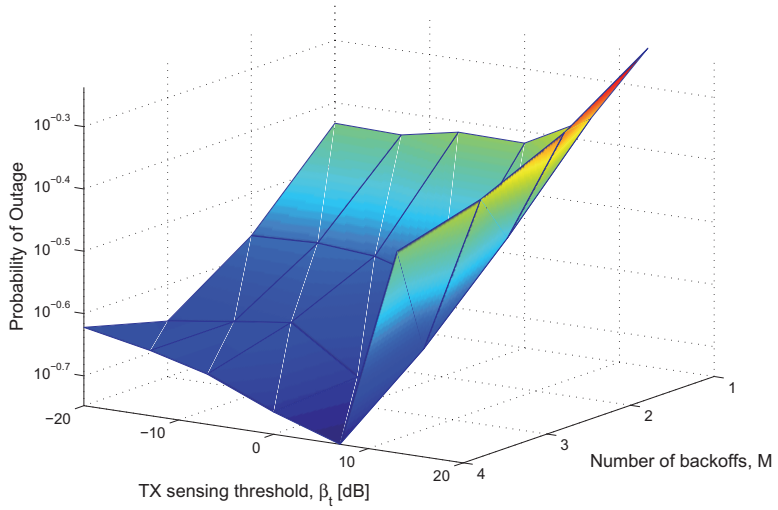

Figure 4.15: Outage probability of $\text{CSMA}_{\text{TXRX}}$ as a function of β_t and M, for a non-fading network with $\lambda = 0.1$, $\beta = \beta_r = 0$ dB, and $N = 0$.

sensing is allowed before the packet is dropped, $\text{CSMA}_{\text{TXRX}}$ exhibits up to 10% higher outage probability than CSMA_{RX} and up to 20% lower outage probability than CSMA_{TX}. As M increases, the benefit of the joint channel sensing of $\text{CSMA}_{\text{TXRX}}$ becomes more evident; for $M = 4$, $\text{CSMA}_{\text{TXRX}}$ outperforms CSMA_{RX} by 40% and CSMA_{TX} by a factor 2. Hence, we conclude that by applying joint transmitter-receiver sensing in a network with $M > 1$, the outage performance of CSMA can be improved beyond that of CSMA_{RX}. Moreover, the optimal sensing thresholds are $\beta_r^{opt} = \beta$ and β_t^{opt} is found approximately by solving Eq. (4.58).

The impact of retransmissions is opposite to that of backoffs. As seen from Figure 4.17, where the outage probability is plotted for a fixed density of $\lambda = 0.03$ and $M = 2$ backoffs, the outage probability of CSMA_{RX} reduces below that of $\text{CSMA}_{\text{TXRX}}$, as the number of retransmissions, N, increases. E.g., when $(M, N) = (2, 0)$, $\text{CSMA}_{\text{TXRX}}$ outperforms CSMA_{RX} by 10%, while for $(M, N) = (2, 3)$, we have 20% higher outage probability for $\text{CSMA}_{\text{TXRX}}$ than for CSMA_{RX}. While significant gain is obtained by increasing N from 0 to 2, little benefit is observed for $N > 2$. Note that we have included results on the impact of M and N only in non-fading networks, as similar conclusions are drawn from fading networks.

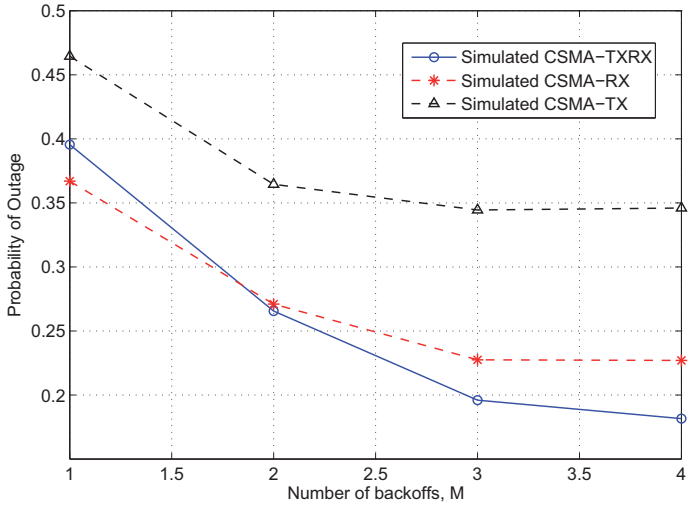

Figure 4.16: Outage probability of $\text{CSMA}_{\text{TXRX}}$ as a function of the number of backoffs, M, for a non-fading network with $\lambda = 0.1$ and $N = 0$.

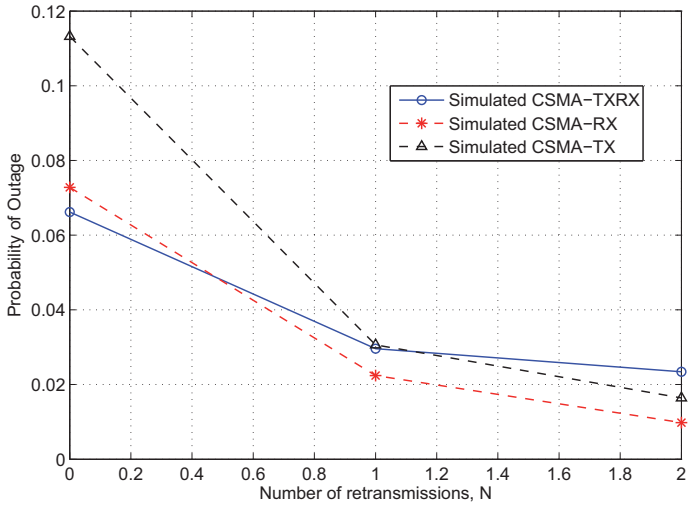

Figure 4.17: Outage probability of $\text{CSMA}_{\text{TXRX}}$ as a function of the number of retransmissions, N, for a non-fading network with $\lambda = 0.03$ and $M = 2$.

4.3 Summary

In this chapter, we proposed modifications to the CSMA protocol in order to improve the performance of point-to-point wireless ad hoc networks. For the proposed schemes, both non-fading and fading networks are considered, and Monte Carlo simulations are generated to validate the derived outage probability expressions.

Firstly, we optimize the sensing threshold based on which the backoff decision is made. We observe that for CSMA_{TX} there is no advantage in allowing for channel sensing when the density is low, whereas a 50% reduction in the outage probability can be obtained in CSMA_{RX}, by setting $\beta_b^{opt} = \beta$. For higher densities, the significance of optimizing the sensing threshold becomes evident also in CSMA_{TX}, reducing the outage probability by up to 40% (for $(M, N) = (2, 1)$). The optimal sensing threshold β_b is derived to be equal to β, although the simulations reveal it to be slightly greater than β at high densities. This is because a greater β_b provides more protection against the aggregate interference from the transmitters outside $B(\text{RX}_0, s)$, which is more severe at higher densities.

Next, we propose a modification to the CSMA protocol, $\text{CSMA}_{\text{TXRX}}$, where the transmitter and receiver both sense their channels and jointly make the backoff decision. This protocol is denoted as $\text{CSMA}_{\text{TXRX}}$, and its outage probability is derived. Furthermore, the optimal sensing thresholds for both the transmitter and receiver are found, and an understanding is established for how these optimal thresholds balance between the inherent hidden and exposed node problems of CSMA. It is shown that using optimal sensing thresholds can provide significant performance gain for all transmission densities. Moreover, when multiple backoffs are allowed, $\text{CSMA}_{\text{TXRX}}$ outperforms CSMA_{RX}. E.g., when $M = 4$, this improvement is 40%.

Chapter 5

Performance Improvement Through Bandwidth Partitioning

The concept of bandwidth partitioning is a well-studied topic. This technique is concerned with dividing the system bandwidth into smaller partitions, called subbands, with the aim of reducing the amount of interference detected for each user. Within uncoordinated decentralized networks, optimization of the frequency reuse has been studied in many works, such as [76] and [77], and references therein. In [78], the authors evaluate the tradeoffs between the time-bandwidth product of the signals and the amount of power that must be transmitted to achieve reliable communication. In [79], the tradeoff between the bandwidth utilized and the achieved spectral efficiency per transmission has been studied within the context of centrally-planned cellular networks. Moreover, in a one-dimensional, evenly spaced, multi-hop wireless network, the issue of frequency reuse is assessed in [80]. Although some similar general insights are derived in the above-mentioned works, the obtained results do not apply to irregular decentralized systems, such as ad hoc or unlicensed networks.

In the context of decentralized networks, the performance of multi-channel wireless networks is investigated in [81–83]. In [81], MAC layer protocols are introduced for efficient utilization of the multiple channels available. However, [81] considers coordinated networks, as opposed to our treatment of uncoordinated networks. The work of [82] proposes algorithms for dynamic bandwidth allocation for cognitive radio networks.

Perhaps the closest work to ours is that of [83], where the number of simultaneous transmissions in a multiuser decentralized network is maximized by optimizing the number of subbands the system bandwidth is divided into. In both [81] and [83], however, only ALOHA-like protocols are considered, whereas in our work, we take a step further to also consider the performance of CSMA-like protocols.

In the following, we introduce bandwidth partitioning into our ad hoc network, both with and without fading, and we obtain the optimal number of subbands that minimizes the outage probability using different MAC protocols. The work of this chapter is partly published in [84] and submitted to IEEE Trans. on Communications [85].

5.1 System Model

Our system model considers, as before, a mobile network where transmitter-receiver pairs are located randomly on a plane according to a 2-D Poisson point process (PPP) with density λ^s [nodes/m^2]. Packets arrive at each transmitter according to a 1-D temporal PPP with density λ^t [packets/sec/node]. Upon the arrival of each packet it is transmitted to its destination located a fixed distance R away. The transmit power ρ is fixed for all users, and each packet has a fixed length of T [sec]. The system bandwidth W is uniformly partitioned into $K \geq 1$ subbands. Each packet uses a single subband for its transmission, where $K = 1$ indicates that each user employs the entire bandwidth. Based on this model, the spatial density of new packet arrivals during $[0, T)$ is given by $\lambda = \lambda^s \lambda^t T$ [packets/m^2], while the spatial density of packets transmitting within the *same subband* is given as $\frac{\lambda}{K}$.

Packet transmissions are initiated across one subband according to either the ALOHA or CSMA MAC protocols. In order to account for the impact that bandwidth partitioning has on all network parameters (i.e., not only the interference), we now turn our attention to the channel capacity. In the ALOHA protocol, a packet is received erroneously and must be retransmitted, if the channel capacity, $\mathcal{C}$, is below the transmission rate required for correct reception of a packet, R_{req}. After N retransmissions, the packet is dropped. In the CSMA protocol, channel sensing is performed at the beginning of each packet. If this is below $R_{req,b}$ (which can be equal to R_{req}, as we initially assume in Section 5.2)[1], the packet is backed off a random time. This is repeated at most M times, before the packet is dropped and counted

[1]The subscript b denotes that this threshold is used for the backoff decision making.

to be in outage. Once a packet transmission is initiated, but the capacity is below R_{req} during its transmission, the packet is received in error and must be retransmitted. Each packet is given a maximum of N retransmission attempts, before the packet is counted to be in outage.

Note that our traffic model consists of highly mobile node pairs, meaning that different and independent sets of nodes are observed on the plane from one slot (of length T) to the next. Upon retransmission of a packet, it is treated as a new packet arrival, i.e., it is placed in a new location and assigned a new subband, resulting in no spatial correlations between transmission attempts. Moreover, the waiting time between each transmission attempt, t_{wait}, is by design ensured to be more than T, which in addition to the high mobility assumption, results in no temporal correlations between retransmission attempts. For more explanations regarding the traffic generation model, please refer to Section 2.1.

For the channel model, we again consider two cases: I) only deterministic path loss attenuation effects (with exponent $\alpha > 2$), and II) path loss attenuation in addition to fading effects. The former yields

$$\text{SINR}_i = \frac{\rho R^{-\alpha}}{\eta/K + \sum_i \rho r_i^{-\alpha}}, \tag{5.1}$$

where r_i is the distance between the node under observation (this could be either the transmitter or receiver of the packet we are considering) and the i-th interfering transmitter, and the sum is over all active interferers on the plane. $\frac{\eta}{K}$ is the noise observed in each subband

Adding fading effects to the deterministic path loss attenuation effects, in the same manner as was done in Subsection 3.1.1, results in

$$\text{SINR}_i^f = \frac{\rho R^{-\alpha} h_{00}}{\eta/K + \sum_i \rho r_i^{-\alpha} h_{0i}}, \tag{5.2}$$

where h_{00} represents, as before, the fading effects between the receiver under observation and its own transmitter. r_i and h_{0i} are, respectively, the distance and fading coefficient between the node under observation and the i-th interfering transmitter.

As bandwidth partitioning affects the amount of information that can be carried over a channel, we start with a different definition for the outage probability[2] than has been considered thus far. Based on the Shannon capacity formula for AWGN channels [17], we may express the probability

[2]This was briefly given by Eq. (1.2) in the Introduction.

of an erroneous packet reception as

$$\begin{aligned} P_{error} &= \Pr\left[\mathcal{C} \leq R_{req}\right] &= \Pr\left[\frac{W}{K}\log(1+\text{SINR}) \leq R_{req}\right] \\ &&= \Pr\left[\text{SINR} \leq 2^{KR_{req}/W}-1\right]. \end{aligned} \tag{5.3}$$

where the SINR is given by Eq. (5.1) in non-fading networks and by Eq. (5.2) for fading networks. This means that packet i is received erroneously if its SINR at the receiver falls below the SINR threshold, $\beta(K)$, given as

$$\beta(K) = 2^{KR_{req}/W}-1, \tag{5.4}$$

where KR_{req}/W is the required spectral efficiency of the system. In the case of CSMA, we also define $\beta_b(K) = 2^{NR_{req,b}/W}-1$, where $R_{req,b}$ is applied for backoff decision making of the transmitter in CSMA_{TX} and the receiver in CSMA_{RX}.

5.2 Performance in the Absence of Fading

In this section, we assume no fading effects in the channel, i.e., the signal degradation is only due to path loss, resulting in an SINR given by Eq. (5.1). Denote the channel capacity in the backoff decision making stage of CSMA by $\mathcal{C}_0$, and the capacity at some $t \in [0, T)$ by C_t. The outage probability of ALOHA and CSMA can then be given by

$$\begin{aligned} P_{out}(\text{ALOHA}) &= \Pr\left[\mathcal{C}_t < R_{req}\ N+1 \text{ times}\right], \\ P_{out}(\text{CSMA}) &= \Pr\left[\mathcal{C}_0 < R_{req,b}\ M \text{ times} \ \cup\ \mathcal{C}_t < R_{req}\ N+1 \text{ times}\right]. \end{aligned} \tag{5.5}$$

In the following subsections, we derive expressions for the outage probability of the ALOHA and CSMA protocols in their various incarnations.

5.2.1 The ALOHA Protocol

In slotted ALOHA, packet transmissions are initiated at the start of the next time slot after they have been formed, unconditioned on the quality of the channel. Given the probability of a packet being retransmitted within a randomly selected subband is $P_{rt,s}(K)$, the density of packets on the plane within the same subband (when the network is in a steady state) is

$$\begin{aligned} \lambda_{slotted}(K) &= \frac{\lambda}{K}\left[1+P_{rt,s}(K)+P_{rt,s}(K)^2+...+P_{rt,s}(K)^N\right] \\ &= \frac{\lambda}{K}\,\frac{1-P_{rt,s}(K)^{N+1}}{1-P_{rt,s}(K)}. \end{aligned} \tag{5.6}$$

In order to derive the outage probability, we employ the concept of guard zones, as was also used earlier in this thesis. Given that the bandwidth is divided into K subbands, we derive the distance to the single closest interferer that would cause the SINR to fall just below the threshold $\beta(K)$, to be

$$s(K) \;=\; \left(\frac{R^{-\alpha}}{\beta(K)} - \frac{\eta(K)}{\rho}\right)^{-\frac{1}{\alpha}}, \tag{5.7}$$

where $\eta(K) = \frac{\eta}{K}$ is the noise observed in each subband, and $\beta(K)$ is given by Eq. (5.4). In a strictly interference-limited system, we may set $\eta(K) = 0$ resulting in $s(K) = R\beta(k)^{1/\alpha}$. In the same manner as before, denote the circle of radius $s(K)$ around the receiver under observation, RX_0, by $B(\mathrm{RX}_0, s(K))$. If one or more interferers are located inside $B(\mathrm{RX}_0, s(K))$ and within the same subband as RX_0 at some $t \in [0, T)$, the packet is received erroneously. Knowing that interferers are Poisson distributed with density $\lambda_{slotted}(K)$ within each subband, we employ the expression $P_{rt,s}(K) = 1 - e^{-\mathbb{E}[\#\text{ of interferers inside } B(\mathrm{RX}_0, s(K)) \text{ in } \mathrm{RX}_0\text{'s subband}]}$. This yields a tight lower bound to the error probability of slotted ALOHA [18]. Allowing for N retransmission attempts for each packet, we arrive at the following theorem.

Theorem 5.1 (Slotted ALOHA)
The outage probability of slotted ALOHA (in the absence of fading), when the bandwidth is divided into K subbands, may be lower bounded by $P_{out}^{lb}(\textit{Slotted ALOHA}) = P_{rt,s}^{N+1}(K)$, *where* $P_{rt,s}(K)$ *is the solution to*

$$P_{rt,s}(K) \;=\; 1 - \exp\left\{-\frac{\lambda}{K}\,\frac{1 - P_{rt,s}(K)^{N+1}}{1 - P_{rt,s}(K)}\,\pi\, s(K)^2\right\}. \tag{5.8}$$

with $s(K)$ *as given by Eq.* (5.7).

In unslotted ALOHA, there is no slotting of time, meaning that packets are transmitted as soon as they are formed. This degrades the probability of correct packet reception as a packet can now either be in error upon its arrival at $t = 0$, or an error can occur during its transmission at some $t \in (0, T)$. This yields the following theorem.

Theorem 5.2 (Unslotted ALOHA)
The outage probability of unslotted ALOHA (in the absence of fading), when the bandwidth is divided into K subbands, may be lower bounded by

$P_{out}^{lb}(\textit{Unslotted ALOHA}) = P_{rt,u}(K)^{N+1}$, *where* $P_{rt,u}(K)$ *is the solution to*

$$P_{rt,u}(K) \;=\; 1 - \exp\left\{-2\,\frac{\lambda}{K}\,\frac{1-P_{rt,u}(K)^{N+1}}{1-P_{rt,u}(K)}\,\pi\,s(K)^2\right\}. \tag{5.9}$$

with $s(K)$ *as given by Eq.* (5.7).

Note that when K increases, so does $\beta(K)$ (as to uphold a constant R_{req} when the size of a subband decreases). This corresponds to an increase in $s(K)$, which means that a greater area around the receiver must be free of interferers in order to avoid an erroneous packet reception. However, a greater K also means that there are fewer interferers within *each* subband. Hence, there is clearly a trade-off between the density of packets and the robustness against interference for a correct packet reception.

In a network where no retransmissions are allowed, we can analytically assess the optimal number of subbands, K_{opt}, that minimizes the outage probability. For simplicity of the analysis, we assume a strictly interference-limited system, i.e., $s(K) = R^2\,(2^{KR_{req}/W}-1)^{2/\alpha}$. For the moment, treating K as a non-integer, and setting the derivative of $P_{out}(\text{Slotted ALOHA})$ with respect to K equal to 0, we obtain:

$$\begin{aligned}\frac{d}{dK}\left(1-\exp\left\{-\frac{\lambda}{K}\,\pi\,R^2\,(2^{KR_{req}/W}-1)^{2/\alpha}\right\}\right) \;&=\; 0\\ 1-\frac{2\ln(2)}{\alpha}\,\frac{K\,R_{req}}{W}-2^{-KR_{req}/W} \;&=\; 0.\end{aligned} \tag{5.10}$$

The solution to Eq. (5.10) is given in terms of the Lambert function, $\mathcal{W}_0(\cdot)$ [54];

$$\begin{aligned}K_{opt} \;&=\; \frac{W}{2R_{req}\ln(2)}\left[\alpha + 2\mathcal{W}_0\left(-\frac{1}{2}\,\alpha\,e^{-\alpha/2}\right)\right]\\ &=\; \frac{W}{R_{req}\ln(2)}\left[\frac{\alpha}{2}+\sum_{n=1}^{\infty}\frac{(-n)^{n-1}}{n!}\left(-\frac{\alpha}{2}\,e^{-\alpha/2}\right)^n\right],\end{aligned} \tag{5.11}$$

K_{opt} is the same for both slotted and unslotted ALOHA, due to the fact that the total number of interferers in both systems is the same when $N = 0$. For $N > 0$, we are not able to find K_{opt} analytically, and so we rely on simulations for this.

5.2.2 The CSMA Protocol With Random Selection of a Subband

In this subsection, we assume that each transmitter makes a *random* selection of one subband to transmit each of its packets over. Moreover,

we assume that the required transmission rate is the same for the backoff decision making and for correct packet reception at the receiver, i.e., $R_{req,b} = R_{req}$. Hence, the SINR sensing threshold and the SINR communication threshold are also equal, $\beta_b(K) = \beta(K)$.

Denote the SINR at the start of the packet by SINR_0 and the SINR at some $t \in [0, T)$ by SINR_t. Based on Eq. (5.5) we have

$$P_{out}(\text{CSMA}) = \Pr\left[\text{SINR}_0 < \beta_b(K)\right]^M + \left(1 - \Pr\left[\text{SINR}_0 < \beta_b(K)\right]^M\right) \times \Pr\left[\text{SINR}_t < \beta(K) \text{ at } 1^{\text{st}} \text{ attempt}\right] \Pr\left[\text{SINR}_t < \beta(K)\right]^N. \quad (5.12)$$

The density of packets attempting to access each subband is

$$\lambda_{csma}(K) = \frac{\lambda}{K}\left[\frac{1 - P_b(K)^M}{1 - P_b(K)} + \left(1 - P_b(K)^M\right) P_{rt1}(K) \frac{1 - P_{rt}(K)^N}{1 - P_{rt}(K)}\right], \quad (5.13)$$

where $P_b(K)$ is the backoff probability, $P_{rt1}(K)$ is the probability that the packet is received in error at its first transmission attempt (once it has been activated), and $P_{rt}(K)$ is the probability of erroneous reception in a retransmission attempt. Each of these probabilities will be derived by using the concept of guard zones, as described in Subsection 5.2.1 for ALOHA.

In CSMA_{TX}, the transmitter senses the channel and makes the backoff decision based on the estimation of the SINR at its receiver. To derive the backoff probability, we assume that the number of *active* interferers on the plane follows a PPP (which is proven by the simulation results to be reasonable). The density of active packets on the plane, once the network is in a steady state, is

$$\lambda_{active}(K) = \frac{\lambda}{K}\left[1 - P_b(K)^M + \left(1 - P_b(K)^M\right) P_{rt1}(K) \frac{1 - P_{rt}(K)^N}{1 - P_{rt}(K)}\right]. \quad (5.14)$$

The reason only the first term is multiplied by $(1 - P_b(K))$ is that once a transmitter-receiver pair has decided to transmit, it does not make a new decision in the case of retransmissions. Hence, the number of channel accesses due to retransmissions is not reduced by a factor $(1 - P_b(K))$. Applying the outage probability expression for PPPs, we have that $P_b(K) = 1 - e^{-\mathbb{E}[\#\text{ of interferers in a subband}]}$.

For more details on the derivation of the outage probability of CSMA, in particular when the sensing and communication thresholds are different, we refer the reader to Section 4.1. With $\beta_b = \beta$ and based on the above derivations, we reach the following theorem.

Theorem 5.3 ($\mathbf{CSMA_{TX}}$)
The outage probability of $CSMA_{TX}$ (in the absence of fading), when the bandwidth is divided into K subbands, is given by

$$P_{out}(CSMA_{TX}) \;=\; P_b(K)^M + \Big(1 - P_b(K)^M\Big)\; P_{rt1}(K)\, P_{rt}(K)^N, \qquad (5.15)$$

where:

- $P_b(K)$ *is the backoff probability, approximated by the solution to*

$$\tilde{P}_b(K) \;=\; 1 - e^{-\pi\, s(K)^2\, \frac{\lambda}{K}\left(1-\tilde{P}_b(K)^M+\left(1-\tilde{P}_b(K)^M\right)\tilde{P}_{rt1}(K)\,\frac{1-\tilde{P}_{rt}(K)^N}{1-\tilde{P}_{rt}(K)}\right)}, \quad (5.16)$$

  where $s(K)$ is given by Eq. (5.7).
- $P_{rt}(K) = P_b(K) + (1 - P_b(K))\, P_{during}(K)$ *is the probability that a packet is received in error during a retransmission attempt. $P_{during}(K)$ is the probability that the error has occurred at some $t \in (0, T)$, approximated by*

$$\tilde{P}_{during}(K) \;=\; 1 - e^{-\int_{s(K)-R}^{s(K)} \lambda_{csma}^{TX}(K)\left[2\pi-2\,\cos^{-1}\left(\frac{r^2+R^2-s(K)^2}{2Rr}\right)\right] r\, dr}, \quad (5.17)$$

  with $\lambda_{csma}^{TX}(K)$ given by Eq. (5.13).
- $P_{rt1}(K) = P_{rx|transmit}(K) + \big(1 - P_{rx|transmit}(K)\big)\; P_{during}(K)$ *is the probability that the packet is received in error at its first transmission attempt. $P_{rx|transmit}(K)$ is the probability that the received packet is in outage upon arrival, approximated by*

$$\tilde{P}_{rx|transmit}(K) = \tilde{P}_b(K)\left[1-\frac{2}{\pi}\cos^{-1}\left(\frac{R}{2s(K)}\right)+\frac{R}{\pi s(K)}\sqrt{1-\frac{R^2}{4\,s(K)^2}}\right].$$

In $\mathrm{CSMA_{RX}}$, the receiver senses the channel and makes the backoff decision based on the measured SINR. The outage probability of this version of CSMA, is derived in the same manner as for $\mathrm{CSMA_{TX}}$, with the main difference that once a packet is activated, it is certain to not be in error at the start of its first transmission. Extending the results of Chapter 2, we obtain the following theorem.

Theorem 5.4 ($\mathbf{CSMA_{RX}}$)
The outage probability of $CSMA_{RX}$ (in the absence of fading), when the bandwidth is divided into K subbands, is given by Eq. (5.15), *where:*

- *$P_b(K)$ is the backoff probability, approximated by the solution to Eq.* (5.16).
- *$P_{rt}(K) = P_b(K) + (1 - P_b(K))\ P_{during}(K)$ is the probability that a packet is received in error in a retransmission attempt, with $P_{during}(K)$ approximated by*

$$\tilde{P}_{during}(K) \ = \ 1 - e^{-\int_{s(K)-R}^{s(K)} \int_{\nu(r)}^{2\pi-\nu(r)} \lambda_{csma}^{RX}(K)\, P(active|r,\phi)\, r\, d\phi\, dr}, \qquad (5.18)$$

with $P(active|r,\phi)$ and $\nu(r)$ given by

$$P(active|r,\phi) = 1 - \frac{1}{\pi}\cos^{-1}\left(\frac{r^2 + 2R^2 - s(K)^2 - 2Rr\cos\phi}{2R\sqrt{r^2 + R^2 - 2Rr\cos\phi}}\right)$$

$$\nu(r) = \cos^{-1}\left(\frac{r^2 + 2Rs(K) - s(K)^2}{2Rr}\right). \qquad (5.19)$$

- *$P_{rt1}(K) = P_{during}(K)$ is the probability that the packet is received in error at its first transmission attempt. The density of packets attempting to access the channel is given by Eq.* (5.13)*, with $P_b(K)$, $P_{rt}(K)$, and $P_{rt1}(K)$ given above.*

Note that because of the inter-dependence between $P_b(K)$, $P_{during}(K)$, and $\lambda_{csma}(K)$ in both the theorems given above, their values are found through numerical iterations. The procedure for this was explained in Section 2.4.

5.2.3 The CSMA Protocol With Sensing Across Subbands

In the following, we improve the performance of our multi-band system by allowing the nodes to sense the channel conditions across all subbands first, in order to locate those (if any) subbands where the SINR is above the required threshold $\beta_b(K)$. In this section, we assume that $\beta_b(K) = \beta(K)$.[3] Then the sensing node makes a random selection of one subband from this chosen set, over which it initiates its packet transmission. Due to this *random* selection of a subband among those that have a measured SINR above $\beta(K)$, we may still assume that the number active of nodes within each subband follows a PPP. This is an approximation that our simulation results will show to be reasonable. Consequently, a packet is backed off if it does not find any subbands where its SINR $\geq \beta(K)$. Such sensing across

[3]For results on the outage probability when $\beta_b(K) \neq \beta(K)$, please refer to Section 4.1.

the entire bandwidth is expected to reduce the outage probability, at the expense of increased complexity and cost of implementation of the hardware. Note that once a transmission is initiated, no further sensing is performed across subbands if a packet has to be retransmitted. With sensing across all subbands, the outage probability of CSMA is given by the following theorem.

Theorem 5.5 (CSMA_{TX} and CSMA_{RX})
The outage probability of CSMA (in the absence of fading), when channel sensing is performed across all K subbands prior to transmission, is given by

$$P_{out}(CSMA) \;=\; P_b(K)^{KM} + \left(1 - P_b(K)^{KM}\right)\, P_{rt1}(K)\, P_{rt}(K)^N, \qquad (5.20)$$

where:

- $P_b(K)$ *is the backoff probability within each subband, and is approximated by the solution to*

$$\tilde{P}_b(K) = 1 - e^{-\pi\, s(K)^2\, \frac{\lambda}{K}\left(1-\tilde{P}_b(K)^{MK}+\left(1-\tilde{P}_b(K)^{MK}\right)\tilde{P}_{rt1}(K)\,\frac{1-\tilde{P}_{rt}(K)^N}{1-\tilde{P}_{rt}(K)}\right)}, \quad (5.21)$$

- $P_{rt1}(K)$ *and* $P_{rt}(K)$ *are given in Theorem 5.3 for* $CSMA_{TX}$ *and in Theorem 5.4 for* $CSMA_{RX}$.
- *The density* $\lambda_{csma}(K) = \{\lambda^{TX}_{csma}(K), \lambda^{RX}_{csma}(K)\}$ *is given as*

$$\lambda_{csma}(K) = \frac{\lambda}{K}\left[\frac{1-P_b(K)^{MK}}{1-P_b(K)^K} + \left(1-P_b(K)^{MK}\right)\, P_{rt1}(K)\,\frac{1-P_{rt}(K)^N}{1-P_{rt}(K)}\right], \qquad (5.22)$$

As we will see in Section 5.4, such sensing across subbands provides significant performance gain, in particular when K increases. Such improvement is obtained at the expense of increased hardware complexity.

5.3 Performance in the Presence of Fading

In this section, we add fading effects to the channel model, as described in Section 5.1. In particular, we consider Rayleigh fading, as this is the only distribution that provides closed form expressions for the error probability [65]. As also mentioned earlier, due to the distance-independence of the channel fading coefficients, the closest interferer does not necessarily cause error in the reception of a packet. Instead, we again consider the *dominant*

interferer, which is a single interferer whose received interference power *alone* is strong enough to result in an erroneous reception for the packet under observation.

Due to the Poisson distribution of interferers in space, we may express the probability that an erroneous packet reception occurs as

$$\begin{aligned} P^f_{error}(K) &= \Pr\left[\text{SINR} \leq 2^{KR_{req}/W} - 1\right] \\ &\geq \mathbb{E}_{h_{00},h_{0i}}\left[1 - e^{-\text{Average number of dominant interferers}}\right] \\ &\approx 1 - e^{-\mathbb{E}_{h_{00},h_{0i}}[\text{ Average number of dominant interferers }]}. \end{aligned} \tag{5.23}$$

In the following subsections, we present the derived expressions for the outage probability of the different flavors of the ALOHA and CSMA protocols by applying the error probability expression given in Eq. (5.23).

5.3.1 The ALOHA Protocol

Following a modified version of the guard zone concept, in the same manner as in Section 3.1, define $s^f(h_{00}, h_{0i})$ as the distance to the *strongest* interferer on the plane. With K subbands and an SINR requirement of $\beta(K)$, as given in Eq. (5.4), we have

$$s^f(h_{00}, h_{0i}) \;=\; h_{0i}^{1/\alpha}\left(\frac{h_{00}R^{-\alpha}}{\beta(K)} - \frac{\eta(K)}{\rho}\right)^{-1/\alpha}. \tag{5.24}$$

Consequently, the expected number of dominant interferers within a distance $s^f(h_{00}, h_{0i})$ away and with arrival time during $[-T, 0)$, is

$$\mathcal{I}_{avg} \;=\; \pi\,\lambda_{slotted}(K)\,s^f(h_{00}, h_{0i})^2, \tag{5.25}$$

where $\lambda_{slotted}(K)$ is given by Eq. (5.6) with $P_{rt}(K)$ replaced by its expected value with respect to h_{00} and h_{0i}, as derived in the following. Considering a strictly interference-limited channel and inserting Eq. (5.25) into Eq. (5.23), yields

$$P^f_{error}(K) \;\approx\; 1 - \exp\left\{-\pi\,\lambda_{slotted}(K)\,\mathbb{E}\left[h_{0i}^{\frac{2}{\alpha}}\right]\mathbb{E}\left[\left(\frac{h_{00}R^{-\alpha}}{\beta(K)}\right)^{-\frac{2}{\alpha}}\right]\right\}, \tag{5.26}$$

Furthermore, knowing that for Rayleigh fading channels, $\mathbb{E}\left[h_{00}^{-2/\alpha}\right]$ and $\mathbb{E}\left[h_{0i}^{2/\alpha}\right]$ are Gamma functions, we apply the result of Eq. (3.8). By allowing for a maximum of N retransmissions per packet, each occurring with probability $\overline{P}_{rt,s}(K) = P^f_{error}(K)$, we arrive at the following theorem.

Theorem 5.6 (Slotted ALOHA)
The outage probability of slotted ALOHA in the presence of Rayleigh fading, when the bandwidth is divided into K subbands, can be approximated by $\tilde{P}_{out}(\textit{Slotted ALOHA}) = \overline{P}_{rt,s}^{N+1}(K)$, *where* $\overline{P}_{rt,s}(K)$ *is the solution to*

$$\overline{P}_{rt,s}(K) \;=\; 1 - \exp\left\{ -\pi \frac{\lambda}{K} \frac{1-\overline{P}_{rt,s}(K)^{N+1}}{1-\overline{P}_{rt,s}(K)} R^2 \beta(K)^{2/\alpha} \frac{2\pi/\alpha}{\sin(2\pi/\alpha)} \right\}, \quad (5.27)$$

with $\beta(K)$ *as given by Eq.* (5.4).

To derive the outage probability of unslotted ALOHA, we use the same procedure as for slotted ALOHA, except that we now need to consider *two* time slots. This yields the following theorem.

Theorem 5.7 (Unslotted ALOHA)
The outage probability of unslotted ALOHA in the presence of Rayleigh fading, when the bandwidth is divided into K subbands, can be approximated by $\tilde{P}_{out}(\textit{Unslotted ALOHA}) = \overline{P}_{rt,u}(K)^{N+1}$, *where* $\overline{P}_{rt,u}(K)$ *is the solution to*

$$\overline{P}_{rt,u}(K) = 1 - \exp\left\{ -2\pi \frac{\lambda}{K} \frac{1-\overline{P}_{rt,u}(K)^{N+1}}{1-\overline{P}_{rt,u}(K)} R^2 \beta(K)^{2/\alpha} \frac{2\pi/\alpha}{\sin(2\pi/\alpha)} \right\}. \quad (5.28)$$

Evaluating the optimal number of subbands, we obtain the exact same expression for K_{opt} as in the absence of fading, given by Eq. (5.11). That is, no matter if fading is present or not, or whether the system is slotted or unslotted, the bandwidth should be partitioned into the same K_{opt} subbands in order to minimize the outage probability.

5.3.2 The CSMA Protocol

As in the absence of fading in Subsection 5.2.2, we start by assuming that each packet transmits over a randomly selected subband. To analytically evaluate the outage probability of CSMA, we divide the outage event into independent error events, as in Eq. (5.12). In this section, we allow the required rate for correct packet reception, R_{req}, to be different than the requested rate for making the backoff decision $R_{req,b}(K)$. The density of packets that attempt to access the channel when the network is in a steady state, is

$$\lambda_{csma}(K) \;=\; \frac{\lambda}{K}\left[\frac{1-\overline{P}_b(K)^M}{1-\overline{P}_b(K)} + (1-\overline{P}_b(K)^M)\,\overline{P}_{rt1}(K)\,\frac{1-\overline{P}_{rt}(K)^N}{1-\overline{P}_{rt}(K)} \right], \quad (5.29)$$

where λ/K being the density of new packet arrivals within each subband; $\overline{P}_b(K)$, $\overline{P}_{rt1}(K)$, and $\overline{P}_{rt}(K)$ are, respectively, the backoff probability, the probability that the packet is received in error at its first transmission attempt, and the probability that the packet is probability of erroneous reception in retransmission attempts, *averaged* with respect to the fading coefficients.

In the same manner as for fading networks without bandwidth partitioning (Section 4.1), we derive expressions for the above-mentioned probabilities. The procedure for deriving the backoff probability is as before, and we will thus not repeat this here. In order to obtain $\overline{P}_{during}$, we derive the expected density of active dominant interferers to be

$$\mu^f(K) \;=\; \frac{\lambda}{K}\left(1-e^{-\frac{h_{ii}R^{-\alpha}r^{\alpha}}{\beta_b(K)}}\right)e^{-\frac{h_{00}R^{-\alpha}r^{\alpha}}{\beta(K)}}. \tag{5.30}$$

This yields $P_{during}(K) = 1 - \mathbb{E}_{h_{00},h_{ii}}\left[\exp\left\{-\iint\limits_A \mu^f(K)\, r\, dr\, d\phi\right\}\right]$.

Finally, by replacing β and β_b in Eq (3.4) with $\beta(K) = 2^{KR_{req}/W} - 1$ and $\beta_b(K) = 2^{KR_{req,b}/W} - 1$, respectively, we have

$$s^f(K) \;=\; h_{0i}^{1/\alpha}\left(\frac{h_{00}R^{-\alpha}}{\beta(K)}\right)^{-1/\alpha} \quad\wedge\quad s_b^f(K) \;=\; h_{0i}^{1/\alpha}\left(\frac{h_{00}R^{-\alpha}}{\beta_b(K)}\right)^{-1/\alpha}.$$

Using a geometrical analysis, we obtain that $P_{rx|transmit}(K; h_{00}, h_{0i}) \approx P_{rx}(K)\frac{\text{Area of } B(\text{RX}_0, s(K)) \cap \overline{B(\text{TX}_0, s_b(K))}}{\text{Area of } B(\text{RX}_0, s(K))}$. Taking the expectation with respect to h_{00} and h_{0i} in the above expressions, we arrive at the following theorem.

Theorem 5.8 (CSMA_{TX})
The outage probability of $CSMA_{TX}$ in the presence of Rayleigh fading, when the bandwidth is divided into K subbands, is given by

$$P_{out}^f(CSMA_{TX}) \;=\; \overline{P}_b(K)^M + \left(1-\overline{P}_b(K)^M\right)\overline{P}_{rt1}(K)\,\overline{P}_{rt}(K)^N, \tag{5.31}$$

where:

- *$\overline{P}_b(K)$ is the average backoff probability, approximated by the solution to*

$$\overline{P}_b(K) = 1 - e^{-\frac{\lambda}{K}\left(1-\overline{P}_b(K)^M+\left(1-\overline{P}_b(K)^M\right)\overline{P}_{rt1}(K)\frac{1-\overline{P}_{rt}(K)^N}{1-\overline{P}_{rt}(K)}\right)\pi R^2\beta_b(K)^{2/\alpha}\frac{2\pi/\alpha}{\sin(2\pi/\alpha)}}. \tag{5.32}$$

  $\overline{P}_{rx}(K)$ is the average probability that a packet is in error at the start of each of its retransmission attempts. This is given by Eq. (5.32) *with $\beta_b(K)$ replaced by $\beta(K)$.*

- $\overline{P}_{rt}(K) = \mathbb{E}_{h_{00}}\left[\overline{P}_{rx}(K) + \left(1-\overline{P}_{rx}(K)\right) P_{during}(K;h_{00})\right]$ *is the average probability that a packet is received in error during a retransmission attempt.* $P_{during}(K;h_{00})$ *is the probability that the error has occurred during the transmission given* h_{00}*, approximated by*

$$\tilde{P}_{during}(K;h_{00}) = 1 - e^{-\int_0^\infty 2\pi\lambda_{csma}^{TX}(K)\left(1-e^{-\mathbb{E}[h_{ii}]R^{-\alpha}r^{\alpha}/\beta_b(K)}\right)e^{-h_{00}R^{-\alpha}r^{\alpha}/\beta(K)}r\,dr}, \tag{5.33}$$

where $\lambda_{csma}^{TX}(K)$ *is the density of packets attempting to access the channel, given by Eq.* (5.29)*.*

- $\overline{P}_{rt1}(K) = \mathbb{E}_{h_{00}}\left[P_{rx|transmit}(K;h_{00}) + [1-P_{rx|transmit}(K;h_{00})]P_{during}(K;h_{00})\right]$ *is the average probability that the packet is received in error at its first transmission attempt, with* $P_{rx|transmit}(K;h_{00})$ *approximated by*

$$P_{rx|transmit}(K;h_{00}) = \overline{P}_{rx}(K)\,\mathbb{E}_{h_{0i}}\left[\frac{\pi s^f(K)^2 - A_{ol}\left(s^f(K), s_b^f(K)\right)}{\pi\, s^f(K)^2}\right], \tag{5.34}$$

where $A_{ol}\left(s^f(K), s_b^f(K)\right)$ *is given by Eq.* (4.21)*.*

The outage probability of CSMA_{RX} is derived in the same way as for CSMA_{TX} with some minor differences. The main difference is in $\overline{P}_{rx|transmit}(K)$, which is now concerned with the overlap area between $B(\text{RX}_0, s)$ and $B(\text{RX}_0, s_b)$ (as opposed to $B(\text{RX}_0, s_b)$). This area is shown in Figure 4.2. This yields the following theorem.

Theorem 5.9 (CSMA_{RX})
The outage probability of $CSMA_{RX}$ *in the presence of Rayleigh fading, when the bandwidth is divided into K subbands, is given by Eq.* (5.31)*, where:*

- $\overline{P}_b(K)$ *is the average backoff probability, approximated by the solution to Eq.* (5.32)*.* $\overline{P}_{rx}(K)$ *is also given by Eq.* (5.32)*, with* $\beta_b(K)$ *replaced by* $\beta(K)$*.*
- $\overline{P}_{rt}(K) = \mathbb{E}_{h_{00}}\left[\overline{P}_{rx}(K) + \left(1-\overline{P}_{rx}(K)\right) P_{during}(K;h_{00})\right]$ *is the average probability that a packet is received in error during a retransmission attempt.* $P_{during}(K;h_{00})$ *is the probability that the error has occurred during the transmission given* h_{00}*, and is approximated by Eq.* (5.33)*.*
- $\overline{P}_{rt1}(K) = \mathbb{E}_{h_{00}}\left[P_{rx|transmit}(K) + \left(1-P_{rx|transmit}(K)\right) P_{during}(K;h_{00})\right]$ *is the average probability that the packet is received in error at its first trans-*

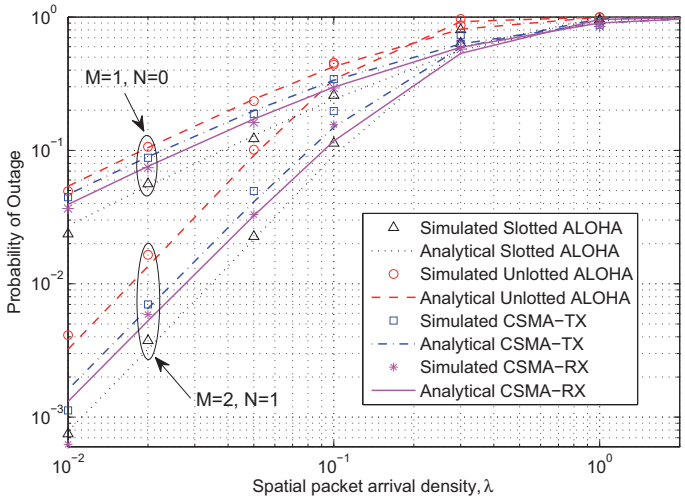

Figure 5.1: Outage probability of ALOHA and CSMA in a non-fading network with $\beta = 0$ dB and $K = 3$ subbands.

mission attempt, with $P_{rx|transmit}(K)$ *approximated by*

$$\tilde{P}_{rx|transmit}(K) = \begin{cases} 0 & ; \textit{for } \beta_b(K) \geq \beta(K) \\ \overline{P}_{rx}(K)\, \dfrac{\beta(K)^{2/\alpha} - \beta_b(K)^{2/\alpha}}{\beta(K)^{2/\alpha}} & ; \textit{otherwise} \end{cases} \tag{5.35}$$

Allowing the decision-making nodes to sense all subbands prior to choosing *one* subband to transmit over (as in Subsection 5.2.3), yields the same outage probability expression in the presence of fading as in the case of non-fading channels. This is given by Theorem 5.5, with $P_b(K)$, $P_{rt1}(K)$, and $P_{rt}(K)$ replaced respectively by $\overline{P}_b(K)$, $\overline{P}_{rt1}(K)$, and $\overline{P}_{rt}(K)$, as given by Theorem 5.8 for CSMA_{TX} and Theorem 5.9 for CSMA_{RX}.

5.4 Numerical Results

Monte Carlo simulations are generated in order to confirm the derived expressions of this section. Unless specified otherwise, we assume a fixed transmitter-receiver distance $R = 1$ m, transmission power $\rho = 1$ mW, path-loss exponent $\alpha = 4$, normalized required transmission rate $\frac{R_{req}}{W} =$

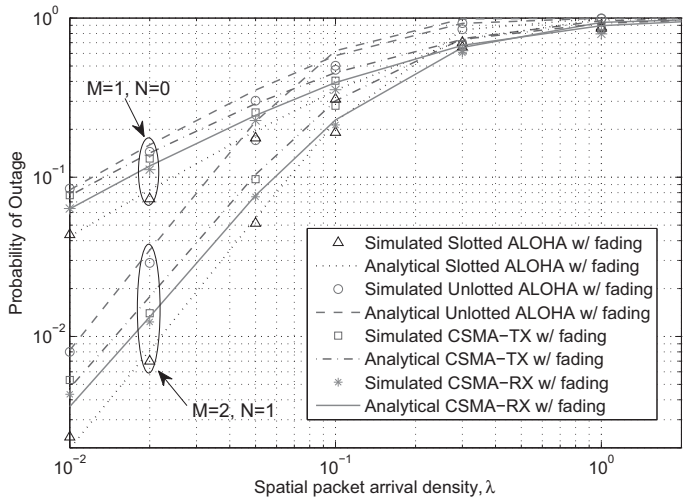

Figure 5.2: Outage probability of ALOHA and CSMA in a fading network with $\beta = 0$ dB, and $K = 3$ subbands.

$\frac{R_{req,b}}{W} = 1$, number of backoffs $M = 2$, and number of retransmissions $N = 1$.

In Figures 5.1 and 5.2, the outage probability of ALOHA and CSMA with $K = 3$ subbands is plotted as a function of the density of new packet arrivals, λ, for a non-fading network and a fading network, respectively. The simulation results validate our derived analytical expressions, as the two curves follow each other tightly for lower densities. As the density increases, some discrepancies are observed between the analytical results and the simulations, in particular for $(M, N) = (2, 1)$. This is due to the guard zone approximation in our analysis; at high interferer densities, the aggregate interference becomes a significant contributor to the outage probability, and thus, the approximation that error is caused only by the closest or dominant interferer, yields a loose lower bound. However, these deviations occur at higher outage probabilities than what is often applied in practical networks. Most systems operate at $P_{out} < 0.1$, where our analytical approximations are seen to be reasonable.

Comparing the performance of the various MAC protocols, we first note that the outage probability of both versions of the CSMA protocol outperform unslotted ALOHA. This is primarily due to backoff property of CSMA, which results in a lower level of interference in the channel. In-

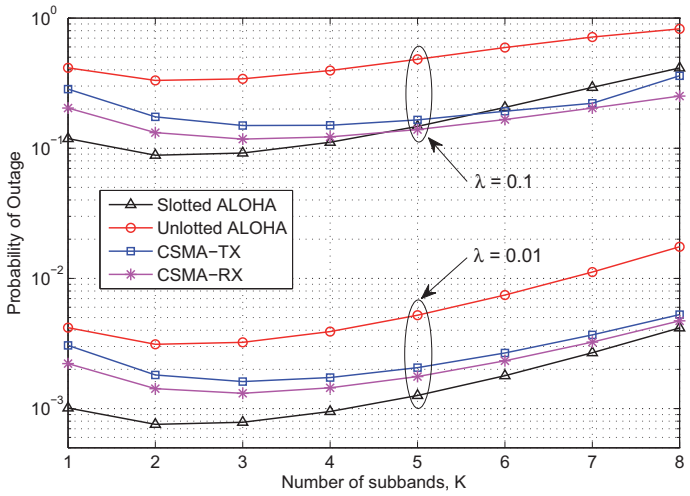

Figure 5.3: Outage probability of ALOHA and CSMA in a non-fading network with $(M, N) = (2, 1)$, as a function of K.

terestingly, this was not the case in a network with no bandwidth partitioning and $(M, N) = (1, 0)$, where CSMA_{TX} exhibits 10% higher outage probability than unslotted ALOHA. The reason for this difference is that for $K = 3$, which is the case in Figures 5.1 and 5.2, CSMA yields an optimal performance, while for ALOHA, the optimal number of subbands is $K = 2$. Clearly, slotted ALOHA yields the lowest outage probability, as it does not allow for partial overlap of packets. Compared to unslotted ALOHA, it reduces the outage probability by a factor of 2^{N+1} both in non-fading and fading networks. However, this slotted protocol would require synchronization between users, which is not only costly, but in some networks, even impossible to implement perfectly, among others because of hardware constraints.

Of all the unslotted protocols, CSMA_{RX} yields the lowest outage probability both in the absence and presence of fading, providing up to 15% improvement compared to CSMA_{TX} when $(M, N) = (1, 0)$ and 25% improvement when $(M, N) = (2, 1)$. However, also note that we have not considered the "stealing" of resources that the additional feedback channel in CSMA_{RX} requires. We have simply assumed that the same separate control channel that is used by the receiver to inform its transmitter of erroneous packet receptions, is also used for sending the "transmit/don't

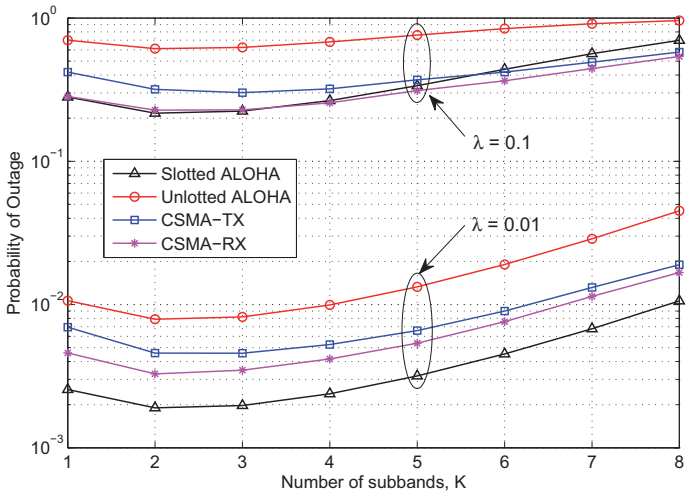

Figure 5.4: Outage probability of ALOHA and CSMA in a fading network with $(M, N) = (2, 1)$, as a function of K.

transmit" signal to the transmitter. Finally, evaluating the impact of fading, which we assume to be Rayleigh, we observe that a non-fading network yields up to 35% lower outage probability than a fading network.

In Figure 5.3, the outage probability of a non-fading network with $(M, N) = (2, 1)$ is plotted as a function of the number of subbands, K, for both a low density of $\lambda = 0.01$ and a high density of $\lambda = 0.1$. As expected, we observe that for both ALOHA and CSMA there exist optimal values of K for which the outage probability is minimized. For both versions of ALOHA, $K_{opt} = 2$. For $N = 0$, we also obtain $K_{opt} = 2$, which is in accordance with our analytical result of $K_{opt,anal} = 2.299 \approx 2$ based on Eq. (5.11). For both CSMA protocols, $K_{opt} = 3$. This means that a higher sensing threshold should be used in the case of CSMA, due to the fact that there are fewer interferers than in ALOHA. Moreover, a higher K_{opt} also implies a higher obtainable spectral efficiency.

When Rayleigh fading is present in the network, as shown in Figure 5.4, we observe a similar behavior as in non-fading networks. As noted in Subsection 5.2.1, the same optimal number of subbands is derived for ALOHA in the presence of fading as in the absence of it. In fact, this conclusion seems to hold for CSMA also. Moreover, we note that the error percentage due to a wrong choice of $K \neq K_{opt}$ is quite high for all protocols. E.g., if the

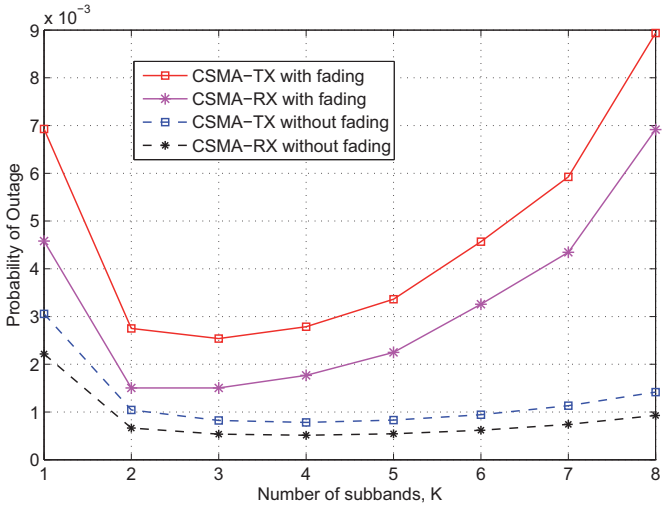

Figure 5.5: Outage probability of CSMA with and without fading with sensing across all K subbands, for $\lambda = 0.01$ and $(M, N) = (2, 1)$.

bandwidth is divided into $K = 6$ subbands, rather than 2 for ALOHA and 3 for CSMA, the system yields about 140% higher outage probability for ALOHA, and about 100% higher for CSMA. For a high density of $\lambda = 0.1$ with $K = 6$, both versions of CSMA can outperform even slotted ALOHA both in non-fading and fading networks.

In Figure 5.5, the outage probability of CSMA_{TX} and CSMA_{RX} when they have the capability to sense across all subbands, is plotted as a function of K, both in the absence and presence of fading. As expected, we witness a significant improvement compared to random selection of a subband. As K increases, this advantage becomes more evident; for $K = 3$ subbands (for which the outage probability of CSMA_{RX} in Figures 5.3 and 5.4 is minimized), the introduction of sensing across subbands in a non-fading network, reduces the minimum outage probability of CSMA_{TX} by approximately 50%, and that of CSMA_{RX} by 32%. In the presence of fading, this improvement is 67% for CSMA_{TX} and 27% for CSMA_{RX}. Moreover, the outage probability remains relatively constant for $K > 3$ in the case of non-fading (with the minimum occurring at $K = 4$), while in the case of fading, the outage probability increases above its minimum value, as K surpasses 3. Note that bandwidth partitioning improves the outage performance of CSMA more than the improvement obtained through optimization of the

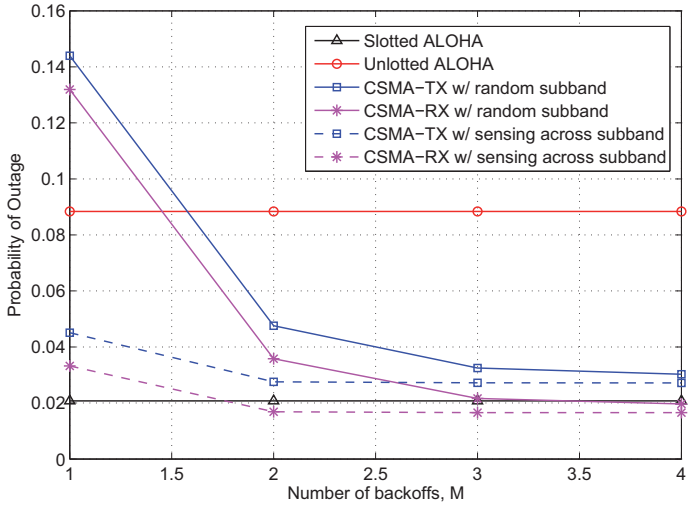

Figure 5.6: Outage probability of ALOHA and CSMA with and without fading as a function of M, for $\lambda = 0.01$ and $(M, N) = (2, 1)$.

sensing threshold or joint transmitter-receiver sensing (which were evaluated in Chapter 4).

Finally, we investigate the impact of the number of backoffs, M, on the performance of CSMA. In Figure 5.6, the outage probability is plotted as a function of M for $\lambda = 0.01$, $N = 1$ retransmission, and $K = 2$ subbands (for which ALOHA yields an optimal performance). As expected, when $M = 1$, both versions of CSMA perform better than unslotted ALOHA, but still yield a higher outage probability than slotted ALOHA. However, as the number of backoffs increases, the outage probability of CSMA starts approaching that of slotted ALOHA. For $M > 2$, sensing across subbands makes CSMA_{RX} outperform slotted ALOHA by approximately 20%. Similar conclusions are drawn in a fading network.

5.5 Summary

In this chapter, bandwidth partitioning is introduced to improve the performance of point-to-point wireless ad hoc networks. Expressions are derived for the outage probability both in the absence and presence of fading, and Monte Carlo simulations are carried out to validate the analytical results.

It is shown that increasing the number of subbands results in a lower level of interference within each subband, while at the same time, a lower transmission rate may be achieved. The optimal number of subbands, K_{opt}, thus represents the optimal trade-off between these two factors. K_{opt} is derived in the case of ALOHA, while in CSMA, due to the complexity of its outage probability expressions, the optimal number of subbands is obtained through simulations only.

Furthermore, rather than randomly selecting the subband to transmit over, we introduce sensing across subbands prior to transmission in CSMA. That is, all subbands are sensed upon the arrival of a packet, and a subband is randomly selected out of those that are sensed to be idle. Such sensing across subbands improves the performance of CSMA considerably, by up to 50% in the absence of fading and 67% in the presence of fading.

Chapter 6

Performance Improvement With MIMO Techniques

Multiple input multiple output (MIMO) systems have achieved great popularity because of their ability to reach remarkably higher transmission rates and improved signal qualities compared to single input single output (SISO) systems [12]. While isolated MIMO systems have been evaluated extensively in the literature [12; 86], MIMO point-to-point *interference channels* have come in focus only in recent years. An interference channel (which we have considered also in the preceding chapters) is a model for studying networks with two or more source-destination pairs, where the source signals interfere with each other at the receivers and all interference is treated as noise (i.e., no constructive use of interference is applied). As mentioned in the introduction, one of the inherent attributes of interference channels is the fact that a change in some system parameters not only affects the performance of the link under observation, but also the impact of this link on the rest of the network. Understanding the behavior of interference channels, in particular with multi-antenna links, is of great importance in today's communication networks, as there is an increasing demand for allowing simultaneous transmissions between independent transmitter-receiver pairs. This is specifically true for networks where it is not always realistic to employ interference in a constructive manner (through multi-user coding, dirty paper coding, etc.), due to the high complexity and cost that this would entail.

Extensive work has been done on understanding the impact of interference in MIMO ad hoc and cellular networks using simulators and test beds [87; 88], and on deriving the distribution of the ordered and unordered

eigenvalues of finite-dimensional channel matrices [89; 90], which is of great significance for the capacity analysis. The particular case of Wishart matrices are considered in [91], where the eigenvalue distribution, as well as the symbol error probability of M-ary PSK signals, are derived. In [92], the distribution of the capacity of a MISO broadcast channel with a random beamformer is derived. However, the impact of interference between users is ignored, as the broadcast channel considers only a single transmitter. For point-to-point MIMO interference channels, analytical expressions are derived in [93] for the *asymptotic* ergodic capacity, i.e., when the number of transmitter and receiver antennas go to infinity. For the non-asymptotic case, the performance of MIMO systems with interference has been evaluated in [94], for the case when the transmitters have full channel state information (CSI). Moreover, much effort has been put into characterizing the degrees of freedom in MIMO interference channels [1; 2; 95] and developing interference alignment schemes when some coordination is allowed between the transmitters [2; 3; 8]. Also other schemes involving precoding, space-time codes, and optimal combining techniques have been proposed to overcome the interference problem [96].

In the following sections, we evaluate the usage of antennas in MIMO interference channels. Two types of networks are considered; 1) a κ link MIMO channel where the transmitters have no CSI (Section 6.1), and 2) a κ link MIMO channel where all nodes in the network are assumed to have partial CSI and apply interference alignment techniques (Section 6.2). We define here partial CSI for a node as having instantaneous information about the channels directly connected to that node, but not the channels between other nodes pairs.

The work of this chapter is partly published in [97; 98].

6.1 Usage of Antennas in Absence of CSI

Obtaining exact or even partial CSI at the transmitter is not always feasible, due to delay constraints or hardware limitations. Only a few works have studied the capacity of MIMO systems in the presence of co-channel interference when the transmitters have no CSI. Most of the works considering interference channels rely on simulation results or approximations. In particular, in [99], a cellular system is simulated utilizing 3×3 MIMO transmission techniques, along with adaptive modulation and frequency reuse. The simulation results confirm that co-channel interference can profoundly degrade the capacity of MIMO links in cellular networks. Also in [21] and [86], the mutual information of MIMO systems in the presence of

co-channel interference is evaluated. It is concluded that for certain signal-to-noise ratio (SNR) and signal-to-interference ratio (SIR) values, the use of multiple antennas in fact degrades the performance of the system compared to SISO networks. These results are constrained to 2 transmit and 2 receive antennas, and the observations are made through simulations only. Jorswieck and Boche also prove in [23] that using fewer antennas can actually improve the system performance in some scenarios. However, their network model does not constitute an interference channel, as they only consider a single multi-antenna link with different network configurations.

In [22], the performance of MIMO interference channels with optimum combining and an arbitrary number of users is considered, and exact expressions are derived for the cdf of the SINR and the outage probability. However, in this work, the interference model is simplified by counting the number of interfering signals rather than the physical interfering users, meaning that each transmit antenna of an interferer is considered as a separate single-antenna interferer. Such assumption makes the analysis tractable, but loses the impact of diversity when the same stream of data is sent over several antennas. In the very recent work of [100], Chiani *et. al.* evaluate the effect of interference on the capacity of MIMO interference channels. Closed-form expressions are derived for the ergodic capacity of both single-user MIMO systems, and MIMO systems with multiple MIMO interferers. The work of this thesis serves as a parallel to this work, where we extend the research domain to also consider outage probability, and evaluate the particular case of multiple input single output (MISO) channels, where an interesting behavior is observed as the system parameters vary.

Despite the recent interest in applying MIMO in cellular and ad hoc wireless networks, the performance of such networks is not yet fully understood. The goal of this section is thus to establish an understanding of the ergodic capacity and outage probability performance of uncoordinated MIMO interference channels with a finite number of antennas and with no CSI at the transmitters (CSIT). Ergodic capacity is the average capacity for each link, whereas outage is characterized as the event when the instantaneous capacity falls below the transmission rate required for correct packet reception. The reason for focusing on these two metrics is that high transmission rates and ensuring correct reception of packets are two of the most desired features in today's wireless networks. The use of multiple antennas plays a key role in achieving these attributes.

In the following, we start by considering a MIMO interference channel with κ communication links, where each link consists of a transmitter and a receiver, each with a finite number of antennas. Next, in Subsection 6.1.3,

we set the number of antennas at the receiver to 1, while that at the transmitter is arbitrary, and we evaluate the system performance. In particular, the key contributions of this section are as follows:

- Upper and lower bounds are derived on the ergodic capacity and outage probability of κ link MIMO interference channels with an arbitrary number of transmitter and receiver antennas.
- The probability density function of the capacity of MISO interference channels with an arbitrary number of transmit antennas is derived.
- Exact expressions for the ergodic capacity and outage probability of MISO interference channels with an arbitrary number of transmitter antennas are developed.
- Analysis is performed on the different behaviors observed in the outage probability of MISO networks as the system parameters vary. Furthermore, time division multiple access (TDMA) is introduced to improve the system performance.

6.1.1 System Model

Consider a wireless network with κ transmitting nodes, TX_i (these could be base stations or sensor nodes), each communicating with its own dedicated receiver, RX_i (e.g., mobile stations or forecast centers). Denote the number of transmit and receive antennas at each of the transmitters and receivers by N_t and N_r, respectively. This MIMO network is illustrated in Figure 6.1. The channel response between each transmitter and its own receiver is specified through an $N_r \times N_t$ random matrix $\mathbf{G}_{ii}$, whose random process is presumed to be zero-mean and ergodic. The elements of $\mathbf{G}_{ii}$ are independent and identically distributed complex Gaussian random variables, each with zero mean and constant variance g_{ii}. Moreover, we define a normalized $N_r \times N_t$ channel matrix $\mathbf{H}_{ii}$ with unit-variance entries such that $\mathbf{G}_{ii} = \sqrt{g_{ii}}\,\mathbf{H}_{ii}$. Similarly, the channel between a receiver i and its interfering transmitter j is denoted by $\mathbf{G}_{ij} = \sqrt{g_{ij}}\,\mathbf{H}_{ij}$.

At the transmitters, the angular spread tends to be small, and the antennas are assumed to be decorrelated. Perfect channel estimation is assumed at the receivers, while the transmitters have no CSI. The transmitted signals are presumed to be independent and equi-powered, as this setting maximizes the mutual information in the case of no CSIT [12]. Transmitter i transmits with a total power ρ_i. The channel entails additive white Gaussian noise (AWGN), and the interference from the other links in the

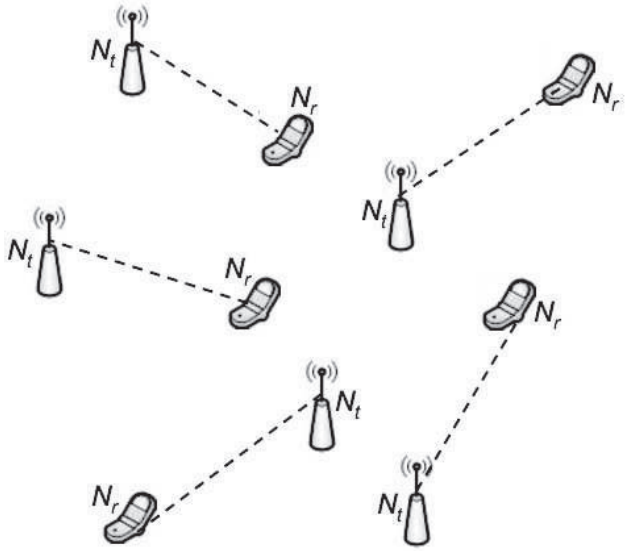

Figure 6.1: Illustration of a κ link MIMO network.

network adds to the impairment of the received signal. Denoting the data to be transmitted by TX_i as $\mathbf{x}_i$ and the noise signal as $\mathbf{n}_i$, we have that the signal received at RX_i is

$$\mathbf{y}_i \;=\; \sqrt{g_{ii}}\,\mathbf{H}_{ii}\mathbf{x}_i + \sum_{j\neq i}^{\kappa} \sqrt{g_{ij}}\,\mathbf{H}_{ij}\mathbf{x}_j + \mathbf{n}_i. \tag{6.1}$$

We assume slow fading [1], and single user detection at the receivers. The ergodic capacity of link i then becomes

$$\mathcal{C}_{erg,i} \;=\; \mathbb{E}\left[\log_2 \det\left(\mathbf{I}_{N_r} + \frac{\rho_i\, g_{ii}}{N_t}\,\mathbf{H}_{ii}\,\mathbf{H}_{ii}^{\dagger}\,\mathbf{Q}_i^{-1}\right)\right], \tag{6.2}$$

where $\mathbf{Q}_i$ is the covariance of the channel impairment, consisting of noise (with power η) plus interference;

$$\mathbf{Q}_i \;=\; \sum_{j\neq i}^{\kappa} \frac{\rho_j\, g_{ij}}{N_t}\,\mathbf{H}_{ij}\mathbf{H}_{ij}^{\dagger} + \eta\mathbf{I}_{Nr}. \tag{6.3}$$

[1] In the case of fast fading, with a sufficiently long coding horizon, we can code over the short-term channel fluctuations.

Outage occurs on a channel when the rate required for correct reception is higher than the capacity of the interference channel. Thus, denoting the required rate at each receiver antenna by R_{req}, the outage probability of link i is defined mathematically as

$$P_{out,i} \;=\; \Pr\left\{\log_2 \det\left(\mathbf{I}_{N_r} + \frac{\rho_i g_{ii}}{N_t}\mathbf{H}_{ii}\,\mathbf{H}_{ii}^{\dagger}\,\mathbf{Q}_i^{-1}\right) < N_r R_{req}\right\}, \tag{6.4}$$

where the sources of randomness in the probability expression are the matrices $\mathbf{H}_{ii}$ and $\mathbf{Q}_i$. In the following, we assume that all transmitter-receiver pairs in the network have the same channel characteristics, and moreover that g_{ii} are equal for all i. This means that we may choose any link i to evaluate the network performance, with the outage probability being $P_{out} = P_{out,i} \;\; \forall i$, and the ergodic capacity in the network being $\mathcal{C}_{erg} = \mathcal{C}_{erg,i} \;\; \forall i$.

6.1.2 MIMO Interference Channels

In this subsection, we evaluate the performance of the MIMO network described above in terms of ergodic capacity and outage probability. In order to derive the former, we need to know the distribution of the capacity. When the number of antennas goes to infinity, the average performance of the network becomes deterministic, and the analysis is thus tractable (as will be shown in Subsection 6.1.2.1). For a finite number of antennas, on the other hand, the situation changes completely. With no interferers in the channel (equivalent to $g_{ij} = 0$ for all i, j, resulting in $\mathbf{Q} = \eta\,\mathbf{I}_{N_r}$), the distribution of the capacity is known [101; 102]. However, with the addition of the interference term (i.e., as g_{ij} increases), these distributions are no longer valid. By decomposing the capacity formula into terms with known distributions (e.g., the determinant or trace of a Wishart matrix), we can derive bounds or approximate expressions for the ergodic capacity and outage probability, as is done in Subsections 6.1.2.2 and 6.1.2.3.

Due to the complexity of the expressions, in this section, we concentrate on a $\kappa = 2$ link network, as shown in Figure 6.2. The results of this section are scalable to larger networks, although the analytical expressions in some cases would become more complex. With $\kappa = 2$, we focus on link $i = 1$ in our analysis, and for the sake of simplicity of our expressions, we refer to ρ_1, g_{11}, $\mathbf{H}_{11}$ and $\mathbf{Q}_1$ by ρ, g, $\mathbf{H}$ and $\mathbf{Q}$, respectively. Hence, we have that the instantaneous capacity of link 1 is given as

$$\mathcal{C}_1 \;=\; \log_2 \det\left(\mathbf{I}_{N_r} + \frac{\rho\, g}{N_t}\,\mathbf{H}\,\mathbf{H}^{\dagger}\,\mathbf{Q}^{-1}\right), \tag{6.5}$$

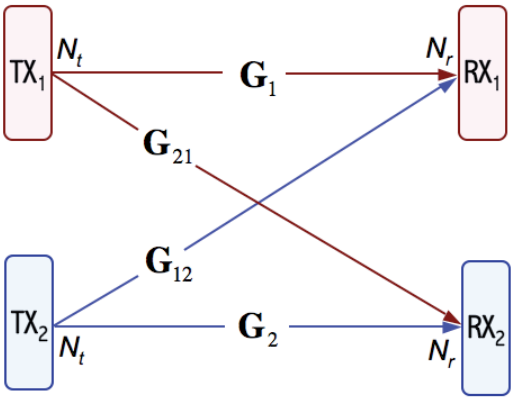

Figure 6.2: Illustration of a 2 link MIMO interference channel.

where $\mathbf{Q} = \frac{\rho_2 g_{12}}{N_t}\mathbf{H}_{12}\mathbf{H}_{12}^{\dagger} + \eta\, \mathbf{I}_{Nr}$.

6.1.2.1 Asymptotic Ergodic Capacity

The exact capacity of a multi-user MIMO interference channel was derived in [93] for the limiting case when the number of transmit and receive antennas approaches infinity. For such an asymptotic case, the sources of randomness disappear and the ergodic capacity becomes a deterministic function. For a 2 link MIMO channel and $\tau = N_t/N_r$, this asymptotic capacity is given as

$$\begin{aligned} C_{asymp} &= \tau \log_2\left(\frac{\mathrm{SIR} + \mathrm{SNR}\frac{\eta_1}{\tau}}{\mathrm{SIR} + \mathrm{SNR}\frac{\eta_2}{\tau}}\right) + \tau \log_2\left(1 + \mathrm{SNR}\frac{\eta_1}{\tau}\right) \\ &\quad + \log_2\frac{\eta_2}{\eta_1} + (\eta_1 - \eta_2)\log_2(e), \end{aligned} \tag{6.6}$$

where $\mathrm{SNR} = \frac{\rho\, g}{\eta}$, $\mathrm{SIR} = \frac{\rho\, g}{\rho_2 g_{12}}$, and η_1 and η_2 are given by

$$\eta_1 + \frac{\mathrm{SNR}\,\eta_1}{\mathrm{SNR}\frac{\eta_1}{\tau} + 1} + \frac{\mathrm{SNR}\,\eta_1}{\mathrm{SNR}\frac{\eta_1}{\tau} + \mathrm{SIR}} = 1 \tag{6.7}$$

$$\eta_2 + \frac{\mathrm{SNR}\,\eta_2}{\mathrm{SNR}\frac{\eta_2}{\tau} + \mathrm{SIR}} = 1. \tag{6.8}$$

For $N_t, N_r < \infty$, Eq. (6.6) becomes an approximation, which is shown to be reasonable for N_t and N_r as low as 6. For lower values of N_t and

N_r, however, Eq. (6.6) no longer serves as a valid approximation, and so we turn to other techniques to analyze the ergodic capacity and the outage probability.

6.1.2.2 Trace Bound

As mentioned above, assuming infinite or even large number of antennas often gives a wrong representation of a real network. In many of today's MIMO networks, such as cellular or sensor networks, the transmitters and receivers can only carry 2 or 3 antennas. In this case, the results of Subsection 6.1.2.1 are no longer valid, and so we attend to bounds in order to evaluate the performance of MIMO interference channels.

In the following, we derive an upper bound to the ergodic capacity, and equivalently a lower bound to the outage probability, by using the *trace* of the SINR matrix. For this, we apply the arithmetic-geometric inequality [103]

$$\left(\prod_{i=1}^{\min(N_t,N_r)} x_i\right)^{1/\min(N_t,N_r)} \leq \frac{1}{\min(N_t,N_r)} \sum_{i=1}^{\min(N_t,N_r)} x_i\,. \tag{6.9}$$

Knowing that the determinant of a square matrix (here: $\mathbf{H}\mathbf{H}^\dagger\mathbf{Q}^{-1}$) is equal to the product of its non-zero eigenvalues λ_i [101], we have that the instantaneous capacity is:

$$\begin{aligned} \mathcal{C}_{erg} &= \mathbb{E}\left[\log_2 \det\left(\mathbf{I}_{N_r} + \frac{\rho\, g}{N_t}\,\mathbf{H}\mathbf{H}^\dagger\mathbf{Q}^{-1}\right)\right] \\ &= \mathbb{E}\left[\log_2 \prod_{i=1}^{\min(N_t,N_r)} \left(1+\frac{\rho\, g}{N_t}\lambda_i\right)\right]. \end{aligned} \tag{6.10}$$

Furthermore, we know that the trace of a square matrix is equal to the sum of its distinct eigenvalues. Denoting the eigenvalues of $\mathbf{H}\mathbf{H}^\dagger\mathbf{Q}^{-1}$ by λ_i, we have that $\sum_{i=1}^{\min(N_t,N_r)} \lambda_i = \mathrm{tr}(\mathbf{H}\mathbf{H}^\dagger\mathbf{Q}^{-1})$. Let $x_i = (1+\frac{\rho\, g}{N_t}\lambda_i)$ in Eq. (6.9). The ergodic capacity can then be upper bounded as follows:

$$\begin{aligned} \mathcal{C}_{erg} &\leq \mathbb{E}\left[\log_2\left(\frac{1}{\min(N_t,N_r)} \sum_{i=1}^{\min(N_t,N_r)} 1+\frac{\rho\, g}{N_t}\lambda_i\right)^{\min(N_t,N_r)}\right] \\ &= \min(N_t,N_r)\,\mathbb{E}\left[\log_2\left(1+\frac{\rho\, g}{N_t\min(N_t,N_r)} \sum_{i=1}^{\min(N_t,N_r)} \lambda_i\right)\right] \\ &= \min(N_t,N_r)\,\mathbb{E}\left[\log_2\left(1+\frac{\rho\, g}{N_t\min(N_t,N_r)}\,\mathrm{tr}(\mathbf{H}\mathbf{H}^\dagger\mathbf{Q}^{-1})\right)\right]. \end{aligned} \tag{6.11}$$

Consequently, given the required rate for correct reception of packets per receive antenna is R_{req}, the outage probability may be lower bounded by

$$P_{out}^{lb} \;=\; \Pr\left[\mathrm{tr}(\mathbf{H}\mathbf{H}^{\dagger}\mathbf{Q}^{-1}) < \frac{N_t \min(N_t, N_r)}{\rho\, g}\left(2^{\frac{N_r R_{req}}{\min(N_t,N_r)}} - 1\right)\right]. \quad (6.12)$$

When there is no interference, i.e., $g_{12} = 0$, we know the distribution of the trace of a Wishart matrix [101]. In this case, the trace bound yields a decent upper bound to the instantaneous capacity. Similarly, a lower bound to the outage probability in the absence of interference is derived in [102] to be

$$P_{out}^{lb}\,|_{(g_{12}=0)} \;=\; 1 - \frac{1}{(N_t N_r - 1)!}\,\Gamma\left[N_t N_r,\, l\right] \;=\; e^{-l}\sum_{k=0}^{N_t N_r - 1}\frac{l^k}{k!}, \quad (6.13)$$

where $l = \frac{\min(N_t,N_r)\,\eta}{\rho\, g/N_t}\left(2^{\frac{N_r R_{req}}{\min(N_t,N_r)}} - 1\right)$.

As the interference channel gain, g_{12}, increases, this lower bound loses its tightness and is no longer valid. In this case, the distribution of $\mathrm{tr}(\mathbf{H}\mathbf{H}^{\dagger}\mathbf{Q}^{-1})$ is unknown, meaning that for the sake of evaluating the trace bounds given in Eqs. (6.11) and (6.12), we must still rely on Monte Carlo simulations. The reason for this evaluation is that if the trace bound turns out not to give a reasonable representation of the actual performance of the network with $g_{12} = 0$ (which we will see in Subsection 6.1.2.4 to be the case), there is no need to derive the distribution of $\mathrm{tr}(\mathbf{H}\mathbf{H}^{\dagger}\mathbf{Q}^{-1})$.

With the aim of finding a tigher bound, we take a step further to consider the lower (resp. upper) bound to the ergodic capacity (resp. outage probability) in the next subsection.

6.1.2.3 Determinant Bound

In this subsection, we employ another technique to derive bounds on the ergodic capacity and outage probability of MIMO interference channels. As before, we assume $\kappa = 2$ links in the network.

We start with Eq. (6.10), assuming without loss of generality that $N_r \leq N_t$. Now, applying the following inequality [102]

$$\prod_{i=1}^{N_r}(1 + x_i) \;\geq\; \left[1 + \left(\prod_{i=1}^{N_r} x_i\right)^{1/N_r}\right]^{N_r} \qquad \forall\; x_i > 0, \quad (6.14)$$

we derive the lower bound on the instantaneous capacity of link 1 to be

$$\begin{aligned}\mathcal{C}_1 &\geq \log_2\left\{1+\frac{\rho\, g}{N_t}\left(\prod_{i=1}^{N_r}\lambda_i\right)^{1/N_r}\right\}^{N_r}\\ &= N_r\,\log_2\left\{1+\frac{\rho\, g}{N_t}\left(\det(\mathbf{H}\mathbf{H}^{\dagger}\mathbf{Q}^{-1})\right)^{1/N_r}\right\}\\ &= N_r\,\log_2\left\{1+\frac{\rho\, g}{N_t}\left(\frac{\det(\mathbf{H}\mathbf{H}^{\dagger})}{\det(\mathbf{Q})}\right)^{1/N_r}\right\}. \qquad (6.15)\end{aligned}$$

The distribution $f_X(x)$ of the determinant of a Wishart matrix, $X = \det(\mathbf{H}\mathbf{H}^{\dagger})$, is derived in [102] and [104]. Based on this, the distribution of $Y = \det(\mathbf{Q})$, denoted as $f_Y(y)$, can also be easily derived. Hence, a lower bound on the ergodic capacity is given as

$$\mathcal{C}_{erg} = \int_0^{\infty}\int_0^{\infty} N_r \log_2\left[1+\frac{\rho\, g}{N_t}\left(\frac{x}{y}\right)^{1/N_r}\right] f_X(x)\, f_Y(y)\, dx\, dy. \qquad (6.16)$$

Furthermore, the outage probability of the MIMO interference channel may be upper bounded by

$$\begin{aligned}P_{out}^{ub} &= \Pr\left[\frac{\det(\mathbf{H}\mathbf{H}^{\dagger})}{\det(\mathbf{Q})} < \left(\frac{N_t}{\rho g}(2^{R_{req}}-1)\right)^{N_r}\right]\\ &= \int_0^{\infty}\Pr\left[X < \left(\frac{N_t}{\rho g}(2^{R_{req}}-1)\right)^{N_r} Y \mid Y=y\right]\cdot f_Y(y)dy \qquad (6.17)\\ &= \int_0^{\infty} 1-\sum_{k=0}^{|N_t-N_r|}\left(\prod_{n=1}^{N_t-1}\frac{(N_r-n-k)!}{(N_r-n)!}\right)\frac{(\varepsilon y)^{kN_t}}{k!}e^{-\frac{(N_r-N_t-k)!}{(N_r-1-k)!}(\varepsilon y)^{N_t}} f_Y(y)dy,\end{aligned}$$

where $\varepsilon = \frac{N_t}{\rho\, g}(2^{N_r R_{req}/\min(N_t,N_r)}-1)$.

When there is no interference in the network, i.e., when $g_{12}=0$, the determinant bound is tight around the ergodic capacity and outage probability. An upper bound to the outage probability when interference is absent is derived in closed form to be

$$P_{out}^{ub}\,|_{(g_{12}=0)} = 1-\sum_{k=0}^{|N_t-N_r|}\left(\prod_{n=1}^{N_t-1}\frac{(N_r-n-k)!}{(N_r-n)!}\right)\frac{a^{k\,N_t}}{k!}e^{-\frac{(N_r-N_t-k)!}{(N_r-1-k)!}a^{N_t}} \qquad (6.18)$$

where $a = \frac{N_t}{\rho\, g}(2^{N_r R_{req}/\min(N_t,N_r)}-1)$.

Since Eq. (6.18) is derived based on the distribution of $\det(\mathbf{H}\mathbf{H}^{\dagger})$ and not $\det(\mathbf{H}\mathbf{H}^{\dagger}\mathbf{Q}^{-1})$, it loses its validity as the interference channel coefficient g_{12} increases. Then we use the integral expression of Eq. (6.17).

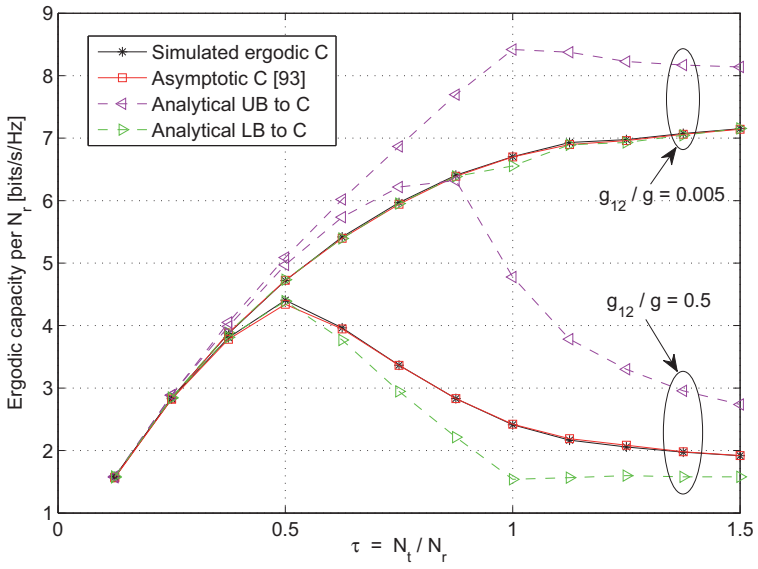

Figure 6.3: Ergodic link capacity, along with derived lower and upper bounds, of a 2 link MIMO channel, as a function of $\tau = N_t/N_r$ with $N_r = 8$.

6.1.2.4 Numerical Results for 2 Link MIMO Networks

In Figure 6.3, the lower and upper bounds to the ergodic capacity of the MIMO interference channel are plotted along with Monte Carlo simulation results, as a function of $\tau = N_t/N_r$, for $N_r = 8$. Firstly, we observe from the figure that the determinant bound is a reasonable lower bound, although it loses its tightness as g_{12}/g increases. The trace bound[2], on the other hand, fails to give a decent upper bound, especially for higher values of g_{12}/g.

Furthermore, we observe that for $\tau \leq 1/2$, the capacity increases with τ, because the total number of transmit antennas in the network ($2 \times N_t$) does not exceed the number of receive antennas, N_r, at each receiver. Hence, the receiver approaches capacity by completely suppressing the interfering signal while simultaneously detecting the desired signal. Furthermore, as noted in [93], as the SNR grows, the capacity becomes independent of the SIR for $\tau \leq 1/2$. For $1/2 < \tau \leq 1$, the number of receive antennas is less than the combined number of desired and interfering antennas, and the receiver must hence compromise between assigning its degrees of

[2]This is found through Monte Carlo simulations for the distribution of $\mathrm{tr}(\mathbf{H}\mathbf{H}^{\dagger}\mathbf{Q}^{-1})$.

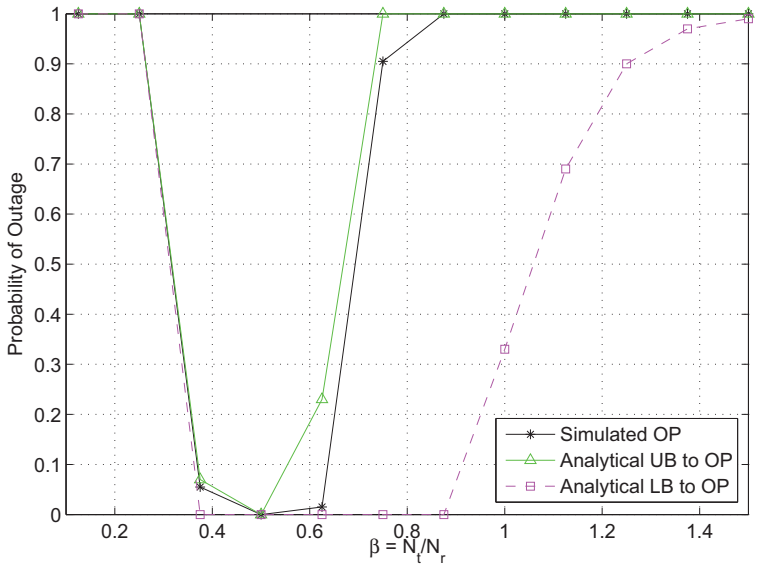

Figure 6.4: Outage probability of a 2 link MIMO interference channel for $g_{12}/g = 0.5$ and $R_{req} = 3$, as a function of $\tau = N_t/N_r$.

freedom to interference suppression and to signal detection. This means that $\tau^{opt} = 1/2$. For $\tau > 1$, the number of interfering antennas exceeds N_r, meaning that the receiver can no longer suppress the totality of the interference, and the capacity is thus determined mainly by the SIR. Interestingly, it is observed in [93] that when $\kappa > 2$, we still have $\tau_{opt} = 1/2$.

In Figure 6.4, the outage probability of the MIMO interference channel is plotted as a function of $\tau = N_t/N_r$, when the interference is strong. As expected, the outage probability is minimized when $N_t = N_r/2$. The determinant upper bound works reasonably, while the trace lower bound is clearly too loose to give a correct picture of the network performance. This holds true also for other values of g_{12}/g. When the interference is weak, the outage probability decreases abruptly in the same manner as the left part of the curve in Figure 6.4, and it continues reducing monotonically with τ. In this case, the determinant bound is extremely tight around the simulation results, while the trace bound still fails to give a decent representation of the outage probability.

6.1.3 MISO Interference Channels

As deriving the exact expressions for the ergodic capacity and outage probability of MIMO interference channels appeared to be an intractable task, we could only derive bounds for these metrics. In order to obtain an exact picture of the performance of a multi-antenna interference channel, we consider in this section, the particular case of a MISO channel. That is, we assign only a single antenna to the receiver (i.e., $N_r = 1$) in our network, while the transmitter still has $N_t < \infty$ antennas. That means that the channel matrices $\mathbf{H} = \mathbf{H}_{ii}$ and $\mathbf{H}_{ij}$ are reduced to $1 \times N_t$ channel vectors $\mathbf{h} = \mathbf{h}_{ii}$ and $\mathbf{h}_{ij}$.

Also, we return to a $\kappa \geq 2$ link network (we still let g_{ii} be equal for all i, and denote it by g). The ergodic capacity and outage probability of link i is then given by

$$\mathcal{C}_{erg,i} = \mathbb{E}\left[\log_2\left(1+\frac{\rho\, g}{N_t}\frac{\mathbf{h}\mathbf{h}^\dagger}{\eta+\frac{1}{N_t}\sum_{j\neq i}^{\kappa}\rho_j\, g_{ij}\mathbf{h}_{ij}\mathbf{h}_{ij}^\dagger}\right)\right] \tag{6.19}$$

$$P_{out,i} = \Pr\left\{\log_2\left(1+\frac{\rho\, g}{N_t}\frac{\mathbf{h}\mathbf{h}^\dagger}{\eta+\frac{1}{N_t}\sum_{j\neq i}^{\kappa}\rho_j\, g_{ij}\mathbf{h}_{ij}\mathbf{h}_{ij}^\dagger}\right) < R_{req}\right\}, \tag{6.20}$$

where the expectation is taken with respect to the entries of $\mathbf{h}$ and $\mathbf{h}_{ij}$. In the following, we derive exact expressions for these metrics in a κ link MISO interference channel.

6.1.3.1 Ergodic Capacity

To find $\mathcal{C}_{erg}$, we first derive the distribution of the capacity. Consider a strictly interference-limited network and thus set $\eta = 0$. Since the elements of $\mathbf{h}$ and $\mathbf{h}_{ij}$ are complex Gaussian random variables, it follows that $|h_{1n}|$ is Rayleigh distributed. Thus, we have that $|\mathbf{h}|^2 = \sum_{n=1}^{N_t}|h_{1n}|^2$ is χ^2_k-distributed with $k = 2N_t$ degrees of freedom. The pdf and cdf of a χ^2_k-distributed random variable X are, respectively,

$$f_X(x) = \frac{\left(\frac{1}{2}\right)^{k/2}x^{k/2-1}e^{-x/2}}{\Gamma(k/2)} \quad \text{for } x>0, \tag{6.21}$$

$$F_X(z) = \frac{\gamma(k/2,z/2)}{\Gamma(N_t)} = \frac{1}{\Gamma(k/2)}\int_0^{z/2} t^{k/2-1}e^{-t}dt, \tag{6.22}$$

where $\Gamma(k/2) = (\frac{k}{2}-1)!$.

The interference term is a weighted sum (with weights $\rho_j g_{ij}$) of $\chi^2_{2N_t}$-distributed random variables. The distribution of the weighted sum of

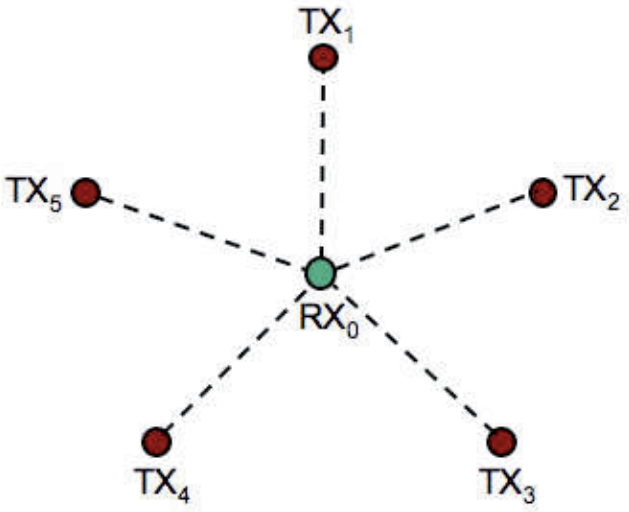

Figure 6.5: Example of a star configuration where the distances between a given receiver and its interferers are equal.

Chi-squared random variables is derived in [105] in the form of a Laguerre series expansion, and the series was approximated in [106]. Due to the complexity of this expression, in the following, we will focus on a particular case of our MISO network. Specifically, we assume a symmetric network where the powers ρ_j and average interference channel gains g_{ij} are equal for all $j \neq i$, where i denotes the link of interest. These are denoted by ρ_I and g_I, respectively. Such an assumption is valid for networks where the product of the path loss attenuation and the variance of the fading is constant for all links. One example of such a network is a symmetric star configuration, as shown in Figure 6.5, where the distance between a node under consideration to all of its interferers is the same. Consequently, our results can only act as pointers to the behavior of more general MISO networks.

By allowing $\rho_j = \rho_I$ and $g_{ij} = g_I$ for all $j \neq i$, our interference terms becomes a (non-weighted) sum of Chi-squared random variables. Now we have that the addition of Chi-squared random variables is also Chi-squared. That is, the interference term, $\sum_{j\neq i}^{\kappa} |\mathbf{h}_{ij}|^2$, is $\chi^2_{2N_t(\kappa-1)}$-distributed.

Denote $X = |\mathbf{h}|^2$ and $Y = \sum_{j\neq i}^{\kappa} |\mathbf{h}_{ij}|^2$. This yields $\mathcal{C} = \log_2\left(1 + \frac{\rho g X}{\rho_I g_I Y}\right)$.

Using that $\frac{dx}{dc} = \frac{\rho_I g_I}{\rho g} y\, 2^c \ln(2)$, we have

$$\begin{aligned} f_C(c) &= \int_0^\infty f_{C|Y}(c|y)\; f_Y(y)\, dy \\ &= \int_0^\infty f_X(x)\, f_Y(y)\, \frac{dx}{dc}\, dy. \\ &= \frac{\rho_I\, g_I}{\rho\, g} \ln(2)\; 2^c \int_0^\infty y \frac{\left(y(2^c-1)\frac{\rho_I g_I}{\rho g}\right)^{N_t-1} e^{-(y(2^c-1)\,\frac{\rho_I g_I}{\rho g})/2}}{2^{N_t}(N_t-1)!} \\ &\qquad \times \frac{y^{N_t(\kappa-1)-1} e^{-y/2}}{2^{N_t(\kappa-1)}(N_t(\kappa-1)-1)!}\, dy \\ &= k_c \int_0^\infty y^{N_t\kappa-1} e^{-y\frac{1+(2^c-1)\rho_I g_I/\rho g}{2}}\, dy, \end{aligned} \tag{6.23}$$

where $k_c = \left(\frac{\rho_I\, g_I}{\rho\, g}\right)^{N_t} \frac{\ln(2)\, 2^c\, (2^c-1)^{N_t-1}}{2^{N_t}(N_t-1)!\, 2^{N_t(\kappa-1)}\, (N_t(\kappa-1)-1)!}$. Now using the result $\int_0^\infty y^\nu\, e^{-\mu y} dy = \frac{\Gamma(\nu+1)}{\mu^{\nu+1}}$, we can solve the integral, and thus we arrive at the following theorem.

Theorem 6.1

The distribution of the capacity of a symmetric κ link MISO network is given by

$$\begin{aligned} f_C(c) &= \left(\frac{\rho_I\, g_I}{\rho\, g}\right)^{N_t} \ln(2)\, 2^c\, (2^c-1)^{N_t-1} \frac{(N_t\kappa-1)!}{(N_t-1)!(N_t(\kappa-1)-1)!} \\ &\quad \times \left(\frac{1}{1+(2^c-1)\,\rho_I\, g_I/\rho\, g}\right)^{N_t\kappa}. \end{aligned} \tag{6.24}$$

Using the distribution of the capacity as given by Eq. (6.24), we can easily derive the ergodic capacity as

$$\begin{aligned} \mathcal{C}_{erg} &= \int_0^\infty c \left(\frac{\rho_I\, g_I}{\rho\, g}\right)^{N_t} \ln(2) 2^c (2^c-1)^{N_t-1} \frac{(N_t\kappa-1)!}{(N_t-1)!(N_t(\kappa-1)-1)!} \\ &\qquad \times \left(\frac{1}{1+(2^c-1)\,\rho_I\, g_I/\rho\, g}\right)^{N_t\kappa} dc, \end{aligned} \tag{6.25}$$

which remains in integral form as its closed form expression (using MAPLE) is too long and involved to present here.

6.1.3.2 Outage Probability

Based on Eq. (6.20), with $X = |\mathbf{h}|^2$ and $Y = \sum_{j \neq i}^{\kappa} |\mathbf{h}_{ij}|^2$, the outage probability of a κ link MISO interference channel may be expressed as

$$P_{out} = \int_0^\infty \Pr\left[|\mathbf{h}|^2 < \frac{\rho_I g_I}{\rho g}\left(2^{R_{req}} - 1\right) Y \mid Y = y\right] f_Y(y)\, dy.$$

Let $\varepsilon = \frac{\rho_I g_I}{\rho g}(2^{R_{req}} - 1)$. The outage probability is then derived as

$$P_{out} = \int_0^\infty \int_0^{\varepsilon y/2} x^{N_t-1} e^{-x} dx \, \frac{y^{N_t(\kappa-1)-1} e^{-y/2}}{2^{N_t(\kappa-1)}\Gamma(N_t)\,\Gamma(N_t(\kappa-1))}\, dy. \quad (6.26)$$

Expanding the inner integral of Eq. (6.26) into a series, as follows

$$\begin{aligned}
&\int_0^{\varepsilon y/2} x^{N_t-1} e^{-x} dx \\
&= -e^{-\frac{\varepsilon y}{2}}\left[\left(\frac{\varepsilon y}{2}\right)^{N_t-1} + \sum_{k=1}^{N_t-1}(N_t-1)(N_t-2)\cdots(N_t-k)\left(\frac{\varepsilon y}{2}\right)^{N_t-k-1}\right] \\
&= -e^{-\frac{\varepsilon y}{2}}\sum_{k=0}^{N_t-1}\left[\frac{(N_t-1)!}{(N_t-k-1)!}\left(\frac{\varepsilon y}{2}\right)^{N_t-k-1}\right], \quad (6.27)
\end{aligned}$$

results in

$$P_{out} = \int_0^\infty -\frac{e^{-y(1+\varepsilon)/2}}{2^{N_t(\kappa-1)}(N_t(\kappa-1)-1)!}\sum_{k=0}^{N_t-1}\frac{y^{N_t\kappa-k-2}}{(N_t-k-1)!}\left(\frac{\varepsilon}{2}\right)^{N_t-k-1} dy. \quad (6.28)$$

Finally by using the result $\int_0^\infty y^\nu e^{-\mu y} dy = \frac{\Gamma(\nu+1)}{\mu^{\nu+1}}$, we arrive at the following theorem.

Theorem 6.2
The outage probability of a symmetric κ link MISO network is given by

$$P_{out} = \sum_{k=0}^{N_t-1}\frac{(N_t\kappa-k-2)!}{(N_t\kappa-N_t-1)!(N_t-k-1)!}\frac{\varepsilon^{N_t-k-1}}{(1+\varepsilon)^{N_t\kappa-k-1}}, \quad (6.29)$$

where $\varepsilon = \frac{\rho_I g_I}{\rho g}(2^{R_{req}} - 1)$.

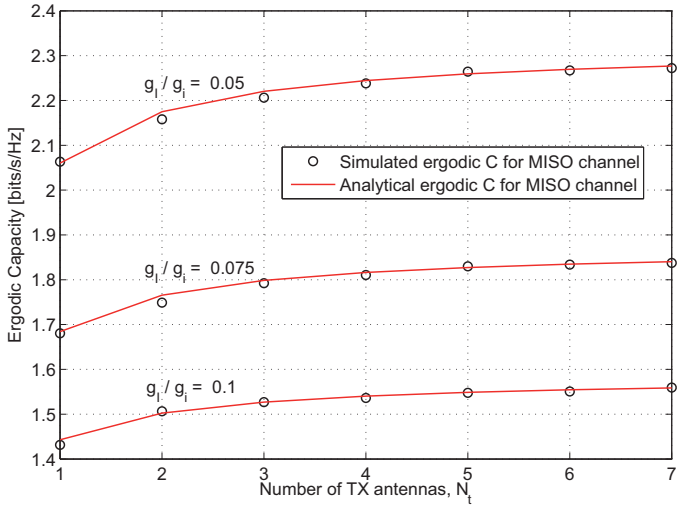

Figure 6.6: Ergodic capacity of a $\kappa = 5$ link MISO interference channel as a function of N_t, both for different channel gain ratios.

6.1.3.3 Numerical Results for MISO Channels

Figures 6.6 and 6.7 show the ergodic capacity and the outage probability of the κ link MISO channel, respectively. The analytical results follow the simulations tightly, confirming our derived expressions. Clearly, as the ratio of the interference channel gain over the direct channel gain, g_I/g, increases, the ergodic capacity decreases. Nevertheless, the ergodic capacity increases with the number of transmit antennas, N_t, due to the diversity gain, i.e., the reduced randomness in the channel coefficients.

The effect of the average channel gains on the outage probability is the reverse; when the amount of interference increases, so does the outage probability. However, we note an interesting behavior in Figure 6.7. Depending on the channel conditions, the outage probability behaves differently with respect to N_t. When the interference is high, the outage probability increases with N_t, while for low interference channel gains, it decreases. And for a certain channel condition, it remains approximately constant, no matter how many transmit antennas are used.

To better understand why this is the case, we note that the increase in N_t decreases the randomness in the received signal. When $N_t \to \infty$, the expected capacity per link is: $\mathcal{C}_\infty = \log_2\left(1 + \frac{\rho g}{(\kappa-1)\rho_I g_I}\right)$. For $N_t < \infty$, the

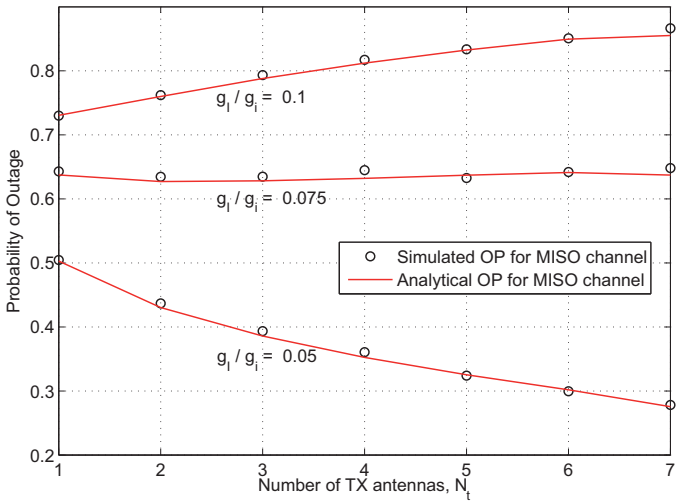

Figure 6.7: Outage probability of a $\kappa = 5$ link MISO interference channel as a function of N_t, both for different channel gain ratios.

capacity has a distribution around the mean $\mathcal{C}_\infty$, as shown in Figure 6.8. As N_t increases, the standard deviation shrinks, making the probability distribution more concentrated around $\mathcal{C}_\infty$. Hence, depending on whether the requested transmission rate R_{req} is greater or smaller than $\mathcal{C}_\infty$, the outage probability increases or decreases (respectively) with N_t. This is elaborated in the next subsection.

6.1.4 Optimal Use of Antennas in MISO Channels

In the previous sections, we observed different behaviors in the outage probability of MIMO interference channels as a function of N_t depending on the network parameter values. To find out for what ranges of the system parameters the outage probability increases or decreases as a function of N_t, we evaluate the following discrete differential

$$\begin{aligned}\Delta P_{out} &= P_{out}(N_t+1) - P_{out}(N_t) \qquad (6.30)\\ &= \sum_{k=0}^{N_t} \frac{((N_t+1)\kappa - k - 2)!}{((N_t+1)\kappa - N_t - 2)!(N_t-k)!} \cdot \frac{\varepsilon^{N_t-k}}{(1+\varepsilon)^{(N_t+1)\kappa-k-1}} \\ &\quad - \sum_{k=0}^{N_t-1} \frac{(N_t\kappa - k - 2)!}{(N_t\kappa - N_t - 1)!(N_t-k-1)!} \cdot \frac{\varepsilon^{N_t-k-1}}{(1+\varepsilon)^{N_t\kappa-k-1}},\end{aligned}$$

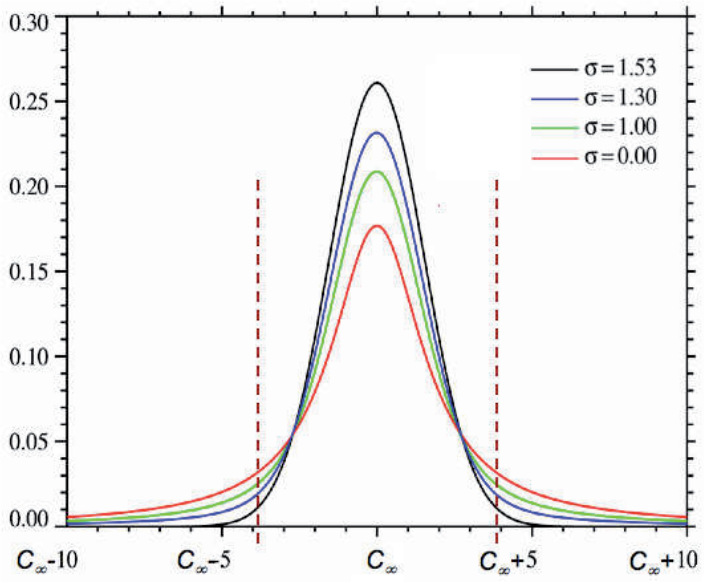

Figure 6.8: An example for the distribution of the capacity.

where $\varepsilon = \frac{\rho_I g_I}{\rho g}\left(2^{R_{req}} - 1\right)$. The optimal value of ε, denoted ε_t,[3] is derived by setting the difference $\Delta P_{out} = 0$. This yields

$$\varepsilon_t^{-\kappa+1}\frac{(N_t\kappa - N_t - 1)!}{(N_t\kappa - N_t + \kappa - 2)!}\sum_{k=0}^{N_t}\left(\frac{\varepsilon_t}{1+\varepsilon_t}\right)^{\kappa-k-1}\frac{(N_t\kappa + \kappa - k - 2)!}{(N_t - k)!} = \sum_{k=0}^{N_t-1}\left(\frac{\varepsilon_t}{1+\varepsilon_t}\right)^{-k-1}\frac{(N_t\kappa - k - 2)!}{(N_t - k - 1)!}. \quad (6.31)$$

Since we have that P_{out} is monotonically increasing or decreasing as a function of N_t, we may insert any value of N_t in Eq. (6.31) in order to find the optimal number of transmit antennas to employ. We chose $N_t = 1$, which results in

$$\frac{(\kappa-2)!}{(2\kappa-3)!}\left[(1+\varepsilon_t)^{1-\kappa}(2\kappa-2)! + \frac{(1+\varepsilon_t)^{2-\kappa}(2\kappa-3)!}{\varepsilon_t}\right] = \left(1+\frac{1}{\varepsilon_t}\right)(\kappa-2)! \quad (6.32)$$

After some manipulations, we arrive at the following theorem.

[3]The subscript t in ε_t specifies that this is a $t$hreshold value.

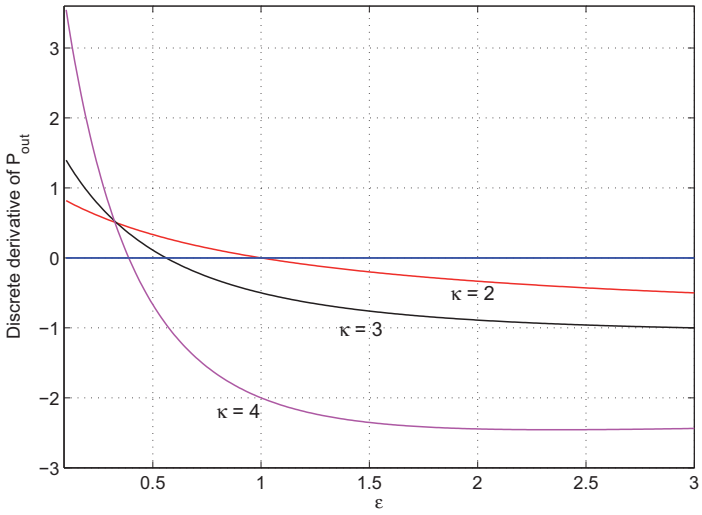

Figure 6.9: Derivative of the outage probability of a $\kappa = 2, 3, 4$ link MISO network to find ε_t.

Theorem 6.3
In an uncoordinated κ link channel with $\varepsilon = \frac{\rho_I g_I}{\rho g}(2^{R_{req}} - 1)$ and symmetric Gaussian random uncorrelated channels, and where the threshold ε_t is the solution to

$$(1+\varepsilon_t)^{1-\kappa}(2\kappa - 2) + \frac{(1+\varepsilon_t)^{2-\kappa}}{\varepsilon_t} = 1 + \frac{1}{\varepsilon_t}, \tag{6.33}$$

we have that

- *if $\varepsilon \leq \varepsilon_t$, the maximum number of transmit antennas available should be applied, i.e., $N_t^{opt} = N_t^{max}$.*
- *if $\varepsilon > \varepsilon_t$, the SISO channel yields the optimal performance, i.e., $N_t^{opt} = 1$.*

Figure 6.9 shows the discrete derivative of the outage probability with respect to N_t, as a function of ε. The point where the curve equals 0, is the solution to Eq. (6.33), ε_t. As seen from the figure, ε_t decreases as the number of links in the network, κ, increases. This means that the optimal strategy to minimize the outage probability is for higher κ more often to apply a SISO channel.

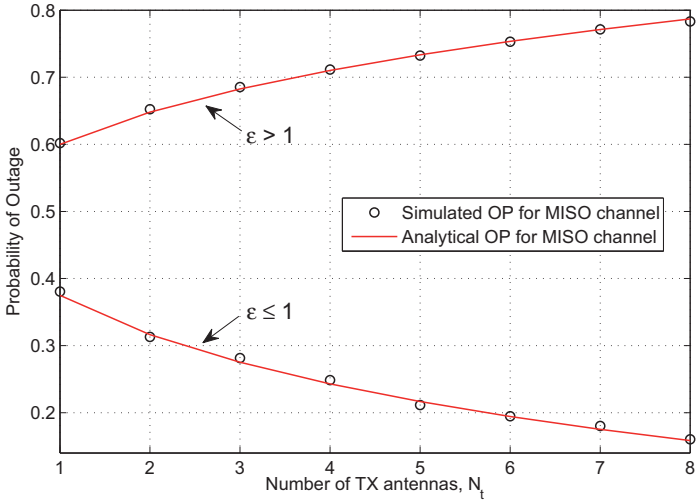

Figure 6.10: Outage probability of a 2 link MISO interference channel as a function of N_t, both for $\varepsilon = \frac{\rho_I g_I}{\rho g}(2^{R_{req}} - 1) \leq 1$ and $\varepsilon > 1$.

At the end of Subsection 6.1.3.3, we noted that when $R_{req} > \mathcal{C}_\infty = \log_2\left(1 + \frac{\rho g}{(\kappa-1)\rho_I g_I}\right)$, the outage probability increases with N_t. Rearranging this expression yields that it is optimal to apply $N_t = 1$ antenna when $\varepsilon > \frac{1}{\kappa-1}$. In fact, we observe that the value of ε_t found as the solution to Eq. (6.33) may be approximated by $\tilde{\varepsilon}_t = \frac{1}{\kappa-1}$. This can be confirmed by inserting $\tilde{\varepsilon}_t$ into Eq. (6.33) and comparing both sides of the equality sign. The lower κ is, the more exact is the approximation $\varepsilon \approx \tilde{\varepsilon}_t$.

For the particular case of a $\kappa = 2$ link channel, we obtain from Eq. (6.33) that $\varepsilon_t = 1$. This yields the following corollary.

Corollary 1 *In an uncoordinated 2 link MISO system with symmetric random uncorrelated channels, we have that*

- *if* $\frac{\rho_I g_I}{\rho g}(2^{R_{req}} - 1) \leq 1$, *the maximum number of transmit antennas available should be applied, i.e.,* $N_t^{opt} = N_t^{max}$.
- *if* $\frac{\rho_I g_I}{\rho g}(2^{R_{req}} - 1) > 1$, *we have that* $N_t^{opt} = 1$.

Note that the condition $\varepsilon \lesseqgtr 1$ corresponds to $R_{req} \lesseqgtr \log_2\left(1 + \frac{\rho g}{\rho_I g_I}\right)$, where the right hand side is the expected capacity per link when $N_t \to \infty$.

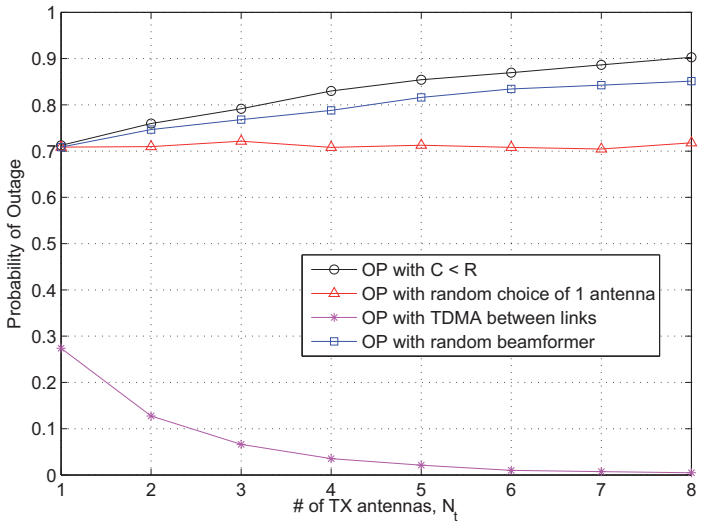

Figure 6.11: Outage probability of a 2 link MISO interference channel when $\varepsilon > 1$, with various techniques applied.

The behavior of the outage probability of a κ link MISO channel was shown in Figure 6.7, while that of a 2 link MISO channel is illustrated in Figure 6.10. As seen from the curves, when $\varepsilon = \frac{\rho_I g_I}{\rho g}(2^{R_{req}} - 1) < 1$, the outage probability decreases with N_t, while for $\varepsilon > 1$, it increases. This is because when N_t increases, the destruction from the reduction in randomness in the interfering signal is greater than the diversity improvement that a higher N_t provides in the desired signal. Hence, for $\varepsilon > 1$, we have that the SISO channel yields the best performance.

The conclusion of $N_t^{opt} = 1$ when $\varepsilon > 1$ indicates an inefficient use of the transmit antennas. Hence, we must employ additional techniques in order to decrease the outage probability as a function of N_t. Firstly, note that when the interference is strong, i.e., $g_I > g$, traditional interference cancellation techniques can be applied [12], making the network interference-free. This leaves us with the region when $\frac{\rho g}{\rho_I(2^{R_{req}}-1)} < g_I \leq g$. Since the outage probability increases as a function of N_t, it means that increasing randomness when $\varepsilon > 1$ is in fact beneficial. Hence, by introducing a random beamformer at the transmitters, we can improve the network performance, as seen from Figure 6.11. However, although at a lower rate, the outage probability still increases with N_t, and our conclusion on $N_t^{opt} = 1$ remains

intact. Also randomly choosing one single transmit antenna does not add to the randomness and the outage probability is not reduced below the SISO channel outage probability.

6.1.4.1 Introducing TDMA

Realizing that we cannot add more randomness than what is inherent in a SISO channel, we introduce time division multiple access (TDMA) into our $\kappa = 2$ link MISO system. This is done by dividing each time frame in two, and let each link transmit over *one* of these subframes, thus precluding interference between the links. Clearly, the division of the time frame also reduces the channel capacity by a factor of 2. The ergodic capacity and outage probability (in the presence of noise) then becomes

$$\begin{aligned} \mathcal{C}_{erg} &= \frac{1}{2}\,\mathbb{E}\left[\log_2\left(1+\frac{\rho\, g}{N_t}\,\frac{|\mathbf{h}|^2}{\eta}\right)\right] && (6.34)\\ P_{out} &= \frac{1}{\Gamma(N_t)}\int_0^{\varepsilon_{tdma}x/2} x^{N_t-1}e^{-x}dx. && (6.35)\\ &= -\frac{e^{-\frac{\varepsilon_{tdma}}{2}}}{(N_t-1)!}\sum_{k=0}^{N_t-1}\frac{1}{(N_t-k-1)!}\left(\frac{\varepsilon_{tdma}}{2}\right)^{N_t-k-1}, \end{aligned}$$

where $\varepsilon_{tdma} = \frac{\eta N_t}{\rho\, g}\left(2^{2R_{req}}-1\right)$.

TDMA improves the outage performance of our 2 link MISO network considerably, as seen in Figure 6.11. This is because the channel of each link becomes interference-free and the decrease in randomness in the desired signal power yields a better performance. As N_t increases, TDMA becomes more beneficial, as the figure confirms. TDMA can also be applied for the case when $g_I > g$, if the system has no interference cancellation abilities.

Note that we obtain such great improvement with TDMA simply because we here assumed only 2 links in the system. As the number of links increases, dividing the time slot between all users could become more hurtful than the amount of improvement it provides in the received signal. Comparing the outage probability expressions of the MISO channel with and without TDMA, i.e.,

$$\begin{aligned} P_{out}^{MISO} &= \Pr\left[|\mathbf{h}|^2 < \frac{\rho_I\, g_I}{\rho\, g}(2^{R_{req}}-1)\sum_{j\neq i}^{\kappa}|\mathbf{h}_{ij}|^2\right] && (6.36)\\ P_{out}^{TDMA} &= \Pr\left[|\mathbf{h}|^2 < \frac{\eta}{\rho\, g}(2^{2R_{req}}-1)\right], && (6.37) \end{aligned}$$

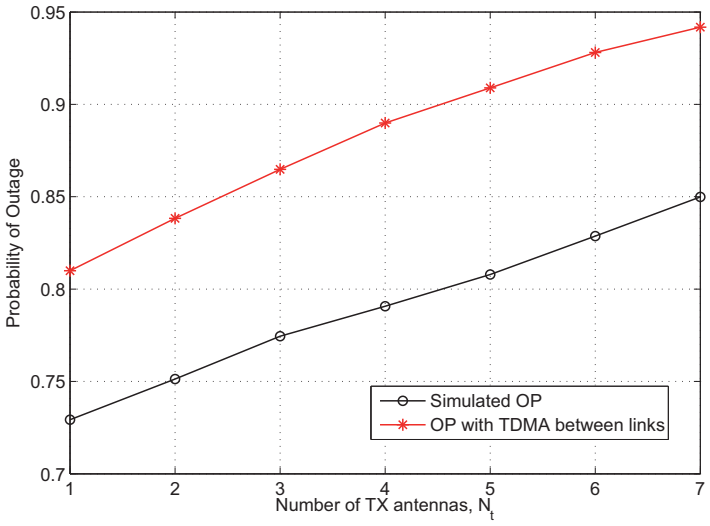

Figure 6.12: Outage probability of a $\kappa = 6$ link MISO interference channel with $g_I/g = 0.08$, where TDMA does not improve the performance.

we may conclude that the addition of TDMA is advantageous in terms of outage probability in a κ link channel when the following condition holds true:

$$\frac{2^{\kappa R_{req}} - 1}{2^{R_{req}} - 1} \frac{\eta}{\rho_I g_I} < \sum_{j \neq i}^{\kappa} |\mathbf{h}_{ij}|^2. \tag{6.38}$$

An example of the case where TDMA does not provide any improvement in the outage probability is a network with $\kappa = 6$ links and $g_I/g = 0.08$, as shown in Figure 6.12. In terms of instantaneous capacity, TDMA is beneficial when

$$\sqrt{1 + \frac{\rho g |\mathbf{h}|^2}{\rho_I g_I \sum_{j \neq i}^{\kappa} |\mathbf{h}_{ij}|^2}} < 1 + \frac{\rho g |\mathbf{h}|^2}{\eta}. \tag{6.39}$$

Note that these results are not design guidelines, due to the fact that transmitters do not have instantaneous CSI and can thus not change back and forth between TDMA and non-TDMA from one time slot to another. However, if the conditions in Eqs. (6.38) and (6.39) are observed (by the system designer, or a centralized unit) to be valid over *many channel instances*, then it can be concluded that TDMA should be employed in the network.

6.2 Use of CSI to Improve System Performance

In Section 6.2, we were mainly concerned with characterizing and optimizing the average performance of a κ link MIMO network through appropriate use of antennas. Due to the absence of CSI, transmitters could not perform precoding (except for random beamforming, which was shown for some network conditions to improve the performance of a MISO channel slightly), and the question of interest was thus concerned with *how many* antennas that should be used in order to improve the performance of the MIMO and MISO interference channels. In this section, on the other hand, we assume that each node (transmitters and receivers alike) have access to partial CSI, and we investigate how the performance of the MIMO interference channels can be improved. We define partial CSI at node i as the access to full information about all channels directly connected to node i.

Much work has been done on the use of antennas in MIMO channels with CSIT using beamforming techniques [2–4]. A newly proposed interference management technique that has recently gained considerable popularity is *interference alignment* [1; 8]. In this scheme, precoding and postcoding vectors are applied to align the interference signals in the null space of the desired signals, in order to completely cancel the interference between users. This scheme was shown to achieve significant improvement in the sum rate of MIMO networks, thus providing a linear increase of the sum rate for increasing SNR values.

Different modifications of the interference alignment scheme exists in the literature. In [107; 108], the authors investigate some of these, and establish that there is a compromise between the beamforming gain at the intended receiver (egoistic approach) and the mitigation of interference created towards other receivers (altruistic approach). An optimal balance between the egoistic and altruistic games is derived in order to maximize the network sum rate. In [98], the above beamforming scheme was extended to allow for multiple streams to be transmitted, and we introduced a heuristic power control scheme to improve the sum rate performance of the network for high SNR values. This section serves as an extension to [98], in that an understanding is established on the feasibility of interference alignment, and the power control algorithm is further improved to provide a higher sum rate.

6.2.1 System Model

The network model we consider resembles that of Section 6.1, with the difference that now also the transmitters have partial CSI. That is, our ad hoc

network consists of κ links distributed randomly in a restricted area, communicating simultaneously. Each transmitter and receiver have N_t transmit antennas and N_r receive antennas, respectively. The channel from transmitter j to receiver i, is $\mathbf{G}_{ij} = \sqrt{g_{ij}}\,\mathbf{H}_{ij}$. Each transmitter is assumed to transmit one stream of data, although the results can be easily extended to the multi-stream case [98]. The transmit power of user j is $\rho_j = \{0, \rho\}$, where ρ is assumed to be the same for all users. This means that either a sender is active and transmitting with maximum power ρ, or it is not transmitting at all.

As mentioned above, we assume that each node has full knowledge about the channel coefficients directly connected to it. E.g., transmitter and receiver i know the channels $\mathbf{G}_{ij}$, $\forall j$. Whether such an assumption is realistic in a real ad hoc network depends on many factors. Firstly, the transmitters or receivers must have the ability to perform channel estimation. If the transmitter does not have this possibility, the receiver must send its channel estimation over to its transmitter, and this process must have low enough latency such that the channel does not change in the duration of the process. Secondly, the channel must not change rapidly, i.e., full CSI is only valid in slow fading scenarios with low mobility of nodes (which we assume in this chapter, as opposed to the preceding ones). Finally, the noise in the channel must be small enough such that the estimation of the channel gains becomes accurate. If the channel noise is too high, the time interval needed to cancel it out (e.g., using a Wiener filter) prior to the channel estimation, will be too long and the channel conditions could change in the meantime. Note that, because of the question on practicality, most of the work in this section is more of conceptual value, simply having the aim of bringing a new idea to the table.

Due to the assumption on CSIT, each transmitter can now perform precoding. The transmit beamforming vector of transmitter i is denoted $\mathbf{w}_i \in \mathbb{C}^{N_t \times 1}$ and the receive beamforming vector of receiver i is $\mathbf{v}_i \in \mathbb{C}^{N_r \times 1}$. As in several prior contributions dealing with coordination on the interference channels, we assume linear precoding (beamforming) [2; 109–112]. With a noise power of η, the received SINR of receiver i may be expressed as

$$\mathrm{SINR}_i \;=\; \frac{\rho_i \left|\mathbf{v}_i^{\dagger}\mathbf{G}_{ii}\mathbf{w}_i\right|^2}{\sum_{j\in\mathbb{I}_i}\rho_j \left|\mathbf{v}_i^{\dagger}\mathbf{G}_{ij}\mathbf{w}_j\right|^2 + \eta}\,, \tag{6.40}$$

where ρ_i is the transmit power of transmitter i, and $\mathbb{I}_i$ is the set of interferers for receiver i.

At the receivers, we assume that maximum SINR beamforming is performed. That is, the receive beamformer of receiver i, $\mathbf{v}_i$, is selected so as to

maximize their own SINR [24]. This is classically given by[4]

$$\mathbf{v}_i^{\kappa} = \frac{\mathbf{C}_i^{\kappa^{-1}}\mathbf{G}_{ii}\mathbf{w}_i^{\kappa}}{|\mathbf{C}_i^{\kappa^{-1}}\mathbf{G}_{ii}\mathbf{w}_i^{\kappa}|}, \tag{6.41}$$

where $\mathbf{C}_i^{\kappa}$ is the covariance matrix of the detected interference plus noise at receiver i;

$$\mathbf{C}_i^{\kappa} = \sum_{j \in \mathbb{I}_i} \rho_j \mathbf{G}_{ij}\mathbf{w}_j^{\kappa}\mathbf{w}_j^{\kappa^{\dagger}}\mathbf{G}_{ij}^{\dagger} + \eta\,\mathbf{I}. \tag{6.42}$$

The noise term captures thermal noise effects in addition to any interference originating from the rest of the network, i.e., from transmitters located beyond the coordination cluster. We assume that the out of cluster interference to be white due to the large number of transmitters in the network and the relatively small cluster sizes, meaning that η is modeled as AWGN.

6.2.2 Interference Alignment and Feasibility

At the transmitters, many different schemes can be applied, where interference alignment is seen to have the potential to provide the best system performance in terms of sum rate. Recently, various interference alignment schemes have been proposed and shown to bring about significant performance gains [2–4; 107]. The main idea of interference alignment is to steer the interference coming from other transmitters in the network to superpose into a subspace of the received signal space at each receiver. This is shown in Figure 6.13 for a 3 link interference channel, and a more visual and simplified illustration is provided in Figure 6.14 for a 2 link interference channel. With interference alignment, the subspace over which the desired signal is transmitted has the potential of being completely interference-free. When this is the case, the interference alignment is said to be *feasible*.

When interference alignment is feasible, the sum rate of the network at high SNR values increases linearly with the SNR. When interference alignment is *infeasible*, on the other hand, the sum rate saturates to a constant as the SNR increases. Thus, in order to obtain the highest possible sum rate with interference alignment, it is essential to find the channel state for which it is beneficial to drive the interference alignment from infeasibility to feasibility.

A necessary condition for interference alignment among κ links to be feasible is that $\kappa \leq N_t + N_r - 1$. This is obtained by setting up $\kappa(\kappa - 1)$

[4]The superscript κ indicates that the beamforming vectors are obtained in a κ link network.

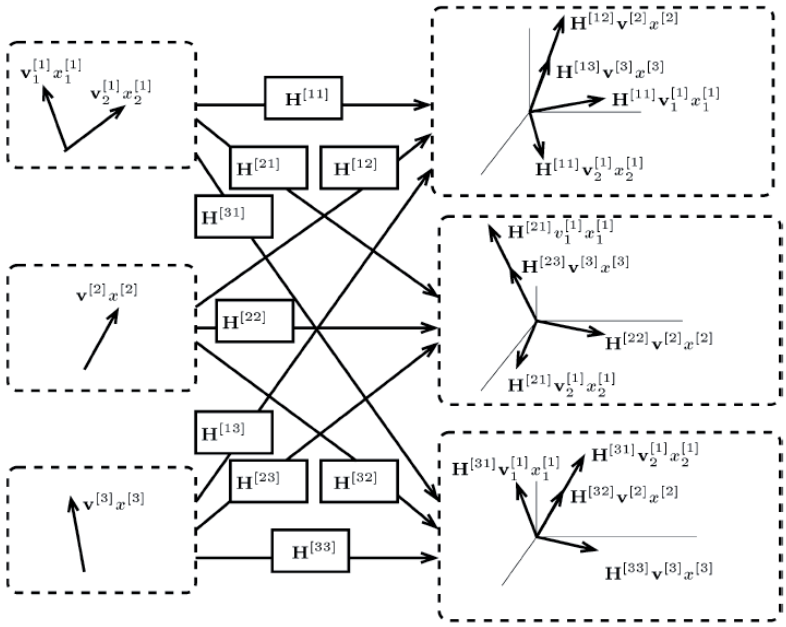

Figure 6.13: Interference alignment of a 3 user interference channel [1].

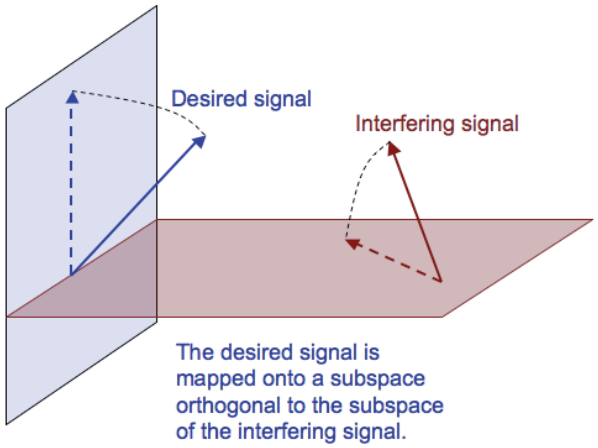

Figure 6.14: Simplified illustration of mapping the desired signal onto a subspace orthogonal to the interfering signal.

equations with $\kappa\left[(N_t-1)+(N_r-1)\right]$ unknowns (these are the beamforming vectors) [1], which has a solution only if $\kappa \leq N_t+N_r-1$. For $\kappa > N_t+N_r-1$ users, interference alignment is infeasible and the inter-user interference powers cannot be fully aligned, resulting in some interference in the subspace of the desired signal. When the SNR is low, operating in the infeasible interference alignment regime can in fact be beneficial, due to the low levels of interference. For higher SNR values, however, the interference within the subspace of the signal of interest can become too destructive and the sum rate of the network will saturate as SNR increases indefinitely. In this case, allowing fewer links in the network to be active with interference alignment being feasible can in fact provide a higher sum rate. Hence, in the following, we propose a power algorithm that uses instantaneous CSIT to ensure the highest achievable sum rate, regardless of the interference alignment scheme at hand.

We consider 3 different interference alignment schemes. These are the "*maximizing SINR*" method, proposed in [2], the "*alternated minimization*" technique for interference alignment, as proposed in [3], and the "*sum rate optimization*" technique, proposed in [4]. The latter method is by construction optimal, but it is more complex and requires additional sharing or feedback of pricing information among the transmitters. As our objective is not to evaluate the various interference alignment schemes, we do not go into more details about their procedures.

6.2.3 Binary Power Control to Ensure Feasibility

It was shown for single antenna systems that *binary* power control is in fact optimal for maximizing the sum rate of a 2 link system [113], and near-optimal for a κ link system. Based on this, we develop a binary power control algorithm to be applied on top of the interference alignment scheme used in the network. Our power control operates in a fully distributed manner. We do not claim optimality for our power control algorithm, only that it improves the sum rate performance without changing the beamforming technique already applied in the network.

Denote the sum capacity of the κ link network by $\mathcal{C}_\Sigma^\kappa$. Since the beamforming at all transmitters and receivers is dependent on the number of links in the channel, the SINR of link i (given by Eq. (6.40)) changes based on the number of active links in the network. When the SNR is small, such that there is little interference at each receiver, we have that

$$\mathcal{C}_\Sigma^\kappa \;=\; \sum_{k=1}^{\kappa}\log_2(1+\mathrm{SINR}_k) \;>\; \sum_{l=1}^{\kappa-1}\log_2(1+\mathrm{SINR}_l) \;=\; \mathcal{C}_\Sigma^{\kappa-1}. \qquad (6.43)$$

On the other hand, we know that for high SNRs, when interference alignment is feasible, the sum rate increases linearly with SNR, thus surpassing the saturated sum rates of its equivalent infeasible interference alignment regime. This means that there is a certain SNR value, SNR_t, above which it is beneficial for the sum rate that the network goes from κ to $\kappa - 1$ active links. In other words,

$$\mathcal{C}_\Sigma^\kappa \; < \; \mathcal{C}_\Sigma^{\kappa-1} \quad ; \text{when SNR} \; > \text{SNR}_t \tag{6.44}$$

For the sake of readability, denote $\overline{\mathbf{G}}_{ij}^\kappa = |\mathbf{v}_i^{\kappa^\dagger} \mathbf{G}_{ij} \mathbf{w}_j^\kappa|^2$ for all i, j. Now we have that for each $\mathbf{G}_{ij}$ instance, one user should be shut down if

$$\begin{aligned} \kappa \log_2 \left(1 + \frac{\rho \, \overline{\mathbf{G}}_{ii}^\kappa}{\eta + \rho \sum_{j \neq i}^\kappa \overline{\mathbf{G}}_{ij}^\kappa} \right) \; &< \; (\kappa - 1) \log_2 \left(1 + \frac{\rho \, \overline{\mathbf{G}}_{ii}^{\kappa-1}}{\eta + \rho \sum_{j \neq i}^{\kappa-1} \overline{\mathbf{G}}_{ij}^{\kappa-1}} \right) \\ \left(1 + \frac{\rho \, \overline{\mathbf{G}}_{ii}^\kappa}{\eta + \rho \sum_{j \neq i}^\kappa \overline{\mathbf{G}}_{ij}^\kappa} \right)^\kappa \; &< \; \left(1 + \frac{\rho \, \overline{\mathbf{G}}_{ii}^{\kappa-1}}{\eta + \rho \sum_{j \neq i}^{\kappa-1} \overline{\mathbf{G}}_{ij}^{\kappa-1}} \right)^{\kappa-1}, \end{aligned} \tag{6.45}$$

Due to the altruistic part of the transmit beamforming (i.e., the fact that each transmitter tries to minimize its interference to other users), the residual coordinated interference at receiver i should be on the order of the noise power, $\mathcal{O}(\eta)$, which we set equal to η. Note that this should not be interpreted as an assumption in a proof, but rather as a proposed design guideline for the interference alignment scheme that is applied. This yields

$$\begin{aligned} \left(1 + \frac{\rho \, \overline{\mathbf{G}}_{ii}^\kappa}{\eta + \rho \sum_{j \neq i}^\kappa \overline{\mathbf{G}}_{ij}^\kappa} \right) \; &< \; \left(1 + \frac{\rho \, \overline{\mathbf{G}}_{ii}^{\kappa-1}}{2\,\eta} \right)^{\frac{\kappa-1}{\kappa}} \\ &\overset{(a)}{\approx} \; \left(1 + \frac{\rho \, \overline{\mathbf{G}}_{ii}^\kappa}{2\,\eta} \right)^{\frac{\kappa-1}{\kappa}}, \end{aligned} \tag{6.46}$$

where in (a) we use the approximation that $\mathbf{G}_{ii}^\kappa < \mathbf{G}_{ii}^{\kappa-1}$. The reason for this is that when the number of links is reduced, transmitter i will have fewer receivers to minimize its interference against, resulting in more degrees of freedom for its own transmission. In fact, as long as interference alignment is infeasible both in the case κ and $\kappa - 1$ links, the change between $\overline{\mathbf{G}}_{ii}^\kappa$ and $\overline{\mathbf{G}}_{ii}^{\kappa-1}$ is expected to be small. As mentioned before, bear in mind that our derivations do not function as a proof; they only provide some justification for the binary power control algorithm we propose.

Based on the above reasoning, we develop the following binary power control algorithm:

1. Each transmitter-receiver pair calculates its transmit and receive beamformers, $\mathbf{w}_i^\kappa$ and $\mathbf{v}_i^\kappa$, based on the current channel coefficients and the desired beamforming algorithm. Here we assume that the number of users κ in the network is known to all users.

2. Each user i compares its current $\text{SINR}_i = \frac{\rho|\mathbf{v}_i^{\kappa\dagger}\mathbf{G}_{ii}\mathbf{w}_i^\kappa|^2}{\eta+\sum_{j\neq i}^{\kappa}\rho|\mathbf{v}_i^{\kappa\dagger}\mathbf{G}_{ij}\mathbf{w}_j^\kappa|^2}$ with the threshold $\text{SINR}_t = \left(\frac{\rho|\mathbf{v}_i^{\kappa\dagger}\mathbf{G}_{ii}\mathbf{w}_i^\kappa|^2}{2\eta}\right)^{1+\frac{1}{\kappa}}$. If $\text{SINR}_i < \text{SINR}_t$, then that link will shut down with probability $1/\kappa$.

3. Repeat steps (1) and (2) until SINR_i is no longer less than SINR_t.

A few comments are in place concerning the performance of the proposed binary power control scheme:

- **Remark 1:** Once the feasibility region has been reached, we will always have that $\text{SINR}_i \geq \text{SINR}_t$, and thus, no more nodes will try to shut down.
- **Remark 2:** Our power control scheme is semi-heuristic, due to the fact that the exact value of $\overline{\mathbf{G}}_{ii} = |\mathbf{v}_i^{\kappa-1^\dagger}\mathbf{G}_{ii}\mathbf{w}_i^{\kappa-1}|^2$ after one user has been shut down is unknown. However, our simulations show that using the $\mathbf{v}_i^\kappa$ and $\mathbf{w}_i^\kappa$ already generated in the κ link channel is a good approximation.

In Figures 6.15, 6.16, and 6.17, the sum rate of the $\kappa \geq 3$ link MIMO networks is plotted with $N_t = N_r = 2$. Our proposed binary power control algorithm is plotted along with various interference alignment schemes, which are feasible when $\kappa \leq 3$. The figures show that the proposed distributed binary power control (the dotted lines) does in fact achieve a higher sum rate for high SNRs compared to applying any of the interference alignment schemes among $\kappa > 3$ links. As discussed earlier, for low SNR values, the sum rate of a network with 6 active links is higher than that with fewer links. This is due to the fact that the amount of rate that each link adds to the system is greater than the degradation its interference causes for other users' rates. For high SNR values, on the other hand, the amount of interference the users cause to each other is more destructive in terms of rate, than the amount of rate increase they provide to the network sum rate. Hence, as SNR increases indefinitely, the highest sum rate is achieved by turning off all excessive users beyond $N_t + N_r - 1$.

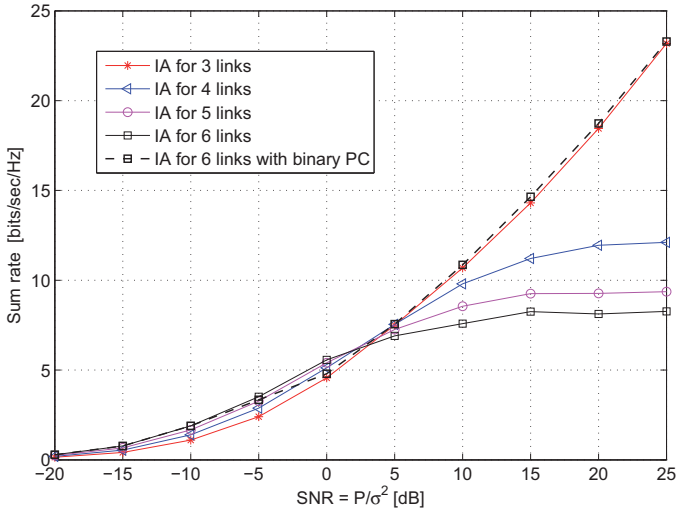

Figure 6.15: The sum rate of "maximizing SINR" interference alignment [2] of a network with 3, 4, 5, or 6 users, as a function of SNR.

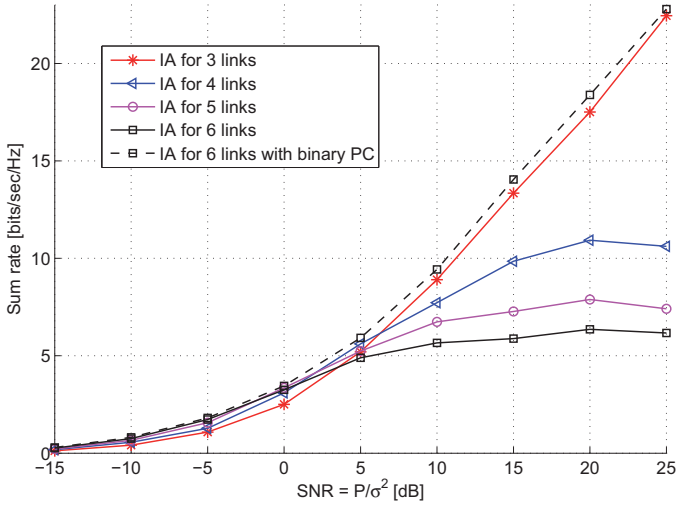

Figure 6.16: The sum rate of the "alternated minimization" interference alignment [3] of a network with 3, 4, 5, or 6 users, as a function of SNR.

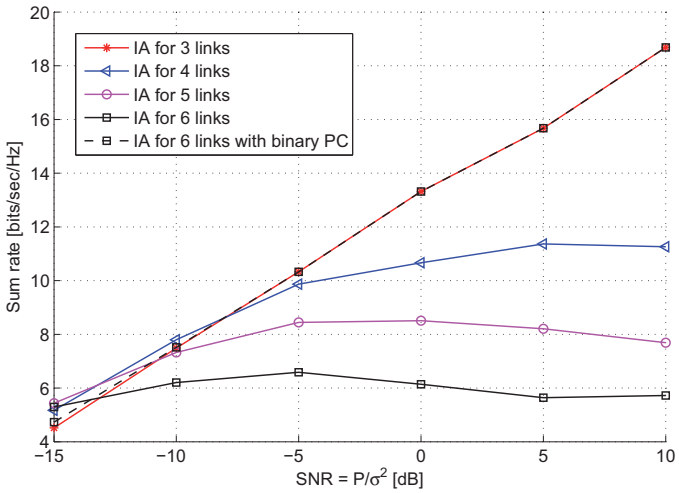

Figure 6.17: The sum rate of the "sum rate optimization" interference alignment [4] of a network with 3, 4, 5, or 6 users, as a function of SNR.

Note that our binary power control scheme not only improves the sum rate performance of a κ link system (assuming $\kappa > N_t + N_r - 1$, but it also provides power savings. For high SNR values, this saving is equal to $\rho(\kappa - N_t - N_r + 1)$. E.g., in a $\kappa = 10$ user network with a transmit power of 1 mW and $N_t = N_r = 2$ antennas, up to 7 mW of power may be saved, at the same time as ensuring the maximum sum rate achievable with any desired precoding scheme.

6.3 Summary

In Section 6.1, we were mainly concerned with characterizing and understanding the average performance of a κ link MIMO network with no CSIT. Upper and lower bounds are derived for the ergodic capacity and outage probability, and we observe that while determinant bound provides a tight bound, the trace bound fails to give a correct picture of the network performance. We also learned that when the transmitters have no CSI, different number of antennas yield an optimal performance for different system parameters. When the interference is weak, the ergodic capacity increases (equivalently, the outage probability decreases) with the number of transmit antennas, N_t. On the other hand, for a strong interference channel, the optimal strategy is always to apply double the number of receive antennas compared to transmit antennas, i.e., $N_r = 2N_t$.

The particular case of a MISO channel is also considered, where exact expressions are derived for the ergodic capacity and outage probability. It is shown that when $\varepsilon = \frac{\rho_I g_I}{\rho g}(2^{R_{req}} - 1) \leq \varepsilon_t$, the outage probability decreases with the number of transmit antennas, while for $\varepsilon > \varepsilon_t$, it increases. ε_t is found numerically and is in a 2 link network simplified to be equal to 1. As a consequence, when $\varepsilon \leq \varepsilon_t$, the capacity achieving approach is to utilize all antennas available, while for $\varepsilon > \varepsilon_t$, the SISO channel provides the best performance. In the latter case, we introduce TDMA between the links, showing that for low values of κ, it reduces the outage probability of the MISO channel below that of the SISO channel, and again using the maximum number of transmit antennas available is optimal.

We also investigate the performance of MIMO networks with CSIT. Applying various interference alignment techniques, we propose a binary power control algorithm that improves the sum rate performance of whichever interference alignment scheme at hand. The binary power control algorithm shuts down users one by one as the SNR increases, until interference alignment is feasible again. The decision on whether or not to shut down is made based on the instantaneous channel quality for each packet. Once interference alignment is feasible again, the sum rate increases linearly with the SNR. The proposed power control algorithm is fully distributed.

Chapter 7

Conclusions and Future Work

This thesis considers the performance of single-hop wireless ad hoc networks with point-to-point communication links, with the objective of establishing a fundamental understanding of their behavior and to propose schemes to improve their performance. Due to the inherent nature of mobile ad hoc networks, i.e., their composition of an unknown number of users, with unknown and varying position of their peers, counteracting the negative impact of interference in such networks is a challenging task. However, through specific modeling techniques and by introducing appropriate analytical frameworks, the complex task of analyzing the average performance of random ad hoc networks is made tractable.

In a large portion of this work, presented in Chapters 2 - 5, the viewpoint is through the MAC layer, and the main metric used for performance evaluation is *outage probability*. This is defined as the probability that a transmitted message is received in such a way that it cannot be decoded correctly at its destination. It can be characterized either by the SINR at the receiver falling below a predefined threshold at some time along the message duration, or by determining when the capacity of the channel is lower than the transmission rate required for correct decoding of a packet. These two characterizations are related and interchangeable. This metric is stochastic, pragmatic, and closely related to the ubiquitous notions of throughput and transmission capacity.

In addition to establishing the network model and analytical framework for evaluating the performance of ad hoc networks (Chapter 2), different network topologies and channel models are considered (Chapter 3). Specifically, fading is first added to the network model and its impact is evaluated. Moreover, the communication domain is bounded, and the resulting edge effects are accounted for both in non-fading and fading en-

vironments. Having established an understanding for the behavior of ad hoc networks, various MAC layer techniques are then proposed to improve their performance (Chapters 4 and 5). In particular, we optimize the sensing threshold of CSMA, and add a simple feedback channel between each sender and its destination for more efficient decision making. Furthermore, we introduce bandwidth partitioning, and find the optimal number of subbands that minimizes the outage probability of the various MAC protocols.

Taking a step further, we also investigate the benefit of applying multiple antennas in each of the point-to-point communication links of the network (Chapter 6). Within an ad hoc setting, where nodes have no information about their surroundings, the average capacity and outage probability performance of these networks are analyzed. With the addition of channel knowledge, a binary power control algorithm is proposed for already-established precoding techniques, to improve their performance in networks with many users.

7.1 Detailed Contributions of This Thesis

In the following, we list the main findings and conclusions of this thesis:

- Approximate analytical expressions are derived for the outage probability of slotted and unslotted ALOHA, CSMA with transmitter sensing (denoted CSMA_{TX}), and CSMA with receiver sensing (denoted CSMA_{RX}). This is done by translating the randomness of transmitter locations on the 2-D plane and the randomness of packet arrivals in time to a 3-D space-time model, allowing us to consider only a single random process describing both the temporal and spatial variations of the system. Moreover, the analysis is made tractable by using the concept of guard zones [36].

- Slotted ALOHA yields the best outage probability, outperforming its unslotted version by a factor of 2^{N+1}, where N is the number of permitted retransmissions. However, this protocol requires synchronization. When no backoffs or retransmissions are allowed, the conventional CSMA protocol, CSMA_{TX}, actually performs worse than unslotted ALOHA for low densities. This is due to the exposed node problem, i.e., transmitters back off in situations where their transmissions would not have caused errors for others.

- By allowing the *receiver* to sense the channel in CSMA_{RX}, and to

inform its transmitter over a separate control channel whether or not to initiate its transmission, the performance of the conventional CSMA protocol is improved significantly. We also observed that significant performance gain can be provided by increasing the number of backoffs and retransmissions. In fact, for large number of backoffs, CSMA with receiver sensing can even outperform slotted ALOHA.

- The addition of fading to the channel model changes the analytical derivations significantly, as we can no longer consider only the closest interferers. However, a modified version of the guard zone technique is proposed, where only the *dominant* interferers are considered. Approximate outage probability expressions are derived, and fading is seen to degrade the system performance considerably.

- For a bounded network domain, new outage probability expressions are derived both in the absence and presence of fading. The boundedness of the communication region reduces the amount of interference in the channel, resulting in up to 50% lower outage probability, because there are no interferers outside the communication domain. As the network size increases with a given node density, so does the outage probability, until it converges to that induced from an infinite network. Practical implications of these results include the possibility of deploying a greater density of nodes in indoor networks than predicted by previous models, due to the presence of walls and obstacles.

- In order to improve the outage probability of CSMA, we optimize the sensing threshold based on which the backoff decision is made. We observe that for CSMA_{TX} there is no advantage in allowing for channel sensing when the density is low, whereas a small gain can be obtained in CSMA_{RX}. For higher densities, however, the effect of optimizing the sensing threshold becomes more significant, and the outage probability of both CSMA protocols can then be reduced by up to 40%.

- We also propose a modification to the CSMA protocol, $\text{CSMA}_{\text{TXRX}}$, where the transmitter and receiver jointly make the backoff decision. Based on derived outage probability expressions, the optimal sensing thresholds for both the transmitter and receiver are obtained, and an understanding is established on how these optimal thresholds

balance between the inherent hidden and exposed node problems of CSMA.

- Bandwidth partitioning is introduced in both non-fading and fading networks, and the outage probability is evaluated. Increasing the number of subbands results in a lower level of interference within each subband, while at the same time, a lower transmission rate may be achieved. The optimal number of subbands represents the optimal trade-off between these two factors. In the case of ALOHA with no retransmissions, the optimal number of subbands is found analytically. For CSMA, it is obtained through simulations.

- In the case of CSMA in the presence of bandwidth partitioning, we introduce sensing across all subbands prior to each transmission. This improves the performance of CSMA considerably, by up to 50% in the absence of fading and 67% in the presence of fading.

- Multiple antennas are introduced at the transmitters and receivers in an ad hoc network, and upper and lower bounds on the ergodic capacity and outage probability of MIMO interference channels (with no CSIT) are obtained. It is shown that using double the number of receive antennas compared to transmit antennas yields the optimal performance in strong interference channels, while when the interference is weak, the maximum number of transmit antennas available should be employed.

- For the particular case of the MISO interference channel, exact analytical expressions are derived for both the ergodic capacity and the outage probability. An interesting behavior is observed in the outage probability, resulting in the conclusion that for certain ranges of the system parameters, the capacity achieving approach is to utilize all transmit antennas available, while for other ranges, the SISO channel provides the best performance. In the latter case, we introduce TDMA between the links. In a 2 link network, this reduces the outage probability below that of the SISO channel, and again using the maximum number of transmit antennas available is optimal.

- The performance of MIMO ad hoc networks is also evaluated when CSI is available at the transmitters. Applying various interference alignment techniques, we propose a binary power control algorithm

that improves the sum rate of the network compared to when interference alignment is applied among all users in the network. The binary power control algorithm shuts down users one by one as the SNR increases, until interference alignment is feasible again. The decision on whether or not to shut down is made in a distributed manner, based on the instantaneous channel qualities.

7.2 Subjects for Further Research

Much work remains to be done in the design and analysis of wireless ad hoc networks. In the following, we suggest some research extensions to the work of this thesis.

- In the CSMA protocol considered in Chapters 2-5, a rather simple backoff mechanism was employed; namely exponential random backoff. However, other backoff schemes are also possible. The common one used in the IEEE 802.11 and 802.16 standards family is *binary exponential backoff*. Variations to this algorithm have been proposed to improve the performance of CSMA [114; 115], and it would be interesting to investigate the impact of different backoff schemes on the outage probability performance of wireless ad hoc networks.

- Our assumption on fixed transmitter-receiver distance is not always reasonable. One way to justify this assumption, as noted in Chapter 2, is to view the network with a fixed R as a snapshot of a multi-hop wireless network, where R is the bounded *average* inter-relay distance resulting from the specific routing protocol used. However, relaxing this constraint could give new insight in the performance of single-hop and multi-hop networks, and allow us to derive the optimal distance to the destination, e.g., based on a given outage constraint. A variable transmitter-receiver distance is expected to have a more severe impact in bounded networks, considered in Chapter 3, than in infinite ones.

- Various MAC layer techniques were proposed in Chapters 4 and 5 to improve the outage probability of ad hoc networks, and each one was shown to provide significant performance gain. Consequently, a natural extension would be to combine the various proposed schemes. E.g., with the introduction of bandwidth partitioning,

each node can then perform sensing threshold optimization within each subband prior to transmission. Moreover, in case good channel conditions are detected over several subbands, a packet can transmit over *multiple* subbands. Here we would have a trade-off between density of interferers and the achieved transmission rate, meaning that one can expect an optimal number of subbands that each packet should be transmitted over.

- Another natural extension to this thesis is to consider *multi-hop* networks. The results obtained in Chapter 2 can be applied for each hop, assuming a fixed distance between relays and no spatial and temporal correlations between transmissions. With these assumptions, we have performed some introductory work on this topic in [30–32]. However, these assumptions are often not reasonable in real ad hoc networks. Moreover, we have assumed perfect routing, i.e., a packet travels on a straight line from its transmitter to its destination. This is again a simplification that needs to be improved or removed. Finally, within a multi-hop setting, the number of and distance between hops may be optimized in order to minimize the outage probability. A further advancement would be to also optimize the transmission rate in each hop.

- Our work in Chapter 6 has room for many extensions, due to the recent expanding interest in MIMO interference channels and techniques to improve their performance. Firstly, exact expressions for the ergodic capacity and outage probability should be derived for MIMO systems with few antennas (instead of our lower and upper bounds). However, based on our extensive attempts and consulting with other prominent researchers within this field, this appears to be an intractable problem. For MISO interference channels, it would be interesting, if possible, to propose schemes to increase the channel randomness beyond that of a SISO channel.

- In a MIMO interference channel with CSIT, we proposed a binary power control algorithm to improve the performance of interference alignment schemes. In order to reduce the heuristic nature of this power control and improve its performance, a fundamental understanding must be established on the performance of interference alignment in the infeasible regime. One approach is to characterize the SNR for which a node should shut down in order to reach feasibility of interference alignment. A subsequent task is then to deter-

mine *which* node to shut down in order to maximize the sum rate of the network. Finally, this power control scheme should be compared with clustering techniques, i.e., instead of shutting down users, one should create clusters of users in such a way that interference alignment within each cluster becomes feasible.

References

[1] V. R. Cadambe and S. A. Jafar, "Interference alignment and degrees of freedom in the *K*-user interference channel," *IEEE Trans. on Information Theory*, vol. 54, no. 8, pp. 3425–3441, Aug. 2008.

[2] K. S. Gomadam, V. R. Cadambe, and S. A. Jafar, "Approaching the capacity of wireless networks through distributed interference alignment," *preprint*, 2008, available at http://arxiv.org/abs/0803.3816.

[3] S. W. Peters and R. W. Heath, "Interference alignment via alternating minimization," in *Proc. IEEE International Conference on Acoustics, Speech and Signal Processing (ICASSP)*, pp. 2445–2448, May 2009.

[4] C. Shi, D. A. Schmidt, R. A. Berry, M. L. Honig, and W. Utschick, "Distributed interference pricing for the MIMO interference channel," in *Proc. IEEE International Conference on Communications (ICC)*, pp. 1–5, June 2009.

[5] L. Kleinrock and F. A. Tobagi, "Packet switching in radio channels: Part I - Carrier sense multiple-access modes and their throughput-delay characteristics," *IEEE Trans. on Communications*, vol. 23, pp. 1400–1416, Dec. 1975.

[6] D. Bertsekas and R. Gallager, *Data Networks*. Prentice-Hall, Inc., New Jersey, 1987.

[7] A. Paulraj and T. Kailath, "Increasing capacity in wireless broadcast systems using distributed transmission/directional reception (DTDR)," in *US Patent 5,345,599*, Sept. 1994.

[8] M. Maddah-Ali, A. Motahari, and A. Khandani, "Communication over MIMO X channels: Interference alignment, decomposition, and performance analysis," *IEEE Trans. on Information Theory*, vol. 54, no. 8, pp. 3457–3470, Aug. 2008.

[9] N. Jindal, S. Weber, and J. Andrews, "Fractional power control for decentralized wireless networks," *IEEE Trans. on Wireless Communications*, vol. 7, no. 12, pp. 5482–5492, 2008.

[10] N. Abramson, "The ALOHA system - Another alternative for computer communications," in *Proc. Fall Joint Computer Conference*, pp. 281–296, Nov. 1970.

[11] P. Muhlethaler and A. Najid, "Throughput optimization in multihop CSMA mobile ad hoc networks," in *Proc. IEEE European Wireless Conference*, Febr. 2004.

[12] A. Goldsmith, *Wireless Communications*. Cambridge University Press, New York, 2005.

[13] Y. Wang and J. J. Garcia-Luna-Aceves, "Performance of collision avoidance protocols in single-channel ad hoc networks," in *Proc. IEEE International Conference on Network Protocols*, pp. 68–77, Nov. 2002.

[14] J. Peng and L. Cheng, "Revisiting carrier sense multiple access with collision avoidance," in *Proc. of the 40th Annual Conference on Information Sciences and Systems*, pp. 1236–1241, March 2006.

[15] P. Mohapatra and S. Krishnamoorthy, *Ad Hoc Networks*. Technologies and Protocols, Springer Verlag, New York, 2004.

[16] T. Sheldon and T. Sheldon, *Encyclopedia of Networking and Telecommunications*, 3rd ed. McGraw-Hill, Inc., New York, 2001.

[17] T. M. Cover and J. A. Thomas, *Elements of Information Theory (Wiley Series in Telecommunications and Signal Processing)*. Wiley-Interscience, 2006.

[18] S. Weber, X. Yang, J. Andrews, and G. de Veciana, "Transmission capacity of wireless ad hoc networks with outage constraints," *IEEE Trans. on Information Theory*, vol. 51, no. 12, pp. 4091–4102, Dec. 2005.

[19] P. Gupta and P. R. Kumar, "The capacity of wireless networks," *IEEE Trans. on Information Theory*, vol. 46, no. 2, pp. 388–404, March 2000.

[20] F. Xue, L. Xie, and P. R. Kumar, "The transport capacity of wireless networks over fading channels," *IEEE Trans. on Information Theory*, vol. 51, no. 3, pp. 834–847, March 2005.

[21] R. S. Blum, "MIMO capacity with interference," *IEEE Journal on Selected Areas in Communications*, vol. 21, no. 5, pp. 793–801, June 2003.

[22] M. Kang, L. Yang, and M.-S. Alouini, "Outage probability of MIMO optimum combining in presence of unbalanced co-channel interferers and noise," *IEEE Trans. on Wireless Communications*, vol. 5, no. 7, pp. 1661–1668, July 2006.

[23] E. Jorswieck and H. Boche, "Outage probability in multiple antenna systems," *European Trans. on Telecommunications*, vol. 18, no. 3, pp. 287–304, April 2007.

[24] A. Paulraj, R. Nabar, and D. Gore, *Introduction to Space-Time Wireless Communications*. Cambridge University Press, 2003.

[25] J. Salz, "Digital transmission over cross-coupled linear channels," *AT&T Technical Journal*, vol. 64, no. 6, pp. 1147–1159, Aug. 1985.

[26] L. Zheng and D. N. C. Tse, "Diversity and multiplexing: A fundamental tradeoff in multiple-antenna channels," *IEEE Trans. on Information Theory*, vol. 49, no. 5, pp. 1073–1096, May 2003.

[27] IEEE Computer Society and Microwave Theory and Techniques Society, *IEEE Standard for Local and metropolitan area networks. Part 16: Air Interface for Broadband Wireless Access Systems*. IEEE, May 2009.

[28] Wikipedia (The Free Encyclopedia), *MIMO*. Wikipedia.org, Aug. 2010. [Online]. Available: http://en.wikipedia.org/wiki/MIMO

[29] P. H. J. Nardelli, M. Kaynia, P. Cardieri, and M. Latva-aho, "Optimal transmission capacity of ad hoc networks with packet retransmissions," *IEEE Trans. on Communications*, Sept. 2010, to be submitted.

[30] M. Kaynia, P. H. J. Nardelli, P. Cardieri, and M. Latva-aho, "On the optimal design of MAC protocols in multi-hop ad hoc networks," in *Proc. IEEE International Symposium of Modeling and Optimization in Mobile, Ad Hoc, and Wireless Networks (WiOpt)*, pp. 424–429, June 2010.

[31] P. H. J. Nardelli, M. Kaynia, and M. Latva-aho, "Efficiency of the ALOHA protocol in multi-hop networks," in *Proc. IEEE International Workshop on Signal Processing Advances for Wireless Communications (SPAWC)*, Marrakech, Morocco, June 2010.

[32] M. Kaynia, P. H. J. Nardelli, and M. Latva-aho, "Evaluating the information efficiency of multi-hop networks with carrier sensing capability," in *IEEE International Conference on Communications (ICC)*, Kyoto, Japan, June 2011, submitted.

[33] J. E. Corneliussen, M. Kaynia, and G. E. Øien, "Optimal tradeoff between transmission rate and packet duration in wireless ad hoc networks," in *Proc. IEEE Wireless Communications and Networking Conference (WCNC)*, pp. 1–6, April 2010.

[34] C.-S. Chen, M. Kaynia, G. E. Øien, and A. Gjendemsjø, "Cooperative multi-cell power control under imperfect channel knowledge: A comparative study," in *Proc. 2nd COST 2100 Workshop on MIMO and Cooperative Communications*, Trondheim, Norway, June 2008.

[35] M. Haenggi, "Outage and throughput bounds for stochastic wireless networks," in *Proc. IEEE International Symposium on Information Theory*, pp. 2070–2074, Sept. 2005.

[36] A. Hasan and J. G. Andrews, "The guard zone in wireless ad hoc networks," *IEEE Trans. on Wireless Communications*, vol. 6, no. 3, pp. 897–906, Dec. 2005.

[37] S. Weber, J. G. Andrews, and N. Jindal, "Throughput and transmission capacity of ad hoc networks with channel state information," in *Proc. of the 44th Annual Allerton Conference on Communication, Control, and Computing*, Monticello, IL, Sept. 2006.

[38] G. Ferrari and O. Tonguz, "MAC protocols and transport capacity in ad hoc wireless networks: Aloha versus PR-CSMA," in *Proc. IEEE Military Communications Conference*, vol. 2, pp. 1113–1318, Oct. 2003.

[39] L.-L. Xie and P. R. Kumar, "On the path-loss attenuation regime for positive cost and linear scaling of transport capacity in wireless networks," *IEEE Trans. on Information Theory*, vol. 52, pp. 2313–2328, June 2006.

[40] R. Vaze, "Throughput-delay-reliability tradeoff with ARQ in wireless ad hoc networks," *available on http://arxiv.org/abs/1004.4432*, April 2010.

[41] X. Wang and K. Kar, "Throughput modelling and fairness issues in CSMA/CA based ad-hoc networks," in *Proc. INFOCOM*, Mar. 2005.

[42] M. Garetto, T. Salonidis, and E. Knightly, "Modeling per-flow throughput and capturing starvation in CSMA multi-hop wireless networks," in *Proc. INFOCOM*, 2006.

[43] M. Kaynia and N. Jindal, "Performance of ALOHA and CSMA in spatially distributed wireless networks," in *Proc. IEEE International Conference on Communications (ICC)*, pp. 1108–1112, May 2008.

[44] M. Kaynia, G. E. Øien, and R. Verdone, "Analytical assessment of the effect of backoff and retransmissions on the performance of ALOHA and CSMA in MANETs," in *Proc. IEEE International Conference on Communications (ICC)*, pp. 1–6, 2010.

[45] M. Kaynia, N. Jindal, and G. E. Øien, "Performance analysis and improvement of MAC protocols in wireless ad hoc networks," *IEEE Trans. on Wireless Communications*, Feb. 2010, in revision, available at http://www.iet.ntnu.no/∼kaynia/MAC_Journal.pdf.

[46] G. Song, Y. Zhou, Z. Wei, and A. Song, "A smart node architecture for adding mobility to wireless sensor networks," *Elsevier Sensors and Actuators A: Physical*, vol. 147, no. 1, pp. 216–221, 2008.

[47] R. K. Ganti and M. Haenggi, "Spatial and temporal correlation of the interference in aloha ad hoc networks," *IEEE Communication Letters*, vol. 13, no. 9, pp. 631–633, Sept. 2009.

[48] J. F. C. Kingman, *Poisson Processes*. Oxford University Press, Oxford, 1993.

[49] A. Baddeley, *Spatial Point Processes and Their Applications*. Springer, 2007.

[50] M. B. Yassein and A. A.-T. S. Manaseer, "A performance comparison of different backoff algorithms under different rebroadcast probabilities for MANETs," in *Proc. UK Performance Engineering Workshop*, pp. 182–188, July 2009.

[51] M. Haenggi, "Outage, local throughput, and capacity of random wireless networks," *IEEE Trans. on Wireless Communications*, vol. 8, no. 8, pp. 4350–4359, Aug. 2009, available at http://www.nd.edu/∼mhaenggi/pubs/twc09.pdf.

[52] N. Jindal, J. G. Andrews, and S. Weber, "Optimizing the SINR operating point of spatial networks," in *Workshop on Info. Theory and its Applications*, Jan. 2007.

[53] E. S. Sousa and J. A. Silvester, "Optimum transmission ranges in a direct-sequence spread-spectrum multihop packet radio network," *IEEE Journal on Selected Areas in Communications*, vol. 8, no. 5, pp. 762–771, June 1990.

[54] Wolfram Research, Inc., *Lambert Function*. Mathworld Web Resource, April 2005. [Online]. Available: http://mathworld.wolfram.com/LambertW-Function.html

[55] M. Kaynia, N. Jindal, and G. E. Øien, "Impact of fading on the performance of ALOHA and CSMA," in *Proc. IEEE International Workshop on Signal Processing Advances for Wireless Communications (SPAWC)*, pp. 394–398, June 2009.

[56] M. Kaynia, F. Fabbri, R. Verdone, and G. E. Øien, "Analytical study of the outage probability of ALOHA and CSMA in bounded ad hoc networks," in *Proc. IEEE European Wireless Conference*, pp. 544–550, April 2010.

[57] F. Fabbri, M. Kaynia, and R. Verdone, "The impact of edge effects on the performance of MAC protocols in ad hoc networks with fading," in *Proc. IEEE International Conference on Communications (ICC)*, pp. 1–5, May 2010.

[58] M. Kaynia, F. Fabbri, R. Verdone, and G. E. Øien, "MAC layer perspective on the boundedness of ad hoc networks with and without fading," *IEEE Trans. on Vehicular Communications*, Aug. 2010, submitted.

[59] F. Baccelli, B. Blaszcxyszyn, and P. Muhlethaler, "An Aloha protocol for multihop mobile wireless networks," *IEEE Trans. on Information Theory*, vol. 52, no. 2, pp. 421–436, Feb. 2006.

[60] R. K. Ganti and M. Haenggi, "Interference and outage in clustered wireless ad hoc networks," *IEEE Trans. on Information Theory*, vol. 55, no. 9, pp. 4067–4086, Sept. 2009, available at http://www.nd.edu/∼mhaenggi/pubs/tit09.pdf.

[61] M. Haenggi, "A geometry-inclusive fading model for random wireless networks," in *Proc. International Symp. on Information Theory (ISIT)*, pp. 1329–1333, July 2006.

[62] X. Liu and M. Haenggi, "Performance analysis of Rayleigh fading ad hoc networks with regular topology," in *Proc. IEEE Global Communications Conference (GLOBECOM)*, pp. 1329–1333, Nov. 2005.

[63] J. Ilow and D. Hatzinakos, "Analytic alpha-stable noise modeling in a Poisson field of interferers or scatterers," *IEEE Trans. on Signal Processing*, vol. 46, no. 6, pp. 1601–1611, June 1998.

[64] S. Weber, J. Andrews, and N. Jindal, "The effect of fading, channel inversion, and threshold scheduling on ad hoc networks," *IEEE Trans. on Information Theory*, vol. 53, no. 11, pp. 4127–4149, 2007.

[65] M. Haenggi and R. K. Ganti, *Interference in large wireless networks*. Foundations and Trends in Networking, 2008, vol. 3, no. 2.

[66] L. E. Miller, "Distribution of link distances in a wireless network," *NIST Journal Research*, vol. 106, no. 2, pp. 401–412, April 2001.

[67] C. Rose, "Mean internodal distance in regular and random multihop networks," *IEEE Trans. on Communications*, vol. 40, no. 8, pp. 1310–1318, Aug. 1992.

[68] J. A. Silvester and L. Kleinrock, "On the capacity of multihop slotted ALOHA networks with regular structure," *IEEE Trans. on Communications*, vol. 31, no. 8, pp. 974–982, Aug. 1983.

[69] C. Bettstetter and J. Zangl, "How to achieve a connected ad hoc network with homogeneous range assignment: An analytical study with consideration of border effects," in *International Workshop on Mobile and Wireless Communications Network*, pp. 125–129, Sept. 2002.

[70] F. Fabbri and R. Verdone, "A statistical model for the connectivity of nodes in a multi-sink wireless sensor network over a bounded region," in *Proc. IEEE European Wireless Conference*, pp. 1–6, 2008.

[71] M. Kaynia, G. E. Øien, and N. Jindal, "Joint transmitter and receiver sensing capability of CSMA in MANETs," in *Proc. IEEE International Conference on Wireless Communications and Signal Processing (IC-WCSP)*, pp. 1–5, Nov. 2009, (Best Paper Award).

[72] M. Kaynia and G. E. Øien, "Improving performance of CSMA in non-fading and fading networks with joint transmitter and receiver sensing," *IEEE Trans. on Wireless Communications*, Aug. 2010, submitted.

[73] J. Zhu, X. Guo, L. Yang, and W. Conner, "Leveraging spatial reuse in 802.11 mesh networks with enhanced physical carrier sensing," in *Proc. IEEE International Conference on Communications (ICC)*, pp. 4004–4011, June 2004.

[74] J. A. Fuemmeler, N. H. Vaidya, and V. V. Veeravalli, "Selecting transmit powers and carrier sense thresholds for CSMA protocols," in *University of Illinois at Urbana-Champaign Technical Report*, Oct. 2004.

[75] B. J. B. Fonseca, "A distributed procedure for carrier sensing threshold adaptation in CSMA-based mobile ad hoc networks," in *Proc. Vehicular Technology Conference (VTC)*, pp. 66–70, Oct. 2007.

[76] T. Rappaport, *Wireless Communications: Principles & Practice*. Prentice Hall, 1996.

[77] J. G. Andrews, A. Ghosh, and R. Muhamed, *Fundamentals of WiMAX*. Prentice Hall, 2007.

[78] M. Pursley and T. Royster, "Resource consumption in dynamic spectrum access networks: Applications and Shannon limits," in *Proc. Workshop on Inform. Theory and its Applications*, 2007.

[79] K. L. Yeung and S. Nanda, "Channel management in microcell/macrocell cellular radio systems," *IEEE Trans. on Vehicular Technology*, vol. 45, no. 4, pp. 601–612, Nov. 1996.

[80] M. Sikora, J. N. Laneman, M. Haenggi, D. J. Costello, and T. Fuja, "Bandwidth- and power-efficient routing in linear wireless networks," *IEEE Trans. on Information Theory*, vol. 52, pp. 2624–2633, June 2006.

[81] P. Kyasanur, S. Jungmin, C. Chereddi, and N. Vaidya, "Multichannel mesh networks: Challenges and protocols," *IEEE Wireless Communications*, vol. 13, no. 2, pp. 30–36, 2006.

[82] Y. Yuan, P. Bahl, R. Chandra, T. Moscibroda, S. Narlanka, and Y. Wu, "Allocating dynamic time-spectrum blocks in cognitive radio networks," in *Proc. ACM MobiHoc*, Sept. 2007.

[83] N. Jindal, J. G. Andrews, and S. Weber, "Bandwidth partitioning in decentralized wireless networks," *IEEE Trans. on Wireless Communications*, vol. 7, no. 12, pp. 5408–5419, Dec. 2008.

[84] M. Kaynia, G. E. Øien, N. Jindal, and D. Gesbert, "Comparative performance evaluation of MAC protocols in ad hoc networks with bandwidth partitioning," in *Proc. IEEE International Symposium on Personal, Indoor and Mobile Radio Communications (PIMRC)*, pp. 1–6, Sept. 2008.

[85] M. Kaynia and G. E. Øien, "Outage probability of fading and non-fading ad hoc networks with bandwidth partitioning," *IEEE Trans. on Communications*, Aug. 2010, submitted.

[86] R. S. Blum, J. H. Winters, and N. Sollenberger, "On the capacity of cellular systems with MIMO," *IEEE Communication Letters*, vol. 6, no. 6, pp. 242–244, June 2002.

[87] J. W. Silverstein and Z. D. Bai, "On the empirical distribution of eigenvalues of a class of large dimensional random matrices," *Journal of Multivariate Analysis*, vol. 54, pp. 175–192, 1995.

[88] N. Czink, B. Bandemer, G. Vazquez-Vilar, L. Jalloul, C. Oestges, and A. Paulraj, "Spatial separation of multi-user MIMO channels," in *Proc. IEEE International Symposium on Personal, Indoor and Mobile Radio Communications (PIMRC)*, Sept. 2009.

[89] L. G. Ordoez, D. P. Palomar, and J. R. Fonollosa, "Ordered eigenvalues of a general class of Hermitian random matrices with application to the performance analysis of MIMO systems," *IEEE Trans. on Signal Processing*, vol. 57, no. 2, pp. 672–689, Feb. 2009.

[90] G. Alfano, A. M. Tulino, A. Lozano, and S. Verdú, "Eigenvalue statistics of finite-dimensional random matrices for MIMO wireless communication," in *Proc. IEEE International Conference on Communications (ICC)*, June 2006.

[91] M. Chiani, M. Z. Win, and A. Zanella, "The distribution of eigenvalues for correlated Wishart matrices applied to optimum combining with unequal power interferers and noise," in *Proc. IEEE Information Theory Workshop*, pp. 203–205, March 2003.

[92] M. Sharif and B. Hassibi, "On the capacity of MIMO broadcast channels with partial side information," *IEEE Trans. on Information Theory*, vol. 51, no. 2, pp. 506–522, Feb. 2005.

[93] A. Lozano and A. M. Tulino, "Capacity of multiple-transmit multiple-receive antenna architecture," *IEEE Trans. on Information Theory*, vol. 48, no. 12, pp. 3117–3128, Dec. 2002.

[94] J. M. Romero-Jerez, J. P. Peña-Martin, G. Aguilera, and A. J. Goldsmith, "Performance of MIMO MRC systems with co-channel interference," in *Proc. IEEE International Conference on Communications (ICC)*, vol. 3, pp. 1343–1349, June 2006.

[95] T. Gou and S. A. Jafar, "Degrees of freedom of the k user $m \times n$ MIMO interference channel," in *Proc. IEEE Global Communications Conf. (GLOBECOM)*, Sept. 2008.

[96] J. Proakis, *Digital Communications*, 3rd ed. McGraw-Hill, Inc., New York, 1995.

[97] M. Kaynia, A. J. Goldsmith, D. Gesbert, and G. E. Øien, "On the usage of antennas in MIMO and MISO interference channels," in *Proc. IEEE International Workshop on Signal Processing Advances for Wireless Communications (SPAWC)*, June 2010.

[98] K. M. Ho, M. Kaynia, and D. Gesbert, "Distributed power control and beamforming on MIMO interference channels," in *Proc. IEEE European Wireless Conference*, pp. 654–660, April 2010.

[99] S. Catreux, P. F. Driessen, and L. J. Greenstein, "Simulation results for an interference-limited multiple-input multiple-output cellular system," *IEEE Communication Letters*, vol. 4, no. 11, pp. 334–336, Nov. 2000.

[100] M. Chiani, M. Z. Win, and H. Shin, "MIMO networks: The effects of interference," *IEEE Trans. on Information Theory*, vol. 56, no. 1, Jan. 2010.

[101] A. M. Tulino and S. Verdú, *Random Matrix Theory and Wireless Communications*. Foundations and Trends in Communications and Information Theory, 2004, vol. 1, no. 1.

[102] Y. Zhu, P.-Y. Kam, and Y. Xin, "A new approach to the capacity distribution of MIMO rayleigh fading channels," in *Proc. IEEE Global Communications Conference (GLOBECOM)*, pp. 1–5, Nov. 2006.

[103] D. Schattschneider, "Proof without words: The arithmetic mean-geometric mean inequality," *Mathematics Magazine*, vol. 59, no. 1, p. 11, 1986.

[104] N. R. Goodman, "The distribution of the determinant of a complex Wishart distributed matrix," *Ann. Mathematical Statistics*, vol. 34, no. 1, pp. 178–180, March 1963.

[105] M. A. Castaño and B. F. Lopez, "Distribution of a sum of weighted central Chi-squared variables," *Communications in Statistics - Theory and Methods*, vol. 34, pp. 515–524, 2005.

[106] M. Yilmaz, "Edgeworth series approximation for Chi-squared type chance constraints," *Communications, Faculty of Science, Univ. of Ankara, Series A1*, vol. 56, no. 2, pp. 27–37, 2007.

[107] Z. K. M. Ho and D. Gesbert, "Balancing egoism and altruism on MIMO interference channel," *IEEE Trans. on Signal Processing*, 2009, submitted.

[108] K. M. Ho and D. Gesbert, "Balancing egoism and altruism on the interference channel: The MIMO case," in *Proc. IEEE International Conference on Communications (ICC)*, pp. 1–5, 2010.

[109] M. Ku and D. Kim, "Tx-Rx beamforming with multiuser MIMO channels in MUltiple-cell systems," in *ICACT*, 2008.

[110] W. Choi and J. G. Andrews, "Base station cooperatively scheduled transmission in a cellular MIMO TDMA system," in *Proc. Annual Conference on Information Sciences and Systems*, 2006.

[111] E. A. Jorswieck and E. G. Larsson, "Complete characterization of pareto boundary for the MISO interference channel," *IEEE Trans. on Signal Processing*, vol. 56, no. 10, pp. 5292–5296, Oct. 2008.

[112] S. Y. Shi, M. Schubert, and H. Boche, "Rate optimization for multiuser MIMO systems with linear processing," *IEEE Trans. on Signal Processing*, vol. 56, no. 8, Aug. 2008.

[113] A. Gjendemsjø, D. Gesbert, G. Øien, and S. G. Kiani, "Binary power control for sum rate maximization over multiple interfering links," *IEEE Trans. on Wireless Communications*, Aug. 2008.

[114] P. Chatzimisios, A. C. Boucouvalas, V. Vitsas, A. Vafiadis, A. Oikonomidis, and P. Huang, "A simple and effective backoff scheme for the IEEE 802.11 MAC protocol," in *Proc. CITSA*, Orlando, Florida, July 2005.

[115] J. Wang and M. Song, "An efficient traffic adaptive backoff protocol for wireless MAC layer," in *Proc. IEEE International Conference on Wireless Algorithms, Systems and Applications (WASA)*, pp. 169–173, Aug. 2007.